Chemical Synthesis of Fluorescent Lugdunins for Mode-Of-Action Studies

as well as

Strategical Derivatization for Structure- Activity-Relationship Studies

Dissertation

der Mathematisch-Naturwissenschaftlichen Fakultät
der Eberhard Karls Universität Tübingen
zur Erlangung des Grades eines
Doktors der Naturwissenschaften
(Dr. rer. nat.)

vorgelegt von
M.Sc. Sebastian Niklas Wirtz
aus Düsseldorf

Tübingen
2023

Gedruckt mit Genehmigung der Mathematisch-Naturwissenschaftlichen Fakultät der Eberhard Karls Universität Tübingen.

Tag der mündlichen Qualifikation:	26.05.2023
Dekan:	Prof. Dr. Thilo Stehle
1. Berichterstatterin:	Prof. Dr. Stephanie Grond
2. Berichterstatter:	Prof. Dr. Harald Groß

Ich erkläre hiermit, dass ich die zur Promotion eingereichte Arbeit mit dem Titel: „Chemical Synthesis Of Fluorescent Lugdunins For Mode-Of-Action Studies as well as Strategical Derivatization For Structure-Activity-Relationship Studies“ selbständig verfasst, nur die angegebenen Quellen und Hilfsmittel benutzt und wörtlich oder inhaltlich übernommene Stellen als solche gekennzeichnet habe. Ich erkläre, dass die Richtlinien zur Sicherung guter wissenschaftlicher Praxis der Universität Tübingen (Beschluss des Senats vom 25.5.2000) beachtet wurden. Ich versichere an Eides statt, dass diese Angaben wahr sind und dass ich nichts verschwiegen habe. Mir ist bekannt, dass die falsche Abgabe einer Versicherung an Eides statt mit Freiheitsstrafe bis zu drei Jahren oder mit Geldstrafe bestraft wird.

_____

Sebastian N. Wirtz

Dedicated to

My Grandmother

Margot Fleschenberg

I. Preface

The following cumulative thesis comprises of four different approaches to gain further insight into the novel antibiotic lugdunin. An introduction describing the state of the art in antimicrobial research and the relevance thereof, a summary of published and unpublished peer-reviewed articles and patents as well as their respective supporting information are included.

This work was carried out at the Institute of Organic Chemistry of Eberhard Karls Universität Tübingen, Germany, in the period from June 2017 to January 2022 under the supervision of Prof. Dr. Stephanie Grond.

II. Acknowledgements

First and foremost, I would like to thank my advisor Prof. Dr. Stephanie Grond. Thank you for providing me with this very interesting research topic as well as your valuable insights and helpful advices in any scientific issues. You not only pushed us to become better researchers but also allowed us to grow. Thank you for giving me the opportunity to attend conferences to present my work and exchange with other scientists.

I would like to thank Prof. Dr. Harald Groß for his support as my second advisor.

Additionally, I would like to thank my previous (Martin, Patrik, Klaus) and current (Pascal, Taulant, Timm, Chema, Ela, Nadine, Julian, Larissa) colleagues for the time in Tübingen. Especially, I would like to thank my lab partner Julian for the time next to each other during experiments. I would also like to thank colleagues outside my group (Tamara, Marlen, Ameira) for their support.

I would also like to thank my lab interns for their support during my research projects.

This whole work would also not have been possible without my cooperation partners in Tübingen (B. Krismer and Prof. Peschel, M. Meixner and Prof. Huhn, T. Rammler and Prof. Meixner as well as various cooperations with the university clinic), in Stuttgart (Prof. Jendrossek), in Göttingen (D. Ruppelt and Prof. Steinem), in Heidelberg (K. Heeyoung and Prof. Bartenschlager) as well as industry partners.

III. Table of Contents

IV. Abbreviations

4-DMAP	4-Dimethylaminophthalimide
6-DMN	6-Dimethylaminonaphthalimide
AIDS	Acquired Immunodeficiency Syndrome
AMR	Antimicrobial Resistance
ATP	Adenosine Triphosphate
BM	Buffered Medium
Boc	tert-Butyloxycarbonyl
BRIC	Brazil, Russia, India, China
CC_{50}	Half maximal cytotoxic concentration
CCCP	Carbonyl Cyanide m-chlorophenyl hydrazone
CDI	Carbonyl diimidazole
CoV	Coronavirus
DAP	Diamino propionic Acid
DCM	Dichloromethane
DMP	Dess–Martin Periodinane
DMSO	Dimethyl Sulfoxide
DVB	Divinylbenzene
EC_{50}	Half maximal effective concentration
EMRSA-15	Epidemic methicillin-resistant Staphylococcus aureus
ESKAPE	Enterococcus faecium, Staphylococcus aureus, Klebsiella pneumoniae, Acinetobacter baumannii, Pseudomonas aeruginosa, and Enterobacter spp
FLIM	Fluorescence-Lifetime Imaging Microscopy
Fmoc	Fluorenylmethoxycarbonyl
GDP	Gross Domestic Product
HIV	Human Immunodeficiency Viruses
HPLC	High-Performance Liquid Chromatography
HTH	Helix-turn-Helix
MIC	Minimal Inhibitory Concentration
MOA	Mode-of-Action
MRSA	Methicillin-resistant Staphylococcus aureus
MS	Mass Spectrometry
NBD	7-Nitro-2,1,3-Benzoxadiazol

NIR	Near Infrared
NMR	Nuclear Magnetic Resonance
NRPS	Non-Ribosomal Peptide Synthetase
PAH	Poly Aromatic Hydrocarbon
PCP	Peptidyl carrier protein
PEG	Polyethylene glycol
PS	Polystyrene
SAR	Structure-Activity-Relationship
SARS	Severe Acute Respiratory Syndrome
SPPS	Solid Phase Peptide Synthesis
Thico	Thiazolidine-containing
TR-FAIM	Time-Resolved Fluorescence Anisotropy Imaging
Trp	Tryptophan
UV	Ultraviolet
Vis	Visible

V. Abstract

Lugdunin is a novel antibiotic initially discovered in the human nose and extracted from *Staphylococcus lugdunensis*. It is a non-ribosomally synthesized cyclic peptide consisting of seven amino acids with alternating stereo-chemistry. The amino acids valine and cysteine are linked via an intramolecular thiazolidine formation. The cyclized peptide exhibits micromolar activity (3 µM) against Gram-positive bacteria such as methicillin-resistant *Staphylococcus aureus* as well as resistant *Enterococcus faecium*.

After fundamental stereo- and alanine-scan derivatives were synthesized, more extensive structure-activity-relationship (SAR) studies were carried out, replacing the amino acids at positions two, three and four. In total, hundreds of lugdunin derivatives were synthesized and evaluated, however only 6-tryptophan-lugdunin displayed higher antimicrobial activity in *in-vitro* assay Staphylococcus assays compared to natural lugdunin. In addition, the SAR-study aimed towards a fluorescent lugdunin proved to be successful with pyrenylalanine-lugdunin being highly active as well as fluorescent under excitation at 342 nm wavelength and emission at 375 nm wavelength.

A wide variety of lugdunin-derivatives from chemical synthesis, as well as more complex deviations from the natural compound, were synthesized and sets of compounds were evaluated for distinct applications. These tasks included, but are not limited to, assays for antibacterial activity (Gram-positive and Gram-negative), antiviral potency, membrane-permeation and ion exchange kinetics assays. Additionally, lugdunin and its derivatives were evaluated for their physicochemical character in solvents, concentrations and charge.

All in all, it is shown that lugdunin is a very potent compound with highly antibacterial activity across a wide range of derivatives. In addition to that, lugdunin also possesses antimicrobial activity against various viruses and bacteria. With two different synthetic routes available, a potential upscaling for industrial use as well as more strategic derivatization (e.g. focus on hydrophilicity or crystallization properties) is readily available. The available fluorescent derivatives (mg scale as pure compound) also enable more in-depth visualization experiments in order to fully elucidate the mode-of-action.

More complex structural deviations of lugdunin were also studied with interesting results, however more extensive research is needed in order to develop the next class of antibiotic in the combat against antimicrobial resistance.

VI. Zusammenfassung

Lugdunin ist ein neues Antibiotikum aus der menschlichen Nase, das aus *Staphylococcus lugdunensis* gewonnen wird. Es ist ein nicht-ribosomal synthetisiertes zyklisches Peptid, das aus sieben Aminosäuren mit einer alternierenden Stereochemie besteht. Die Aminosäuren Valin und Cystein sind über eine intramolekulare Thiazolidinbildung miteinander verbunden. Das zyklische Peptid weist eine mikromolare Aktivität (3 µM) gegen grampositive Bakterien wie Methicillin-resistenten *Staphylococcus aureus* sowie resistenten *Enterococcus faecium* auf. Nach der Synthese grundlegender Stereo- und Alanin-Scan-Derivate wurden umfangreichere Struktur-Aktivitäts-Beziehungen (SAR) untersucht, wobei die Aminosäuren an den Positionen zwei, drei und vier ersetzt wurden. Insgesamt wurden Hunderte von Lugdunin-Derivaten synthetisiert und bewertet, wobei nur 6-Tryptophan-Lugdunin im Vergleich zu natürlichem Lugdunin eine höhere antimikrobielle Aktivität in In-vitro-Tests mit Staphylococcus zeigte. Darüber hinaus erwies sich die SAR-Studie, die auf ein fluoreszierendes Lugdunin abzielte, als erfolgreich, wobei das Pyrenylalanin-Lugdunin sowohl hochaktiv als auch fluoreszierend bei einer Anregungswellenlänge von 342 nm und einer Emissionswellenlänge von 375 nm war. Es wurde eine breite Palette von Lugdunin-Derivaten aus chemischer Synthese sowie komplexere Abweichungen von der natürlichen Verbindung synthetisiert und eine Reihe von Verbindungen für verschiedene Anwendungen hergestellt. Zu diesen Aufgaben gehörten unter anderem Tests zur antibakteriellen Aktivität (Gram-positiv und Gram-negativ), zur antiviralen Potenz, zur Membranpermeation und zur Ionenaustauschkinetik. Außerdem wurden Lugdunin und seine Derivate auf ihre physikochemischen Eigenschaften in verschiedenen Lösungsmitteln, Konzentrationen und Ladungen untersucht. Alles in allem zeigt sich, dass Lugdunin eine sehr potente Verbindung mit hoher antibakterieller Aktivität in einem breiten Spektrum von Derivaten ist. Darüber hinaus besitzt Lugdunin auch eine antimikrobielle Aktivität gegen verschiedene Viren und Bakterien. Da zwei verschiedene Synthesewege zur Verfügung stehen, ist ein potenzielles Upscaling für die industrielle Nutzung sowie eine strategischere Derivatisierung (z. B. mit Fokus auf Hydrophilie oder Kristallisationseigenschaften) ohne weiteres möglich. Die verfügbaren fluoreszierenden Derivate (im mg-Maßstab als reine Verbindung) ermöglichen eingehendere Visualisierungsexperimente, um die Wirkungsweise vollständig aufzuklären. Auch komplexere Strukturabweichungen von Lugdunin wurden mit interessanten Ergebnissen untersucht, doch sind noch umfangreichere Forschungsarbeiten erforderlich, um die nächste Klasse von Antibiotika im Kampf gegen die antimikrobielle Resistenz zu entwickeln.

VII. Scientific Publications

Declaration according to § 5 Abs. 2 No. 8 of the PhD regulations of the Faculty of Science of the Eberhard Karls University Tübingen

All publications are displayed in the appendix. Journal entries are also displayed with their corresponding supporting information. Publications are also accessible via the provided link online.

Collaborative Publications

Last Name, First Name(s): Wirtz, Sebastian Niklas

List of Peer Reviewed Publications

Paper 1 Synthetic Lugdunin Analogues Reveal Essential Structural Motifs for Antimicrobial Action and Proton Translocation Capability
Dr. Nadine A. Schilling, Dr. Anne Berscheid, Johannes Schumacher, Julian S. Saur, Dr. Martin C. Konnerth, **Sebastian N. Wirtz**, José M. Beltrán-Beleña, Dr. Alexander Zipperer, Dr. Bernhard Krismer, Prof. Andreas Peschel, Dr. Hubert Kalbacher, Prof. Heike Brötz-Oesterhelt, Prof. Claudia Steinem, Prof. Stephanie Grond
Angew. Chem. Int. Ed. **2019**, *58*, 9234-9238
https://doi.org/10.1002/anie.201901589
Angew. Chem. **2019**, *131*, 9333
https://doi.org/10.1002/ange.201901589

Paper 2 Secretion of and Self-Resistance to the Novel Fibupeptide Antimicrobial Lugdunin by Distinct ABC Transporters in Staphylococcus lugdunensis
Sophia Krauss, Dr. Alexander Zipperer, **Sebastian N. Wirtz**, Julian Saur, Dr. Martin C. Konnerth, Dr. Simon Heilbronner, Benjamin O. Torres Salazar, Prof. Stephanie Grond, Dr. Bernhard Krismer, Prof. Andreas Peschel
Antimicrob, Agents and Chemother, **2020**, *65*, e01734-20
https://doi.org/10.1128/AAC.01734-20

Paper 3 Distinct Lugdunins from a New Efficient Synthesis and Broad Exploitation of Its MRSA-Antimicrobial Structure
Julian S. Saur, **Sebastian N. Wirtz**, Nadine A. Schilling, Dr. Bernhard Krismer, Prof. Andreas Peschel, Prof. Stephanie Grond
J. Med. Chem. **2021**, *64*, 7, 4034-4058
https://doi.org/10.1021/acs.jmedchem.0c02170

Published Patents

Patent 1 Novel cyclic compounds, method for their preparation and their use in cosmetic compositions
Sebastian N. Wirtz, Julian S. Saur, Prof. Stephanie Grond, Dr. Bernhard Krismer
EP4001296 (A1), WO2022106667 (A1), filed on 20.11.2020, published on 25.05.2022

Unpublished Peer Reviewed Publications

Paper 4 Development of fluorescent derivatives as tools to validate the in vivo mode of action of the antibiotic lugdunin
Sebastian N. Wirtz, Dominik Ruppelt, Dr. Martin Meixner, Prof. Carolin Huhn, Prof. Claudia Steinem, Prof. Stephanie Grond
Manuscript not yet published

Paper 5 Unveiling the mode of action: The antimicrobial fibupeptide lugdunin forms water-filled channel structures in lipid membranes
Dominik Ruppelt, Taulant Dema, **Sebastian N. Wirtz**, Hendrik Flegel, Sophia Mönnikes, Prof. Stephanie Grond, Prof. Claudia Steinem
Manuscript not yet published

Personal Contribution

Personal Contribution to Peer Reviewed Publications

Paper 1 I synthesized compounds for the alanine scan and performed one- and two-dimensional NMR spectroscopic analysis. I also performed mass spectrometric analysis for liquid chromatography and MSMS fragmentation as well as edited the manuscript. All compounds were synthesized on multi-mg scale in purities over 90%.

Paper 2 I synthesized lugdunin, 6-tryptophan-lugdunin as well as 4-alanine-lugdunin and performed one- and two-dimensional NMR spectroscopic analysis. I also performed mass spectrometric analysis for liquid chromatography and MSMS fragmentation as well as edited the manuscript. All compounds were synthesized on multi-mg scale in purities over 90%.

Paper 3 I designed and synthesized various compounds and performed one- and two-dimensional NMR spectroscopic analysis. I also performed mass spectrometric analysis for liquid chromatography and MSMS fragmentation. All compounds were synthesized on multi-mg scale in purities over 90%.

Personal Contribution to Published Patents

Patent 1 All compounds were planned, synthesized and analyzed by myself. Analyses include, but are not limited to one- and two-dimensional NMR spectroscopic methods, UV/Vis spectroscopic methods as well as mass spectrometric methods. Bioactivity assays against *S. aureus* were performed by Dr. Bernhard Krismer. The manuscript was written in collaboration with Julian S. Saur.

Personal Contribution to Unpublished Peer Reviewed Publications

Paper 4 All 15 compounds were planned, synthesized and analyzed by myself. Analysis include, but are not limited to one- and two-dimensional NMR spectroscopic methods, UV/Vis spectroscopic methods as well as mass spectrometric methods. Bioactivity assays against *S. aureus* were performed by Dr. Bernhard Krismer. The manuscript was also written by me. All compounds were synthesized on multi-mg scale in purities over 95%.

Paper 5 I synthesized lugdunin as well as 6-tryptophan-lugdunin as well as performed one- and two-dimensional NMR. I also performed mass spectrometric analysis for liquid chromatography and MSMS fragmentation as well as edited the manuscript. All compounds were synthesized on multi-mg scale in purities over 90%.

VIII. Aim of this Thesis

The main objective of this thesis is to study lugdunin as a novel antibiotic, to optimize the structure for fluorescence microscopy, reduced resistance towards natural transporter genes and improved synthetic properties.

The Introduction offers a short overview about the evolution of resistant bacteria and the relevance to humanity with a focus on ESKAPE pathogens. Additionally, an insight into the development of current antibiotics is provided, detailing the state of the art of lugdunin research prior to the work that is part of this dissertation. Finally, fluorescence microscopy is briefly described.

In Results and Discussion, the main results of previously published articles are summarized. Afterwards, the emphasis is put on unpublished results, especially concerning the pyrene-containing derivatives and the usage thereof for fluorescence microscopy.

Conclusion and Outlook will combine unpublished and published results and utilize the gained information about lugdunin in order to give an outlook into the future use of and possible research into lugdunin derivatives.

The Appendix is a compilation of publications.

1 Introduction

Historic evolution of antibiotics

When Fleming discovered Penicillin (**1**) in 1928[1], he revolutionized medicine and laid the foundation of many of the greatest medical advances of the 20th century[2]. In the following years, some of the most important antimicrobial compounds were discovered such as sulfonamides, β-lactams, polyketides and glycopeptides resulting in a remarkable downturn of the mortality rate associated with bacterial infections[3]. While these discoveries drastically changed the ability to treat infectious diseases, the rapid availability of a wide variety of antimicrobials also led to a strong decrease in research of new antimicrobials. One of the most remarkable citations describing this period in medicinal research came from US Surgeon General William H Stewart saying that it was time to "close the book on infectious diseases" due to the success of vaccines and antibiotics in 1967[4]. This resulted in the last innovative class of antibiotics being discovered in the late 1980s with carbapenem (**2**)[5] and fluoroquinolone (**3**)[6], both already less relevant due to existing resistant bacteria[7-8].

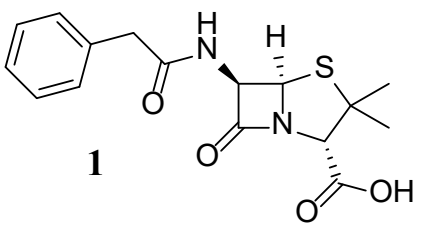

1

Figure 1: Chemical structure of penicillin G (1)

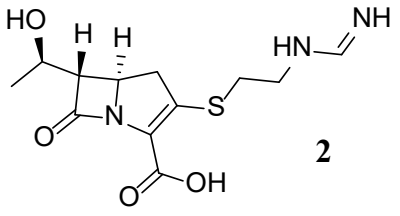

2

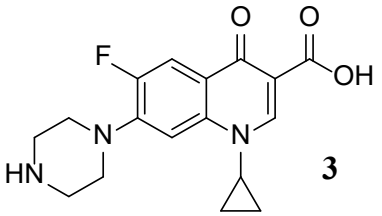

3

Figure 2: Chemical structures of imipenem 2 as the first clinically used carbapenem and ciprofloxacin 3 as a second-generation quinolone antibiotic

This unfortunate lack of research into novel antibiotic systems has continued until today, and it is not expected to improve in the near future. One of the drivers thereof is the excessive health care cost estimated at around US$ 1.5 billion[9-10]. With an estimated revenue generated from antibiotic sales of around US$ 46 million per year, large pharmaceutical corporations have already dropped antibiotic research from their portfolio such as Novartis in Basel, Sanofi in Paris and AstraZeneca in Cambridge[11].

While this reduced amount of novel antimicrobial compounds from industry research is already an alarming state, the vastly growing demand for antibiotics is a different aspect of the current struggles with infectious diseases. Global consumption of antibiotics in human medicine rose by nearly 40% between 2000 and 2010 but this figure

masks patterns of declining usage in some countries and rapid growth in others[12]. The BRIC (Brazil, Russia, India and China) countries plus South Africa accounted for three quarters of this growth, while annual per-person consumption of antibiotics varies by more than a factor of ten across all middle and high-income countries[2, 12]. The strong increase in antibiotic consumption is also predicted to further accelerate, with an estimated growth in consumption of up to 200% from 2015 to 2030[13].

In addition to the total amount of antibiotics consumed, particularly concerning is the type of antibiotics that are being used, with a strong increase in so-called last-resort compounds such as the previously mentioned carbapenems[13]. These, typically broad spectrum antibiotics, are often used when the pathogen has not (yet) been identified[14]. This results in a calculated, unsighted initial therapy in contrast to targeted antibiotic therapy based on available lab diagnostics on the pathogen and known *in vitro* resistance[15]. As a result, in recent years untreatable strains of carbapenem-resistant *Enterobacteriaceae* paved the way into a so-called postantibiotic era[16-17]. This led to the ESKAPE-pathogens (*Enterococcus faecium, Staphylococcus aureus, Klebsiella pneumoniae, Acinetobacter baumannii, Pseudomonas aeruginosa* and *Enterobacter*), capable of "escaping" the biocidal action of antibiotics[18], becoming even more challenging as multidrug resistant (MDR) and extensively drug resistant (XDR) bacteria[19-24]. While resistant strains were detected even before penicillin was introduced[25], highly dangerous, resistant clones such as methicillin-resistant *Staphylococcus aureus* (MRSA) USA300, *Escherichia coli* ST131, and *Klebsiella* ST258 are disseminated rapidly worldwide[16, 26]. Possible spread mechanisms include, but are not limited to, interspecies gene transmission, poor sanitation and hygiene in communities and hospitals as well as the increasing frequency of global travel,

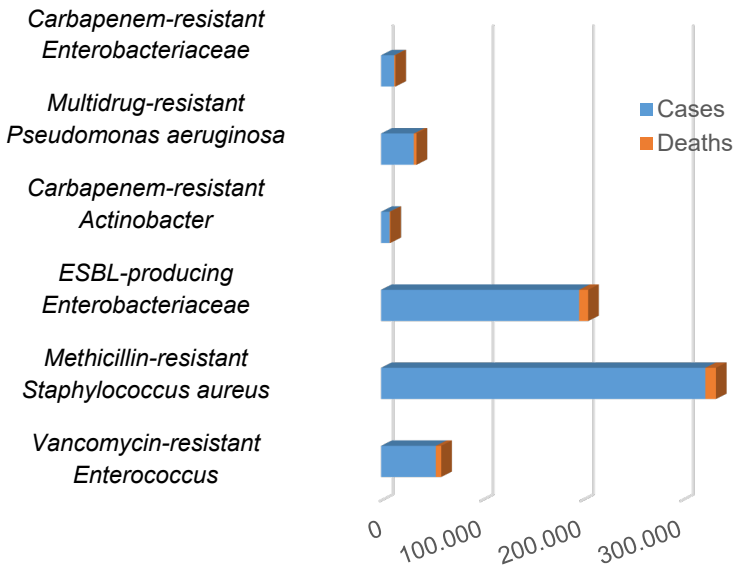

Figure 3: Cases of ESKAPE-pathogens in the USA in 2019. ESBL-producing Enterobacteriaceae include Escherichia coli and Klebsiella pneumoniae. Numbers reported by the CDC[24]

trade and disease transmission[16]. As an example, the evolution of MRSA, which is currently one of the most potent antibiotic-resistant strains, was highly impacted by a health-care associated MRSA epidemic in England in the 1980s. Shortly after the strain EMRSA-15 was reported in England, similar outbreaks occurred in Germany, the Czech Republic, Portugal, New Zeeland, Australia and Singapore[27]. While bacteria are able to adopt resistance genes from other bacteria, the type of resistance can also differ. Bacteria can be resistant to the antibiotic agent because the drug fails to reach its target, the drug is inactivated, the drug target is altered or there is acquisition of a target bypass system[28].

To put this development in a current perspective, in 2019 more than 1.27 million people died due to bacterial antimicrobial resistance (AMR) and an estimated 4.95 million deaths worldwide were associated (infection not the sole cause of death) with bacterial AMR[29]. This is more than the combined amount of deaths from HIV/AIDS (680,000 in 2020)[30] and Malaria (409,000 in 2019)[31].

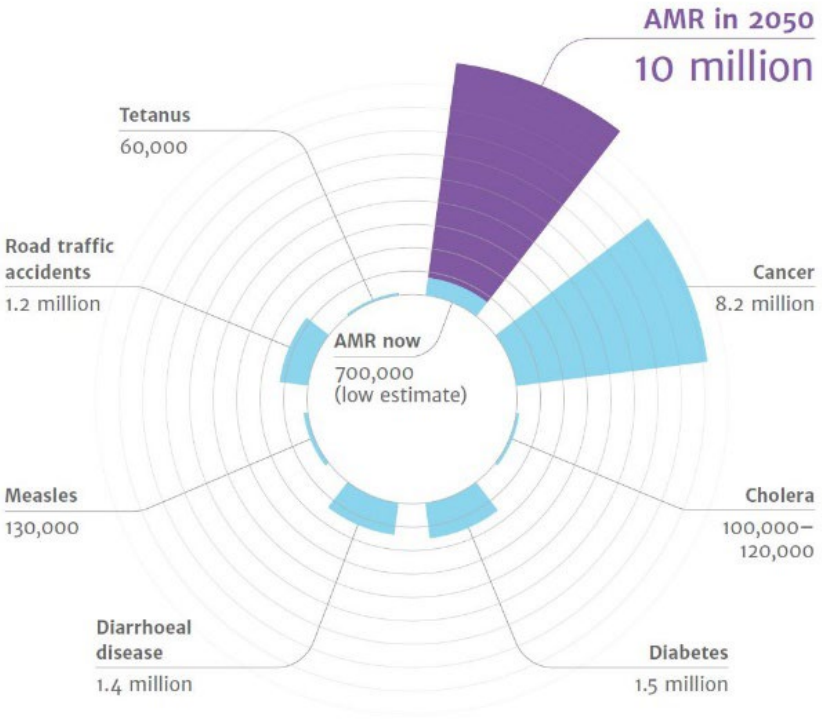

Figure 4: Deaths attributable to AMR every year from 2050 going forward, as displayed by O'Neill [32]

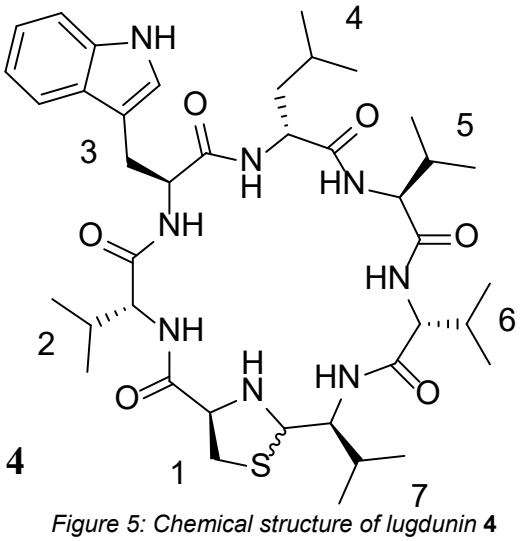

*Figure 5: Chemical structure of lugdunin **4** with highlighted amino acid positions*

The Review on Antimicrobial Resistance also argued that AMR could kill 10 million people per year in 2050, more than currently die from cancer[32], and cost as much as US$ 100 trillion per year in GDP (gross domestic product)[2, 32]. This dra-

matic evolution can only be stopped by extended research on antibiotic resistance and more fundamentally on novel antibiotic compounds.

Novel antibiotic from the human nose

One of these novel antibiotic compounds is lugdunin **4**. This new, thiazolidine-containing cyclic peptide is bactericidal against major gram-positive pathogens with low micro-molar activity against MRSA and vancomycin-resistant *Enterococcus faecium*[33]. **4** was the first antibiotic discovered in the human nose and defined a new class of cyclic peptide through its structural properties. **4** is a cyclic heptapeptide NRPS-product with an unusual reductase. This results in the formation of an aldehyde and thus enabling the cyclisation into a thiazolidine ring[33]. In addition to its antimicrobial activity, **4** also increases expression and release of LL-37 (human, antimicrobial peptide) and CXCL8/MIP-2 (macrophage inflammatory protein) in human keratinocytes[34]. Surprisingly, lugdunin also acts synergistic with LL-37 and dermcidin-derived peptides[34], further highlighting the potential for an MRSA-treatment with this novel compound. We have also previously carried out structure-activity-relationship (SAR) studies[35-36]. First, a basic stereo scan was performed, where each amino acid was replaced by its analogue with an inverted stereo-center at the side chain, thus demonstrating that the alternating D-L-amino acid backbone is crucial to activity[36]. Afterwards, an alanine scan was performed. During this, each amino acid was replaced by alanine in order to display the effect of the respective side chain on the compound's activity[36]. This resulted in the discovery of 6-tryptophan-lugdunin **5**, being the only known derivative with a higher antimicrobial activity than natural lugdunin (1.6 µM against MRSA)[36]. Additionally, non-proteinogenic amino acids were evaluated for activity in lugdunin **4** with a

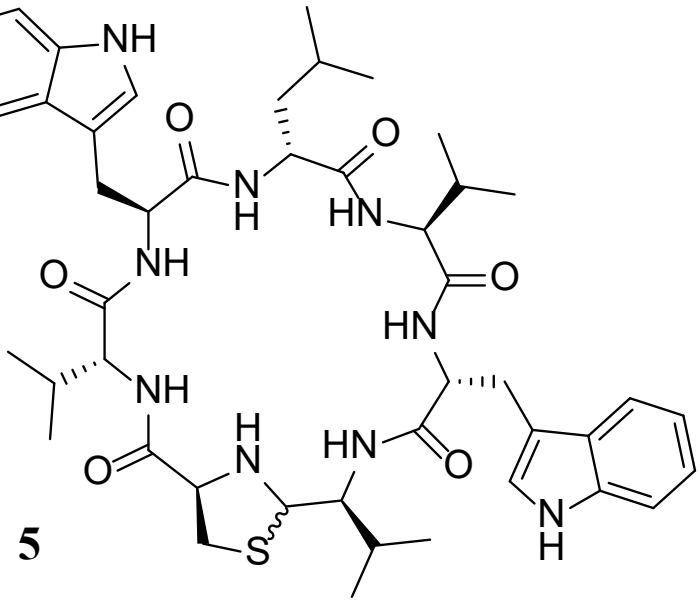

*Figure 6: Chemical structure of 6-tryptophan-lugdunin **5***

set of different amino acids alkyl branching as well as unsaturated residues were tested in exchange for valine (at position two, five and six) and leucin (at position 4)[35].

Furthermore, we studied various (hetero-) aromatic amino acids in place of tryptophan (at position three), however no improvement in bioactivity over the natural compound was possible[35]. Another aspect has been the ABC transporters in lugdunin-producing *Staphylococcus lugdunensis* in collaboration with the Peschel group. It was shown that natural resistance mechanisms from *S. lugdunensis* were highly selective, further promoting lugdunin **4** as a new antibiotic without cross-resistance to other antimicrobials or to optimized lugdunin derivatives (selectivity data shown in collaborative publication by Krauss *et. al*)[37].

Hypothetical Mode-of-Action of lugdunin

In order to further advance the research on lugdunin, we aimed at an insight into the mode-of-action (MOA) of lugdunin. As previously shown, **4** is capable of equalizing pH gradients in artificial membrane vesicles without disrupting the membrane integrity[36]. We therefore propose two possibilities for proton translocation via lugdunin.

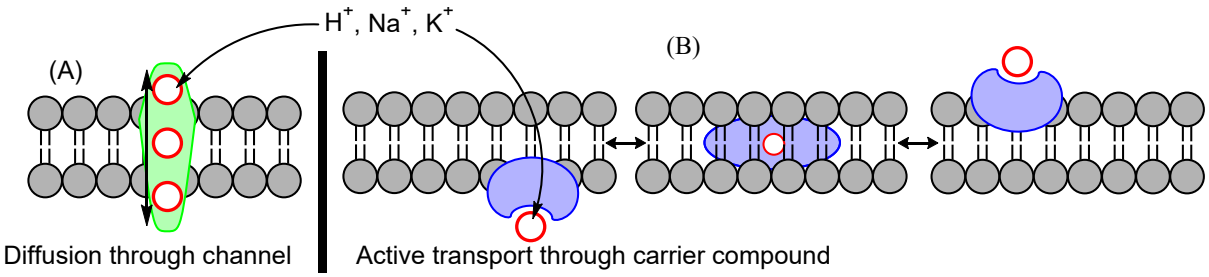

*Figure 7: Possible proton translocation mechanisms from lugdunin **4**. Red indicates proton, sodium or potassium cations, green indicates potential channel of lugdunin molecules (type A) and blue indicates lugdunin acting as cation carrier (type B)*

The first proposed mechanism is the formation of pore-like substructures made from lugdunin molecules (see Figure 7, (A)). In this theory, multiple lugdunin molecules arrange themselves via intermolecular hydrogen bonds in such a three-dimensional structure (see Figure 8), that positively charged cations are able to translocate. This second theory has previously been published by Ghadiri *et al.* for various other cyclopeptides with eight or ten amino acids, also containing an alternating stereo configuration[38-39]. These compounds participate in backbone-backbone intermolecular hydrogen bonding to produce a contiguous β-sheet structure, causing the amino acid side

chains to lie on the outside of the structure[38, 40]. The newly formed channels display good channel-mediated ion-transport activity with rates rivalling the performance of naturally occurring counterparts[41].

The second proposed mechanism is proton translocation via a carrier (see Figure 7, (B)). Considering the inactivity of *N*-methylated thiazolidine-lugdunin (MIC >100 µM against MRSA), it is possible that the secondary amine of the thiazolidine binds to a proton, traverses the membrane and releases the proton on the other side of the membrane, thus equalizing the membrane potential. This possibility was previously calculated in-house and the postulated change in three-dimensional structure of lugdunin, whether protonated or not, does support this theory. It was shown, that **4** should be able to trap a cation and act as a barrier to the membrane. However, we have not yet been able to ultimately confirm or deny lugdunin **4** as a proton carrier.

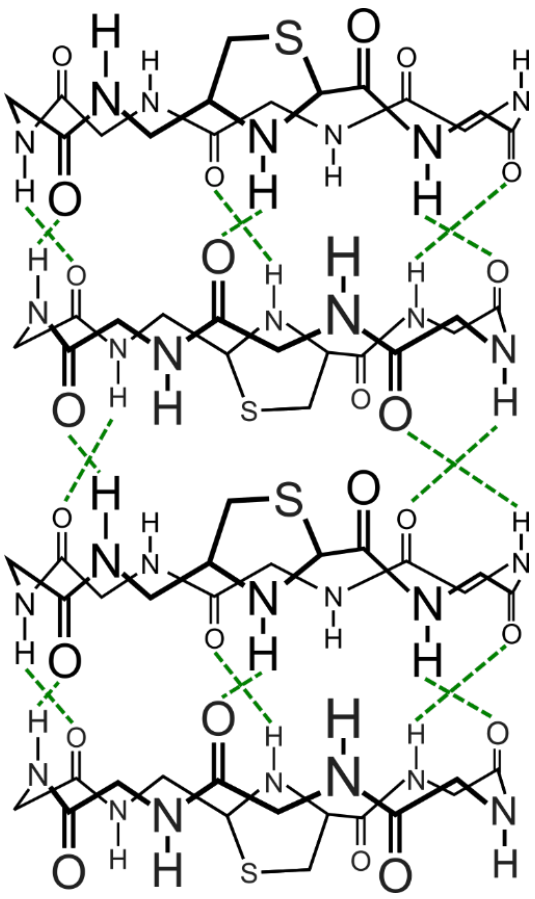

*Figure 8: Possible arrangement of lugdunin **4** in a channel-like three-dimensional shape inside the membrane. Dashed lines propose hydrogen bonds. Amino acid side chains are not shown for clarity*

Particularly interesting is the amino acid sequence used by Ghadiri[41]. Comparable to lugdunin **4**, a cyclic peptide consisting of L-tryptophan and D-leucin showed similar, if not higher activity than gramicidin A and amphotericin B[41]. Additionally, these cyclic peptides are able to transport sodium and potassium cations[42], comparable to lugdunin. Another similarity is the inactivity of both *N*-methylated lugdunin derivatives as well as *N*-methylated cyclic peptide cyclo[(-L-Phe-D-*N*-MeAla-)$_4$-][43]. As a result, potentially through these structural similarities, six and eight-membered D,L-α-peptides act preferentially on Gram-positive and/or Gram-negative bacterial cell membranes, increase membrane permeability and collapse transmembrane ion potentials, resulting in rapid cell death[44]. These intermolecular assemblies are increasingly interesting, as the potential proximity of individual peptides can be used to differentiate between the two proposed MOAs.

Fluorescent spectroscopy of biological systems

One type of spectroscopy that can be used to detect lugdunin in bacteria, and therefrom gain insight in the MOA of lugdunin, is fluorescence microscopy. This type of microscopy has been found to be an ideal technique for the examination of all biological specimens, due to the good signal-to-noise ratio at low concentrations[45-47] but still high resolution[48-49]. These properties make optical microscopy one of the most powerful and versatile diagnostic tools in modern cell biology[50]. In particular the combination of confocal scanning microscopy, which restricts photodetection to the focal point, with the ability to reject out-of-focus light results in only a very small amount of emitted photons being detected[45]. Therefore, fluorescence microscopy is highly interesting when researching living cells, since the required fixation for other spectroscopy methods does not give a clear image of the living sample[51]. Two specific types of fluorescence microscopy are fluorescence lifetime imaging (FLIM) as well as time-resolved fluorescence anisotropy imaging (TR-FAIM)[52]. Both methods are time-dependent and provide additional information compared to standard fluorescence microscopy. In the case of FLIM, it is possible to detect the fluorescence decay as a function of its environment. Therefore, this method can potentially assist in understanding intercellular compartments[52-53].

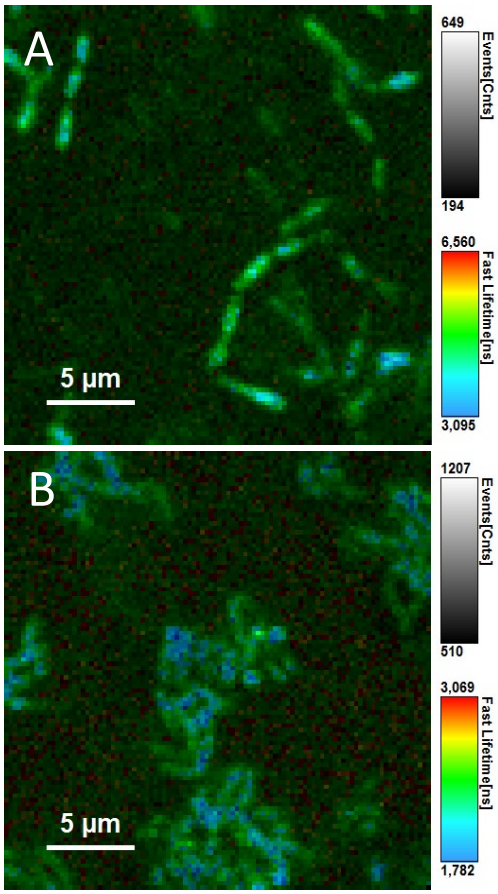

Figure 9: Fluorescent microscopy images of Bacillus subtilis (A) and Bacillus megaterium (B)

In the case of lugdunin **4**, the environmental change (for example the pH) between the outside of a bacterial cell, the membrane and the inside of a cell could lead to a noticeable change in fluorescence decay of the fluorophore[54]. A similar approach can be carried out via TR-FAIM. In this case, the fluorescence decay is measured through the correlation of polarization-resolved fluorescence decays $I_{\parallel}$ and $I_{\perp}$. Due to the environmental impact on the depolarization, effects such as pH, molecular size and viscos-

ity[52, 55-56], TR-FAIM is also a promising approach for visualizing lugdunin **4** in live bacteria. Equally dependent on its environment are the fluorophores required for fluorescence microscopy[57-58].

As mentioned above, the image quality heavily relies on the amount of photons that reach the detector[59], which is strongly influenced by the fluorophore's extinction coefficient, stokes-shift and quantum yield[57]. This is especially important due to the negative impact of phototoxicity in live cell imaging resulting from strong excitation light[60]. Unfortunately, most commonly used fluorophores have their absorption and emission maximums in the ultraviolet (UV) light range[61]. Light in this range is very well absorbed in (bio)molecules such as water, lipids and hemoglobin[62]. As a result, the sample's auto-fluorescence can have a strong impact in signal-to-noise ratios via scattering and absorption[61, 63].

Fluorescent probes

More suitable are fluorescent probes with absorption and emission values in the near infrared (NIR) region of 650-900 nm. In this range, phototoxicity is highly reduced, with deep tissue penetration and low autofluorescence by biomolecules[64-67]. Suitable fluorophores in this range can be seen in Figure 10, however, the relevance for lugdunin studies is questionable. These modern compounds achieve NIR absorption wavelengths through large π-systems (absorption: 536 nm, emission: 733 nm, measured in aqueous buffer with 1% DMSO, see Figure 10

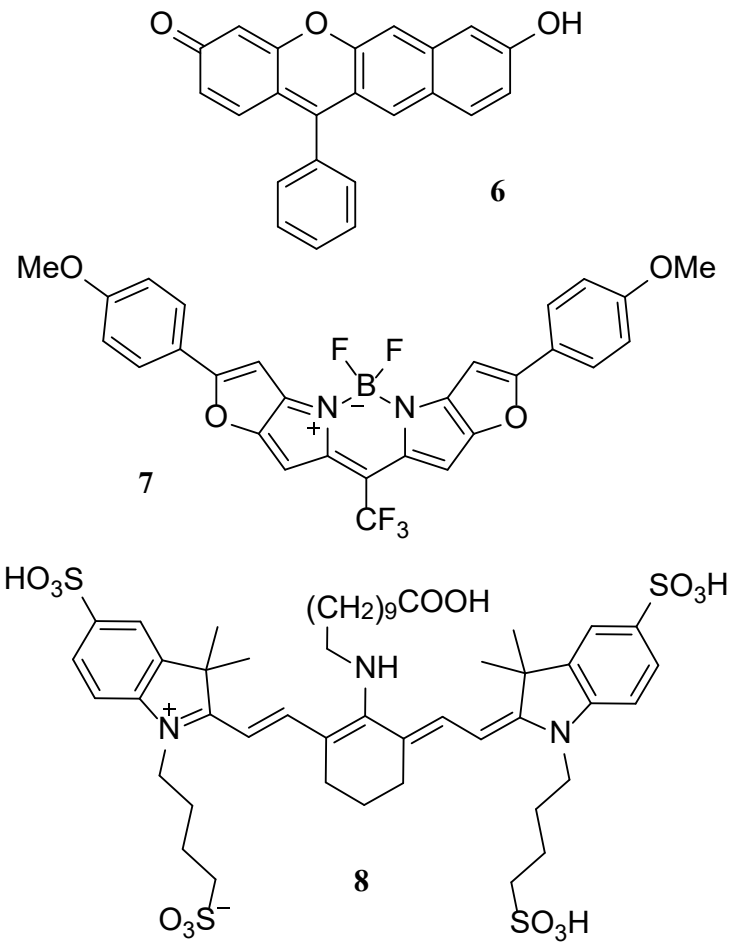

Figure 10: Commonly used fluorophores with NIR absorption and emission wavelengths

6)[68], delocalized charges (absorption: 723 nm, emission: 738 nm, measured in chloroform, see Figure 10 **7**)[69-70] or large hydrophilic anchors (absorption: ~620 nm, emission: 760 nm, see Figure 10 **8**)[71] for necessary solubility improvements. Due to the rather small size of lugdunin, we have previously tested small fluorophores that are able to connect via an amino acid functionality.

These fluorophores include, 4-dimethylaminophthalimide (4-DMAP, **11**), 6-dimethylaminonaphthalimide (6-DMN, **12**), 4-Chloro-7-nitrobenzo-2-oxa-1,3-diazole (NBD, **13**) and Azulene (**14**) as well as commercially available click-fluorophores such as BODIPY®-FL-azid (**9**) and Cyanin-3.5-azid (**10**) as shown in Figure 11.

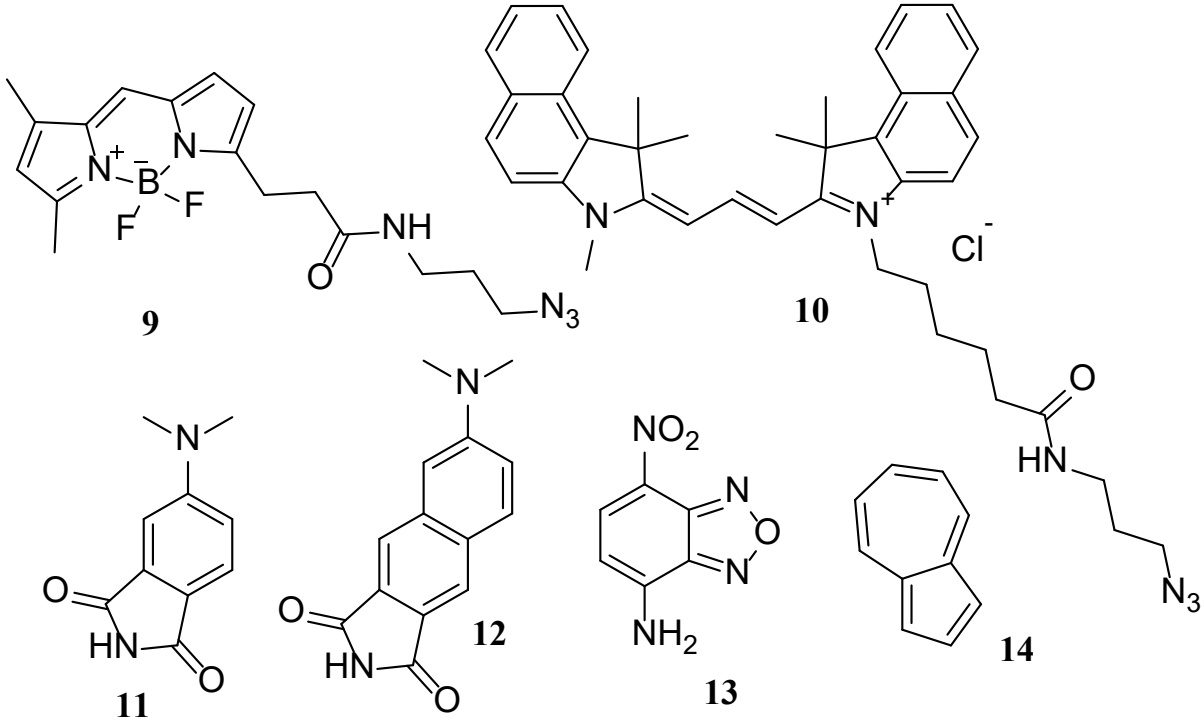

Figure 11: Previously used fluorophores in lugdunin (4)

Unfortunately, all these moieties, except for **14**, have previously been show to render lugdunin inactive in antimicrobial *in-vitro* assays and thus are not suitable for live imaging due to the incompatibility to natural lugdunin[72]. While Azulene-lugdunin did result in a highly active antimicrobial[73], the fluorescence properties were not suitable for fluorescence microscopy. Since even the small 4-DMAP **11** resulted in an inactive lugdunin, we focused on a fluorophore that is similar in size to **11**, but does not bear any heteroatoms such as **9**.

Pyrene as fluorophore

Pyrene-related molecules, more specific *N*-α-(9-Fluorenylmethoxycarbonyl)-3-(1-pyrenyl)-alanine **15** (see Figure 12), are highly promising with a larger π-system than **14**, have no large connective alkyl chain such as **10**, and no heteroatoms such as **13**. Pyrene has been thoroughly studied with regards to optical properties and was used as fluorescent probe par excellence[74]. While it has been shown that pyrene monomers do not associate regardless of concentration[75], it is possible for pyrene molecules to form excimers (special excited dimers)[76].

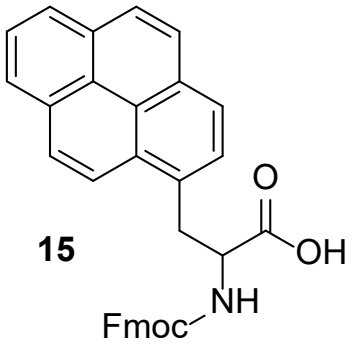

*Figure 12: Fmoc-(1-Pyrenyl)-Ala-OH (**15**)*

An excimer differs from an excited dimer in four aspects. The first aspect is the ground state, which is dissociated in excimers and stable at room temperature in excited dimers. Secondary dimerization aspects follow the act of light absorption in excimers and precedes the act of light absorption in excited dimers. The third aspect is the radiative relaxation, which is forbidden in excimers and allowed in excited dimers. The last aspect is the corresponding absorption, which is not observed in excimers and increases with concentration in excited dimers.[75]

Excimers feature an ultraviolet emission band with vibrational structure and more interestingly a broader, less structured, blue emission band with a Stokes-shift of 115 nm in cyclohexane[77-79]. With regards to the proposed mechanism of stacked lugdunins forming pores, the excimer fluorescence could be especially interesting[80-82]. In addition to excimers, the fluorescence of pyrene monomers is also solvent dependent and the pyrene 3/1 ratio (the relative intensity of peak 3 to peak 1 in the fluorescence vibrational fine structure) provides insights on the close environment of the compound[83-86].

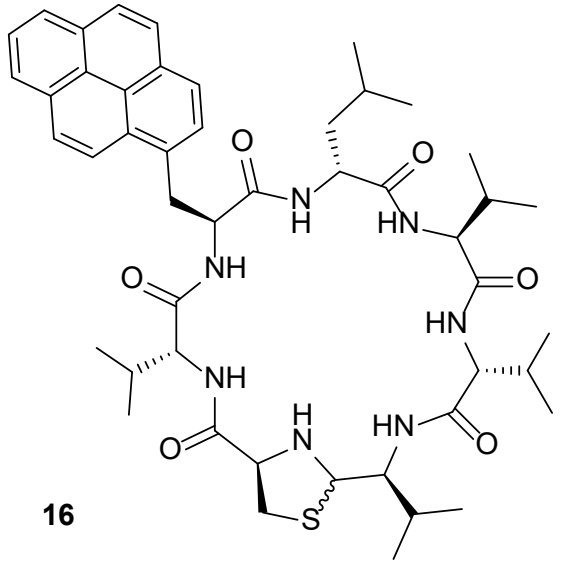

*Figure 13: Chemical structure of 3-Pyrenylalanine-lugdunin (**16**)*

As a result, we combined the promising pyrene fluorophore with our previously acquired expertise in order to gain as much insight into the MOA of lugdunin as possible.

2 Results and Discussion

2.1 Solid phase peptide synthesis to implement SAR lugdunin

This part corresponds to my first publication by Schilling *et al.* and the goal was to establish a general understanding in lugdunin's natural structure and to generate first derivatives to this compound.

The previously published antimicrobial lugdunin has already shown high potential against MRSA in Zipperer *et al.*'s Nature publication[33]. However, in order to gain further insight into a novel compound, the understanding of a compound's MOA is essential. With peptides, more specific cyclic peptides, such as lugdunin **4**, one of the most direct approaches is to understand the function of the amino acid side chains. In order to synthesize these peptides, we used two established solid-phase-peptide-synthesis (SPPS) approaches. SPPS has been developed by Merrifield, who published his method in the1960s[87-88]. In our case, we first used a less common H-Val-H NovaSyn® TG resin, shown in Figure 14, as this resin enabled to synthesis of a peptide aldehyde, similar to the biological way of synthesis.

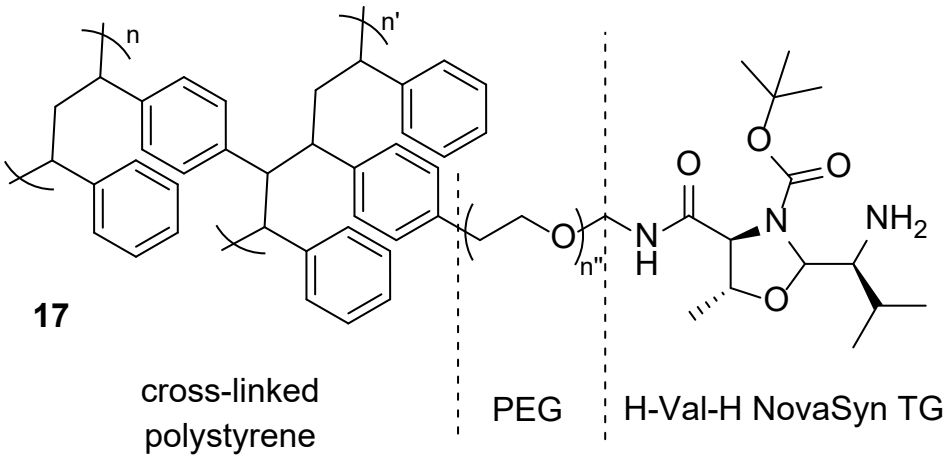

*Figure 14: Chemical Structure of the H-Val-H NovaSyn TG resin from Novabiochem® **17***

The resin consists of a polystyrene (PS) matrix with divinylbenzene (DVB) allowing for a lightly cross-linked polymer. Due to the hydrophobic PS matrix, a polyethylene glycol (PEG) spacer is immobilized onto the PS via graft copolymerization with a PEG content of up to 70%[89]. As a result, the PEG chains dominate the properties of the resin, allowing for better swelling properties when compared to a basic hydrophobic PS matrix. The PEG chain is then connected to the H-Val-H NovaSyn TG® linker, consisting

of a threonine residue with pre-loaded valinal. When cleaved from the resin, the aldehyde can undergo spontaneous cyclisation with the terminal cysteine via thiazolidine ring formation. This enables quick access to a wide variety of peptides since almost all lugdunin derivatives require the thiazolidine ring. Unfortunately, this resin also limits the variability of different lugdunin structures in the synthesis due to the given valine adjacent to the cysteine. While it is possible to synthesize the resin according to specific needs, this proved to be not very time and cost efficient and this resin was only used for basic peptide SAR studies. Therefore, we first started with alanine and stereo scans, published by Schilling *et al.* in 2019[36]. This resulted in 14 different peptides (shown in the appendix), whereas only a selected few were antimicrobially active at all. These active compounds had in common that they had alternating stereo chemistry as well as the aromatic amino acid tryptophan and the aliphatic amino acid leucin. This led us to believe that these are the crucial aspects for bioactivity.

Then, as the last unknown structural aspect of natural lugdunin **4**, we turned our attention to the thiazolidine moiety. The corresponding peptides included linear lugdunin, homodetic lugdunin, methylated and acetylated thiazolidine-lugdunin as well as the homocysteine analogue. This derivatization only resulted in non-active compounds, demonstrating the indispensability of the natural thiazolidine-ring. These experiments were mostly carried out using an aldehyde-generating resin that was commercially available. While this approach was suitable for the initial studies, a larger scale synthesis was necessary for advanced SAR studies[36].

Exploration of a regular resin

Trying to improve the synthesis, while also scaling it up, we focused on multiple aspects[35]. First the resin was not ideal, as the cleavage resulted in isomerization at the α-carbon of the amino acid on the resin due to the aldehyde. Thus, the final product

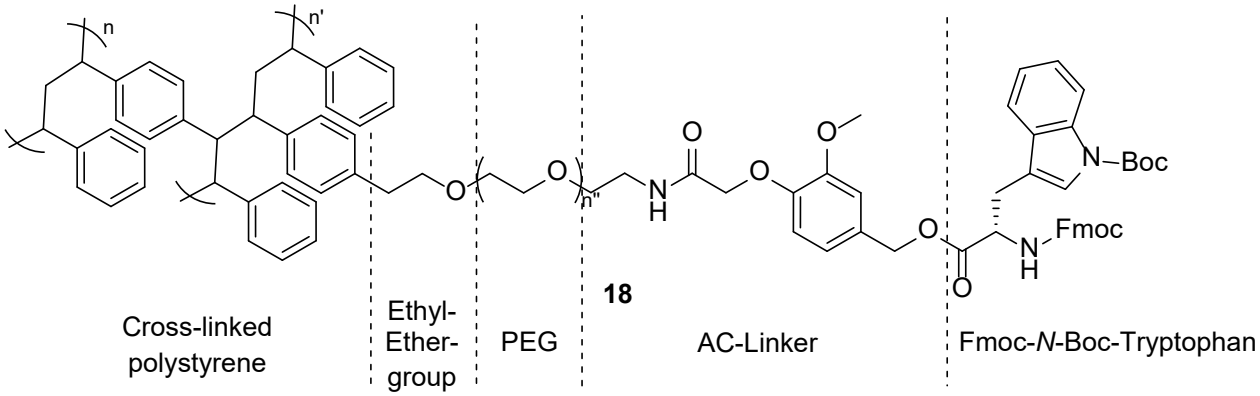

*Figure 15: Chemical structure of Fmoc Trp(Boc) TentaGel® S AC resin **18***

lacked purity and with the great number of different lugdunin-derivatives, individual purification became very complex. Additionally, the aldehyde-generating resin resulted in truncation sequences, lowering the yields. To overcome these challenges, a commercially available Fmoc Trp(Boc) TentaGel® S AC resin was used (see Figure 15).

While this resin is also based on a lightly cross-linked PS matrix with DVB and a PEG spacer, the linker is drastically different. This resulted in a purely acid labile resin, compared to the previous one where the peptide got cleaved off via the water labile oxazolidine ring. This new resin also allowed for more flexibility during the synthesis as all proteinogenic amino acids were commercially available as pre-loaded onto the resin, independently from the stereo center.

We thank the Peschel Group as well as the Krismer Group for their cooperation and for providing antimicrobial activity assays.

2.2 Improved synthesis enables deepened SAR of lugdunin

This part corresponds to my second publication by Saur *et al.* and the goal was to provide a secondary synthesis route as well as provide more diverse derivatives for a more comprehensive SAR study.

This new approach required the additional synthesis of the thiazolidine amino acid beforehand. This was realized starting from basic Fmoc-valine that was reduced to the corresponding amino alcohol via sodium borohydrate ($NaBH_4$) and carbonyl diimidazole (CDI). Afterwards, the alcohol was reoxidized to the amino aldehyde via Dess-Martin periodinane (DMP). The final step was, similar to the previous synthesis, the condensation of the amino aldehyde with cysteine, providing the product in good yields and purity, see Figure 16 and the corresponding publication in the appendix[35].

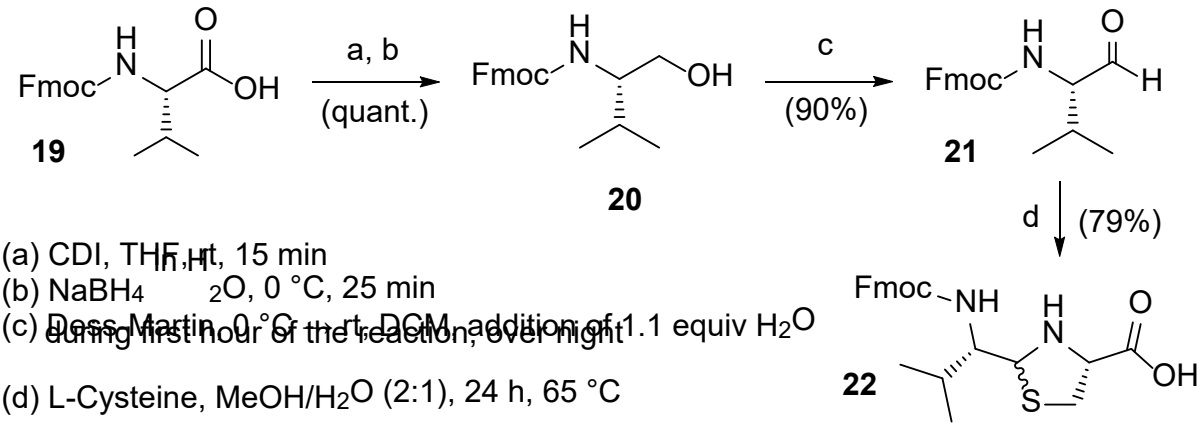

*Figure 16: Synthesis of the thiazolidine building block **22***

With the new thiazolidine amino acid, we were able to use this novel compound in standard SPPS protocols, enabling further derivatives and synthetic approaches. This led us to the second SAR study by Saur *et al.* in 2021[35]. For this publication, we evaluated a wide range of amino acids, proteinogenic as well as non-proteinogenic, for their potential in lugdunin. In contrast to our previous publication from Schilling *et al.*, we focused on positions two, three and four. Unfortunately, we were unable to identify clear trends for either position, other than a consequentially weakened activity when differing from the natural amino acid. The only exemption is the previously published 6-tryptophan-lugdunin with a slightly higher activity than natural lugdunin.

Investigation of the D-Valine at position two

For position two, we based our evaluation on both natural lugdunin and 6-tryptophan-lugdunin. Due to the aliphatic character of valine as the natural amino acid at that position, we focused on similarly aliphatic amino acids such as leucine, iso-leucine, norvaline or tertiary leucine (see Figure 17). While the respective lugdunin derivatives with these four amino acids all had similar antimicrobial activity in antimicrobial *in-vitro* assays (12.5 µM – 25 µM), the derivatives based on 6-tryptophan lugdunin displayed a completely different effect.

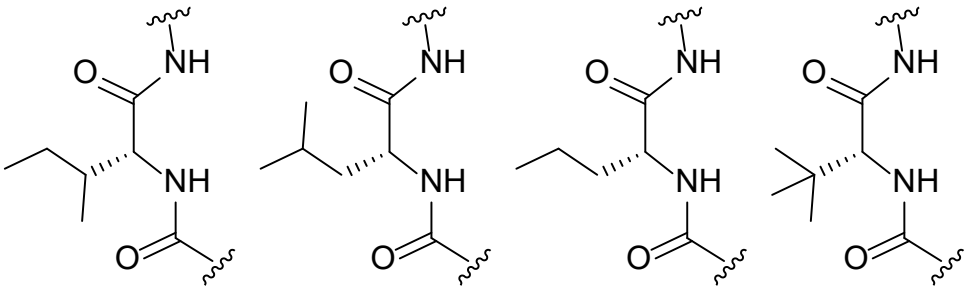

Figure 17: Highlighted changes in bioactive position two derivatives of lugdunin

On one side, the 2-norvaline-6-tryptophan-lugdunin exhibits an activity of 6.25 µM, and thus more active than 2-norvaline-lugdunin. On the other side, 2-leucine-6-tryptophan-lugdunin displayed a complete loss of activity while 2-leucine-lugdunin exhibits decent activity at 12.5 µM. As a result, it was unfortunately not possible to identify a beneficial trend for position two in lugdunin. However, based on our small sample size, further amino acids should be evaluated to assess a trend.

Investigation of the L-tryptophan at position three

For position three, we evaluated a diverse set of aromatic amino acids with a varying number of aromatic rings, different heteroatoms, different sizes of rings as well as different substituents outside of the aromatic rings. Out of these 22 lugdunin analogues, the most potent peptides were the ones with the closest similarity to natural tryptophan. Those lugdunins consisted of (3-benzothienyl)-alanine, (1-naphthyl)-alanine, (9-anthracenyl)-alanine and (1-*N*-Methyl)-tryptophan at position 3 each (see Figure 18).

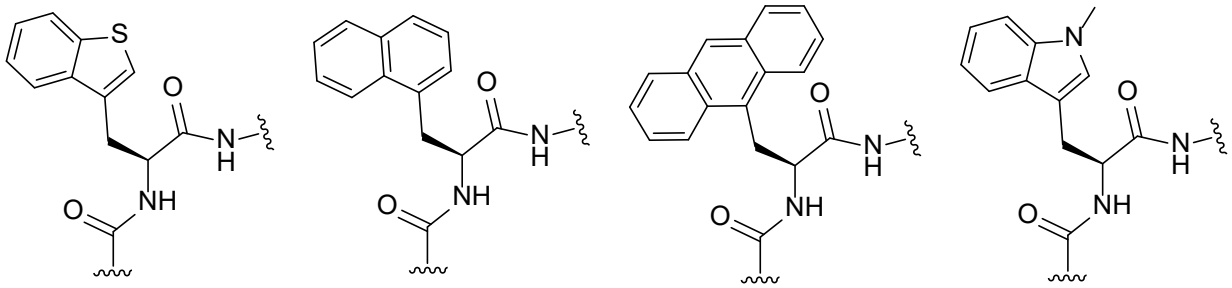

*Figure 18:Highlighted changes in bioactive, position three derivatives of lugdunin **4***

These peptides had antimicrobial activity against MRSA of 6.25 µM (for (1-naphthyl)-alanine and (9-anthracenyl)-alanine) and 12.5 µM (for (3-benzothienyl)-alanine and (1-*N*-Methyl)-tryptophan). While these changes were fairly well tolerated in regards to activity, other amino acids that were less similar to tryptophan, did not result in highly active, or even active at all derivatives. Polar residues (tyrosine and (3-nitro)-phenylalanine), five-membered rings ((4-thiazolyl)-alanine and (2-furyl)-alanine) and cross-linked aromatic rings (diphenylalanine and (4-benzoyl)-phenylalanine) all showed severely weakened antimicrobial properties. Thus, it was not possible to synthesize a derivative with another amino acid at position three yielding a higher antimicrobial activity compared to the original compound **4**. This further displays the importance of natural tryptophan at the position three.

Investigation of the D-Leucine at position four

The final step in this SAR-study was position four, naturally occupied by leucine in lugdunin. We chose the amino acids again according to similarity to the natural standard. This led us to similar amino acids compared to the ones used in the position two derivatives. Additionally, less comparable amino acids were also tested, such as proline, methionine and 1-aminocyclopropane-1-carboxylic acid (see Figure 19).

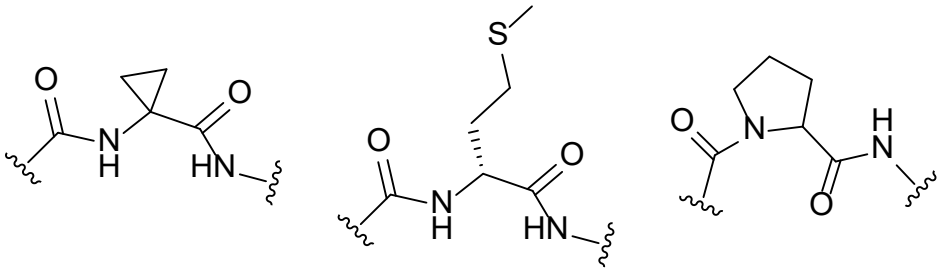

Figure 19: Highlighted changes in bioactive position four derivatives of lugdunin

The previously tested amino acids at position two (for the full list see the corresponding publication in the appendix) also resulted in bioactive compounds at position four with activity similar to the one of natural lugdunin (12.5 µM – 25 µM). However, the newly evaluated amino acids all resulted in inactive compounds (>100 µM).

As a conclusion, we were not able to identify amino acid derivatives that yielded higher activity compared to **4**, by replacing the leucine in natural lugdunin. Thus, we postulate that the natural amino acids are state of the art, with regards to just antimicrobial activity. 6-Tryptophan-lugdunin **5** is to date the only synthetic derivative that is more active than natural lugdunin.

Interestingly, we also identified that the sequence of lugdunin is not fixed to the natural sequence, with a 3-valine-4-valine-5-leucine-6-tryptophan-lugdunin derivative being only slightly less active at 6.25 µM compared to **4**. This is also supported by structural derivatives of lugdunin with the same amino acid side chains. Colleagues were able to show that the enantiomer, as well as the enantiomer with the reversed amino acid sequence were also highly bioactive. While it was not possible to improve lugdunin's activity through other amino acids, the wide variety of available compounds enables even further derivatization, such as Click-chemistry, solubility experiments, combinations with other compounds as well as various applications as a novel antibiotic.

We thank the Peschel Group as well as the Krismer Group for their cooperation and for providing antimicrobial activity assays.

2.3 ABC-transporter of *S. lugdunensis*

This part corresponds to my third publication by Krauss *et al.* and the goal was to provide more insights into the origin of lugdunin as well as researching potential resistance mechanisms to this novel antibiotic.

Since many derivatives were synthesized without a clear improvement in terms of antimicrobial activity, it might be beneficial to better understand lugdunin in its natural environment. Additionally, the discovery of a novel antibiotic such as lugdunin might be drastically diminished with an equally fast rising resistance to such an antibiotic. Therefore, we turned our focus to lugdunin producing *Staphylococcus lugdunensis*. When cultivating *S. lugdunensis* and *S. aureus* on the same agar plate, we were able to detect lugdunin on the interface of the two species. This suggests that *S. lugdunensis* is able to transport lugdunin to the targeted area. In combination with the previously published inability of *S. aureus* to develop resistance to lugdunin[33], this suggests that there are specific transporters in *S. lugdunensis* that facilitate producer self-resistance and release the final antimicrobial compound. This is especially interesting due to the fact that we have not yet been able to identify a target for lugdunin (**4**).

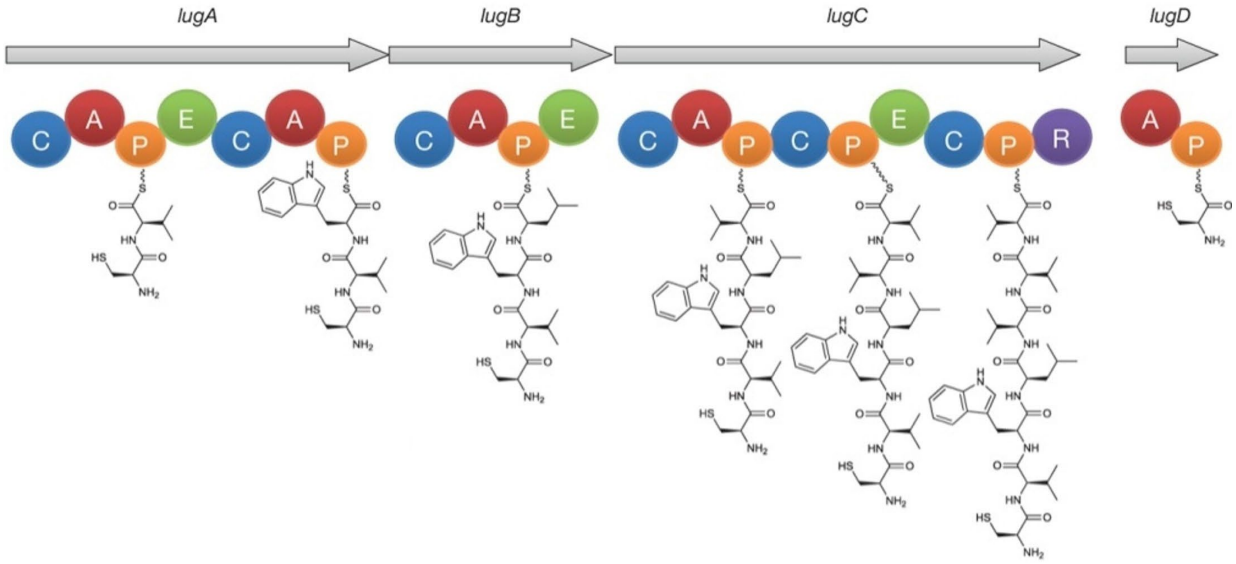

Figure 20: Gene cluster of the lugdunin with proposed biosynthetic pathway. Figure from Zipperer et. al [33]

When lugdunin was first discovered, the gene cluster responsible for the production of lugdunin was only partially identified[33] (see Figure 20). While the *lugABCD* genes are non-ribosomal peptide synthase (NRPS) enzymes and encode the biosynthesis, *lugR* was identified as putative regulator.

Gene cluster of S. lugdunensis

Thus, we turned our focus to the remaining gene cluster. As shown in Figure 21, we identified several additional genes of the BGC and their functional assignment may code for the resistance mechanism. The already known *lugD* is flanked by two genes that encode LugT and LugZ, respectively. LugT is a putative type II thioesterase that may repair stalled peptidyl carrier protein (PCP) domains[90]. LugZ is homologous to 4'-phosphopantetheinyl transferases and is believed to convert apo-PCP to the active holo-form by attachment of the 4-phosphopantetheine cofactor[90]. Those two genes are primarily important for the biosynthesis. They can be neglected for evaluation of self-resistance and transportation properties of *S. lugdunensis*. Following in the sequence is *lugM*, whose role unfortunately remains unclear.

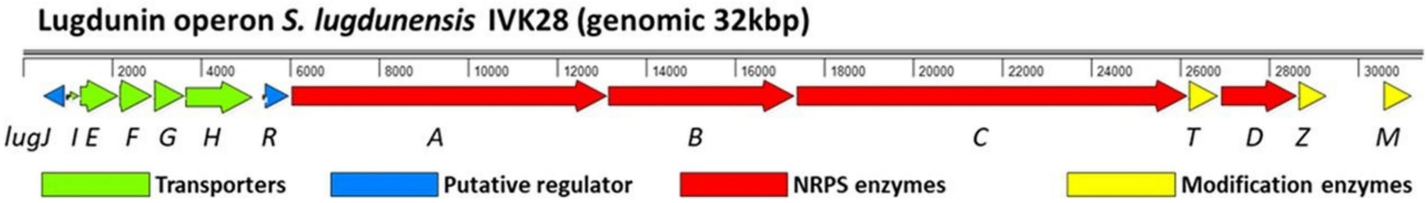

Figure 21: Genetic organisation of the lugdunin gene cluster with functional assignment[37]

Corresponding to *lugR*, another putative regulator gene in *lugJ* was identified. LugJ most likely belongs to the winged-helix type HTH-containing transcriptional regulators. Most natural product biosynthetic gene clusters encode additional proteins required for self-resistance properties such as antibiotic-insensitive variants of target proteins, enzymes for the modification of target structures or antibiotic exporters[91]. However, none of the genes in the lugdunin cluster fit with the first two types of self-resistance, highlighting the importance of the remaining *lugIEFGH* genes. The functions of each gene are detailed in Table 1.

Since neither the regulator genes, nor the modification enzymes correspond to known properties, the potential role of the ABC transporters in lugdunin export and producer self-resistance were analyzed. Therefore, different combinations of *lugEFGH* deletions and the co-transcribed gene *lugI* were expressed in the lugdunin producing strain *S. lugdunensis* IVK28. Mutants were then evaluated for activity against lugdunin-susceptible *S. aureus*.

Table 1: Newly identified transporter genes in lugdunin biosynthetic gene cluster

Gene	Function
lugI	Encodes a 79-amino-acid-long integral membrane protein with two transmembrane helices and no similarity to proteins of known function
lugE	Contain conserved Walker motifs probably representing the ATP-binding components of ABC transporter complexes[92]
lugF	Related to the integral membrane parts of putative ABC transporters of other Firmicutes, containing 6 putative transmembrane segments
lugG	Contain conserved Walker motifs probably representing the ATP-binding components of ABC transporter complexes[92]
lugH	Related to the integral membrane parts of putative ABC transporters of other Firmicutes, containing 12 putative transmembrane segments

As proof-of-concept, the *lugIEFGH* mutant showed no inhibition, indicating the necessity of at least some of these genes for activity and the suitability of this assay. After all mutants were evaluated, it was shown that *lugI* has a moderate but *lugEFGH*-indepedent role in lugdunin release, however only the deletion of *lugI* had no impact on the lugdunin release. *lugEF* displayed a dominant role in lugdunin export, almost as strong as the mutant without *lugEFGH*. *lugGH*-missing mutants on the other hand revealed a larger amount of lugdunin release, suggesting a role in resistance, rather than export.

Additionally, the different gene combinations were expressed in *S. aureus* and the resulting mutants were then evaluated for activity against natural lugdunin **4**. *lugGH* expression led to a significantly increased MIC, confirming the relevant impact of these genes to lugdunin resistance. The additional expression of *lugEF* further increased the resistance of the *S. aureus* mutant. This further underlines the importance of ABC-transporters on lugdunin self-resistance. In contrast, *lugI* only showed a supporting role with *lugGH*, as the exclusive expression of *lugI* did not result in different susceptibility to lugdunin in *S. aureus*.

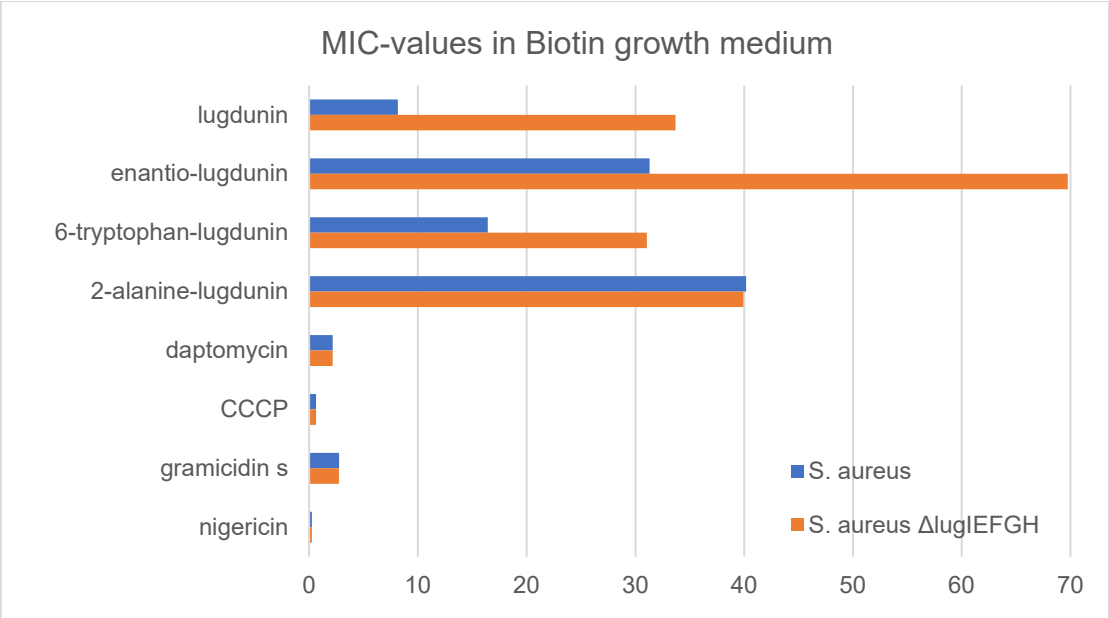

Figure 22: MIC-values in µM for selected compounds tested in BM-medium against S. aureus (blue bars) as well as S. aureus lugIEFGH mutant (orange bars)[37]

After the various mutants were established, the specificity of the transporters was evaluated. A *lugIEFGH* containing *S. aureus* pRB474 was subjected to the following set of lugdunin derivatives as well as other antimicrobial compounds in order to measure the difference in MIC values compared to unmodified *S. aureus*. The compounds used were natural lugdunin **4**, 2-alanine-lugdunin (as less active) and 6-tryptophan-lugdunin **5** (as more active). daptomycin, gramicidin s, CCCP and nigericin were also tested and used as controls. The transporters showed a highly specific identification of natural lugdunin with a more than four times increase in MIC compared to natural *S. aureus* (see Figure 22). While both the enantiomer of lugdunin **4** and 6-tryptophan-lugdunin **5** are also recognized by the *S. aureus* mutant, the difference in activity is already reduced to a two-fold increase. However, the small change of two methyl-groups from natural lugdunin to 2-alanin-lugdunin already resulted in the transporters not recognizing the derivative and thus no change in MIC in *lugIEFGH* containing *S. aureus*. The non-lugdunin related controls were also not affected by the modification of the *S. aureus*.

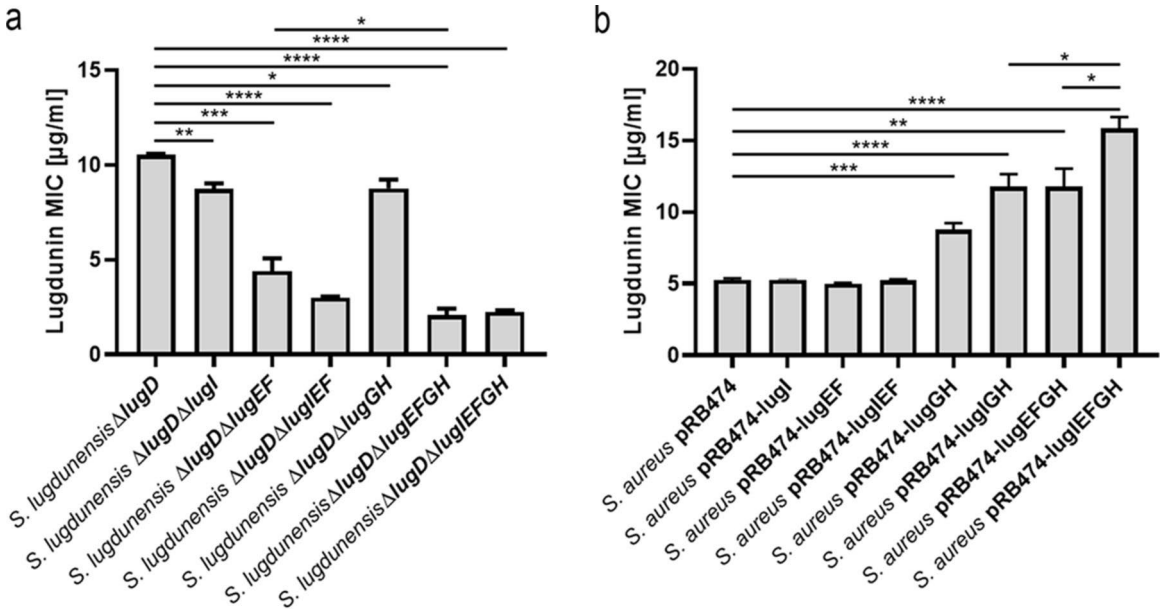

Figure 23: Impact of lugIEFGH deletion in the S. lugdunensis ΔlugD strain (a) or constitutive expression in S. aureus (b) on lugdunin susceptibility. Means and SEM of at least five independent experiments are shown. Significant differences were calculated by one-way ANOVA (Brown-Forsythe and Welsh) (, P ≤ 0.05; **, P ≤ 0.01; ***, P ≤ 0.001; ****, P < 0.0001)[37]*

As a result, we postulate that slight modifications of lugdunin's structure can strongly decrease the possibility for self-resistance even if *lugIEFGH* could spread horizontally across different species. The obvious selectivity of the available resistance mechanisms give rise to optimism for lugdunin derivatives to be used for the treatment of *S. aureus* infections. Since non-natural lugdunin derivatives proved to be beneficial for avoiding self-resistant genes, we focused on non-natural amino acids as well as fluorescent amino acid tags.

We thank the Peschel Group as well as the Krismer Group for their cooperation and we appreciate being part of this publication.

2.4 Fluorescent lugdunin

This part corresponds to my fourth manuscript by Wirtz *et al.* and the goal was to provide fluorescent lugdunin derivatives in order to enable a visualization of lugdunin in bacterial cells to better understand the MOA.

Due to lugdunin's structure as a peptide, we focused on fluorescent amino acids rather than a connecting amino acid that enables further derivatization with a fluorophore.

For preliminary experiments, 4-chloro-7-nitro-benzo-2-oxa-1,3-diazole (NBD-Cl) was coupled to diamino propionic acid (DAP) with triethylamine in methanol in order to produce fluorescent amino acid **25,** see Figure 24.

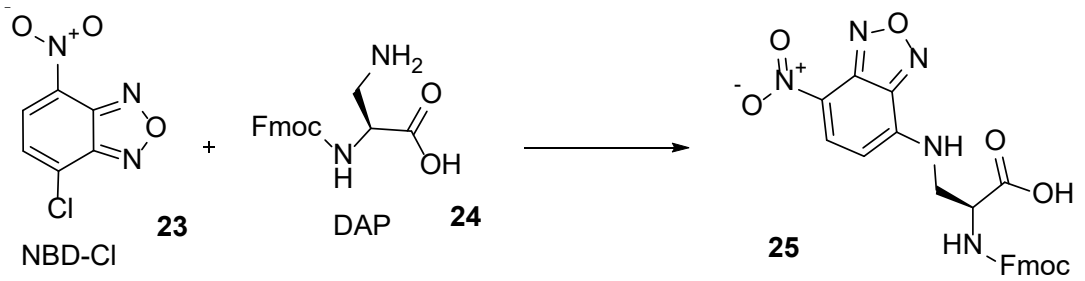

*Figure 24: Synthesis of fluorescent amino acid **25***

After successful characterization via NMR, HPLC-MS as well as UV/Vis, this novel amino acid was incorporated into lugdunin **4**, resulting in the first ever fluorescent lugdunin **26**, see Figure 25. However, after subjecting **26** to antimicrobial assays against MRSA and *B. subtilis,* no activity was detected. This further demonstrates lugdunin's intolerance to even slightly charged molecules such as the nitro group in NBD. Since the desired absorption wavelength was determined to be between 300 nm and 400 nm, the beneficial mesomeric impact of nitro-, hydroxyl- or carboxylic groups and halogen atoms had to be replaced by larger aromatic systems. As a result, I turned my focus to 4-dimethylaminophthalimide (4-DMAP) and 6-dimethylaminonaphthalimide (6-DMN) as previously published environment-sensitive fluorophores[93].

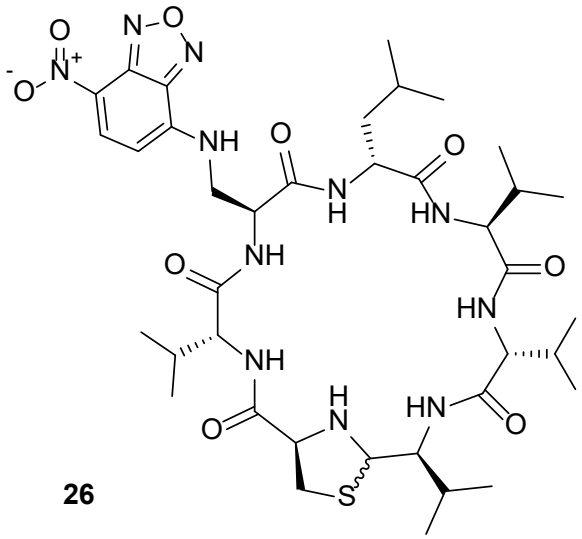

*Figure 25: The first fluorescent lugdunin **26** with an NBD-tag in position three*

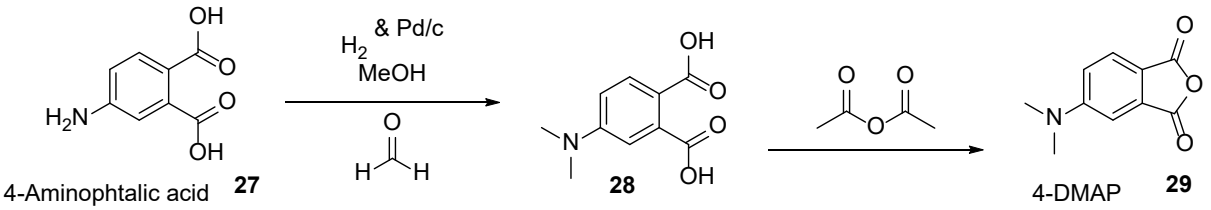

*Figure 26: Synthesis of fluorescent anhydride **29***

After successful synthesis of the precursor anhydride (see Figure 26), the corresponding fluorescent amino acids were incorporated into lugdunin (see Figure 27). However, similar to **26**, when subjected to antimicrobial assays, the fluorescent lugdunins **30** and **31** showed no activity against MRSA. These compounds also required much more attention during synthesis, resulting in lower yields (less than 25%) and less pure products (less than 70%). Due to the already intensive purification process for lugdunin via HPLC, we decided not to further pursue experiments with these compounds as the loss during purification would be too substantial for further experiments.

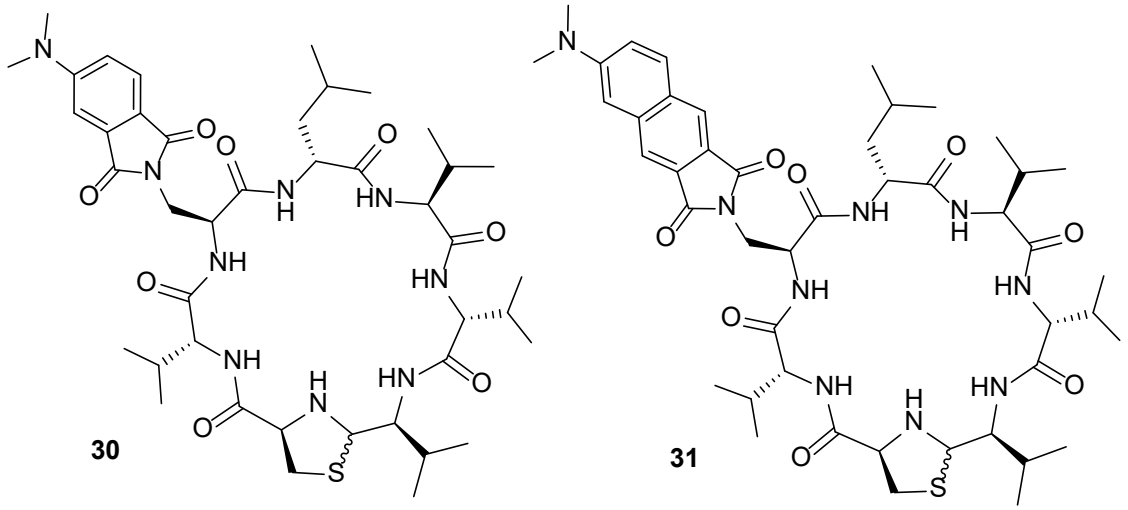

*Figure 27: Fluorescent lugdunins **30** and **31** with fluorescent tags 4-DMAP **29** and 6-DMN respectively*

As a result, we chose to explore other fluorophores instead of optimizing the existing peptides. The generally more active 6-tryptophan derivatives were also evaluated for their impact due to the improvement in activity and also beneficial impact on fluorescence from the additional tryptophan.

This led us to polycyclic aromatic hydrocarbons (PAHs), which are essentially compounds consisting of multiple aromatic rings. The simplest structures of PAHs are for example naphthalene and anthracene, which have both been previously used in lugdunin SAR studies, demonstrating high antimicrobial activity, both against MRSA at 6.25 µM [35]. While larger compounds such as pentacene, coronene or ovalene suggest

decent UV properties from their large π-system, their size presumably renders these compounds inactive in antimicrobial assays as lugdunin does not tolerate large side chains. Thus, a lugdunin containing one of these larger PAHs is most likely not usable as comparison to natural lugdunin and a synthesis was not carried out.

We therefore focused on pyrene, a compact PAH, consisting of four peri-fused benzene rings, resulting in a flat aromatic system. Pyrene **32** (see Figure 28) is widely used in commercial dyes, such as pyranine, and as probe molecule in fluorescence spectroscopy. UV/Vis absorption spectra of pyrene show, similar to most PAHs[94], three distinct bands at 310 nm, 320 nm and 330 nm in dichloromethane (DCM) (see Figure 31). Since the desired use for the compounds is fluorescence experiments, the high quantum yields as well as fluorescence lifetime at 0.65 and 410 ns respectively is also highly important[95-96]. Pyrene is also the first compound for which excimer behavior was discovered in 1954[97]. Additionally, in this thesis, pyrene was also commercially available as Fmoc-protected amino acid, enabling rapid peptide synthesis.

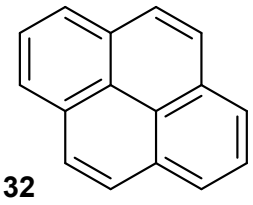

32

*Figure 28: Chemical structure of pyrene (**32**)*

As a result, we designed a set of fluorescent lugdunin derivatives based on pyrenylalanine as the fluorescent tag (see Figure 29 and Figure 30). For a detailed descript of the individual derivatives see the manuscript provided in the appendix. Due to our previous insights into lugdunin's tolerance towards various amino acids, we designed each pyrene derivative with valine as well as leucine at position two. This resulted in twelve fluorescent lugdunins, with an additional two pyrene lugdunins containing propargylglycine for further derivatization and another pyrene lugdunin with two alanine moieties as designed inactive derivative for negative control[98].

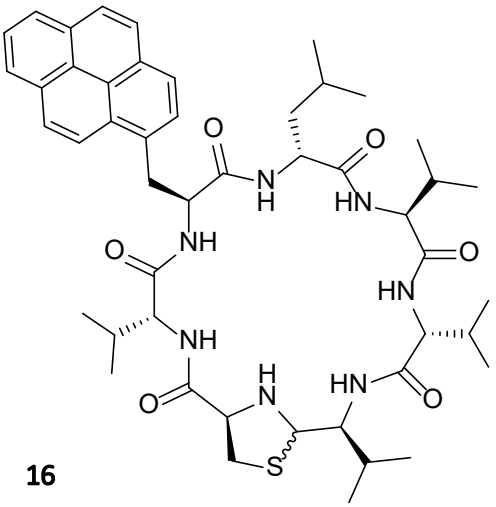

16

*Figure 29: Chemical structure of fluorescent 3-pyrenylalanine-lugdunin (**16**)*

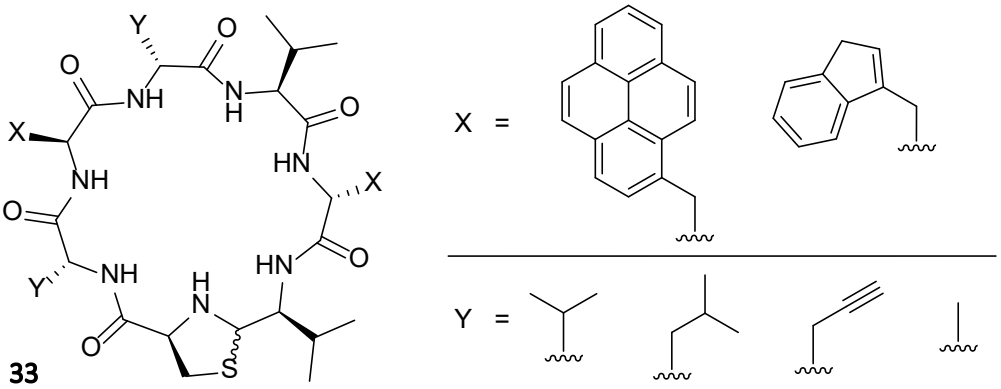

*Figure 30: Schematic presentation of the designed set of fluorescent lugdunins (**33**)*

While the antimicrobial properties for the 3-pyrenylalanine derivative followed known trends (see previous SAR studies), the 6-pyrenylalanine derivatives interestingly displayed unknown trends as the 3-tryptophan-6-pyrenylalanine lugdunin was less active than its 3-valine counterpart. For lugdunin **4**, the additional tryptophan always resulted in better antimicrobial properties. On the other hand, all 2-leucine derivatives followed the trend of natural lugdunin with a slightly reduced activity when compared to the 2-valine derivatives. Interestingly, the designated inactive derivative with two alanine residues proved to be antimicrobially active, albeit at higher concentrations. While this might not be as important as highly active derivatives, this does show that the 4-alanine lugdunin, which has previously been regarded and used as negative control, might still be active, just not in the range that we tested as we previously considered a MIC >100 µM to be inactive. The propargyl and pyrenylalanine containing derivatives also showed promising antimicrobial activity and further experiments with these compounds might enable further aspects of lugdunin research, such as immobilization and using Click-chemistry to connect other molecules to bioactive lugdunin.

After all fluorescent derivatives were synthesized and analyzed, they were subject to UV/Vis experiments for absorption and fluorescence spectra (see Figure 31). In the absorption spectra (blue curve), **16** shows the triple band characteristic for pyrene between 310 nm and 345 nm.

As the maximum was found at 342 nm, we decided to use this wavelength for excitation in fluorescence experiments. As a result, we detected two distinct fluorescence signals at 376 nm and 396 nm. They correspond to literature known pyrene monomer fluorescence. In addition to that, a broad shoulder at 420 nm was detected, corresponding to pyrene excited dimer (excimer) fluorescence, which may be due to aggregation in solution. The Stokes-shift (Δ excitation and emission) is at least 34 nm for the first fluorescence signal and should enable fluorescence microscopy, which have not been possible so far due to time restraints in the course of this thesis.

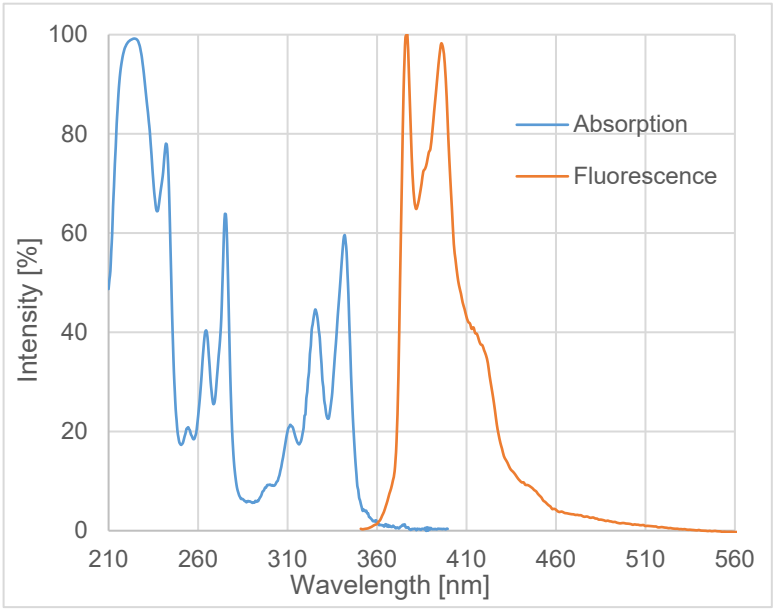

*Figure 31: UV/Vis spectra of 3-pyrenylalanine-lugdunin **16** at a concentration of 0.0125 mg*mL^{-1} in MeOH.*

We thank the Krismer Group for their cooperation and for providing antimicrobial activity assays. We also thank the Steinem Group for their cooperation and for providing UV experiments. In addition to that, we thank the Huhn Group for their cooperation and for providing pK_a experiments. Also, we thank the Jendrossek Group for their cooperation and for providing microscopy experiments.

2.5 Advanced structural changes to lugdunin

This part corresponds to unpublished results. The goal was to explore previously disregarded aspects of lugdunin to gain further insights into the existing MOA as well as discover new approaches to lugdunin.

Ring size of lugdunin

Following the SAR studies mentioned above, more drastic changes to lugdunin's **4** original structure were also evaluated. At first, the number of amino acids were changed. Therefore, the chemical synthesis was inspired from Ghadiri *et. al*[38, 41, 43] and we added or removed two amino acids at once to keep the alternating stereo chemistry (see Figure 32). In literature known Ghadiri-peptides, six-membered as well as eight-membered rings displayed similar antimicrobial activity.[38, 41, 43] For the lugdunin analogue **34** with five amino acids, counting the thiazolidine amino acid as one, we removed two of the valines as the tryptophan, leucine and thiazolidine ring were prioritized. On the other hand, for the larger derivative, we added an additional tryptophan-leucine motif for a total of nine amino acids in **35**, also with alternating stereo centers.

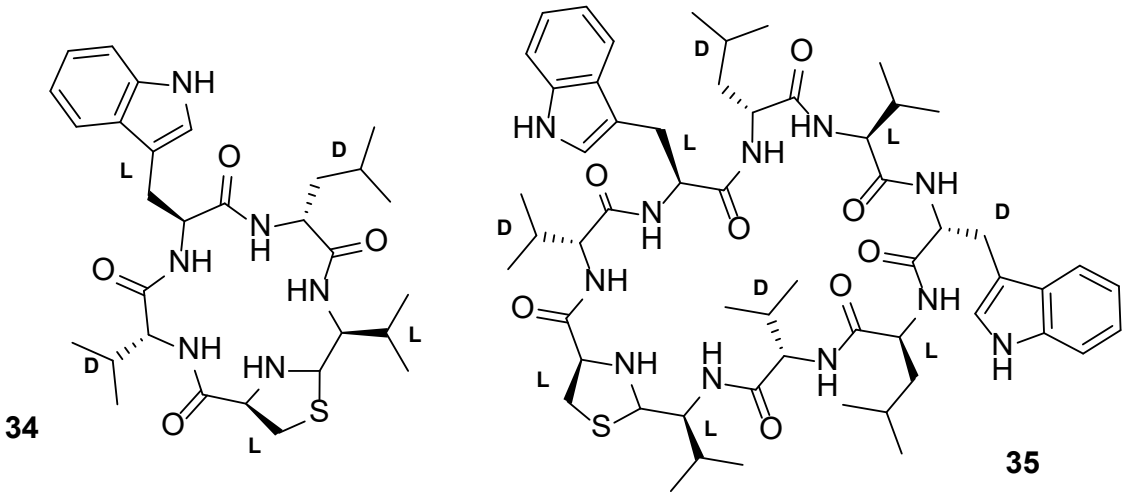

*Figure 32: Shortened and enlarged lugdunin analogues with five amino acids **34** and 9 amino acids **35** with highlighted stereo centers*

However, both peptides showed no antimicrobial activity against MRSA. While it might be an interesting aspect to further investigate, the vast number of necessary derivatives outweighed the benefits of these experiments. These peptides also did not show new behavior in NMR with still two distinct sets of signals from the indole peak or LCMS experiments with still two retention times for the same peptide when compared to natural lugdunin **4**. Instead, the usage of multiple thiazolidine rings was evaluated.

Thiazolidine rings in the macrocycle

Due to the synthesis of the thiazolidine ring, it was not possible to keep the alternating stereo chemistry as well as the uneven number of amino acids. Finally, two compounds were designed (see Figure 33). The first one **36** contains three thiazolidine rings with leucine and tryptophan as connections as all those amino acids proved to be essential in previous SAR-studies. The second compound **37** consists only of four thiazolidine rings, in order to focus on the impact of the thiazolidine ring on its own.

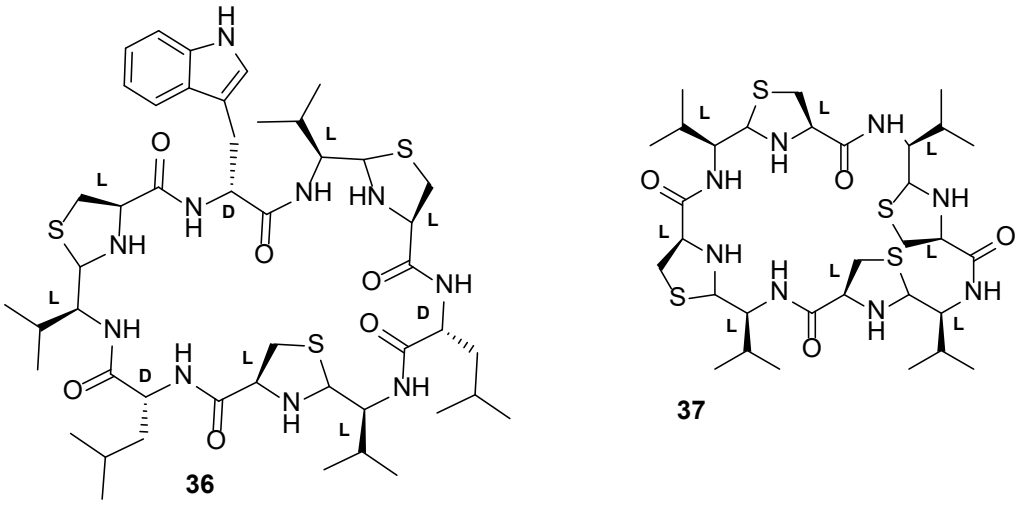

*Figure 33: Compounds based on lugdunin with multiple thiazolidine rings **36** and **37***

Unfortunately, neither of the peptides **36** and **37** showed any antimicrobial activity against Gram-positive or Gram-negative bacteria. For the assays, MRSA and *B.subtilis* were used as Gram-positive bacteria and *E.coli* was used as Gram-negative bacteria. All compounds were subjected to *in-vitro* antimicrobial activity assays ranging in concentrations from 0.18 µM to 100 µM. These compounds did, however, have similar properties to lugdunin when measuring HPLC-MS, further highlighting the importance of the thiazolidine-ring for lugdunin's natural structure. As lugdunin **4** displays two distinct peaks in NMR and LCMS due to its unusual structure with the thiazolidine ring, compounds **36** and **37** displayed multiple sets of signals in their respective analysis, further amplifying the relevance of the thiazolidine ring for the signal anomaly during analysis. Unfortunately, this could not be characterized or quantified due to the imperfect resolution during those experiments. After multiple thiazolidine-rings did not result in an improved activity, the focus was shifted to the five-membered ring itself. Since it has previously been shown, that the changes in the oxidation status, such as a thiazole ring, did not result in any antimicrobially active compounds, the respective thiazoline and thiazole rings were not further explored.

Oxazolidine-lugdunin

Instead, we used threonine rather than cysteine during the peptide synthesis for further derivatization. Together with the spontaneous cyclisation via trapping of the imine[99], this resulted in a cyclic peptide with a methyl-oxazolidine ring **38** (see Figure 34). This compound displayed good antimicrobial activity at 25 µM against MRSA. Since lugdunin defined the class of thiazolidine-containing peptides (Thico-peptides)[33] this is the first lugdunin derivative without a sulfur atom.

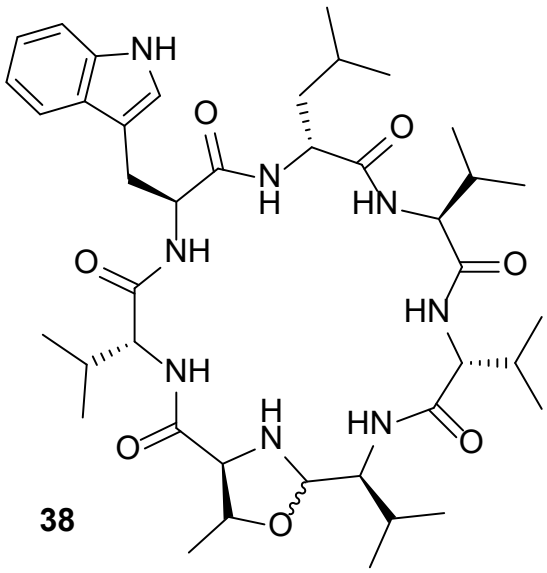

38

*Figure 34: Chemical structure of methyl-oxazolidine containing cyclic peptide **38***

Although the activity is eight times lower compared to lugdunin, this might be a result of the biggest disadvantage of this compound, the instability of the methyl-oxazolidine ring. 2-Alkyl-1,3-oxazolidines are known to be solvent dependent and can undergo ring-opening[100-101]. As a result, the peptide exists as a mixture of imine and oxazolidine tautomers (see Figure 35)[102-105]. The reactivity of the imine then led to the immediate formation of adducts with the solvents during LCMS analysis, rendering it impossible for us to determine purity of the bioactive oxazolidine component. These difficulties during analysis also determines this compound to be not suitable for biological assays, as determination of purity is not possible and the amount of compound used cannot be measured. Thus, the antimicrobial activity mentioned above only describes the activity of an unknown percentage of the compound. Additionally, the instability in an acidic medium renders this compound unsuitable for further optimization during this thesis as all available quantification methods involved an acidic component.

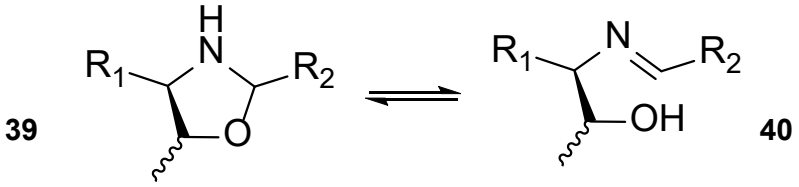

39 **40**

*Figure 35: Schematic display of the oxazolidine-imine-tautomers in **38***

2.6 Applications of lugdunin

This part corresponds to unpublished results. The goal was to apply the existing compounds to various applications in order to further explore the possible applications of lugdunin.

Antimicrobial lugdunin

After all peptides from the topics mentioned above were successfully synthesized and characterized, they were evaluated for their activity and usability in a wide range of assays. These peptides include but are not limited to 4-alanine-lugdunin, 2-alanine-lugdunin, lugdunin **4** and 6-tryptophan-lugdunin **5** as a set of peptides with ascending antimicrobial activity. Additionally, 3-pyrenylalanine-lugdunin, 6-pyrenylalanine-lugdunin, 3-pyrenylalanine-6-pyrenylalanine-lugdunin and 6-tryptophan-lugdunin were used as a set of fluorescent analogues. Also, the peptides **34**-**37** derived in chapter 2.5 were used as a set of more enhanced deviations. In addition to that, multiple other peptides were used for a total of 25 peptides, ranging through the whole time of this thesis. While all peptides were routinely evaluated for their activity against MRSA, we also subjected the derivatives mentioned above to various other bacteria such as *Escherichia coli, Lactobacillus acidifaerinae, Bacillus kochii, Bacillus megaterium* as well as other laboratory strains that do not have a name yet. There were a lot of interesting results, such as lugdunin's activity against *Staphylococcus hawaiiensis* at 6.25 µM and against *Lactobacillus acidifaerinae* at 0.39 µM in *in-vitro* antimicrobial activity assays. 3-pyrenylalanine-lugdunin's activity against *Escherichia coli* at 50 µM was also the first lugdunin analogue that displays antimicrobial activity against both, Gram-positive and Gram-negative bacteria. Unfortunately, no clear trend was detected along multiple derivatives or across multiple bacteria. For example, *B.megaterium* proved to be highly suitable for biological profiling with eight out of 13 fluorescent lugdunins displaying antimicrobial activity. On the other side, multiple strains, such as Gö4010 or *Streptomyces coelicolor,* did not show any biologic activity for any derivative. However, it might be an interesting idea for future studies to map all available lugdunin derivatives across all involved researchers and their activities in order to fully evaluate possible correlations between amino acid sequences and antimicrobial activity.

Antiviral lugdunin

Due to the emerging COVID-19 pandemic during the time that this thesis was carried out, the search for potential antiviral compounds quickly became one of the key aspects for the fight against the coronavirus.

Therefore, we evaluated selected lugdunin derivatives for their antiviral activity against SARS-CoV-2 in two different cell lines (A549-ACE2 and CaJu-3 cells). We evaluated for two specific values. The first value was the EC_{50}-value, which determines the effective concentration of the compound that inhibits at least 50% of virus growth. The second value is the CC_{50}-value, which determines the cytotoxic concentration that kills at least 50% of the cells and therefore displays the cell viability. For A549-ACE2 cells, lugdunin **4** displayed notable activity with an EC_{50}-value of 19.77 µM and a CC_{50}-value of >50 µM. This proved to be very interesting as the usually more active 6-tryptophan-lugdunin proved to be less active in both EC_{50} and CC_{50} assays. For CaJu-3 cells, the antiviral activity of lugdunin was unfortunately not measurable due to errors in detection, however, the CC_{50} value of lugdunin as well as the EC_{50} and CC_{50} value of 6-tryptophan-lugdunin were comparable to the previous cell line. All measured data are shown in Table 2.

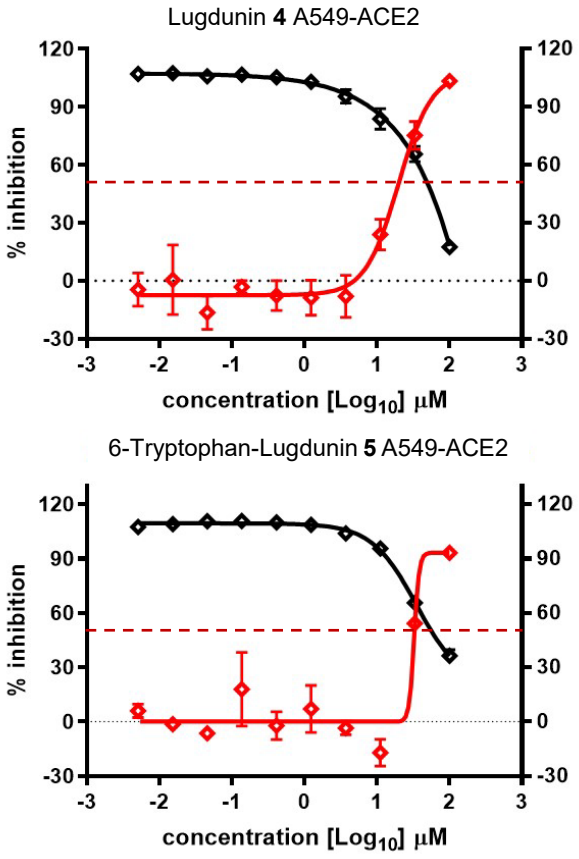

*Figure 36: Antiviral activity of lugdunin **4** and 6-tryptophan-lugdunin **5** against SARS-CoV-2 in A549-ACE2 cells*

*Table 2: Values of antiviral activity of lugdunin **4** and 6-tryptophan-lugdunin **5** against SARS-CoV-2 in different cells*

A549-ACE2 cells		
Compound	EC_{50} (µM)	CC_{50} (µM)
Lugdunin **4**	19,77	~50
6-Tryptophan-Lugdunin **5**	32,50	34,78
Calu-3 cells		
Compound	EC_{50} (µM)	CC_{50} (µM)
Lugdunin **4**	Not detectable	~50
6-Tryptophan-Lugdunin **5**	34,21	34,78

These results further highlight lugdunin's specific interaction with non-polar membranes. Especially the physico-chemical similarities and highly complex structural differences between the envelope of virus particles and bacteria cells are of interest. As lugdunin **4** is able to interact with both, viruses and microbes, this might be a relevant approach for further derivatization, also of other antimicrobials in order to achieve new classes and bioactive compounds.

Immobilization of lugdunin on implants

Another possible application was evaluated by immobilizing lugdunin on a titanium surface for medical applications and the subsequent analysis of activity against *Streptococcus gordonii*. Titanium has been widely used in various medical application such as dental implants or artificial joints. While lugdunin displayed significant antimicrobial activity against *S. gordonii* in culture assays, it was unfortunately not possible to detect a reduction in bacteria vitality, bacteria adhesion or bacteria proliferation in the coated titanium plates. However, this inactivity is most likely due to lugdunin not staying on the surface properly as it has not been shown that lugdunin remains on the surface. This could be solved by more in-depth SAR studies that focus on metal-interactions rather than pure antimicrobial activity. A different approach could also be to use the existing propargyl residues to immobilize lugdunin via Click-chemistry. However, if lugdunin **4** inserts into the membrane, a longer linker might solve the problem and enable immobilized lugdunin **4** to be bioactive.

We thank the Bartenschlager Group for their cooperation and for providing antiviral activity assays. We also thank the Rupp Group for their cooperation and for providing titanium immobilization experiments.

3 Conclusion and Outlook

This thesis is a combination of various publications on lugdunin, a novel antibiotic from the human nose. Lugdunin is a thiazolidine-containing cyclopeptide with micromolar *in-vitro* activity against multi-resistant *S. aureus* (3.13 µM). It is a non-ribosomally synthesized peptide with an alternating stereo chemistry and an intra molecular thiazolidine formation resulting in the final heptapeptide.

This PhD thesis comprises the most detailed and comprehensive insight into lugdunin to date. This work consists of three peer-reviewed publications and two manuscripts which are, at the time of writing being reviewed by the co-authors. Additionally, a patent application, of which I am the main author of, is added to the appendix.

The first publication consists of the first SAR study with basic alanine- and stereo-scan that displayed the importance of the alternating stereo centers. The strong fluctuation in activity among the derivatives during the alanine scan also highlighted the structural complexity of lugdunin. Therefore, tryptophan, leucine and the thiazolidine proved to be essential for activity. The thiazolidine ring was also evaluated for possible changes in size (five- or six-membered ring) or nitrogen connectivity. Unfortunately, none of the derivates showed any activity, highlighting the necessity of the unaltered thiazolidine ring.

The second publication was designed to further understand the biological aspects of the lugdunin-producing strain as well as the interaction between lugdunin and MRSA. With regards to the continuous evolution of resistances against new antibiotics, it is becoming more and more important to develop new types of antimicrobials instead of derivatives of existing compounds. The high specificity of individual transporter genes is very promising as the small derivatization in 2-alanine-lugdunin is already enough to not be recognized. This suggests that cross-resistance to other antimicrobials is unlikely and lugdunin, especially highly optimized lugdunin derivatives, are a potential candidate for *S. aureus* treatment.

Consequentially, we focus on a highly diversified set of natural as well as non-natural amino acids for the SAR study in our third publication. We established a new synthesis route with improvements in resin availability, work-up and yields. Thus, positions two, three and four were readily available for substitution. For positions two and four, the

focus was put on aliphatic amino acids while the tryptophan at position three was replaced by various other aromatic amino acids in order to keep to natural theme at the respective position. Additionally, we carried out multiple-position substitutions in the attempt to evaluate different motifs and combinations of amino acids in the lugdunin sequence. While we did not succeed in generating derivatives with higher activity than the original compound, the sheer number of 50 peptides provided a lot of insight into possible derivatization.

All these insights were then considered when designing the experiments for the manuscript of the fourth publication. In order to further investigate the MOA, we evaluated various fluorescent tags for their fluorescence properties. This resulted in pyrenylalanine being a suitable fluorophore for lugdunin. We then designed a set of fluorescent lugdunin derivatives and evaluated these for their fluorescence as well as their activity against a set of bacteria. Even though all peptides had similar fluorescence spectra, the difference in antimicrobial activity enables interesting experiments that are, at the time of writing, being investigated by cooperation partners.

For the patent application, we modified the thiazolidine ring although it was previously shown that many derivatizations were not tolerated. In addition to the thiazolidine modification, various non-natural amino acids were used for the derivatization.

As summarized above, the insights gained in this work highlight lugdunin's possibilities for treatment against MRSA. Having synthesized hundreds of peptides during my PhD time, it was possible to provide valuable insight into the MOA of lugdunin. However, even though there are already that many derivatives, there are still a lot of opportunities for further investigation.

For example, it might be beneficial to use artificial intelligence, such as OpenAI, on the existing data in order to further investigate unknown relationships. With the number of derivatives available, this should result in a library large enough for various calculations. Depending on the availability of data about various membrane compositions, this approach might also show more possible applications for lugdunin as well as suggest complex structural derivatives of lugdunin.

In case this is not possible, a more simplistic approach might be to subject a variety of lugdunin derivatives to a broader spectrum of microbials such as fungi or viruses. Especially with the promising results against Sars-CoV-2, this research area might be

very auspicious as there is currently not much data available. There have also been an increasing number of antiviral peptide (AVP) drugs undergoing clinical trials against human immunodeficiency virus (HIV), influenza virus as well as hepatitis virus (B and C)[106] further highlighting the significance of this approach. While carrying out this SAR study against viruses, it might also be beneficial to consult existing repositories such as the antiviral peptide database AVPdb[107].

4 Bibliography

5 References

[1] A. Fleming, On the Antibacterial Action of Cultures of a Penicillium, with Special Reference to their Use in the Isolation of *B. influenzæ*, *Br. J. Exp. Pathol.* **1929**, *10*, 226-236.

[2] J. O'Neill, Antimicrobial Resistance: Tackling a Crisis for the Health and Wealth of Nations: December 2014, *Review on Antimicrobial Resistance*, **2014**.

[3] F. von Nussbaum, M. Brands, B. Hinzen *et al.*, Antibacterial Natural Products in Medicinal Chemistry-Exodus or Revival? *Angew. Chem. Int. Ed.* **2006**, *45*, 5072-5129.

[4] N. Bristol, William H Stewart, *Lancet* **2008**, *372*, 110.

[5] M. I. El-Gamal, I. Brahim, N. Hisham*, et al.*, Recent updates of carbapenem antibiotics, *Eur. J. Med. Chem.* **2017**, *131*, 185-195.

[6] J. S. Wolfson, D. C. Hooper, Fluoroquinolone antimicrobial agents, *Clin. Microbiol. Rev.* **1989**, *2*, 378-424.

[7] N. Gupta, B. M. Limbago, J. B. Patel *et al.*, Carbapenem-Resistant Enterobacteriaceae: Epidemiology and Prevention, *Clin. Infect. Dis.* **2011**, *53*, 60-67.

[8] D. C. Hooper, Mechanisms of fluoroquinolone resistance, *Drug Resist. Updat.* **1999**, *2*, 38-55.

[9] A. Towse, C. K. Hoyle, J. Goodall *et al.*, Time for a change in how new antibiotics are reimbursed: Development of an insurance framework for funding new antibiotics based on a policy of risk mitigation, *Health Policy* **2017**, *121*, 1025-1030.

[10] J. Mestre-Ferrandiz, J. Sussex, A. Towse, The R&D cost of a new medicine, *Monogr.* **2012**.

[11] B. Plackett, Why big pharma has abandoned antibiotics, *Nature* **2020**, *586*, 0828-0836.

[12] T. P. Van Boeckel, S. Gandra, A. Ashok *et al.*, Global antibiotic consumption 2000 to 2010: An analysis of national pharmaceutical sales data, *Lancet Infect. Dis.* **2014**, *14*, 742-750.

[13] E. Y. Klein, T. P. Van Boeckel, E. M. Martinez *et al.*, Global increase and geographic convergence in antibiotic consumption between 2000 and 2015, *Proc. Natl. Acad. Sci. USA* **2018**, *115*, E3463-E3470.

[14] H. Hahn, S. H. Kaufmann, T. F. Schulz *et al.*, Medizinische Mikrobiologie und Infektiologie, *Springer-Verlag*, **2009**.

[15] Landeszentrum Gesundheit Nordrhein-Westfalen, Reserve-Antibiotika, Antibiotika-Verbrauch, Antibiotika-Reserve - *Sachstandsbericht*, **2016**.

[16] R. Laxminarayan, A. Duse, C. Wattal *et al.*, Antibiotic resistance—the need for global solutions, *Lancet Infect. Dis.* **2013**, *13*, 1057-1098.

[17] Centers for Disease Control and Prevention, Vital signs: carbapenem-resistant Enterobacteriaceae, *U.S. Department of Health and Human Services*, **2013**.

[18] J. N. Pendleton, S. P. Gorman, B. F. Gilmore, Clinical relevance of the ESKAPE pathogens, *Expert Rev. Anti Infect. Ther.* **2013**, *11*, 297-308.

[19] M. S. Mulani, E. E. Kamble, S. N. Kumkar *et al.*, Emerging strategies to combat ESKAPE pathogens in the era of antimicrobial resistance: A Review, *Front. Microbiol.* **2019**, *10*, 539.

[20] S. Santajit, N. Indrawattana, Mechanisms of antimicrobial resistance in ESKAPE pathogens, *Biomed. Res. Int.,* **2016**, *2314*.

[21] D. M. P. D. Oliveira, B. M. Forde, T. J. Kidd *et al.*, Antimicrobial Resistance in ESKAPE Pathogens, *Clin. Microbiol. Rev.* **2020**, *33*, e00181-00119.

[22] R. Benkő, M. Gajdács, M. Matuz *et al.*, Prevalence and Antibiotic Resistance of ESKAPE Pathogens Isolated in the Emergency Department of a Tertiary Care Teaching Hospital in Hungary: A 5-Year Retrospective Survey, *Antibiotics* **2020**, *9*, 624.

[23] H. A. El-Mahallawy, S. S. Hassan, M. El-Wakil *et al.*, Bacteremia due to ESKAPE pathogens: An emerging problem in cancer patients, *J. Egypt Natl. Canc. Inst.* **2016**, *28*, 157-162.

[24] Centers for Disease Control and Prevention, Antibiotic Resistance Threats in the United States, *U.S. Department of Health and Human Services*, **2019**.

[25] E. P. Abraham, E. Chain, An Enzyme from Bacteria able to Destroy Penicillin, *Nature* **1940**, *146*, 837-837.

[26] B. Zacher, S. Haller, N. Willrich *et al.*, Application of a new methodology and R package reveals a high burden of healthcare-associated infections (HAI) in Germany compared to the average in the European Union/European Economic Area, 2011 to 2012, *Eurosurveillance* **2019**, *24*, 1900135.

[27] M. T. Holden, L.-Y. Hsu, K. Kurt*, et al.*, A genomic portrait of the emergence, evolution, and global spread of a methicillin-resistant *Staphylococcus aureus* pandemic, *Genome Res.* **2013**, *23*, 653-664.

[28] S. Rachakonda, L. Cartee, Challenges in Antimicrobial Drug Discovery and the Potential of Nucleoside Antibiotics, *Curr. Med. Chem.* **2004**, *11*, 775-793.

[29] C. J. L. Murray, K. S. Ikuta, F. Sharara*, et al.*, Global burden of bacterial antimicrobial resistance in 2019: a systematic analysis, *Lancet* **2022**, *399*, 629-655.

[30] UNAIDS, accessed on 11.02.2022, https://www.unaids.org/sites/default/files/media_asset/UNAIDS_FactSheet_en.pdf.

[31] WHO, accessed on 11.02.2022, https://www.who.int/docs/default-source/malaria/world-malaria-reports/9789240015791-double-page-view.pdf?sfvrsn=2c24349d_5.

[32] J. O'Neill, Tackling drug-resistant infections globally: final report and recommendations, Government of the United Kingdom, **2016**.

[33] A. Zipperer, M. C. Konnerth, C. Laux*, et al.*, Human commensals producing a novel antibiotic impair pathogen colonization, *Nature* **2016**, *535*, 511-516.

[34] K. Bitschar, B. Sauer, J. Focken*, et al.*, Lugdunin amplifies innate immune responses in the skin in synergy with host- and microbiota-derived factors, *Nat. Commun.* **2019**, *10*, 2730-2744.

[35] J. S. Saur, S. N. Wirtz, N. A. Schilling*, et al.*, Distinct Lugdunins from a New Efficient Synthesis and Broad Exploitation of Its MRSA-Antimicrobial Structure, *J. Med. Chem.* **2021**, *64*, 4034-4058.

[36] N. A. Schilling, A. Berscheid, J. Schumacher*, et al.*, Synthetic lugdunin analogues reveal essential structural motifs for antimicrobial action and proton translocation capability, *Angew. Chem., Int. Ed.* **2019**, *58*, 9234-9238.

[37] S. Krauss, A. Zipperer, S. Wirtz*, et al.*, Secretion of and Self-Resistance to the Novel Fibupeptide Antimicrobial Lugdunin by Distinct ABC Transporters in Staphylococcus lugdunensis, *Antimicrob. Agents Chemother.* **2020**, *65*, e01734-01720.

[38] M. R. Ghadiri, J. R. Granja, R. A. Milligan*, et al.*, Self-assembling organic nanotubes based on a cyclic peptide architecture, *Nature* **1993**, *366*, 324-327.

[39] D. T. Bong, T. D. Clark, J. R. Granja*, et al.*, Self-Assembling Organic Nanotubes, *Angew. Chem. Int. Ed.* **2001**, *40*, 988-1011.

[40] J. D. Hartgerink, J. R. Granja, R. A. Milligan *et al.*, Self-Assembling Peptide Nanotubes, *JACS* **1996**, *118*, 43-50.

[41] M. R. Ghadiri, J. R. Granja, L. K. Buehler, Artificial transmembrane ion channels from self-assembling peptide nanotubes, *Nature* **1994**, *369*, 301.

[42] J. D. Hartgerink, T. D. Clark, M. R. Ghadiri, Peptide Nanotubes and Beyond, *Chem. Eur. J.* **1998**, *4*, 1367-1372.

[43] M. R. Ghadiri, K. Kobayashi, J. R. Granja*, et al.*, The Structural and Thermodynamic Basis for the Formation of Self-Assembled Peptide Nanotubes, *Angew. Chem. Int. Ed.* **1995**, *34*, 93-95.

[44] S. Fernandez-Lopez, H.-S. Kim, E. C. Choi *et al.*, Antibacterial agents based on the cyclic D,L-α-peptide architecture, *Nature* **2001**, *412*, 452-455.

[45] R. Yuste, Fluorescence microscopy today, *Nat. Methods* **2005**, *2*, 902-904.

[46] J. W. Lichtman, J.-A. Conchello, Fluorescence microscopy, *Nat. Methods* **2005**, *2*, 910-919.

[47] A. Small, S. Stahlheber, Fluorophore localization algorithms for super-resolution microscopy, *Nat. Methods* **2014**, *11*, 267-279.

[48] B. Huang, M. Bates, X. Zhuang, Super-Resolution Fluorescence Microscopy, *Annu. Rev. Biochem.* **2009**, *78*, 993-1016.

[49] M. J. Sanderson, I. Smith, I. Parker*, et al.*, Fluorescence Microscopy, *Cold Spring Harb. Protoc.* **2014**, pdb.top071795.

[50] L. Schermelleh, R. Heintzmann, H. Leonhardt, A guide to super-resolution fluorescence microscopy, *J. Cell Biol.* **2010**, *190*, 165-175.

[51] J. R. Pringle, R. A. Preston, A. E. M. Adams *et al.*, in *Methods Cell Biol., Vol. 31* (Ed.: A. M. Tartakoff), Academic Press, **1989**, pp. 357-435.

[52] K. Suhling, P. M. W. French, D. Phillips, Time-resolved fluorescence microscopy, *Photochem. Photobiol. Sci.* **2005**, *4*, 13-22.

[53] J. A. Levitt, M. K. Kuimova, G. Yahioglu *et al.*, Membrane-Bound Molecular Rotors Measure Viscosity in Live Cells via Fluorescence Lifetime Imaging, *J. P. Chem. C* **2009**, *113*, 11634-11642.

[54] T. Nakabayashi, H.-P. Wang, M. Kinjo *et al.*, Application of fluorescence lifetime imaging of enhanced green fluorescent protein to intracellular pH measurements, *Photochem. Photobiol. Sci.* **2008**, *7*, 668-670.

[55] I. E. Steinmark, P.-H. Chung, R. M. Ziolek *et al.*, Time-Resolved Fluorescence Anisotropy of a Molecular Rotor Resolves Microscopic Viscosity Parameters in Complex Environments, *Small* **2020**, *16*, 1907139.

[56] K. Suhling, Y. Teijeiro-Gonzalez, I. E. Steinmark *et al.*, *Fluorescence lifetime imaging for viscosity and diffusion measurements, Vol. 10882*, SPIE, **2019**.

[57] J. C. Waters, Accuracy and precision in quantitative fluorescence microscopy, *J. Cell Biol.* **2009**, *185*, 1135-1148.

[58] A. Diaspro, G. Chirico, C. Usai*, et al.*, in *Handbook of biological confocal microscopy*, Springer, **2006**, pp. 690-702.

[59] P. Montero Llopis, R. A. Senft, T. J. Ross-Elliott *et al.*, Best practices and tools for reporting reproducible fluorescence microscopy methods, *Nat. Methods* **2021**, *18*, 1463-1476.

[60] J. Icha, M. Weber, J. C. Waters *et al.*, Phototoxicity in live fluorescence microscopy, and how to avoid it, *Bioessays* **2017**, *39*, 1700003.

[61] L. Yuan, W. Lin, K. Zheng *et al.*, Far-red to near infrared analyte-responsive fluorescent probes based on organic fluorophore platforms for fluorescence imaging, *Chem. Soc. Rev.* **2013**, *42*, 622-661.

[62] R. Weissleder, V. Ntziachristos, Shedding light onto live molecular targets, *Nat. Med.* **2003**, *9*, 123-128.

[63] M. G. Müller, I. Georgakoudi, Q. Zhang *et al.*, Intrinsic fluorescence spectroscopy in turbid media: disentangling effects of scattering and absorption, *Appl. Opt.* **2001**, *40*, 4633-4646.

[64] J. V. Frangioni, In vivo near-infrared fluorescence imaging, *Curr. Opin. Chem. Biol.* **2003**, *7*, 626-634.

[65] R. Weissleder, A clearer vision for in vivo imaging, *Nat. Biotechnol.* **2001**, *19*, 316-317.

[66] C.-H. Tung, Y. Lin, W. K. Moon *et al.*, A Receptor-Targeted Near-Infrared Fluorescence Probe for In Vivo Tumor Imaging, *ChemBioChem* **2002**, *3*, 784-786.

[67] J. O. Escobedo, O. Rusin, S. Lim *et al.*, NIR dyes for bioimaging applications, *Curr. Opin. Chem. Biol.* **2010**, *14*, 64-70.

[68] Y. Yang, M. Lowry, X. Xu *et al.*, Seminaphthofluorones are a family of water-soluble, low molecular weight, NIR-emitting fluorophores, *PNAS* **2008**, *105*, 8829-8834.

[69] K. Umezawa, A. Matsui, Y. Nakamura *et al.*, Bright, Color-Tunable Fluorescent Dyes in the Vis/NIR Region: Establishment of New “Tailor-Made” Multicolor Fluorophores Based on Borondipyrromethene, *Chem. Eur. J.* **2009**, *15*, 1096-1106.

[70] K. Umezawa, Y. Nakamura, H. Makino *et al.*, Bright, Color-Tunable Fluorescent Dyes in the Visible−Near-Infrared Region, *JACS* **2008**, *130*, 1550-1551.

[71] W. Pham, L. Cassell, A. Gillman *et al.*, A near-infrared dye for multichannel imaging, *Chem. Commun.* **2008**, 1895-1897.

[72] S. N. Wirtz, J. S. Saur, N. A. Schilling *et al.*, Deepened insights into lugdunin, *Unpublished Work*, **2021**.

[73] N. A. Schilling, S. Grond, Biologisch aktive Peptide mit verbesserter Wirksamkeit, *DE102021002122A1*, **2021**.
[74] L. Piñeiro, M. Novo, W. Al-Soufi, Fluorescence emission of pyrene in surfactant solutions, *Adv. Colloid Interface Sci.* **2015**, *215*, 1-12.
[75] B. Stevens, Evidence for the Photo-Association of Aromatic Hydrocarbons in Fluid Media, *Nature* **1961**, *192*, 725-727.
[76] B. Stevens, E. Hutton, Radiative Life-time of the Pyrene Dimer and the Possible Role of Excited Dimers in Energy Transfer Processes, *Nature* **1960**, *186*, 1045-1046.
[77] J. B. Birks, L. G. Christophorou, Excimer Fluorescence of Aromatic Hydrocarbons in Solution, *Nature* **1962**, *194*, 442-444.
[78] J. B. Birks, L. G. Christophorou, Excimer fluorescence spectra of pyrene derivatives, *Spectrochim. Acta* **1963**, *19*, 401-410.
[79] J. B. Birks, Excimers and Exciplexes, *Nature* **1967**, *214*, 1187-1190.
[80] Y. Shiraishi, Y. Tokitoh, T. Hirai, pH- and H_2O-Driven Triple-Mode Pyrene Fluorescence, *Org. Lett.* **2006**, *8*, 3841-3844.
[81] N. Ashkenasy, W. S. Horne, M. R. Ghadiri, Design of self-assembling peptide nanotubes with delocalized electronic states, *Small,* **2006**, *2*, 99-102.
[82] R. J. Brea, M. E. Vázquez, M. Mosquera *et al.*, Controlling Multiple Fluorescent Signal Output in Cyclic Peptide-Based Supramolecular Systems, *JACS,* **2007**, *129*, 1653-1657.
[83] K. Kalyanasundaram, J. K. Thomas, Environmental effects on vibronic band intensities in pyrene monomer fluorescence and their application in studies of micellar systems, *JACS,* **1977**, *99*, 2039-2044.
[84] J. Aguiar, P. Carpena, J. A. Molina-Bolívar *et al.*, On the determination of the critical micelle concentration by the pyrene 1:3 ratio method, *J. Colloid Interface Sci.* **2003**, *258*, 116-122.
[85] M. M. Amiji, Pyrene fluorescence study of chitosan self-association in aqueous solution, *Carbohydr. Polym.* **1995**, *26*, 211-213.
[86] D. C. Dong, M. A. Winnik, The Py Scale of solvent polarities. Solvent effects on the vibronic fine structure of Pyrene fluorescence and empirical correlations with ET and Y values, *Photochem. Photobiol.* **1982**, *35*, 17-21.
[87] R. B. Merrifield, Solid Phase Peptide Synthesis. I. The Synthesis of a Tetrapeptide, *JACS,* **1963**, *85*, 2149-2154.
[88] R. B. Merrifield, Automated Synthesis of Peptides, *Science* **1965**, *150*, 178-185.
[89] B. Yan, *The properties of resin supports and their effects on solid-phase organic synthesis, Vol. 1*, **1998**.
[90] M. Kotowska, K. Pawlik, Roles of type II thioesterases and their application for secondary metabolite yield improvement, *Appl. Microbiol. Biotechnol.* **2014**, *98*, 7735-7746.
[91] M. D. Mungan, M. Alanjary, K. Blin*, et al.*, ARTS 2.0: feature updates and expansion of the Antibiotic Resistant Target Seeker for comparative genome mining, *Nucleic Acids Res.* **2020**, *48*, W546-W552.
[92] K. P. Locher, Mechanistic diversity in ATP-binding cassette (ABC) transporters, *Nat. Struct. Mol. Biol.* **2016**, *23*, 487-493.

[93] M. Sainlos, B. Imperiali, Synthesis of anhydride precursors of the environment-sensitive fluorophores 4-DMAP and 6-DMN, *Nat. Protoc.* **2007**, *2*, 3219-3225.

[94] A. M. Rivera-Figueroa, K. A. Ramazan, B. J. Finlayson-Pitts, Fluorescence, Absorption, and Excitation Spectra of Polycyclic Aromatic Hydrocarbons as a Tool for Quantitative Analysis, *J. Chem. Educ.* **2004**, *81*, 242-245.

[95] T. Medinger, F. Wilkinson, Concentration dependence of quantum yield of triplet-state production of pyrene in ethanol, *Trans. Faraday Soc.* **1966**, *62*, 1785-1792.

[96] C. A. Parker, C. G. Hatchard, Delayed fluorescence of pyrene in ethanol, *Trans. Faraday Soc.* **1963**, *59*, 284-295.

[97] T. Förster, K. Kasper, Ein Konzentrationsumschlag der Fluoreszenz, *Z. Phys. Chem.* **1954**, *1*, 275-277.

[98] S. N. Wirtz, D. Ruppelt, M. Meixner *et al.*, Development of fluorescent derivatives as tools to validate the in vivo mode of action of the antibiotic lugdunin, **2022**, p. 16, unpublished work.

[99] L. R. Malins, J. N. deGruyter, K. J. Robbins*, et al.*, Peptide Macrocyclization Inspired by Non-Ribosomal Imine Natural Products, *JACS,* **2017**, *139*, 5233-5241.

[100] T. H. Fife, L. Hagopian, Oxazolidine hydrolysis. Participation of solvent and buffer in ring opening, *JACS,* **1968**, *90*, 1007-1014.

[101] T. H. Fife, J. Hutchins, General-acid-catalyzed ring opening of oxazolidines. Hydrolysis of 2-[4-(dimethylamino) styryl]-N-phenyl-1, 3-oxazolidine, *J. Org. Chem.,* **1980**, *45*, 2099-2104.

[102] M. J. Wu, L. N. Pridgen, Synthesis of chiral α-alkyl phenethylamines via organometallic addition to chiral 2-aryl-1,3-oxazolidines, *J. Org. Chem.,* **1991**, *56*, 1340-1344.

[103] C. K. Miao, R. Sorcek, P.-J. Jones, A simple and effective enantiomeric synthesis of a chiral primary amine, *Tetrahedron Lett.* **1993**, *34*, 2259-2262.

[104] G. P. Moloney, M. N. Iskander, D. J. Craik, Stability Studies of Oxazolidine-Based Compounds Using 1H NMR Spectroscopy, *J. Pharm. Sci.* **2010**, *99*, 3362-3371.

[105] F. Gosselin, A. Roy, P. D. O'Shea *et al.*, Oxazolidine Ring Opening and Isomerization to (E)-Imines. Asymmetric Synthesis of Aryl-α-fluoroalkyl Amino Alcohols, *Org. Lett.* **2004**, *6*, 641-644.

[106] G. Agarwal, R. Gabrani, Antiviral Peptides: Identification and Validation, *Int. J. Pept. Res. Ther.* **2021**, *27*, 149-168.

[107] A. Qureshi, N. Thakur, H. Tandon *et al.*, AVPdb: a database of experimentally validated antiviral peptides targeting medically important viruses, *Nucleic Acids Res.* **2014**, *42*, D1147-1153.

6 Appendix

6.1 Angewandte Chemie International Edition, 2019

N.A. Schilling, A. Berscheid, J. Schumacher, J.S. Saur, M.C. Konnerth, S.N. Wirtz, J.M. Beltrán-Belena, A. Zipperer, B. Krismer, A. Peschel, H. Kalbacher, H. Brötz-Oesterhelt, C. Steinem, S. Grond

Paper 1

Synthetic Lugdunin Analogues Reveal Essential Structural Motifs for Antimicrobial Action and Proton Translocation Capability

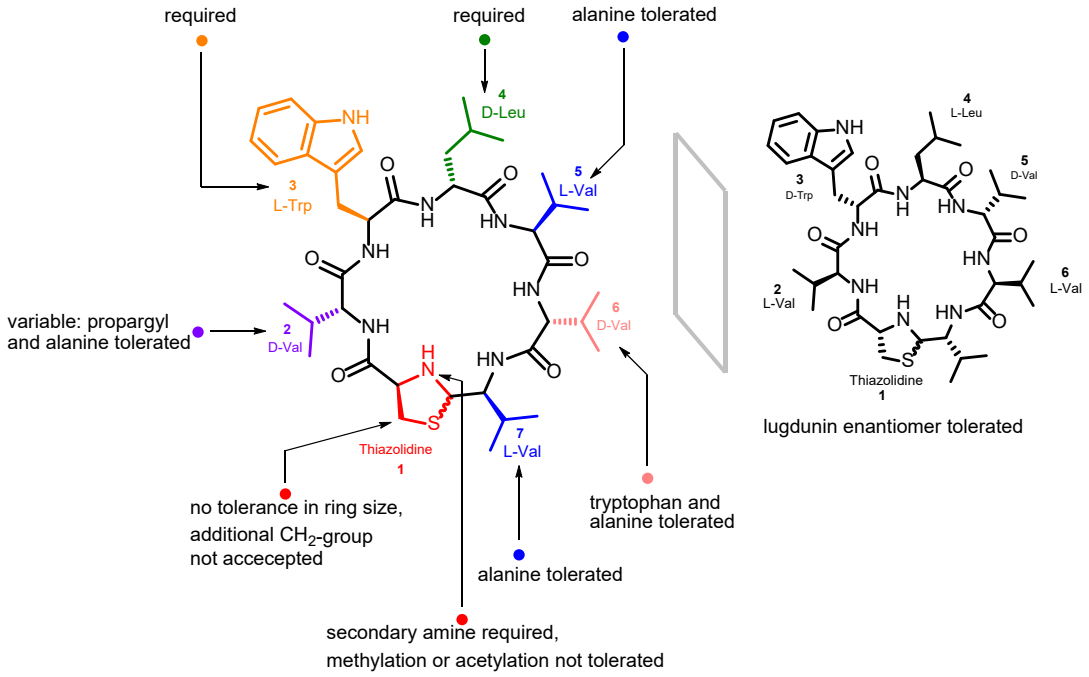

Angew. Chem. Int. Ed. **2019**, *58*, 9234-9238
https://doi.org/10.1002/anie.201901589

VIP Aldehyde Peptide Synthesis Very Important Paper

International Edition: DOI: 10.1002/anie.201901589
German Edition: DOI: 10.1002/ange.201901589

Synthetic Lugdunin Analogues Reveal Essential Structural Motifs for Antimicrobial Action and Proton Translocation Capability

*Nadine A. Schilling, Anne Berscheid, Johannes Schumacher, Julian S. Saur, Martin C. Konnerth, Sebastian N. Wirtz, José M. Beltrán-Beleña, Alexander Zipperer, Bernhard Krismer, Andreas Peschel, Hubert Kalbacher, Heike Brötz-Oesterhelt, Claudia Steinem, and Stephanie Grond**

Dedicated to Professor Axel Zeeck on the occasion of his 80th birthday

Abstract: *Lugdunin, a novel thiazolidine cyclopeptide, exhibits micromolar activity against methicillin-resistant Staphylococcus aureus (MRSA). For structure–activity relationship (SAR) studies, synthetic analogues obtained from alanine and stereo scanning as well as peptides with modified thiazolidine rings were tested for antimicrobial activity. The thiazolidine ring and the alternating* D- *and* L-*amino acid backbone are essential. Notably, the non-natural enantiomer displays equal activity, thus indicating the absence of a chiral target. The antibacterial activity strongly correlates with dissipation of the membrane potential in S. aureus. Lugdunin equalizes pH gradients in artificial membrane vesicles, thereby maintaining membrane integrity, which demonstrates that proton translocation is the mode of action (MoA). The incorporation of extra tryptophan or propargyl moieties further expands the diversity of this class of thiazolidine cyclopeptides.*

Infectious diseases caused by antibiotic-resistant bacteria are an increasing health problem worldwide, especially the fast dissemination of MRSA.[1] As novel antibiotic entities have rarely been discovered in the last decade, we have an urgent need to find new structures. Numerous peptides such as daptomycin add to the great structural diversity of pharmaceutical agents. Modifications of peptide antibiotics are achieved by insertion of particular moieties, for example, double bonds or heterocycles, into the backbone structure. The cyclopeptide callyaerin and one of its analogues differ by a double bond, which confers constraints that correlate directly with their activity.[2] Notably, five- and six-membered carbocycles within the backbone mimic conformationally restricted β- and γ-amino acids.[3] Naturally occurring heterocycles also determine the structural flexibility of peptide macrocycles.[4] Interestingly, thiazolidine rings have not been reported as cyclopeptide components so far. During a screening approach for antibiotics using human bacterial nasal isolates,[5] lugdunin (**1**, Scheme 1) was discovered.[6] **1** is a nonribosomal cyclic peptide produced by *Staphylococcus lugdunensis* and features a thiazolidine ring as part of the backbone. **1** shows potent antimicrobial activity against pathogenic bacteria such as MRSA with a minimum inhibitory concentration (MIC) of 3.1 $\mu g\,mL^{-1}$ (3.9 μM). Furthermore, **1** mediates bactericidal effects when applied to mice after skin infection by *S. aureus*. However, the mode of action (MoA) of **1** has remained elusive.

We previously established the synthesis of **1** for the structural proof of natural lugdunin.[6] Now we present a comprehensive structure–activity relationship (SAR) study to identify the essential motifs of **1** for its antimicrobial activity. Derivatives of **1** were produced by solid-phase peptide synthesis (SPPS) on an aldehyde-generating resin. After assembly of the peptide chain and deprotection of the side chains, the linear aldehyde was released from the resin. Subsequent intramolecular heterocyclization of the C-terminal aldehyde and the N-terminal cysteine afforded the macrocycle **1** through in situ thiazolidine formation.[7] The thiazolidine, and thus **1**, exists in two interconverting and,

[*] Dr. N. A. Schilling, J. S. Saur, Dr. M. C. Konnerth, S. N. Wirtz, J. M. Beltrán-Beleña, Prof. S. Grond
Institute of Organic Chemistry, Biomolecular Chemistry
Eberhard Karls Universität Tübingen
Auf der Morgenstelle 18, 72076 Tuebingen (Germany)
E-mail: stephanie.grond@uni-tuebingen.de
Dr. A. Berscheid, Dr. A. Zipperer, Dr. B. Krismer, Prof. A. Peschel, Prof. H. Brötz-Oesterhelt
Interfaculty Institute of Microbiology and Infection Medicine
German Center for Infection research (DZIF)
Eberhard Karls Universität Tübingen
72076 Tuebingen (Germany)
J. Schumacher, Prof. C. Steinem
Institute of Organic and Biomolecular Chemistry
Georg August Universität Göttingen
37077 Goettingen (Germany)
Dr. H. Kalbacher
Interfaculty Institute of Biochemistry
Eberhard Karls Universität Tübingen
72076 Tuebingen (Germany)

Supporting information (synthesis of the peptides and procedures for the assays and vesicle experiments) and the ORCID identification numbers for the authors of this article can be found under: https://doi.org/10.1002/anie.201901589.

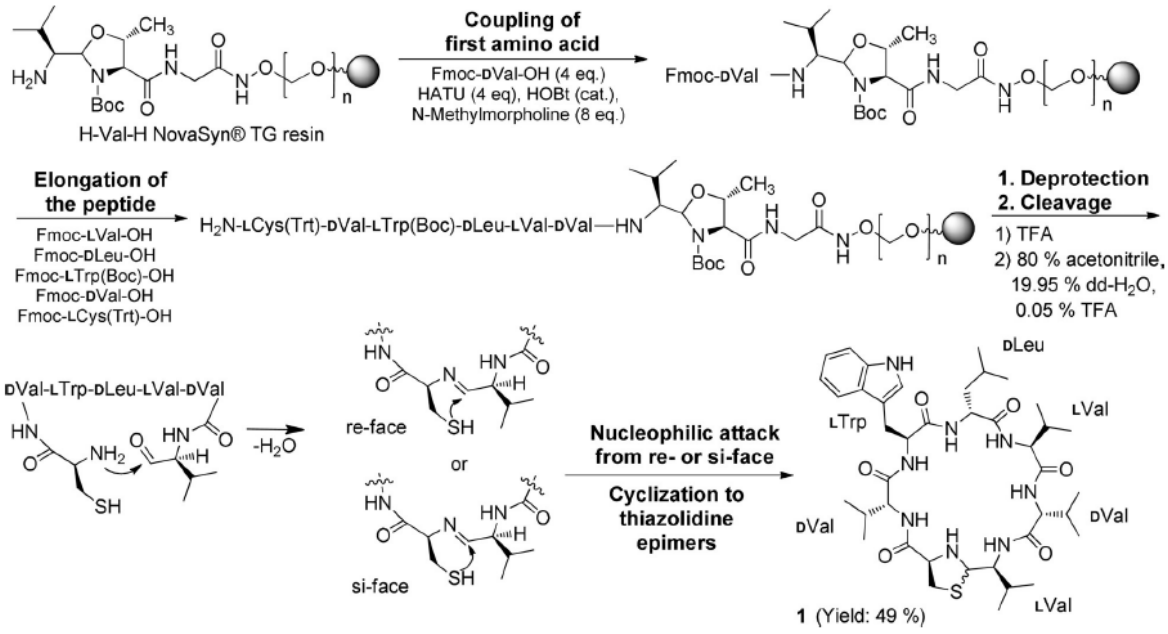

Scheme 1. Solid-phase aldehyde peptide synthesis of **1**.

therefore, inseparable epimeric forms (Scheme 1). The poor coupling of consecutive valine residues (Val^5, Val^6) was addressed by peptide elongation in acetonitrile (see Figure S1 in the Supporting Information). The optimized strategy provided access to many peptides.

All the peptides were tested as crude products for activity against the MRSA strain USA300 LAC (hereafter: USA300, Table 1). During cleavage, the aldehyde α-carbon atom of the valine residue at position 7 (Val^7, Ala^7 in **8**) of the peptides partially racemized, thereby leading to mixtures of L- and D-valine or -alanine adjacent to the thiazolidine ring (see Scheme S1 and Figure S2 in the Supporting Information). Crude peptides with significant activity (MIC $\leq 50\,\mu g\,mL^{-1}$) were purified to determine the exact MIC. We suggest terming the new class of lugdunins fibupeptides (lat. fibula, clasp) to define macrocyclic peptides with a thiazolidine moiety as an "ornament clasp".

The importance of individual amino acids for the activity of **1** was revealed by an alanine scan,[8] which yielded fibupeptides **2**–**8**. Each amino acid of **1** was successively replaced by alanine with the same stereoconfiguration. Antimicrobially inactive peptide **2** neither carries a thiazolidine nor is cyclic because of the lack of cysteine. Mass spectrometry analysis of **2** showed the formation of an aldehyde-methanol adduct ($[M+MeOH]^+$, m/z 801.5232, 0.12 Δppm). This is in agreement with the finding of Enck et al. that the precursor aldehyde of tyrocidine A did not spontaneously cyclize to the imine.[9]

Consequently, cysteine and, hence, the thiazolidine ring is essential. Active alanine peptides **3**, **6**, **7**, and **8** showed MIC values of 12.5 $\mu g\,mL^{-1}$ (16.6 μM) to 25 $\mu g\,mL^{-1}$ (33.1 μM), which is a four- to eightfold reduction in the antimicrobial activity. The most pronounced impact on antibiotic efficacy was detected for the exchange of Trp^3 (**4**) and Leu^4 (**5**) for alanine. Both derivatives showed MIC values $\geq 100\,\mu g\,mL^{-1}$ and were regarded as inactive. Therefore, tryptophan and

Table 1: MIC values of peptides **1**–**25**.

	AA sequence	Differences highlighted	MIC[a]
1	(CVWLVVV)	lugdunin (lug)	3.1 (3.9)
2	AVWLVVValinal[b]	**1-Ala**-lug	≥100
3	(CAWLVVV)	**2-Ala**-lug	12.5 (16.6)
4	(CVALVVV)	**3-Ala**-lug	≥100
5	(CVWAVVV)	**4-Ala**-lug	≥100
6	(CVWLAVV)	**5-Ala**-lug	12.5 (16.6)
7	(CVWLVAV)	**6-Ala**-lug	25.0 (33.1)
8	(CVWLVVA)	**7-Ala**-lug	25.0 (33.1)
9	(CVWLVVV)	**linear** lug (-COOH)	≥100
10	$CVWLVVV_{cycl.}$	**cyclized homodetic** lug	≥100
11	(Me-CVWLVVV)	***N*-methylthiazolidine**-lug	≥100
12	(Ac-CVWLVVV)	***N*-acetylthiazolidine**-lug	≥100
13	(*homo*CVWLVVV)	**1,3-thiazinane**-lug	≥100
14	$PVWLVVV_{cycl.}$	**1-Pro homodetic** lug	≥100
15	(CVWLVVV)	**1-D**-lug	≥100
16	(CVWLVVV)	**2-L**-lug	≥100
17	(CVWLVVV)	**3-D**-lug	≥100
18	(CVWLVVV)	**4-L**-lug	≥100
19	(CVWLVVV)	**5-D**-lug	≥100
20	(CVWLVVV)	**6-L**-lug	≥100
21	(CVWLVVV)	**7-D**-lug	≥100
22	(CVWLVVV)	**enantio**-lug	3.1 (3.9)
23	(CVWLVWV)	**6-Trp**-lug	1.6 (1.8)
24	(CPraWLVWV)	**2-Pra-6-Trp**-lug	3.1 (3.9)
25	$VOLFPVOLFP_{cycl.}$	gramicidin S	6.2 (5.4)

[a] MRSA USA300 LAC (MIC in $\mu g\,mL^{-1}$ (μM). For *S. aureus* NCTC8325 MICs, see Table S3). Single-letter codes for amino acids, brackets indicate cyclic structure (cyclization via thiazolidine), *cycl.* indicates cyclization via the peptide bond, underlined letters represent D-amino acids. [b] Detected as $[M+MeOH]^+$ by ESI-MS, Ala = alanine, Pro = proline, Trp = tryptophan, Pra = propargylglycine.

leucine are crucial for the antibacterial activity, whereas valine versus alanine exchanges are well-tolerated. However, the different activities of **3**, **6**, **7**, and **8** imply a distinct relevance of each valine.

The importance of the thiazolidine ring was investigated, starting with the linear lugdunin peptide **9** (Figure 1). Intramolecular cyclization of **9** yielded homodetic analogue **10** in which the ring is composed exclusively of normal peptide

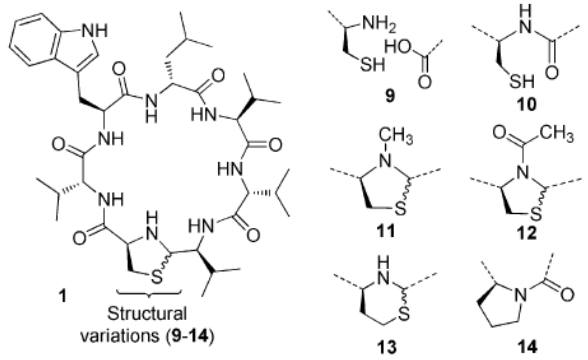

Figure 1. Structure of lugdunin (**1**) and analogues **9–14**.

bonds. Both peptides were inactive against USA300. In addition, the role of the thiazolidine NH proton was addressed by replacing it by a tertiary amine through methylation (**11**) and acetylation (**12**). **11** and **12** are inactive as antibacterial agents, thus demonstrating the indispensability of the secondary amine of the thiazolidine ring. We speculate that the basicity of the thiazolidine amine or its three-dimensional structure are responsible for the bioactivity of **1**. Inactive **13** was prepared with homocysteine to expand the heterocycle by an additional methylene group. The six-membered 1,3-thiazinane affects the structure of **1** adversely in terms of activity, even though it contains a secondary amine. Since the thiazolidine resembles an unusual 2-connected thioproline, we synthesized the proline-containing homodetic **14**, which was inactive. Thus, both, the thiazolidine ring and its secondary amine are essential for the antimicrobial activity of **1**.

The intriguing D-,L-architecture of **1** prompted us to conduct a stereo scan, while retaining the sequence and hydrophobic character of **1**. One amino acid at a time was incorporated as its enantiomer (**15**–**21**). All the diastereomers were ineffective against USA300, which demonstrates that any inversion of a stereogenic center dramatically affects the antimicrobial potency. To clarify whether the inversion of the absolute configuration of **1** also has such an impact on activity, we synthesized its enantiomer **22**. Remarkably, **22** showed identical antibiotic activity as **1**. This situation has been rarely discussed for natural products, for example, for the antiviral feglymycin[8] or the antibiotic lysocin E.[10] The insignificance of the absolute configuration of **1** suggests that the MoA does not depend on a stereospecific receptor–ligand interaction but could involve the recognition of achiral small molecules or ions.[10]

Together, these SAR studies revealed that an unsubstituted thiazolidine, tryptophan, leucine, and an alternating amino acid stereoconfiguration are essential structural motifs of **1**. Tryptophan and leucine are abundant in peptides that interact with bacterial cell membranes such as synthetic poly-(Trp-Leu)-octapeptides.[11] The necessity of tryptophan and leucine and the decrease in the activity of the less hydrophobic alanine fibupeptides **3**, **6**, **7**, and **8** pointed towards an interaction of **1** with the hydrophobic region of bacterial membranes.

A double tryptophan-containing fibupeptide (**23**) was designed to intensify the presumed interaction with the bacterial membrane. D-Tryptophan was incorporated (Trp^6) within the nonpolar flank ($DLeu^4$-$LVal^5$-$DVal^6$-$LVal^7$) of **1**. Fibupeptide **23** showed a twofold increased activity. As could be deduced from the alanine scan, position 2 shows tolerance for side-chain modification while retaining activity. Incorporation of D-propargylglycine (Pra) at this position in **23** resulted in active derivative **24**. **24** is suitable for 1,3-dipolar cycloaddition to enable the production of further analogues, preferably with activity against Gram-negative bacteria.[12]

With the knowledge that the enantiomer (**22**, Figure 2) shows activity identical to **1**, we suspected that **1** might move achiral molecules or ions across lipid membranes. This concurs with our previous observation that bacterial cells exposed to **1** stopped incorporating radioactive DNA, RNA, protein, and cell-wall precursors.[6] Thus, the influence of the active fibupeptides **1**, **3**, **22**, and **23** on the transmembrane potential of *S. aureus* NCTC8325 was compared to that of the less active or inactive **5**, **11**, and **21**. When entering the cell, the green fluorescence of the dye $DiOC_2(3)$ shifts towards a red emission because of a self-association that depends on membrane potential.[13]

All the tested peptides affected the transmembrane potential of *S. aureus* NCTC8325, in full correlation with

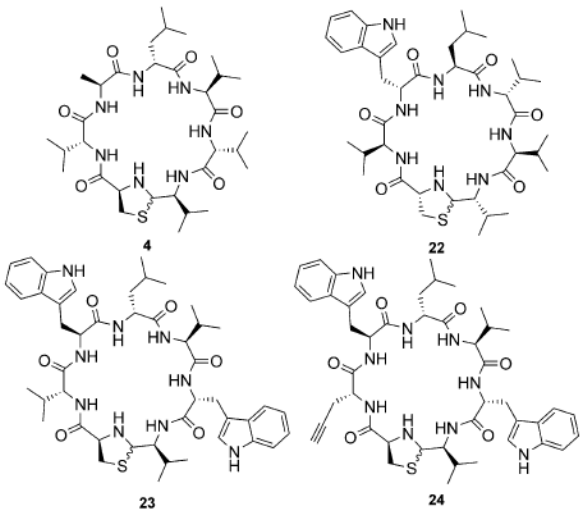

Figure 2. Exemplified derivatives of **1**. **4** is an inactive alanine analogue. The enantiomer **22** shows identical activity as **1**. **23** and **24** are specially designed analogues of **1** with twofold and equal activity, respectively.

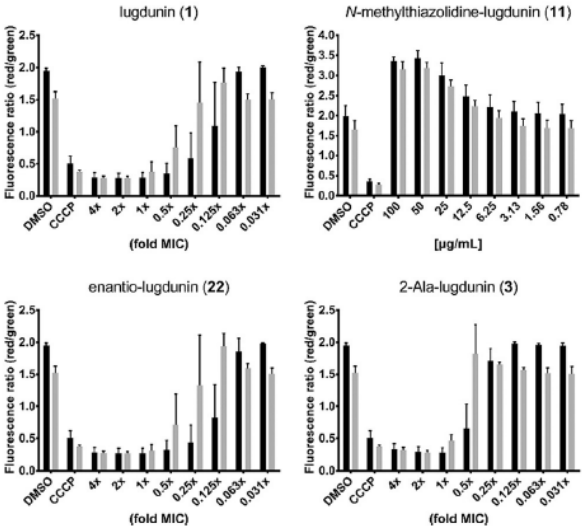

Figure 3. Effect of **1**, **11**, **22**, and **3** on the *S. aureus* NCTC8325 membrane potential after 30 (black bars) and 60 minutes (gray bars) of treatment. The protonophore CCCP (5 μM) was used as a positive and DMSO as a negative control. Error bars represent the standard deviation (SD) of two biological replicates including two technical replicates each.

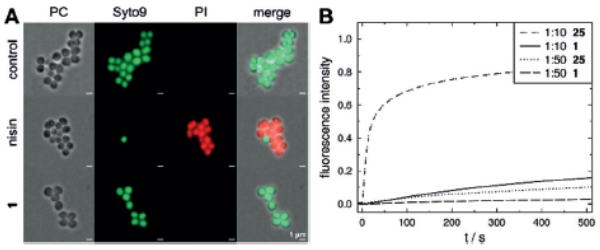

Figure 4. Complementary experiments excluding large pores or lesions. A) Fluorescence microscopy of *S. aureus* treated with pore-forming nisin (1–2 × MIC) or **1** (10 × MIC). Scale bars: 1 μm. B) Time course of normalized CF leakage from POPC vesicles, induced by **25** and **1** at concentrations of 5 μM and 1 μM (P/L 1:10 and 1:50).

their MIC values, and in a concentration-dependent manner (Figure 3, see also Figure S11 and Table S3 in the Supporting Information). Partial membrane depolarization occurred at concentrations slightly below the MIC (0.125–0.5 × MIC), while inactive **11** showed no effect. This is in accordance with the parallel cessation of all biosynthetic pathways and indicates a MoA involving impairment of membrane integrity or ion leakage/transport.

Remarkably, **1** does not tolerate amino acids with polar (Ser, Thr) or protonated (Lys) side chains without losing bioactivity—in contrast to common peptides that disrupt the membrane potential such as gramicidin A.

To analyze the effects on bacterial membranes, we treated *S. aureus* with **1** and subsequently added a mixture of the dyes Syto9 and propidium iodide (PI) to the cells as an indicator for pore formation. The red-fluorescent PI can only cross the cytoplasmic membrane through large pores or lesions. Treatment with **1** up to a concentration of 30 $\mu g\,mL^{-1}$ (10 × MIC) did not allow for PI entry into the *S. aureus* cells, while nisin led to a strong influx of the dye because of its ability to form large pores (Figure 4A).

We further employed unilamellar vesicles composed of POPC (1-palmitoyl-2-oleoyl-*sn*-glycero-3-phosphocholine) as a membrane model system to assess the activity of **1**. The use of artificial lipid bilayers enables the characterization of membrane activity independent of other factors such as proteins. We investigated first whether **1** impairs vesicle integrity.[14] The ability of **1** to induce release of the fluorescent dye carboxyfluorescein (CF) was compared to that of the cyclic decapeptide gramicidin S (**25**), which can destabilize membranes.[15] The dye is entrapped in vesicles in a self-quenching concentration (100 mM) and leakage results in an increase in fluorescence. In contrast to **25**, **1** induced only very slow leakage of the dye even at high concentrations (Figure 4B). This result supports the notion that **1** does not destabilize the membrane, but rather acts by translocating ions.

We investigated the ability of **1** to transport protons by using vesicles filled with the pH-sensitive fluorescent dye pyranine (HPTS).[16] A pH gradient was established across the lipid bilayer and proton transport was observed as a change in fluorescence. As proton translocation across a membrane induces a transmembrane potential that prevents further transport, the change in the internal pH value is also dependent on charge equilibration and, therefore, transport of further ions. A control experiment with the protonophore carbonyl cyanide *m*-chlorophenyl hydrazone (CCCP) and the potassium ionophore valinomycin showed that both ions have to be transported to explain rapid pH equilibration (see Figure S12 in the Supporting Information). Figure 5 shows that **1** causes rapid proton translocation at concentrations as low as 50 nM (peptide to lipid ratio (P/L) 1:1000) irrespective of the direction of the gradient. To exclude dye leakage, pyranine fluorescence was quenched outside the vesicles in a control experiment (see Figure S12 in the Supporting Information).

In this pH assay, **1** demonstrated a significantly higher proton translocation capability than **25**, whereas antimicrobially inactive **11** showed greatly reduced proton transport (Figure 5C). This finding suggests a vital role of the thiazolidine moiety in proton translocation and is in agreement with the membrane depolarization data.

In summary, we established an optimized synthesis of **1** to provide access to manifold analogues. By SAR studies, we revealed the essential motifs for antimicrobial activity, notably, the alternation of D- and L-amino acids, the presence of tryptophan and leucine, as well as the N-unsubstituted thiazolidine ring. The identical activity of the enantiomer **22** suggested that chiral recognition was not relevant for the MoA of **1**. Additionally, **1** and its analogues illustrate a strong correlation between membrane depolarization and MIC values with *S. aureus* cells. Furthermore, **1** did not induce large pores in either *S. aureus* cells or POPC vesicles and acts through proton translocation in synthetic membrane vesicles. In addition, the twofold more active **23** (Trp^6) verified these insights.

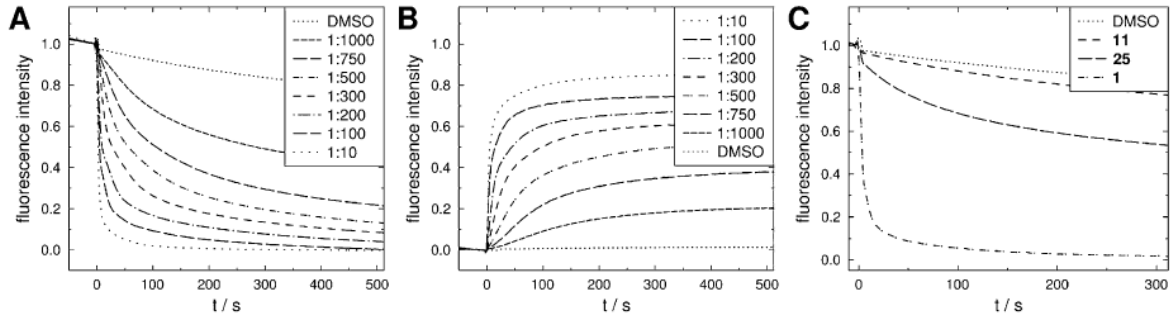

Figure 5. Time course of normalized pyranine fluorescence after addition of: A,B) 5 μM to 50 nM **1** (P/L 1:10 to 1:1000) with A) proton influx from pH 6.4 to 7.4, B) proton efflux from pH 7.4 to 8.4, C) after addition of 1 μM (P/L 1:50) **11**, **25**, and **1**, proton influx from pH 6.4 to 7.4. The vesicles were composed of POPC, total lipid concentration 50 μM containing 0.5 mM pyranine.

The active analogue **24** with a propargyl function paves the way for the production of analogues with optimized bioactivity or fluorescent properties, which will contribute to elucidating the mechanistic interaction between **1** and MRSA on the molecular level. The exact role of the vital thiazolidine ring is the focus of current investigations along with the question of whether **1** translocates protons as a mobile carrier or by channel formation.

Acknowledgements

The work of N.A.S. is supported by the Institutional Strategy of the University of Tübingen (DFG, ZUK 63). We are grateful to RTG 1708 (M.C.K., A.P., H.B.-O., S.G.) and SFB 766 (A.P., H.B.-O., S.G.) for financial support. B.K., A.P., H.B.-O., and A.B. acknowledge support through infrastructural funding from DZIF and Cluster of Excellence EXC 2124. We further acknowledge Jan Straetener and Jutta Gerber-Nolte for technical support and Pascal Rath for NMR measurements.

Conflict of interest

Eberhard Karls University Tübingen holds a patent (EP3072899B1) covering the compound lugdunin, derivatives thereof, and the bacterial infection prevention by lugdunin producing bacteria. The patent has also been filed in the USA (US2018/0155397A1).

Keywords: aldehyde peptide synthesis · methicillin-resistant *Staphylococcus aureus* · proton translocation · synthetic membrane vesicles · thiazolidine antibiotics

How to cite: *Angew. Chem. Int. Ed.* **2019**, *58*, –
Angew. Chem. **2019**, *131*, –

[1] T. R. Walsh, *Nat. Microbiol.* **2018**, *3*, 854–855.
[2] S. Zhang, L. M. De Leon Rodriguez, I. K. H. Leung, G. M. Cook, P. W. R. Harris, M. A. Brimble, *Angew. Chem. Int. Ed.* **2018**, *57*, 3631–3635; *Angew. Chem.* **2018**, *130*, 3693–3697.
[3] J. Montenegro, M. R. Ghadiri, J. R. Granja, *Acc. Chem. Res.* **2013**, *46*, 2955–2965.
[4] S. J. Kaldas, A. K. Yudin, *Chem. Eur. J.* **2018**, *24*, 7074–7082.
[5] D. Janek, A. Zipperer, A. Kulik, B. Krismer, A. Peschel, *PLoS Pathog.* **2016**, *12*, e1005812.
[6] A. Zipperer, M. C. Konnerth, C. Laux, A. Berscheid, D. Janek, C. Weidenmaier, M. Burian, N. A. Schilling, C. Slavetinsky, M. Marschal, M. Willmann, H. Kalbacher, B. Schittek, H. Brötz-Oesterhelt, S. Grond, A. Peschel, B. Krismer, *Nature* **2016**, *535*, 511–516.
[7] L. R. Malins, J. N. deGruyter, K. J. Robbins, P. M. Scola, M. D. Eastgate, M. R. Ghadiri, P. S. Baran, *J. Am. Chem. Soc.* **2017**, *139*, 5233–5241.
[8] F. Dettner, A. Hänchen, D. Schols, L. Toti, A. Nußer, R. D. Süssmuth, *Angew. Chem. Int. Ed.* **2009**, *48*, 1856–1861; *Angew. Chem.* **2009**, *121*, 1888–1893.
[9] S. Enck, F. Kopp, M. A. Marahiel, A. Geyer, *Org. Biomol. Chem.* **2010**, *8*, 559–563.
[10] M. Murai, T. Kaji, T. Kuranaga, H. Hamamoto, K. Sekimizu, M. Inoue, *Angew. Chem. Int. Ed.* **2015**, *54*, 1556–1560; *Angew. Chem.* **2015**, *127*, 1576–1580.
[11] M. R. Ghadiri, J. R. Granja, L. K. Buehler, *Nature* **1994**, *369*, 301.
[12] P. A. Smith, et al. *Nature* **2018**, *561*, 189–194.
[13] D. Novo, N. G. Perlmutter, R. H. Hunt, H. M. Shapiro, *Cytometry* **1999**, *35*, 55–63.
[14] J. N. Weinstein, R. D. Klausner, T. Innerarity, E. Ralston, R. Blumenthal, *Biochim. Biophys. Acta Biomembr.* **1981**, *647*, 270–284.
[15] M. Wenzel, M. Rautenbach, J. A. Vosloo, T. Siersma, C. H. M. Aisenbrey, E. Zaitseva, W. E. Laubscher, W. van Rensburg, J. C. Behrends, B. Bechinger, L. W. Hamoen, *mBio* **2018**, *9*, e00802-18.
[16] K. Kano, J. H. Fendler, *Biochim. Biophys. Acta Biomembr.* **1978**, *509*, 289–299.

Manuscript received: February 6, 2019
Revised manuscript received: March 13, 2019
Accepted manuscript online: May 6, 2019
Version of record online: May 27, 2019

6.2 Antimicrobial Agents and Chemotherapy, 2020

S. Krauss, A. Zipperer, S.N. Wirtz, J.S. Saur, M.C. Konnerth, S. Heilbronner, B.O. Torres Salazar, S. Grond, B. Krismer, A. Peschel

Paper 2

Secretion of and Self-Resistance to the Novel Fibupeptide Antimicrobial Lugdunin by Distinct ABC Transporters in Staphylococcus lugdunensis

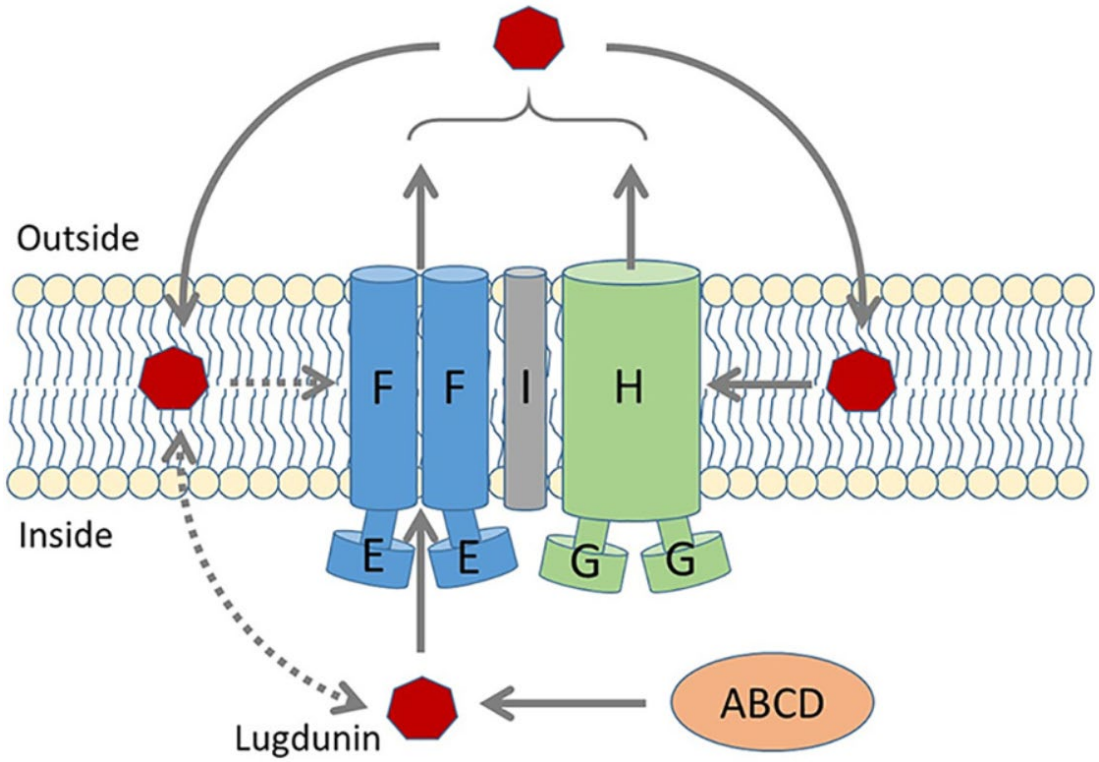

Antimicrob, Agents and Chemother, **2020**, *65*, e01734-20
https://doi.org/10.1128/AAC.01734-20

AMERICAN SOCIETY FOR MICROBIOLOGY | Antimicrobial Agents and Chemotherapy®

MECHANISMS OF RESISTANCE

Secretion of and Self-Resistance to the Novel Fibupeptide Antimicrobial Lugdunin by Distinct ABC Transporters in *Staphylococcus lugdunensis*

Sophia Krauss,[a,b,c] Alexander Zipperer,[a,b*] Sebastian Wirtz,[c,d] Julian Saur,[c,d] Martin C. Konnerth,[c,d*] Simon Heilbronner,[a,b,c] Benjamin O. Torres Salazar,[a,b,c] Stephanie Grond,[c,d] Bernhard Krismer,[a,b,c] Andreas Peschel[a,b,c]

[a]Interfaculty Institute of Microbiology and Infection Medicine, Infection Biology, University of Tübingen, Tübingen, Germany
[b]German Center for Infection Research (DZIF), Tübingen, Germany
[c]Cluster of Excellence: EXC 2124: Controlling Microbes to Fight Infection, Tübingen, Germany
[d]Institute of Organic Chemistry, University of Tübingen, Tübingen, Germany

Sophia Krauss and Alexander Zipperer contributed equally to this work. Author order was determined on the basis of ongoing employment.

ABSTRACT Lugdunin is the first reported nonribosomally synthesized antibiotic from human microbiomes. Its production by the commensal *Staphylococcus lugdunensis* eliminates the pathogen *Staphylococcus aureus* from human nasal microbiomes. The cycloheptapeptide lugdunin is the founding member of the new class of fibupeptide antibiotics, which have a novel mode of action and represent promising new antimicrobial agents. How *S. lugdunensis* releases and achieves producer self-resistance to lugdunin has remained unknown. We report that two ABC transporters encoded upstream of the lugdunin-biosynthetic operon have distinct yet overlapping roles in lugdunin secretion and self-resistance. While deletion of the *lugEF* transporter genes abrogated most of the lugdunin secretion, the *lugGH* transporter genes had a dominant role in resistance. Yet all four genes were required for full-level lugdunin resistance. The small accessory putative membrane protein LugI further contributed to lugdunin release and resistance levels conferred by the ABC transporters. Whereas LugIEFGH also conferred resistance to lugdunin congeners with inverse structures or with amino acid exchange at position 6, they neither affected the susceptibility to a lugdunin variant with an exchange at position 2 nor to other cyclic peptide antimicrobials such as daptomycin or gramicidin S. The obvious selectivity of the resistance mechanism raises hopes that it will not confer cross-resistance to other antimicrobials or to optimized lugdunin derivatives to be used for the prevention and treatment of *S. aureus* infections.

KEYWORDS ABC transporters, *Staphylococcus*, drug resistance mechanisms, natural antimicrobial products

The dynamic changes in microbiome composition are governed by multiple antagonistic or mutualistic microbial interactions (1). Several microbiome members achieve fitness benefits in competition with other bacteria through the production of bacteriocins or related antimicrobials (2, 3). The biosynthetic genes for the production of antimicrobials are located in highly variable and often mobile clusters, which usually also include genes conferring self-resistance to the producer strain (4, 5). Such mechanisms can confer resistance to a more or less narrow range of antimicrobials, thus defining the capacity of antimicrobial-producing bacterial strains to tolerate their own compound plus, potentially, those from competitors. The capacity to produce bacteriocins and related molecules has been found to be particularly abundant in micro-

Citation Krauss S, Zipperer A, Wirtz S, Saur J, Konnerth MC, Heilbronner S, Torres Salazar BO, Grond S, Krismer B, Peschel A. 2021. Secretion of and self-resistance to the novel fibupeptide antimicrobial lugdunin by distinct ABC transporters in *Staphylococcus lugdunensis*. Antimicrob Agents Chemother 65:e01734-20. https://doi.org/10.1128/AAC.01734-20.

Address correspondence to Bernhard Krismer, b.krismer@uni-tuebingen.de.

*Present address: Alexander Zipperer, Roche Innovation Center Basel, F. Hoffmann-La Roche Ltd., Roche Pharma Research & Early Development, Basel, Switzerland; Martin C. Konnerth, EMC Microcollections GmbH, Tübingen, Germany.

Received 11 August 2020
Returned for modification 14 September 2020
Accepted 15 October 2020
Accepted manuscript posted online 26 October 2020
Published 16 December 2020

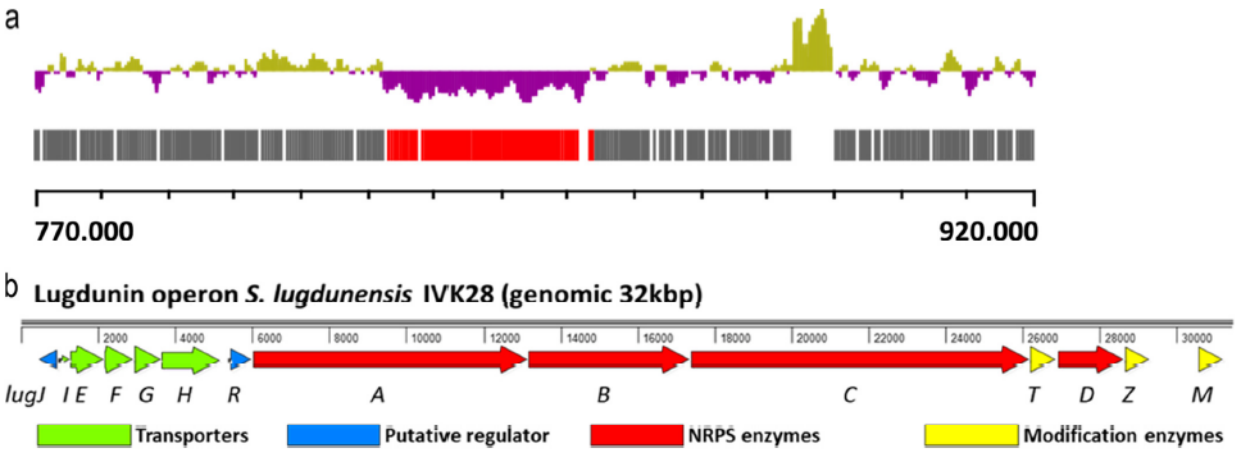

FIG 1 Decreased G+C content (a) and genetic organization (b) of the lugdunin gene cluster. *S. lugdunensis* IVK28 chromosomal section between nucleotides 770,000 and 920,000 (BioProject accession number PRJNA669000 and GenBank accession number CP063143), along with the encoded open reading frames in red (lugdunin gene cluster *lugJ* to *lugM*) and gray (other genes) and the corresponding G+C content in purple (below average; 26.7% for the lugdunin operon) and green (above average; 33.82% for the entire genome), is shown in panel a. Organization of the lugdunin gene cluster with functional assignment in different colors is shown in panel b. Protein accession numbers are listed in Table S3 in the supplemental material.

biome members from nutrient-poor habitats such as the human nose (6). We are only beginning to understand the diversity and relevance of such molecules (7).

We have recently reported that most isolates of *Staphylococcus lugdunensis*, a colonizer of the human skin and nasal mucosa, produce lugdunin, the founding member of a new class of circular antimicrobial peptides named fibupeptides (8, 9). Lugdunin is synthesized by nonribosomal peptide synthetases and inhibits target bacteria by dissipating their membrane potential, probably in a protonophore-like fashion (9). In addition to its direct antimicrobial activity, lugdunin stimulates human skin cells to produce antibacterial host defense peptides that synergize with lugdunin in the elimination of susceptible microbes (10). Lugdunin-producing *S. lugdunensis* can eradicate the major human pathogen *Staphylococcus aureus*, and nasal carriage of *S. lugdunensis* strongly reduces the rate of nasal colonization by *S. aureus* (8). The suitability of lugdunin as a potential new drug for *S. aureus* decolonization and therapy depends also on the risk of resistance development. We found that *S. aureus* cannot develop spontaneous resistance to lugdunin even after several passages in cultures with increasing subinhibitory concentrations of lugdunin (8). It has remained unclear, though, how *S. lugdunensis* achieves self-resistance to its product and if potential resistance genes could be mobilized and transferred to *S. aureus* or other pathogens.

Here, we analyzed the *lugEFGH* genes encoded next to the lugdunin biosynthesis genes and show that the four ABC transporter-encoding genes are necessary and sufficient to confer lugdunin resistance. LugEFGH and the accessory small putative membrane protein LugI were required for both optimal secretion of endogenous lugdunin and resistance to exogenous lugdunin, and even slight changes in lugdunin structure abrogated the capacity of the ABC exporters to protect against these compounds.

RESULTS

The lugdunin gene cluster includes 13 genes, many of which encode proteins of unknown functions. The recent identification of the lugdunin gene cluster comprising the biosynthetic *lugABCD* genes and the putative regulator *lugR* (8) prompted us to elucidate the boundaries of the cluster and identify additional genes potentially involved in lugdunin synthesis, export, regulation, and self-resistance. The cluster, plus some of the adjacent genes, has a significantly lower G+C content than the rest of the chromosome (26.7 versus 33.8%, respectively), and the region spanning *lugH* and *lugR* has even less than 24% G+C (Fig. 1a), suggesting that *lugRABCD* plus nine additional

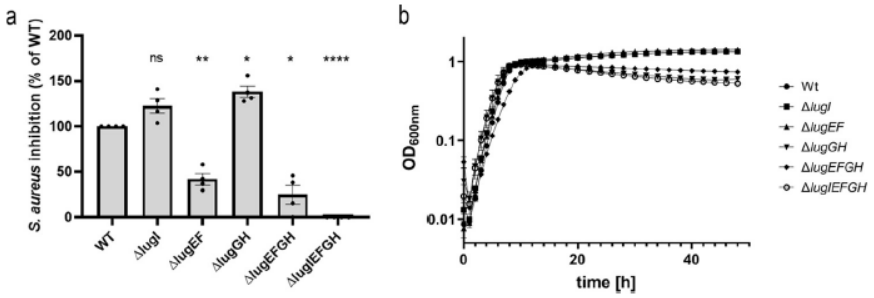

FIG 2 Impact of combinations of deletions of the *lugIEFGH* genes on *S. lugdunensis* lugdunin secretion (a) and growth (b). (a) Differences in inhibition zone distances around colonies of *S. lugdunensis* wild type (WT), set to 100%, or mutants with the indicated deletions on agar containing lugdunin-susceptible *S. aureus*. (b) Growth in broth culture of the strains shown in panel a. Means and SEM of at least 4 (panel a) or 3 (panel b) independent experiments are shown. Significant differences were calculated by one-way ANOVA (Dunnett's multiple-comparison test) (*, $P \leq 0.05$; **, $P \leq 0.01$; ***, $P \leq 0.001$; ****, $P < 0.0001$; ns, not significant).

genes form the full gene cluster (Fig. 1b). *lugD*, coding for the starter unit in lugdunin biosynthesis, is flanked by the genes encoding LugT, a putative type II thioesterase that may repair stalled peptidyl carrier protein (PCP) domains (11), and LugZ, which is homologous to 4′-phosphopantetheinyl transferases and probably converts apo-PCP to the active holo-form by attachment of the 4-phosphopantetheine cofactor (11). Further downstream, probably forming a separate transcriptional unit, *lugM* encodes a putative monooxygenase, whose role in the biosynthesis process remains unclear.

Upstream of *lugR*, five genes (*lugIEFGH*) form another operon (Fig. 1b). LugI is predicted to encode a 79-amino-acid-long integral membrane protein with two transmembrane helices and no similarity to proteins of known function (Fig. S1 in the supplemental material). LugE and LugG contain conserved Walker motifs probably representing the ATP-binding components of ABC transporter complexes (12). LugF and LugH are related to the integral membrane parts of putative ABC transporters of other *Firmicutes*, with LugF containing 6 and LugH 12 putative transmembrane segments (Fig. S1). According to the canonical architecture of ABC transporter complexes, the four proteins could form two distinct transporters, one as a LugEF homodimer and a second with a LugG homodimer linked to one LugH copy. Upstream of *lugI*, the gene *lugJ* is encoded in opposite direction, which may constitute a second regulator gene in addition to *lugR*. LugJ most likely belongs to the winged-helix type HTH-containing transcriptional regulators. Most antibiotic biosynthetic gene clusters encode proteins conferring self-resistance to the producing strain. Usually, these are either antibiotic-insensitive variants of target proteins, enzymes for the modification of target structures (e.g., rRNAs), or antibiotic exporters (13). None of the genes in the lugdunin cluster seemed to reflect the first two types of self-resistance genes, while the putative ABC transporter genes were regarded as candidates for accomplishing lugdunin secretion and self-resistance and were analyzed further.

ABC transporters encoded in the *lug* gene cluster mediate lugdunin release and confer resistance to lugdunin. To analyze a potential role of the ABC transporters in lugdunin export and self-resistance, different combinations of *lugEFGH* and the cotranscribed gene *lugI* were deleted in the lugdunin-producing strain *S. lugdunensis* IVK28. To avoid polar effects on downstream transcripts, an allelic replacement strategy with no insertion of foreign DNA fragments was used. When inhibition zones around spotted bacterial suspensions with identical diameters of the wild type and mutants on agar containing lugdunin-susceptible *S. aureus* cells were compared (Fig. 2a), the *lugIEFGH* mutant (Δ*lugIEFGH*) showed no inhibition, indicating that some or all of the five genes are required for lugdunin export. Deletion of only *lugEFGH* strongly reduced but did not abolish lugdunin release. The inhibitory distance was about 25% compared to the wild type (Fig. 2a), suggesting that LugI has a very modest but LugEFGH-

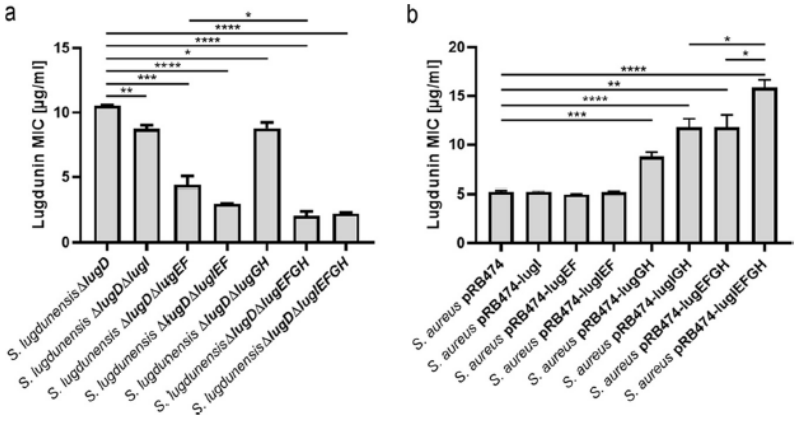

FIG 3 Impact of *lugIEFGH* deletion in the *S. lugdunensis* Δ*lugD* strain (a) or constitutive expression in *S. aureus* (b) on lugdunin susceptibility. Means and SEM of at least five independent experiments are shown. Significant differences were calculated by one-way ANOVA (Brown-Forsythe and Welsh) (*, $P \leq 0.05$; **, $P \leq 0.01$; ***, $P \leq 0.001$; ****, $P < 0.0001$).

independent role in lugdunin release. However, the sole inactivation of *lugI* caused no reduction in lugdunin release. Deletion of *lugEF* had a significant impact on the level of lugdunin export, which was almost as strong as in the Δ*lugEFGH* mutant, indicating that LugEF has a dominant role in lugdunin export. In contrast, the Δ*lugGH* mutant released even slightly larger amounts of lugdunin (about 38%) and exhibited a growth defect in liquid culture compared to the wild type (Fig. 2b), suggesting a role in resistance to lugdunin rather than export. Accordingly, the other *lugGH*-deficient mutant strains Δ*lugEFGH* and Δ*lugIEFGH* displayed similar growth defects (Fig. 2b).

To investigate the role of LugIEFGH in lugdunin self-resistance, several combinations of the genes were deleted in *S. lugdunensis* Δ*lugD*, which does not produce lugdunin (8), and the susceptibility of the resulting mutants to lugdunin was analyzed. Deletion of the entire gene set (*lugIEFGH*) strongly decreased the MIC to exogenous lugdunin from 10.5 μg/ml to 2.0 μg/ml, indicating that the genes are involved in producer self-resistance to lugdunin (Fig. 3a). Deletion of either *lugEF* or *lugGH* also led to reduced lugdunin MIC values, indicating that both ABC transporters play a role in lugdunin self-resistance. Deletion of *lugI* led to a decrease of the MIC to the identical level as the *lugGH* deletion. Deletion of *lugEF*, *lugIEF*, or *lugIEFGH* led to a stepwise MIC decrease to the lowest observed level. Δ*lugEFGH*, still expressing *lugI*, showed the same MIC level as the *lugIEFGH* mutant, indicating that although *lugI* deletion has an effect on the overall MIC level, LugI seems to rely on the presence of one of the transporters to modulate lugdunin self-resistance (Fig. 3a). The lugdunin MIC of the *S. lugdunensis lugEFGH* deletion mutant was at the same level as those of a representative panel of nasal *S. aureus* and *Staphylococcus epidermidis* strains (2.7 μg/ml on average; Fig. S2), suggesting that there is probably no additional self-resistance system involved.

To confirm the capacity of *lugIEFGH* to confer lugdunin resistance, the genes were cloned in different combinations in the pRB474 vector downstream of a constitutive promoter and introduced into *S. aureus* N315. *lugGH* expression led to a significantly increased lugdunin MIC (Fig. 3b), which confirms the important contribution of this subset of genes to lugdunin resistance. The additional expression of *lugEF* further raised the resistance of *S. aureus* to lugdunin, which supports the notion that full lugdunin resistance depends on the presence of all four ABC transporter genes. However, expression of *lugEF* alone did not cause a notable level of resistance. The presence of the entire operon *lugIEFGH* increased the lugdunin MIC to the highest observed level of 15.9 μg/ml, indicating that the small *lugI* also contributes to resistance. When *lugI* was expressed in combination with *lugEF* (pRB474-lugIEF), no increased MIC compared to *lugEF* expression alone was observed. In contrast, *lugI* expression with *lugGH*

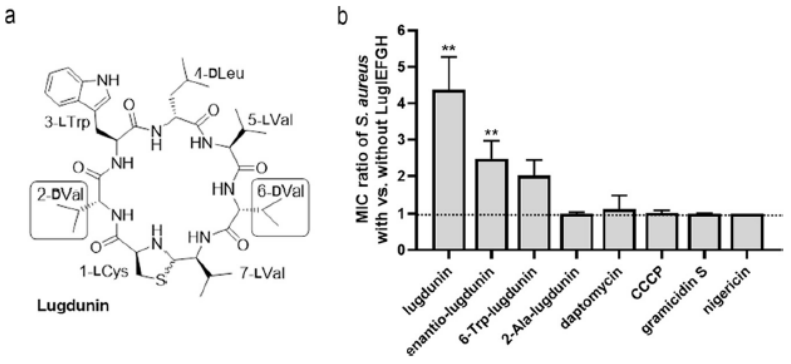

FIG 4 Impact of *lugIEFGH* on *S. aureus* susceptibility to lugdunin variants and other cyclic peptide antimicrobials. (a) Chemical structure of lugdunin and positions of alterations in derivatives used in panel b. (b) Ratios of MICs elucidated for *S. aureus* pRB474-lugIEFGH versus *S. aureus* pRB474. Means ± SEM from at least three independent experiments and significant differences between MICs for the two strains, calculated by Student's multiple unpaired *t* test (with Holm-Sidak correction) are shown (**, $P \leq 0.01$). Mean MIC values for all compounds and both strains are listed in Table S3 in the supplemental material.

(pRB474-lugIGH) enhanced the MIC to the same level as *lugEFGH* expression, indicating that LugI might have a supporting effect with LugGH rather than with LugEF. Accordingly, the exclusive expression of *lugI* did not alter the susceptibility to lugdunin. The lugdunin MIC reached in *S. aureus* pRB474-lugIEFGH was identical to or even higher than that of *S. lugdunensis* IVK28, probably as a consequence of the high plasmid copy number (Fig. 3b).

The resistance conferred by the ABC transporters LugIEFGH is largely specific for native lugdunin. While some ABC drug exporters have broad substrate specificities, others are highly selective for only certain compounds (14). The *lugIEFGH* genes were assessed for their capacity to protect *S. aureus* against lugdunin derivatives (see chemical structures 1 to 4 in Fig. S3) and other antimicrobial compounds to elucidate the transporters' substrate range. The three derivatives enantio-lugdunin, 6-Trp-lugdunin, and 2-Ala-lugdunin were selected because they had similar activities as native lugdunin. 6-Trp-lugdunin was even slightly more active than native lugdunin. Since most other lugdunin derivatives showed no or only residual activity, we could include only the two active versions (9). The constitutive expression of LugIEFGH did not affect the susceptibility of *S. aureus* to the membrane-active cyclic peptide antibiotics daptomycin and gramicidin S, or to the small nonpeptide protonophores carbonyl cyanide *m*-chlorophenylhydrazone (CCCP) and nigericin, indicating that the resistance mechanism has a strict preference for the structure of lugdunin (Fig. 4a). LugIEFGH also conferred some degree of resistance to the lugdunin enantiomer (enantio-lugdunin), which has the same structure as regular lugdunin but an inverse D-/L-amino acid configuration (8, 9), albeit with a much lower efficacy as to native lugdunin. Similar, though even less pronounced, findings were obtained with 6-Trp-lugdunin, which contains a D-tryptophan at position 6 instead of a D-valine (9). In contrast, 2-Ala-lugdunin (D-alanine instead of D-valine at position 2) (9) had equal antimicrobial activity against *S. aureus* with or without LugIEFGH, implying that no resistance against the 2-Ala congener was conferred. Thus, LugIEFGH is largely specific for lugdunin in its native structure, and lugdunin alterations at position 2 are less well tolerated by the transporter than alterations at position 6.

DISCUSSION

Lugdunin, the first nonribosomally synthesized antibiotic from human microbiomes, has a novel structure and an unusual protonophore-like mode of action, which distinguishes it from most of the antibiotics in clinical use (9). Lugdunin causes proton leakage in synthetic, protein-free membrane vesicles, suggesting that it does not need

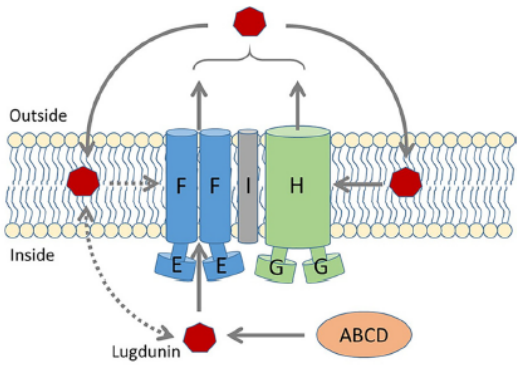

FIG 5 Model for the roles of LugIEFGH in lugdunin secretion and self-resistance. LugEF has a dominant role in lugdunin secretion and a minor role in lugdunin resistance. In contrast, LugGH is mostly responsible for self-resistance, presumably by taking lugdunin up from the membrane bilayer. LugI contributes to secretion and resistance by collaborating with the ABC transporters in a currently unclear fashion. Putative minor lugdunin passageways are shown as dashed arrows. ABCD depicts the intracellular lugdunin-biosynthetic enzymes.

to target a proteinaceous molecule to exert its antibacterial activity (9). The atypical mode of action raised the question of whether the bacterial producer strains would also use an unusual mechanism to achieve self-resistance to lugdunin. As shown for other cyclic peptides, lugdunin may be able to oligomerize in membranes (15–17), which might also have an influence on its recognition by the lugdunin transporters. We demonstrate that *S. lugdunensis* uses the four ABC transporter proteins LugEFGH for lugdunin secretion and self-resistance (Fig. 5), which is reminiscent of several other antimicrobial molecule producers (2, 18). The use of two separate ABC transporters for antimicrobial secretion and self-resistance has previously been documented, for instance, for several lantibiotics and other bacteriocins (18). Moreover, the phenol-soluble modulin (PSM) peptides produced by most *Staphylococcus* species are secreted by an ABC transporter complex, which is encoded by four genes most probably forming two separate transporters, PmtAB and PmtCD (19). They confer self-resistance to PSMs and several other membrane-damaging cationic antimicrobial peptides (CAMPs) (20).

The roles of LugEF and LugGH in lugdunin export and self-resistance overlapped to some degree, which is also reminiscent of some bacteriocin-synthetic systems with two separate ABC transporters (21, 22). LugGH had a dominant role in lugdunin resistance in *S. aureus*, which was even enhanced by the presence of LugI. Accordingly, LugGH had only a weak effect on lugdunin release in *S. lugdunensis*. Although deletion of *lugGH* in *S. lugdunensis* had only a minor effect on the MIC compared to *lugEF* deletion, it had a strong impact on the growth and fitness of lugdunin-producing *S. lugdunensis*, which is in agreement with its capacity to protect the producer against its product. The *S. lugdunensis lugGH* mutant released even slightly more lugdunin than the wild type for unclear reasons, maybe as a consequence of dysregulation of the lugdunin-biosynthetic process in these highly stressed mutant bacteria. This might also be the explanation for the unexpected strong impact of *lugEF* deletion in *S. lugdunensis* on the MIC, although LugEF does not change the MIC level in *S. aureus*. As for several other ABC exporters conferring resistance to membrane-active compounds, it can be assumed that LugH takes up its cargo from the membrane bilayer by opening the channel laterally (Fig. 5). In contrast to LugGH, LugEF did not seem to affect the producer's fitness but had a dominant impact on lugdunin release, probably by acquiring lugdunin from the biosynthetic machinery (LugABCD) in the cytoplasm. Nevertheless, LugEF also contributed to lugdunin resistance, maybe by exporting excess cytoplasmic or membrane-embedded lugdunin (Fig. 5). It is currently not clear if the two transporter systems form indeed a complex together with LugI. It is possible that LugEF may be associated with the biosynthesis machinery formed by LugABCD to

directly export newly synthesized lugdunin, which, in addition to the stoichiometry of the LugIEFGH products, remains to be explored.

It remains unclear how LugI may contribute to lugdunin secretion and self-resistance, but it is obvious that its role in resistance depends on the presence of both ABC transporters. Accessory membrane proteins have been described for other ABC transporters, for instance, the *S. aureus* VraDEH system, which confers resistance to CAMPs. In addition to the ATPase VraD and the integral membrane component VraE, the system includes the small VraH protein, which is required for high-level resistance to gallidermin and daptomycin and has been denoted a "peptide resistance ABC transporter activity modulator" (23), a term also appropriate for LugI. VraH has a similar size and predicted membrane topology as LugI, but no obvious sequence similarity. Accessory integral membrane proteins are also known to complement ABC transporters secreting and conferring producer self-resistance to the lantibiotics epidermin and gallidermin (21, 22).

Only inversion of the lugdunin structure in enantio-lugdunin or a minor change at amino acid position 6 of lugdunin were tolerated by the resistance mechanism, although resistance to these congeners was much less pronounced than for native lugdunin. In contrast, changes at position 2 abrogated the capacity of LugIEFGH to confer resistance completely. The high selectivity distinguishes the lugdunin resistance mechanism from those to other antimicrobial molecules such as PSMs or from multidrug ABC exporters such as Sav1866 (24) or AbcA (25, 26). Slight modifications of lugdunin that maintain or even increase its antimicrobial activity will therefore make it difficult for LugIEFGH to neutralize such variants if they would be developed for clinical use, even if *lugIEFGH* could spread horizontally between different bacterial species. More detailed studies will be necessary to elucidate the molecular basis for the selectivity and elucidate if and which mutations in the self-resistance proteins might alter or broaden its preferences for peptide cargo.

LugIEFGH has never been found outside the *lug* operon of *S. lugdunensis*, neither in *S. aureus* nor other nasal microbiome members. Only a few members of the *Bacillales* order, mainly from the environmental or intestinal bacterial genera *Salinicoccus*, *Planococcus*, *Exiguobacterium*, or *Gracilibacillus*, harbor homologs of the *lugIEFGH* cluster, albeit without the lugdunin biosynthesis genes. Additionally, *Streptococcus mutans* genomes encode an ABC transporter with homology to LugGH, but lack LugI or LugEF homologs. Despite its lower G+C content, the *lug* gene cluster does not seem to constitute a promiscuous genetic element, which may restrict its mobility among species other than *S. lugdunensis*.

MATERIALS AND METHODS

Strains and growth conditions. The *Staphylococcus* strains used in this study were *S. aureus* N315, *S. aureus* USA300 LAC, and *S. lugdunensis* IVK28. Further strains used for MIC determination were *S. aureus* N315 with plasmids pRB474, pRB474-lugI, pRB474-lugEF, pRB474-lugIEF, pRB474-lugGH, pRB474-lugIGH, pRB474-lugEFGH, and pRB474-lugIEFGH. The construction of the plasmids is described below. *Escherichia coli* DC10B was used as the cloning host for further transformation in *S. aureus* N315 (expression of transporter genes) or *S. aureus* PS187 for subsequent phage transduction into *S. lugdunensis* IVK28 (27).

Basic medium (BM; 1% soy peptone A3 [Organotechnie SAS, France], 0.5% Ohly Kat yeast extract [Deutsche Hefewerke GmbH, Germany], 0.5% NaCl, 0.1% glucose, and 0.1% K_2HPO_4, pH 7.2) was used as the standard growth medium and for MIC determinations. If necessary, antibiotic was used at a concentration of 10 μg ml^{-1} for chloramphenicol. *E. coli* transformants were grown in lysogeny broth (LB; Lennox) medium (1% tryptone, 0.5% yeast extract, and 0.5% NaCl; Carl Roth GmbH, Germany) supplemented with 100 μg ml^{-1} ampicillin or corresponding LB agar.

To analyze growth curves, strains were grown overnight in BM with suitable antibiotics under continuous shaking at 37°C. Each strain was adjusted to an optical density at 600 nm (OD_{600}) of 1 in Mueller-Hinton broth (MHB), and 2.5 μl of the bacterial stock solutions were pipetted to 500 μl MHB in a 48-well microtiter plate. The plates were incubated for 48 h under continuous shaking in a microplate reader, and the OD_{600} was measured every 15 minutes.

Synthetic lugdunin congeners and control compounds. All synthetic lugdunin derivatives were synthesized as described elsewhere (9). Daptomycin (Cubicin) was purchased from MSD Sharp & Dohme GmbH (Haar, Germany); CCCP, gramicidin S, and nigericin were obtained from Sigma-Aldrich (now Merck, Germany).

Generation of *S. lugdunensis* IVK28 knockout mutants. DNA manipulation, isolation of plasmid DNA, and transformation of *E. coli* were performed by use of standard procedures. Enzymes for molecular

TABLE 1 Primers used for construction of *S. lugdunensis* IVK28 mutants and their verification[a]

Primer	Sequence (5′–3′)	Assignment
lugI K.O._forw1_SacI	aaa**gagctc**cgttctccacaattctc	Deletion of *lugI* (3′ of *lugJ*)
lugI K.O._rev1_NcoI	ccct**ccatgg**tcattattgataatgataatg	Deletion of *lugI* (5′ of *lugJ*)
lugI K.O._forw2_NcoI	tgat**ccatgg**aaggaggctaataaaaattgatcg	Deletion of *lugI* (5′ of *lugE*)
lugI K.O._rev2_BglII	aat**agatct**ctcatatatcagacaccaactct	Deletion of *lugI* (3′ of *lugE*)
lugJ SacI	aaa**gagctc**cgtcgttctccacaattc	Deletion of *lugIEF* or *lugIEFGH* (3′ of *lugJ*)
lugJ Acc65I u	tatc**ggtacc**cattttcaccctccattatc	Deletion of *lugIEF* or *lugIEFGH* (5′ of *lugJ*)
lugG Acc65I d	agt**ggtacc**cttacattagctgaaagcc	Deletion of *lugEF* or *lugIEF* (5′ of *lugG*)
lugG BglII	gctaagt**agatct**catataccaaatagcca	Deletion of *lugEF* or *lugIEF* (3′ of *lugG*)
lugJI SacI	cca**gagctc**ctaggattaacttgagagg	Deletion of *lugEF* or *lugEFGH* (3′ of *lugJ*)
lugJI Acc65I u	cct**ggtacc**ccaatacactctccctctga	Deletion of *lugEF* or *lugEFGH* (3′ of *lugI*)
lugF SacI	tta**gagctc**cacatattcttgatgatgc	Deletion of *lugGH* (5′ of *lugF*)
lugF Acc65I u	gata**ggtacc**taacacctttatcagaacc	Deletion of *lugGH* (3′ of *lugF*)
lugR Acc65I d	acaa**ggtacc**tgtagtataaaatccac	Deletion of *lugGH*, *lugEFGH*, or *lugIEFGH* (5′ of *lugR*)
lugR BglII	ctt**agatct**tttcagttatcacaacagg	Deletion of *lugGH*, *lugEFGH*, or *lugIEFGH* (3′ of *lugR*)
lugJ region down	gttttggtacctgtacatggtggtggc	5′ of *lugJ* (control)
lugR region up	cttagatcttttcagttatcacaacagg	3′ of *lugR* (control)

[a]Restriction sites used for cloning are indicated as bold letters.

cloning were obtained from Thermo Fisher Scientific and New England Biolabs. For the generation of knockout mutants, the temperature-sensitive shuttle vector pBASE6 was used, and mutants were generated by allelic replacement as described previously (28). Flanking regions of the genes to be deleted were amplified by PCR (Table 1) and ligated to shuttle vector pBASE6 after digestion with suitable restriction enzymes. Cloning was performed in *E. coli* DC10B from where sequence-verified plasmids were transferred to *S. aureus* PS187 by electroporation. Phage ϕ187 was used for transduction of *S. lugdunensis* IVK28 as described elsewhere (27). Mutations in *S. lugdunensis* were confirmed by PCR amplification of the entire *lugJIEFGH* region with control primers and analysis of the fragment sizes in comparison to the wild type. For the construction of the *lugIGH* mutant, the confirmed *lugGH* mutant was transduced with the plasmid for *lugI* deletion, and the second deletion was performed in the Δ*lugGH* background.

Expression of ABC transporter genes in *S. aureus* N315. The transporters of *S. lugdunensis* IVK28 were cloned in pRB474 as follows. For the *lugEF* construct, the primers ABC1-down and ABC2-up (Table 2) were used to amplify *lugEF*, and the primers ABC regulator forw and ABC2-up were used to amplify *lugIEF*. To express only *lugI*, the gene was amplified with primers ABC regulator forw and lugI rev (SacI). *lugGH* was generated with the primers ABC3-down and ABC4-up. For the generation of the *lugIGH* construct, the plasmid pRB474-lugGH was digested with PstI and treated with alkaline phosphatase. Here, *lugI* was amplified with the primers ABC regulator forw and lugI rev (Pst), digested with PstI, and ligated into the PstI-digested pRB474-lugGH. The correct orientation of *lugI* in front of *lugGH* was confirmed by sequencing. *lugEFGH* was generated with the primers ABC1-down and ABC4-up. The PCR fragment for *lugIEFGH* was amplified with the primers ABC regulator forw and ABC4-up. All PCR products resulting constructs pRB474-lugI, pRB474-lugEF, pRB474-lugIEF, pRB474-lugGH, pRB474-lugIGH, pRB474-lugEFGH, and pRB474-lugIEFGH were transferred into *E. coli* DC10B (29) and subsequently into *S. aureus* N315.

Analysis of lugdunin secretion. To analyze the capacity of *S. lugdunensis* IVK28 and its isogenic mutants to export lugdunin, an *S. aureus* inhibition assay was performed. *S. aureus* USA300 LAC was grown overnight in BM, and BM agar, cooled down to 50°C after autoclaving, was inoculated to a final OD of 0.00125 with this overnight culture. From this suspension, defined 15-ml agar plates with 8.4 cm diameter were poured. *S. lugdunensis* strains were grown overnight in BM, centrifuged, and washed in 1/10 volume phosphate-buffered saline (PBS) to remove residual cell-associated lugdunin. After a second centrifugation step, cultures were adjusted to an OD_{600} of 20, and 10 μl of the suspensions were spotted on the solidified BM agar plates containing *S. aureus*. After drying of the spots, the plates were incubated at 37°C for 24 h, and inhibition zones were photographed and analyzed with ImageJ software (version 1.8.0_112). For each experiment, all strains to be analyzed were spotted on the same agar plate, and the

TABLE 2 Primers used for construction of transporter expression vectors[a]

Primer (restriction site)	Sequence (5′–3′)	Amplified gene
ABC1-down (PstI)	ggacctatt**ctgcag**ttgattattggaagga	5′ of *lugE*
ABC3-down (PstI)	tgcat**ctgcag**tcattatcaagaaattc	3′ of *lugF*
ABC2-up (SacI)	tat**gagctc**ttagaatttcttgataatgact	5′ of *lugG*
ABC4-up (SacI)	tgt**gagctc**atcttctaataataag	3′ of *lugH*
ABC regulator forw (PstI)	atgtac**tgcag**cattatcattatcaataatg	5′ of *lugI*
lugI rev (SacI)	cattttattc**gagctc**ttaatctcgatc	3′ of *lugI*
lugI rev (Pst)	cattttattc**ctgcag**ttaatctcgatc	3′ of *lugI*

[a]Restriction sites used for cloning are indicated as bold letters.

inhibition zone, defined as the distance between the *S. lugdunensis* IVK28 colony and the growing *S. aureus* cells, was defined as 100%.

MIC determination. Strains used for MIC determinations were grown overnight in BM, with chloramphenicol for plasmid-containing strains, under continuous shaking at 37°C. Each strain was adjusted to OD_{600} of 0.0625 in BM. The antimicrobial molecule stock solutions were serially diluted in BM in 96-well microtiter plates. Each well with 100 μl medium, and chloramphenicol, if required, was inoculated with 2 μl of the OD_{600} of 0.0625 bacterial stock solution. The plates were incubated at 37°C for 24 h under continuous shaking (160 rpm). The OD_{600} of each well was measured with a microplate reader, and the concentration leading to a 75% growth reduction was calculated and defined as the MIC value.

Statistics. Statistical analyses were performed using GraphPad Prism 8.01. One-way analysis of variance (ANOVA) was used to compare MIC levels of individual strains against the reference strain, and *t* tests were used for the comparison of MIC levels against various compounds with or without transporter genes.

Data availability. Data for *S. lugdunensis* strain IVK28 were deposited in BioProject under accession no. PRJNA669000 and GenBank accession number CP063143.

SUPPLEMENTAL MATERIAL

Supplemental material is available online only.

SUPPLEMENTAL FILE 1, PDF file, 0.6 MB.

ACKNOWLEDGMENTS

We thank Luise Ruda, Vera Augsburger, Gabriele Hornig, Timm Schäfle, and Manuel Beltran for excellent technical support and Nadine A. Schilling for fruitful discussions.

This work was financed by grants from the German Research Foundation (TRR156 to A.P.; TRR261 and GRK1708 to S.H., S.G., and A.P.) and the German Center of Infection Research (DZIF) to B.K. and A.P.

The authors acknowledge infrastructural support by the cluster of Excellence EXC2124 Controlling Microbes to Fight Infection (CMFI).

REFERENCES

1. Krismer B, Weidenmaier C, Zipperer A, Peschel A. 2017. The commensal lifestyle of Staphylococcus aureus and its interactions with the nasal microbiota. Nat Rev Microbiol 15:675–687. https://doi.org/10.1038/nrmicro.2017.104.
2. Cotter PD, Hill C, Ross RP. 2005. Bacteriocins: developing innate immunity for food. Nat Rev Microbiol 3:777–788. https://doi.org/10.1038/nrmicro1273.
3. Otto M. 2020. Staphylococci in the human microbiome: the role of host and interbacterial interactions. Curr Opin Microbiol 53:71–77. https://doi.org/10.1016/j.mib.2020.03.003.
4. Arnison PG, Bibb MJ, Bierbaum G, Bowers AA, Bugni TS, Bulaj G, Camarero JA, Campopiano DJ, Challis GL, Clardy J, Cotter PD, Craik DJ, Dawson M, Dittmann E, Donadio S, Dorrestein PC, Entian KD, Fischbach MA, Garavelli JS, Goransson U, Gruber CW, Haft DH, Hemscheidt TK, Hertweck C, Hill C, Horswill AR, Jaspars M, Kelly WL, Klinman JP, Kuipers OP, Link AJ, Liu W, Marahiel MA, Mitchell DA, Moll GN, Moore BS, Muller R, Nair SK, Nes IF, Norris GE, Olivera BM, Onaka H, Patchett ML, Piel J, Reaney MJ, Rebuffat S, Ross RP, Sahl HG, Schmidt EW, Selsted ME, et al. 2013. Ribosomally synthesized and post-translationally modified peptide natural products: overview and recommendations for a universal nomenclature. Nat Prod Rep 30:108–160. https://doi.org/10.1039/c2np20085f.
5. Medema MH, Kottmann R, Yilmaz P, Cummings M, Biggins JB, Blin K, de Bruijn I, Chooi YH, Claesen J, Coates RC, Cruz-Morales P, Duddela S, Düsterhus S, Edwards DJ, Fewer DP, Garg N, Geiger C, Gomez-Escribano JP, Greule A, Hadjithomas M, Haines AS, Helfrich EJ, Hillwig ML, Ishida K, Jones AC, Jones CS, Jungmann K, Kegler C, Kim HU, Kötter P, Krug D, Masschelein J, Melnik AV, Mantovani SM, Monroe EA, Moore M, Moss N, Nützmann HW, Pan G, Pati A, Petras D, Reen FJ, Rosconi F, Rui Z, Tian Z, Tobias NJ, Tsunematsu Y, Wiemann P, Wyckoff E, Yan X, et al. 2015. Minimum information about a biosynthetic gene cluster. Nat Chem Biol 11:625–631. https://doi.org/10.1038/nchembio.1890.
6. Janek D, Zipperer A, Kulik A, Krismer B, Peschel A. 2016. High frequency and diversity of antimicrobial activities produced by nasal Staphylococcus strains against bacterial competitors. PLoS Pathog 12:e1005812. https://doi.org/10.1371/journal.ppat.1005812.
7. Sugimoto Y, Camacho FR, Wang S, Chankhamjon P, Odabas A, Biswas A, Jeffrey PD, Donia MS. 2019. A metagenomic strategy for harnessing the chemical repertoire of the human microbiome. Science 366:eaax9176. https://doi.org/10.1126/science.aax9176.
8. Zipperer A, Konnerth MC, Laux C, Berscheid A, Janek D, Weidenmaier C, Burian M, Schilling NA, Slavetinsky C, Marschal M, Willmann M, Kalbacher H, Schittek B, Brotz-Oesterhelt H, Grond S, Peschel A, Krismer B. 2016. Human commensals producing a novel antibiotic impair pathogen colonization. Nature 535:511–516. https://doi.org/10.1038/nature18634.
9. Schilling NA, Berscheid A, Schumacher J, Saur JS, Konnerth MC, Wirtz SN, Beltran-Belena JM, Zipperer A, Krismer B, Peschel A, Kalbacher H, Brotz-Oesterhelt H, Steinem C, Grond S. 2019. Synthetic lugdunin analogues reveal essential structural motifs for antimicrobial action and proton translocation capability. Angew Chem Int Ed Engl 58:9234–9238. https://doi.org/10.1002/anie.201901589.
10. Bitschar K, Sauer B, Focken J, Dehmer H, Moos S, Konnerth M, Schilling NA, Grond S, Kalbacher H, Kurschus FC, Gotz F, Krismer B, Peschel A, Schittek B. 2019. Lugdunin amplifies innate immune responses in the skin in synergy with host- and microbiota-derived factors. Nat Commun 10:2730. https://doi.org/10.1038/s41467-019-10646-7.
11. Kotowska M, Pawlik K. 2014. Roles of type II thioesterases and their application for secondary metabolite yield improvement. Appl Microbiol Biotechnol 98:7735–7746. https://doi.org/10.1007/s00253-014-5952-8.
12. Locher KP. 2016. Mechanistic diversity in ATP-binding cassette (ABC) transporters. Nat Struct Mol Biol 23:487–493. https://doi.org/10.1038/nsmb.3216.
13. Mungan MD, Alanjary M, Blin K, Weber T, Medema MH, Ziemert N. 2020. ARTS 2.0: feature updates and expansion of the Antibiotic Resistant Target Seeker for comparative genome mining. Nucleic Acids Res 48:W546–W552. https://doi.org/10.1093/nar/gkaa374.
14. Orelle C, Mathieu K, Jault JM. 2019. Multidrug ABC transporters in bacteria. Res Microbiol 170:381–391. https://doi.org/10.1016/j.resmic.2019.06.001.
15. De Riccardis F, Izzo I, Montesarchio D, Tecilla P. 2013. Ion transport through lipid bilayers by synthetic ionophores: modulation of activity

and selectivity. Acc Chem Res 46:2781–2790. https://doi.org/10.1021/ar4000136.
16. Duax WL, Griffin JF, Langs DA, Smith GD, Grochulski P, Pletnev V, Ivanov V. 1996. Molecular structure and mechanisms of action of cyclic and linear ion transport antibiotics. Biopolymers 40:141–155. https://doi.org/10.1002/(SICI)1097-0282(1996)40:1<141::AID-BIP6>3.0.CO;2-W.
17. Ghadiri MR, Granja JR, Buehler LK. 1994. Artificial transmembrane ion channels from self-assembling peptide nanotubes. Nature 369:301–304. https://doi.org/10.1038/369301a0.
18. Bierbaum G, Sahl HG. 2009. Lantibiotics: mode of action, biosynthesis and bioengineering. Curr Pharm Biotechnol 10:2–18. https://doi.org/10.2174/138920109787048616.
19. Chatterjee SS, Joo HS, Duong AC, Dieringer TD, Tan VY, Song Y, Fischer ER, Cheung GY, Li M, Otto M. 2013. Essential Staphylococcus aureus toxin export system. Nat Med 19:364–367. https://doi.org/10.1038/nm.3047.
20. Cheung GYC, Fisher EL, McCausland JW, Choi J, Collins JWM, Dickey SW, Otto M. 2018. Antimicrobial peptide resistance mechanism contributes to Staphylococcus aureus infection. J Infect Dis 217:1153–1159. https://doi.org/10.1093/infdis/jiy024.
21. Peschel A, Schnell N, Hille M, Entian KD, Gotz F. 1997. Secretion of the lantibiotics epidermin and gallidermin: sequence analysis of the genes gdmT and gdmH, their influence on epidermin production and their regulation by EpiQ. Mol Gen Genet 254:312–318. https://doi.org/10.1007/s004380050421.
22. Hille M, Kies S, Gotz F, Peschel A. 2001. Dual role of GdmH in producer immunity and secretion of the Staphylococcal lantibiotics gallidermin and epidermin. Appl Environ Microbiol 67:1380–1383. https://doi.org/10.1128/AEM.67.3.1380-1383.2001.
23. Popella P, Krauss S, Ebner P, Nega M, Deibert J, Gotz F. 2016. VraH is the third component of the Staphylococcus aureus VraDEH system involved in gallidermin and daptomycin resistance and pathogenicity. Antimicrob Agents Chemother 60:2391–2401. https://doi.org/10.1128/AAC.02865-15.
24. Velamakanni S, Yao Y, Gutmann DA, van Veen HW. 2008. Multidrug transport by the ABC transporter Sav1866 from Staphylococcus aureus. Biochemistry 47:9300–9308. https://doi.org/10.1021/bi8006737.
25. Costa SS, Viveiros M, Amaral L, Couto I. 2013. Multidrug efflux pumps in Staphylococcus aureus: an update. Open Microbiol J 7:59–71. https://doi.org/10.2174/1874285801307010059.
26. Yoshikai H, Kizaki H, Saito Y, Omae Y, Sekimizu K, Kaito C. 2016. Multidrug-resistance transporter AbcA secretes Staphylococcus aureus cytolytic toxins. J Infect Dis 213:295–304. https://doi.org/10.1093/infdis/jiv376.
27. Winstel V, Kuhner P, Rohde H, Peschel A. 2016. Genetic engineering of untransformable coagulase-negative staphylococcal pathogens. Nat Protoc 11:949–959. https://doi.org/10.1038/nprot.2016.058.
28. Geiger T, Francois P, Liebeke M, Fraunholz M, Goerke C, Krismer B, Schrenzel J, Lalk M, Wolz C. 2012. The stringent response of Staphylococcus aureus and its impact on survival after phagocytosis through the induction of intracellular PSMs expression. PLoS Pathog 8:e1003016. https://doi.org/10.1371/journal.ppat.1003016.
29. Monk IR, Shah IM, Xu M, Tan MW, Foster TJ. 2012. Transforming the untransformable: application of direct transformation to manipulate genetically Staphylococcus aureus and Staphylococcus epidermidis. mBio 3:e00277-11. https://doi.org/10.1128/mBio.00277-11.

6.3 Journal of Medicinal Chemistry, 2021

J.S. Saur, S.N. Wirtz, N.A. Schilling, B. Krismer, A. Peschel, S. Grond, 2021

Paper 3

Distinct Lugdunins from a New Efficient Synthesis and Broad Exploitation of Its MRSA-Antimicrobial Structure

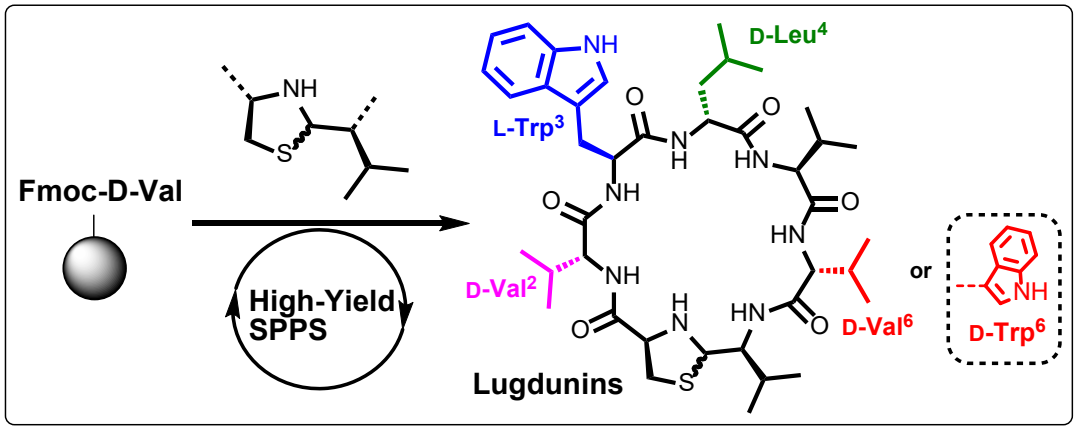

J. Med. Chem. **2021**, *64*, 7, 4034-4058
https://doi.org/10.1021/acs.jmedchem.0c02170

Journal of Medicinal Chemistry

pubs.acs.org/jmc Article

Distinct Lugdunins from a New Efficient Synthesis and Broad Exploitation of Its MRSA-Antimicrobial Structure

Julian S. Saur, Sebastian N. Wirtz, Nadine A. Schilling, Bernhard Krismer, Andreas Peschel, and Stephanie Grond*

Cite This: *J. Med. Chem.* 2021, 64, 4034–4058 Read Online

ACCESS | Metrics & More | Article Recommendations | Supporting Information

ABSTRACT: A new solid-phase peptide synthesis and bioprofiling of the antimicrobial activity of lugdunin, a fibupeptide, enable a comprehensive structure–activity relationship (SAR) study (MRSA *Staphylococcus aureus*). Distinct lugdunin analogues with variation of the three important amino acids Val^2, Trp^3, and Leu^4 are readily available based on the established high-output synthesis. This efficient synthesis concept takes advantage of the presynthesized thiazolidine building block. To gain further knowledge of SAR, D-Val^2, and D-Leu^4 were replaced with aliphatic amino acids. For L-Trp^3 derivatization, a set of non-natural aromatic amino acids with manifold substitution and annulation patterns precisely shows structural imperatives, starting from the exchange of D-Val^6 → D-Trp^6 with a 2-fold improved biological activity. D-Trp^6-lugdunin analogues with additional variation of D-Val^2 and D-Leu^4 residues were designed and synthesized followed by antimicrobial profiling. For the first time, these SAR studies deliver valuable information on the tolerance of other amino acids to D-Val^2, L-Trp^3, and D-Leu^4 in the sequence of lugdunin.

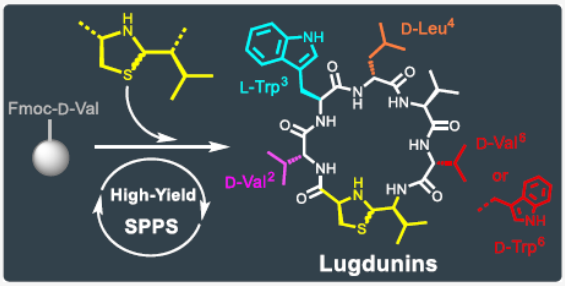

INTRODUCTION

A fundamental procedure for the derivatization of bioactive peptides in medicinal chemistry is the exchange of structurally related amino acids. First, standard proteinogenic amino acids are used to vary the peptide sequence; then, the insertion of non-natural amino acids, especially for structure–activity relationship (SAR) studies of peptidomimetics, is performed.[1,2] This approach is exemplified (Figure 1) by the linear decapeptide icatibant **1**, a bradykinin peptidomimetic and selective antagonist of bradykinin B2 receptors, which has several nonproteinogenic amino acids incorporated in its sequence.[3,4] Additionally, SAR studies of antimicrobial peptides were reported for teixobactin **2** focusing on the identification of essential structural moieties and enhanced pharmacological properties.[5,6] For gramicidin S, which belongs to the membrane-disrupting antimicrobials, the valuable optimization succeeded in terms of side-effect reduction to control its intrinsic hemolytic activity.[7] In contrast, a structure–activity study highlighted only one selected amino acid (2*S*,3*R*, 3-methyl glutamic acid) by chemical mapping for the clinically used lipopeptide antibiotic daptomycin **3** (Cubicin).[8]

Lugdunin **4** is a cyclic peptide showing promising antimicrobial potency (3.9 μM) against a wide range of Gram-positive but not Gram-negative bacteria.[9] Nonpolar **4** is biosynthesized from seven amino acids by a nonribosomal peptide synthase (NRPS), originally isolated from the human nasal commensal *Staphylococcus lugdunensis*, and represents the first member of the novel class of cyclopeptides ("fibupeptides") defined by the backbone-incorporated thiazolidine heterocycle (Figure 2). The thiazolidine heterocycle, L-tryptophan, and D-leucine were previously identified as essential structural motifs of the cyclic heptapeptide by an alanine scan. A stereo scan showed that the alternating D/L configuration is also indispensable for antimicrobial activity.[10] Studies toward the Mechanism of Action (MoA) of lugdunin with synthetic membrane vesicles revealed that lugdunin acts as a protonophore via proton translocation. The resulting membrane depolarization is postulated to correspond with the potency of lugdunin **4** to cause growth inhibition and cell death.[10]

Different from the proposed MoA of lugdunin **4** is the heterogeneous group of antimicrobial peptides (AMPs), the latter acting via rough destruction of the membrane by disruptive mechanisms.[11−15] The majority of AMPs target the membrane bilayer and cause different damaging actions such as large pore-formation, disruption of the membrane integrity,

Received: December 16, 2020
Published: March 29, 2021

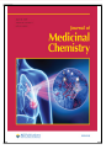

https://doi.org/10.1021/acs.jmedchem.0c02170
J. Med. Chem. 2021, 64, 4034−4058

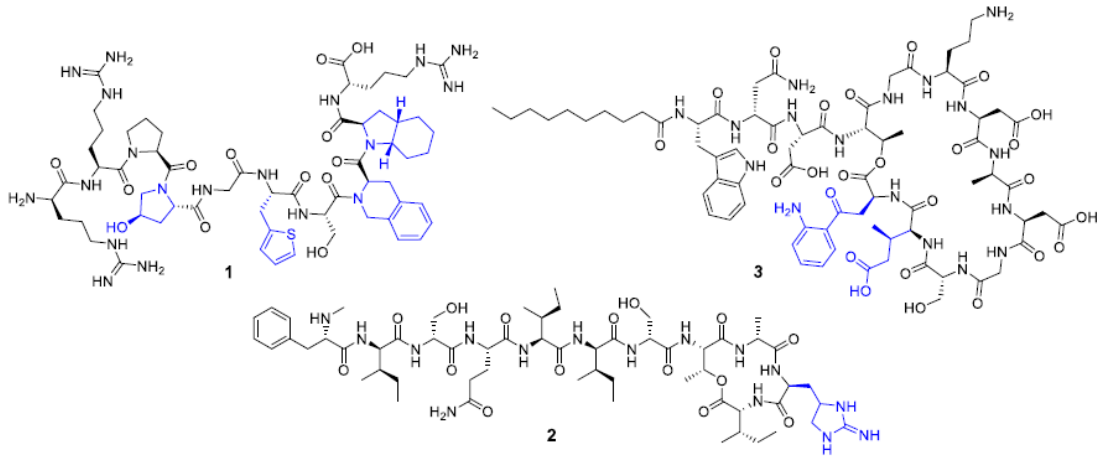

Figure 1. Chemical structures of icatibant 1, teixobactin 2, and daptomycin 3. Incorporated nonproteinogenic amino acids are highlighted in blue.

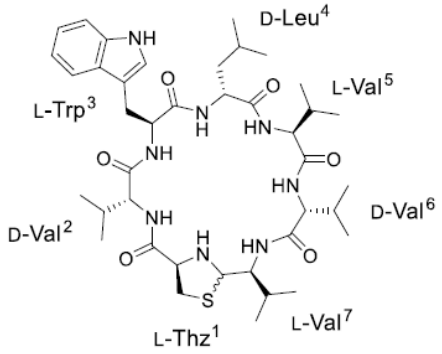

Figure 2. Chemical structure of lugdunin 4.

and membrane depolarization.[16−20] The crucial step for the antimicrobial action of AMPs is a strong membrane−peptide interaction with the lipid−water interphase, which is predominantly caused by cationic and hydrophobic residues.[21−26] Here, tryptophan plays a dominant role in the process of membrane insertion and also penetration, especially into the interfacial layer of the membrane.[27−29] The extraordinary influence of tryptophan on this action is explained by the *Janus*-faced hydrophilic and hydrophobic features.[30] The amphipathic character of tryptophan is caused by a significant quadrupole moment, which is generated by the extended π-electron system of the indole heterocycle.[31,32] The electrostatic properties of tryptophan are well known for cation−π interactions, exemplified by trp−arg, trp−lys, and trp−choline interactions.[33,34] A known SAR study for tryptophan derivatization in AMPs is indolicidin, where tryptophan was replaced by 3-(2-naphtyl)-alanine, leading to a 2-fold increased antimicrobial activity.[35,36] Moreover, the 15-residue containing bovine lactoferricin peptide was optimized in antibacterial efficiency by replacing the tryptophan indole with the sulfur analogue 3-(3-benzothienyl)-alanine.[37]

To obtain detailed chemical knowledge on the variability of structural motifs for the antimicrobial action of lugdunin, we developed a new solid-phase peptide synthesis and synthesized a diverse set of analogues focusing on the three residues D-Val,[2] L-Trp,[3] and D-Leu[4] of 4, which play an essential role in the membrane association process. The selected non-naturally occurring amino acids shed light on the yet unknown structural needs of lugdunin's structure−activity relationships as a structurally new concept of antimicrobial action.

RESULTS AND DISCUSSION

Thiazolidine Building Block Synthesis. First, we were encouraged to develop a new synthetic strategy for lugdunin 4. The synthesis of lugdunin on a resin, which generates an aldehyde during cleavage and subsequent spontaneous cyclization, has several disadvantages as demonstrated in our previous research.[10] This original synthesis provided relatively low yields (40−50%), truncation sequences (about 9%), and uncontrolled cyclization conditions with additional loss of synthetic product 4 by epimerization of L-Val.[7] The final preparative high-performance liquid chromatography (HPLC) separation of 4 from the coeluting epimers of L-Val[7] turned out ineffective, demanding individual isolated optimization for each new analogue on RP-C_{18} columns. To reliably avoid the epimerization of L-Val,[7] the new synthetic route toward 4 was

Scheme 1. Synthesis of Fmoc-Protected Thiazolidine Amino Acid 8[a]

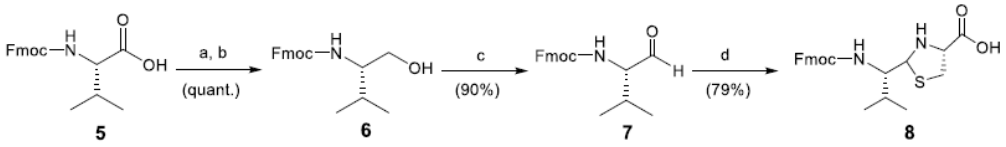

[a]Reagents and conditions: (a) Fmoc-L-Val-OH, CDI, tetrahydrofuran (THF), room temperature (rt), 15 min; (b) $NaBH_4$ in H_2O, 0 °C, 25 min; (c) Dess−Martin periodinane, 0 °C → rt, DCM, addition of 1.1 equiv. of H_2O during the first hour of the reaction, O/N; (d) L-cysteine, MeOH/H_2O (2:1), 24 h, 65 °C.

https://doi.org/10.1021/acs.jmedchem.0c02170
J. Med. Chem. 2021, 64, 4034−4058

Scheme 2. New Solid-Phase Peptide Synthesis (SPPS) Route of 4 from Linear Precursor 9 and Macrolactamization[a]

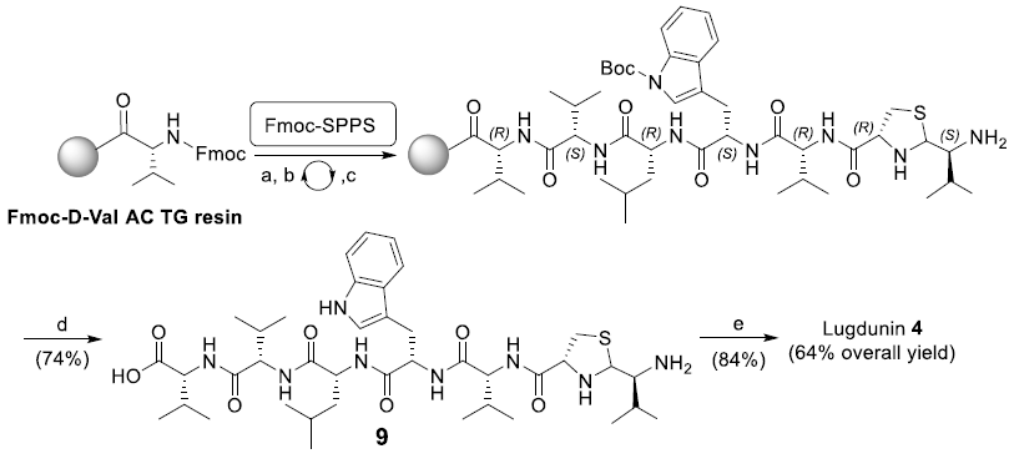

[a]Reagents and conditions: (a) Fmoc deprotection: 2% DBU/10% morpholine (*v*/*v*) in DMF, rt, 3 and 12 min; (b) double coupling: Fmoc-D/L-AA-OH, (1.) HATU, HOBt, 4-methylmorpholine (NMM), DMF, rt, 30−45 min, (2.) PyBOP, HOBt, NMM, DMF, rt, 30−45 min; (c) capping after Val[6] → Val[5] coupling: DMF/Ac_2O/Pyr (6:3:1, *v*/*v*); (d) cleavage: TFA/TIPS/H_2O (90:5:5, *v*/*v*); (e) macrolactamization: 9, HATU, HOAt, DIPEA, DMF (conc. of 9 = 2 mM), rt, 24 h.

conceived via the presynthesis of the thiazolidine heterocycle attached to L-Val[7] to the yet unknown amino acid 8, which was directly subjected to solid-phase peptide synthesis (SPPS) as a regular amino acid in the coupling sequence.

The Fmoc-L-Thz(L-Val) amino acid 8 (Scheme 1) was achieved in three steps by the reduction of the amino acid Fmoc-L-Val-OH 5 to the corresponding amino alcohol Fmoc-L-Valinol 6 with sodiumborohydrate ($NaBH_4$) under preactivation of the carboxylic acid by carbonyldiimidazole (CDI).[38] 6 was reoxidized to the corresponding aldehyde 7 by the well-established Dess−Martin periodinane (DMP).[39,40] Condensation with L-cysteine[41] yields the desired Fmoc-L-Thz(L-Val)-OH amino acid 8, which favorably precipitates during the reaction and was filtered off, ready to use for convenient Fmoc-SPPS protocols by solubilization in *N*,*N*-dimethylformamide (DMF).

Solid-phase peptide synthesis. The solid-phase peptide synthesis (SPPS) was performed on a standard, cost-efficient preloaded TentaGel S resin fused with an acid-labile 3-methoxy-4-(hydroxymethyl)-phenoxyacetic acid (MHMPA) linker (Scheme 2). In general, poly(ethylene glycol) (PEG)-based resins like TentaGel have better swelling properties compared to divinylbenzyl (DVB)-based resins in standard SPPS solvents (DMF, *N*-methyl-2-pyrrolidinone (NMP), etc.). This advantage is relevant for poorly progressing L-Val[5]−D-Val[6] couplings in the lugdunin sequence.[42−44] The tendency of lugdunin for backbone aggregation due to its high content of hydrophobic amino acid should be minimized by a good swelling PEG-based resin.[45−47] In the newly established SPPS protocol, Fmoc deprotection was achieved by treatment of the resin with a mixture of 2,3,4,6,7,8,9,10-octahydropyrimido[1,2-*a*]azepine (DBU, 2%) and morpholine (10%) in DMF, resulting in a fast and efficient Fmoc removal. A double-coupling strategy by the initial use of 1-[bis(dimethylamino)-methylene]-1*H*-1,2,3-triazolo[4,5-*b*]pyridinium 3-oxide (HATU) followed by (Benzotriazol-1-yloxy)-tripyrrolidinophosphonium hexafluorophosphate (PyBOP) was introduced to avoid truncation products. Efforts to reduce the coupling reaction to only one reagent turned out to give unfavorable truncated sequences. Furthermore, a capping step with Ac_2O/Pyr in DMF was included in the SPPS protocol after the consecutive Val[6] → Val[5] coupling to prevent shorted peptide byproducts. The resulting side-product *N*-Ac-L-Val-D-Val-OH is easily removed by basic washing after the final macrolactamization. Complete assembly of the lugdunin peptide sequence on-resin was followed by the removal of the terminal Fmoc group. The linear lugdunin heptapeptide 9 was cleaved off the resin under standardized conditions (trifluoroacetic acid (TFA)/triisopropylsilane (TIPS)/H_2O). After lyophilization, the linear peptide was immediately applied to macrolactamization under high dilution conditions of 9 (2 mM) in DMF using HATU/3-hydroxytriazolo[4,5-*b*]pyridine (HOAt)/*N*-ethyl-*N*-(propan-2-yl)propan-2-amine (DIPEA) as coupling reagents (Table S1).[48] Due to the high hydrophobicity of 4, all residual byproducts after the SPPS and macrolactamization can be extracted by polar solvents, whereas lugdunin remains in the lipophilic $CHCl_3$/*n*-BuOH phase. As a result of that procedure, 4 was obtained in high HPLC purity (>90%) and the application of further purification was renounced. Purity was determined by standard HPLC-electrospray ionization (ESI)-high-resolution mass spectrometry (HRMS)/UV with a calibration curve, and if required, the respective HPLC chromatography made pure cyclic peptides (>95%) available. This advanced convenient synthetic methodology was applied to create a large and diverse ensemble of D-Val,[2] L-Trp,[3] and D-Leu[4] lugdunin analogues (**10**−**46**).

Strategic orientation. We selected three lugdunin residues (D-Val[2], L-Trp[3], and D-Leu[4]) to gain information about the role of these amino acids on the intensity of antimicrobial action to deduce the membrane association processes of lugdunin 4. Therefore, the SAR study was designed to investigate the alteration of the anti-MRSA activity by variation of the side-chain size as well as functional groups. The residues L-Trp[3] and D-Leu[4] were determined to be "crucial" in our previously reported SAR study of lugdunin.[10] Hence, our strategy has focused on minimal variations in the amino acid pattern compared to the natural product 4. Therefore, the effect of amino acid alkyl branching was studied.

https://doi.org/10.1021/acs.jmedchem.0c02170
J. Med. Chem. 2021, 64, 4034−4058

Table 1. MIC[a] of Lugdunin 4 and Lugdunin Analogues 10–59 for *S. aureus* USA300 (LAC)

cmpd	grouped lugdunin analogues	exact sequential modification	MIC
4	natural product	lugdunin	3.1 (3.9)[9,10]
Δ^2-[D-Val] analogues of natural lugdunin			
10		Δ^2-[D-*allo*-Ile]	6.25 (7.9)
11		Δ^2-[D-Leu]	12.5 (15.7)
12		Δ^2-[D-homo Leu]	50.0 (61.7)
13		Δ^2-[D-Nva]	12.5 (16.0)
14		Δ^2-[D-Ile]	25.0 (31.4)
15		Δ^2-[D-Tle]	25.0 (31.4)
16		Δ^2-[D-Phe]	100 (120.5)
17		Δ^2-[D-Trp]	25.0 (28.8)
18		Δ2,4-[D-Leu^2-D-Val^4]	100 (127.7)
Δ^3-[L-Trp] analogues of natural lugdunin			
19		Δ^3-[L-Phe]	12.5 (16.8)
20		Δ^3-[L-Tyr]	100 (132.0)
21		Δ^3-[L-Phg]	>100 (137.2)
22		Δ^3-[L-DOPA]	>100 (129.9)
23		Δ^3-[L-His]	>100 (136.4)
24		Δ^3-[L-Phe(4-chloro)]	>100 (128.7)
25		Δ^3-[L-Phe(3-nitro)]	>100 (126.9)
26		Δ^3-[L-Phe(F_5)]	25.0 (30.0)
27		Δ^3-[L-Ala(4-pyridyl)]	>100 (134.4)
28		Δ^3-[L-Ala(4-thiazolyl)]	100 (133.3)
29		Δ^3-[L-Ala(2-furyl)]	>100 (136.4)
30		Δ^3-[L-Ala(2-thienyl)]	100 (133.5)
31		Δ^3-[L-Ala(2-benzothiazolyl)]	25.0 (31.3)
32		Δ^3-[L-Ala(3-benzothienyl)]	12.5 (15.6)
33		Δ^3-[L-Bip]	25.0 (30.5)
34		Δ^3-[L-Dip]	50.0 (61.1)
35		Δ^3-[L-pBpa]	50.0 (59.0)
36		Δ^3-[L-Ala(1-naphthyl)]	6.25 (7.9)
37		Δ^3-[L-Ala(9-anthracenyl)]	6.25 (7.4)
38		Δ^3-[L-Trp(1-*N*-Me)]	12.5 (15.7)
39		Δ^3-[L-Tic]	> 100 (132.5)
40		Δ^3-[L-Pra]	50.0 (72.4)
Δ^2-[D-Val] analogues of synthetic [D-Trp^6]-lugdunin			
41		Δ^6-[D-Trp]	1.6 (1.8)[10]
42		Δ2,6-[D-Nva^2-D-Trp^6]	6.25 (7.2)
43		Δ2,6-[D-AllylGly^2-D-Trp^6]	12.5 (14.4)
44		Δ2,6-[D-Pra^2-D-Trp^6]	3.1 (3.9)[10]
45		Δ2,6[D-Leu^2-D-Trp^6]	>100 (113.0)
46		Δ2,6-[D-Met^2-D-Trp^6]	>100 (111.0)
Δ^4-[D-Leu] analogues of natural lugdunin			
47		Δ^4-[D-Ile]	25.0 (31.9)
Δ^4-[D-Leu] analogues of synthetic [D-Trp^6]-lugdunin			
48		Δ4,6-[D-*allo*-Ile^4-D-Trp^6]	12.5 (14.4)
49		Δ4,6-[D-Tle^4-D-Trp^6]	25.0 (28.8)
50		Δ4,6-[D-Nva^4-D-Trp^6]	12.5 (14.6)
51		Δ4,6-[D-AllylGly^4-D-Trp^6]	50.0 (58.6)
52		Δ4,6-[D-Pra^4-D-Trp^6]	50.0 (58.8)
53		Δ4,6-[D-Pro^4-D-Trp^6]	>100 (117.2)
54		Δ4,6-[D-Met^4-D-Trp^6]	>100 (112.7)
55		Δ4,6-[D-Phe^4-D-Trp^6]	>100 (110.7)
56		Δ4,6-[D-Trp^4-D-Trp^6]	>100 (106.2)
57		Δ4,6-[ACPC^4-D-Trp^6]	>100 (119.2)
multiple substitution			
58		Δ2,3,6-[D-*allo*-Ile^2-L-Ala(9-anth)^3-D-Trp^6]	>100 (105.9)
59		Δ3,4,5,6-[L-Val^3-D-Val^4-L-Leu^5-D-Trp^6]	6.25 (8.0)

[a]In μg mL^{-1} (μM). Tested MIC range: 0.195–100 μg mL^{-1}. All chemical structures are represented in Figure S29.

In addition, unsaturated (alkene, alkyne) residues were incorporated to increase the polarity gradually. For L-Trp,[3] an "aromatic screening" was performed using a diverse set of (hetero-) aromatic amino acids. We aimed to obtain insights into the role of L-Trp^3 for membrane insertion and penetration. In this context, the here-presented number of unusual, non-naturally occurring amino acids was tested to obtain 24–40. The substitution of L-Trp^3 with small heterocycles of five-membered rings (furyl, thienyl, thiazolyl), large condensed aromatics (naphthyl, anthracenyl), and functionalized phenylalanine analogues was implemented. Furthermore, we addressed the more polar residues L-His, L-Tyr, and L-DOPA to increase the hydrophilicity of lugdunin. Based on this assumption, the highly sensitive D-Leu,[4] with respect to substitution, was replaced carefully by structurally related residues like norvaline, *tert*-leucine, and allylglycine to check the SARs in this region of lugdunin. For the D-Leu^4 studies (48–57), the additional substitution of D-Val^6 → D-Trp^6 was used because of the 2-fold increased activity of D-Trp^6 lugdunin 42 relative to lugdunin.[10] According to that principle, analogues of Δ^6-[D-Trp]-lugdunin (41–46) were generated by additional variation of D-Val^2 with alkyl substituents containing a different degree of branching and desaturation. The sequence inversion from L-Trp^3 → D-Val^6 59 was obtained to study the interchangeability of chemically related amino acids in the lugdunin sequence.

Val^2-, Trp^3-, and Leu^4-SAR Study of Lugdunin. More than 45 analogues were evaluated for their activity against *Staphylococcus aureus* USA300 (LAC). USA300 is a hypervirulent, multidrug-resistant variant, community-acquired, methicillin-resistant *S. aureus* (CA-MRSA) pathogen that started to spread in the United States around the millennium. It predominantly causes severe skin and soft tissue infections (SSTIs) and endovascular-associated infections (endocarditis).[49−52] Here, we report a large number of lugdunin analogues that were synthesized in the 15–25 mg scale for the first time, enabling the antimicrobial profiling and discussion of the SAR for the newly designed fibupeptides. All antimicrobial activities are summarized in Table 1 (also

https://doi.org/10.1021/acs.jmedchem.0c02170
J. Med. Chem. 2021, 64, 4034−4058

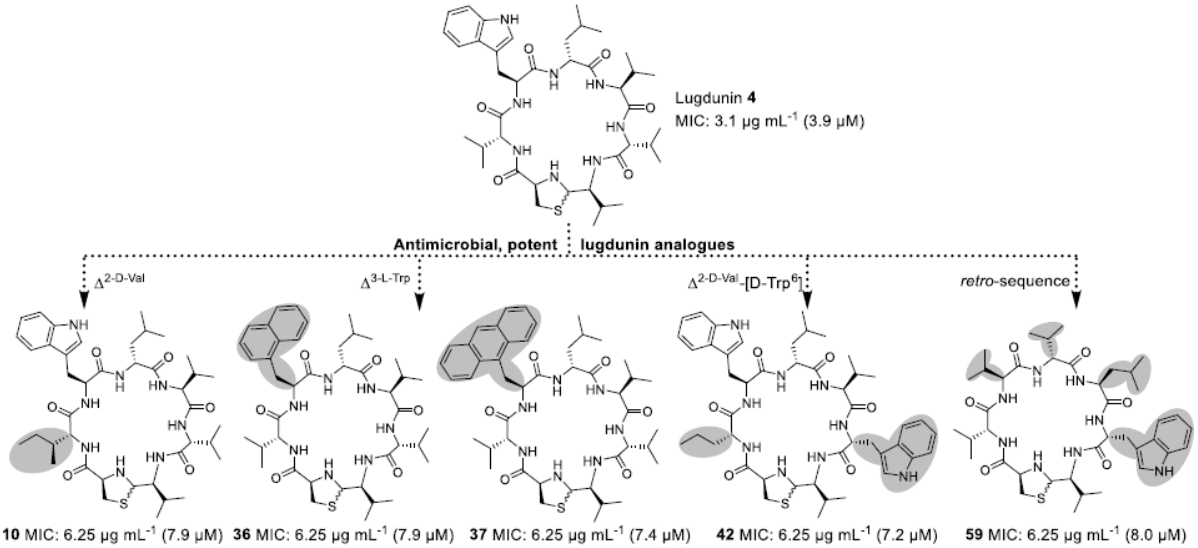

Figure 3. Lugdunins **10**, **36**, **37**, **42**, and **59** with their potent antimicrobial activities.

Table S2); among them, the most potent compounds are shown in Figure 3.

SAR Study of Lugdunin D-Val². First, D-Val² of lugdunin **4** was examined, which is adjacent to the unique thiazolidine heterocycle. The D-Val² isopropyl group was exchanged systematically by a set of eight hydrophobic aliphatic amino acids. With an additional stereo center in the side chain, **10** (Δ^2-[D-*allo*-Ile], 6.25 μg mL^{-1}; Figure 3) is a natural derivative of **4**.[9] Chemical synthesis and antimicrobial evaluation of synthetic **10** revealed the slightly lower activity relative to **4** (3.1 μg mL^{-1}). The related D-Leu² analogue **11** (12.5 μg mL^{-1}) showed a distinct loss of activity, whereas the D-homoleucine exchange in **12** resulted in reduction to 50.0 μg mL^{-1}. Compared to **12**, the debranched valeric acid variation **13** (D-Nva²; 12.5 μg mL^{-1}) with its linear alkyl side chain turned out beneficial as demonstrated by its moderate potency. An interesting finding is the slightly decreased activity of **14** (D-Ile²; 25.0 μg mL^{-1}) compared to **10** (Δ^2-[D-*allo*-Ile]), which differs only in the side-chain stereocenter. The bulkier substituents of **15** (D-Tle²; 25.0 μg mL^{-1}) and **17** (D-Trp², 25.0 μg mL^{-1}) are also barely tolerated, whereas the additional aromatic ring **16** (D-Phe²; 100 μg mL^{-1}) is absolutely detrimental to activity. The swap between the aliphatic amino acids D-Val² ↔ D-Leu⁴ in analogue **18** (100 μg mL^{-1}) resulted in no inhibitory potency. In general, prolongation, extended branching, and increased bulkiness of substituents at D-Val² of lugdunin result in reduced biological activity.

Role of Hydrophobicity in L-Trp³ Derivatization. L-Trp³ was substituted with (hetero-) aromatic amino acids, and the variations were evaluated in terms of its membrane interaction properties by *S. aureus* inhibition assays. The L-Trp³ → L-Phe³ exchange in **19** (12.5 μg mL^{-1}) reduces the activity by 4-fold, whereas the direct attachment of the phenyl unit to the peptide backbone **21** (>100 μg mL^{-1}) results in entire loss of activity. Variations with naturally occurring aromatic amino acids **20** (L-Tyr³; 100 μg mL^{-1}), **22** (DOPA³; >100 μg mL^{-1}) containing hydroxyl groups, and **23** (L-His³; >100 μg mL^{-1}) showed no antimicrobial properties. We set out to use a wider range of unusual, noncanonical, aromatic amino acids to substitute L-Trp³ and to get access to an attractive chemical diversity. The four modified phenylalanine analogues **24**–**27** containing chloro- **24** (>100 μg mL^{-1}), nitro- **25** (>100 μg mL^{-1}), pentafluoro- **26** (25.0 μg mL^{-1}), and nitrogen **27** (>100 μg mL^{-1}) substitution set the stage for the understanding that polarity or charge is not tolerated. The only analogue showing moderate activity was **26** with its pentafluoro electrostatic properties compared to **19**. The presence of one halogen atom in the phenyl ring, as in analogue **24**, led to full loss of activity. These findings indicate that polarized atoms (Cl, OH) and charges like the nitro group are not tolerated. Therefore, L-Trp³ was swapped to heterocyclic analogues **28**–**30** containing the minimized five-ring size; however, it unfortunately resulted in full loss of activity (>100 μg mL^{-1}). Returning to analogues with a higher similarity to the regular L-Trp³ structure of lugdunin **4**, we created **31** and **32** containing the previously used five-membered heterocycle thiazole and thiophene annelated with a benzene unit. Surprisingly, the activity of these two analogues dropped to a medium level, where the more hydrophobic benzothienyl analogue **32** (12.5 μg mL^{-1}) has improved activity compared to **31** (25.0 μg mL^{-1}). To study this trend of enlarged aromaticity, we tested the effect of nonfused diphenyl structures **33**–**35**. The linear arrangement of the biphenyl unit **33** (25.0 μg mL^{-1}) provided the best bioactivity in contrast to **34** (50.0 μg mL^{-1}) with the branched diphenyl arrangement and **35** (50.0 μg mL^{-1}) with the additional carbonyl function. Compared to **4**, the biological activity of **33**–**35** is significantly impaired and unfortunately does not match the anticipated diphenyl trend. The hydrophobically enhanced amino acids with annelated benzene rings **36**–**37** (Figure 3) like naphthalene- **36** (6.25 μg mL^{-1}) and anthracene side chains **37** (6.25 μg mL^{-1}) are only 2-fold less active than the natural product. Naphthalene- and anthracene amino acids have previously been used in SAR studies of immunotherapeutic peptides for cancer therapy,[53] antimicrobial and antifungal screening of hexapeptides[54] as well as for antimicrobial peptides containing unnatural amino acids.[55] Here, the lugdunin congeners with fused hydrocarbon aromatic rings

https://doi.org/10.1021/acs.jmedchem.0c02170
J. Med. Chem. 2021, 64, 4034−4058

36−37 indicate the influence of hydrophobicity on the biological activity of lugdunin. The hydrophobicity of a single amino acid is represented by its hydropathy index,[56] whereas the side-chain logP values for L-Ala(1-naphthyl) and L-Ala(9-anthracenyl) are 3.87 and 5.07, respectively.[57] We attributed the high activity of 36−37 to an enhanced transmembrane insertion capability compared to 20−30. The highly hydrophobic aromatic functionality ensures the fast association as well as insertion into the bacterial membrane, representing the initial step for membrane penetration as a protonophore. It is also evident for lugdunins 36−37 that the number of benzene units and their steric demand is less relevant for the inhibitory properties of 4. To further explore the impact of the L-Trp^3 residue, we synthesized the *N*(1)-methylated analogue 38 (12.5 μg mL^{-1}), which was 4-fold less active than 4. Obviously, the hydrogen bonding of the L-Trp^3-amine has a moderate effect on the hydrogen-bonding pattern and structural integrity for adopting the preferred conformation and interaction. Two inactive analogues of L-Trp^3-lugdunin are the C_α-bridged secondary amine 39 (>100 μg mL^{-1}) and the propargylalanine analogue 40 (50.0 μg mL^{-1}). In the case of 39, the alteration of the cyclopeptide backbone flexibility generating strong structural changes is accompanied by the loss of activity. For the side chain of 40, the significant reduction in size and the lack of aromaticity are assumed to decrease the antimicrobial activity.

Effect of Additional Trp^6 Substitution. With the observed 2-fold improved antimicrobial activity by a single D-Val^6 → D-Trp^6 exchange 41[10] (1.6 μg mL^{-1}), an extended field for lugdunin variations was created. Thus, we replaced [D-Trp^6]-lugdunin at the D-Val^2 position to achieve further decrease in the minimal inhibitory concentration. Therefore, a series of lugdunins with linear alkyl amino acids 42−44 was prepared and the degree of desaturation at position 2 was increased gradually. Here, the propargyl analogue 44[10] (D-Pra^2-D-Trp^6, 3.1 μg mL^{-1}) showed the most promising results, with a MIC similar to that of lugdunin. Also, the fully saturated norvaline analogue 42 (D-Nva^2-D-Trp^6, 6.25 μg mL^{-1}; Figure 3) revealed a doubly diminished MIC. Again, the alkene lugdunin 43 (D-AllylGly^2-D-Trp^6, 12.5 μg mL^{-1}) revealed a 2-fold stagewise reduced activity. The two analogues with extended alkyl side-chain groups 45 (D-Leu^2-D-Trp^6,> 100 μg mL^{-1}) and heteroatom 46 (D-Met^2-D-Trp^6,> 100 μg mL^{-1}) are completely inactive.

Screening of Critical Position 4 (D-Leu^4). D-Leu^4 of lugdunin (4) was proven as "essential" in the comprehensive alanine scan[10] and thereof classified as a critical residue for substitution. To address the prominent importance in dynamic membrane interactions, we opted to introduce D-Ile^4 47 (25.0 μg mL^{-1}), a structural closely related D-Leu^4 → D-Ile^4 analogue of lugdunin, showing a significant loss of activity. Ongoing from the reduced MIC of 41, we synthesized the distinct set of D-Leu^4 analogues 46−57 with D-Trp^6 instead of regular D-Val^6 to use the achieved antimicrobial improvements. Surprisingly, most of the generated analogues 53−57 were inactive: 53 (D-Pro^4; >100 μg mL^{-1}), 54 (D-Met^4; >100 μg mL^{-1}), 55 (D-Phe^4; >100 μg mL^{-1}), 56 (D-Trp^4; >100 μg mL^{-1}), and achiral cyclopropyl analogue 57 (>100 μg mL^{-1}). Also, all consecutively introduced branched amino acids, e.g., 48 (D-*allo*-Ile^4; 12.5 μg mL^{-1}) and 50 (D-Nva^4; 12.5 μg mL^{-1}), revealed a 4-fold reduced biological activity. Analogue 49 (D-Tle^4; 25.0 μg mL^{-1}) with an additional quaternary carbon center and 51 (50.0 μg mL^{-1}) and 52 (50.0 μg mL^{-1}) with a higher degree of desaturation showed an enhanced decrease in activity. We conclude that the Trp^{3}Leu^4 sequence strictly tolerates only a low alteration of polarity and charge as well as spherical demand at that position for potent activity.

Multiple Substitutions. Knowledge from the achieved single amino acid SAR study was the basis for a triple substitution derivative 58. Therefore, we merged the previous results to achieve an amplification of the antimicrobial potency. To prove this hypothesis, we synthesized 58 (D-*allo*-Ile^2, L-Ala(9-anth)^3, D-Trp^6; >100 μg mL^{-1}) with a triple exchange, in which every individual analogue showed a promising antimicrobial activity. Unfortunately, we observed no antimicrobial activity for 58 anymore.

We also point to the fact that the synthetic enantiomer of lugdunin (3.1 μg mL^{-1}) has the same antimicrobial potential as the natural parent compound lugdunin 4.[10] The here-derived hypothesis concludes that also lugdunin 59 (Figure 3) with a full *retro*-sequence under the provision of maintaining the configurations of the original lugdunin (4, (L-Cys^1•L-Val^7)^{Thz}•D-Val^6•L-Val^5•D-Leu^4•L-Trp^3•D-Val^2) shows a sound antimicrobial activity although the structure is completely different. Starting from L-Cys^1, the *retro*-lugdunin 59 sequence is read (L-Cys^1•L-Val^7)^{Thz}•D-Trp^6•L-Leu^5•D-Val^4•L-Val^3•D-Val^2 and showed a MIC value of 6.25 μg mL^{-1}, which is an only 2-fold reduced activity compared to 4. We explain the antimicrobial activity of the *retro*-lugdunin 59 by its similarity to a mirror image of lugdunin, which again nearly resembles the lugdunin enantiomer. We underline that the molecular mechanism of action of lugdunin as a protonophore in the membrane presumably has no (additional) protein target.

■ CONCLUSIONS

In summary, we here report a new and efficient total solid-phase peptide synthesis (SPPS) for the thiazolidine containing cyclopeptide lugdunin, now using a regular solid-phase resin and the new amino acid, 2(1-amino-2-methylpropyl)-thiazolidine-4-carboxylic acid. Moreover, complete antimicrobial cell assays of the distinct series of lugdunin analogues result in a comprehensive structure−activity relationship study. A three-step reaction sequence delivers the thiazolidine moiety ("Val-Thiaz") upfront, which is subsequently applied in the straightforward SPPS protocol. This optimized synthesis route was used to design lugdunin congeners in a multimilligram-scale for the three lugdunin residues D-Val^2, L-Trp^3, and D-Leu^4.

In the case of D-Leu^4, additional D-Val^6 → D-Trp^6 substitution was accomplished to take advantage of a 2-fold lowered MIC of the Δ^6-[D-Trp]-lugdunin analogue. Bioprofiling for inhibition of *S. aureus* (USA300 LAC, MRSA) with these series of analogues revealed that aliphatic replacement of D-Val^2 and D-Leu^4 is marginally tolerated for a bioactive lugdunin structure, whereas groups with higher polarity significantly reduce the biological activity. The derivatization of L-Trp^3 with five-membered heterocycles results in total loss of activity, whereas the loss of activity is much lower when fusing the heterocycle with a benzene unit. Additionally, Trp^3 can be replaced by annelated hydrophobic aromatic functionalities with only a minor loss of activity. These findings indicate that hydrophobic aromaticity is essential for L-Trp^3 of lugdunin, whereas polar or strongly polarized aromatic amino acids are not tolerated. All here-investigated residues (D-Val^2, L-Trp^3, and D-Leu^4) were not amenable to substitution with polar or even charge functionalities, underlining the

https://doi.org/10.1021/acs.jmedchem.0c02170
J. Med. Chem. 2021, 64, 4034−4058

Journal of Medicinal Chemistry pubs.acs.org/jmc Article

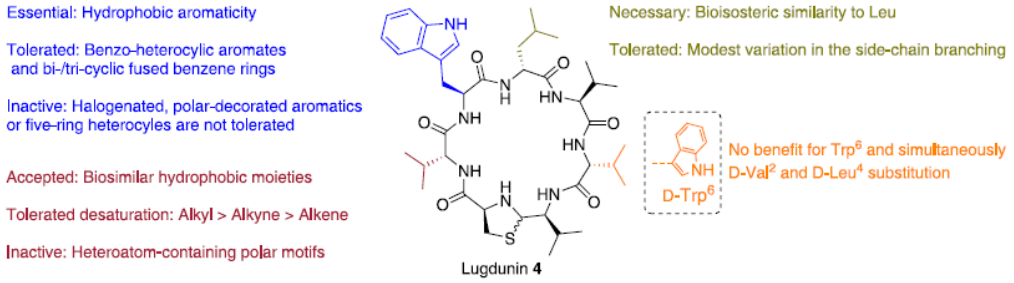

Figure 4. Summarized results of structure−activity relationship (SAR) studies of D-Val[2], L-Trp[3], D-Leu[4], and D-Val[6] of lugdunin (**4**) with respect to antimicrobial potency against Gram-positive methicillin-resistant *S. aureus*.

importance of conserved hydrophobicity as well as structural integrity of lugdunin (Figure 4).

To be effective as a protonophore, lugdunin's ability to transport protons over membranes strictly depends on the efficiency to insert and penetrate through lipid bilayers, also known as the "protonophoric effect." Therefore, our structure−activity relationship study highlighted the increased lipophilicity as a favored structural modification, demonstrating its indispensability for the proton-translocation activity of the protonophorous fibupeptide lugdunin 4.

■ EXPERIMENTAL SECTION

General Procedures. All nonaqueous reactions were performed under an atmosphere of argon, unless otherwise noted. Commercially available reagents and starting materials, especially protected amino acids, were purchased at the highest commercial quality from Sigma-Aldrich, Carbolution, abcr, Chempur, Fluorochem, Iris Biotech, or Bachem and used as received. Preloaded resins for Fmoc-SPPS were purchased from Rapp Polymers (Tuebingen). All solvents were purchased as HPLC grade and used without further purification. Reactions were monitored by analytical thin-layer chromatography (TLC) performed on Merck precoated TLC silica gel 60 F254 plate (5 cm × 10 cm). Compounds were visualized by ultraviolet fluorescence followed by staining with ninhydrin or anisaldehyde. Yields refer to lyophilized peptide analyzed by HPLC-UV-HRMS and ^{1}H NMR, unless otherwise stated. The purity of lyophilized peptide was determined by analytical reversed-phase (RP)-HPLC and ^{1}H NMR spectroscopy. The lyophilized material has a purity of >90%.

Nuclear Magnetic Resonance (NMR). Spectra were recorded at 25 or 30 °C in $(CD_3)_2SO$ or $CDCl_3$ as specified. Routine NMR spectra were recorded on a Bruker Avance-400 spectrometer operating at 400 MHz for ^{1}H nuclei and at 100 MHz for ^{13}C nuclei. All NMR spectra of lugdunin and its analogues were recorded on a Bruker AMX-600 spectrometer operating at 600 MHz for ^{1}H nuclei and at 150 MHz for ^{13}C nuclei or on a Bruker AvanceIII-700 spectrometer operating at 700 MHz for ^{1}H nuclei and at 175 MHz for ^{13}C nuclei. All chemical shifts are reported in parts per million (ppm) relative to the solvent reference peaks: $CDCl_3$ (δ_H 7.26 and δ_C 77.0) or $(CD_3)_2SO$ (δ_H 2.50 and δ_C 39.5). Coupling constants are reported in hertz. ^{1}H NMR spectra are reported as chemical shift in ppm, followed by the number of equivalent nuclei, multiplicity ("s", singlet; "d", doublet; "t", triplet; "q", quartet; "m", multiplet or a combination where necessary).

HPLC. Analytical RP-HPLC was performed on a Dionex Ultimate 3000 (Thermo Scientific) HPLC system. Column: Kromasil 100 C18 (4.0 mm × 250 mm, 5 μm; Dr. Maisch, Ammerbuch, Germany), flow rate: 0.5 mL min^{-1}, gradient: 0 min (10% B), 20 min (100% B), 25 min (100% B), eluting solvents: methanol (system B, containing 0.06% formic acid) and H_2O (system A, containing 0.1% formic acid).

LC-HR-MS. LC-MS data were recorded on a Bruker MaXis 4G ESI-QTOF mass spectrometer equipped with a Dionex Ultimate 3000 HPLC system (Thermo Scientific). HPLC instrumental setup: column: Macherey-Nagel Nucleoshell EC RP-C18 (150/2 RP18, 2.7 μm); flow rate: 0.3 mL min^{-1}; eluting solvents: methanol (system B, containing 0.06% formic acid) and H_2O (system A, containing 0.1% formic acid); gradient: 0 min (10% B), 20 min (100% B), 25 min (100% B), 26 min (10% B), 30 min (10% B). Mass spectrometer instrumental setup: electrospray ionization mass spectra (positive and negative ions) were recorded in the range of 100−1250 Da. The elemental composition was derived from the averaged mass spectra with high mass accuracy below 3 ppm. Sodium formiate was used as the internal calibrant. Nebulizer pressure of the ESI source was set to 0.4 bar with a dry gas flow of 4.0 L min^{-1} and a dry gas temperature of 200 °C. The end plate offset was 500 V, and the capillary voltage was 3000 V.

General Procedure for the Synthesis of *N*-α-(9-Fluorenylmethyloxycarbonyl)-L-valinol (6).[38] *N*-α-(9-Fluorenylmethyloxycarbonyl)-L-valine 5 (5.00 g, 14.75 mmol) was dissolved in THF (50 mL), and 1,1′-carbonyldiimidazole (3.1 g, 19.1 mmol, 1.3 equiv) was added in one portion. The solution was stirred for 15 min at room temperature and cooled down to 0 °C for 10 min. To this solution, $NaBH_4$ (945 mg, 25.0 mmol, 1.7 equiv) in water (15 mL) was injected fast and uniformly and stirred at 0 °C for 25 min. The reaction was quenched by addition of 1 N HCl (10 mL) and 50 mL of water. The reaction mixture was extracted with EtOAc (3 × 60 mL). The combined organic extracts were washed with saturated $NaHCO_3$ (3 × 100 mL) and brine (3 × 100 mL) and dried over Na_2SO_4. The solution was filtered through a thin pad of Celite, and the solvent was evaporated and vacuum-dried to give 6 as a white solid (4.78 g, 14.71 mmol, 99% yield). R_f = 0.57 (hexane/EE 1:1); ^{1}H NMR (400 MHz, $CDCl_3$): δ (ppm) 7.77 (d, J = 7.52 Hz, 2H), 7.60 (d, J = 7.45 Hz, 2H), 7.48−7.28 (m, 4H), 4.87 (s, 1H), 4.54−4.32 (m, 2H), 4.22 (dd, J = 4.39, 7.98 Hz, 1H), 3.84−3.55 (m, 2H), 3.48 (d, J = 7.63 Hz, 1H), 2.42 (s, 1H), 1.86 (q, J = 6.83 Hz, 1H), 0.94 (dd, J = 6.76, 11.56 Hz, 6H). ^{13}C NMR (100 MHz, $CDCl_3$): δ (ppm) 157.2, 144.0, 141.5, 127.8, 127.2, 125.1, 120.1, 66.8, 64.0, 58.8, 47.5, 29.4, 19.6, 18.8. HRMS (ESI) calcd for $C_{20}H_{23}NO_3$: 326.1751 [M + H]$^+$, 348.1570 [M + Na]$^+$; found 326.1756 [M + H]$^+$, 348.1566 [M + Na]$^+$.

General Procedure for the Synthesis of *N*-α-(9-Fluorenylmethyloxycarbonyl)-L-valinal (7).[39,40] *N*-α-(9-Fluorenylmethyloxycarbonyl)-L-valinol 6 (4.78 g, 14.7 mmol) was dissolved in DCM (100 mL) and cooled to 0 °C in an ice-water bath. Dess−Martin periodinane (DMP, 9.3 g, 22 mmol, 1.5 equiv) was added portionwise over 10 min at 0 °C. The ice-water bath was removed after completed DMP addition, and the reaction mixture was allowed to warm to room temperature. During the first hour, water (250 μL, 1.1 equiv) was added in four portions. The reaction mixture was stirred at room temperature overnight. The reaction mixture was quenched by addition of $Na_2S_2O_3$ (4.5 g) and $NaHCO_3$ (1.5 g) in water (300 mL) and stirred for 30 min. The resulting suspension was centrifuged, and residual solids were filtered off. The phases were separated, and the organic phase was washed with 1 N $Na_2S_2O_3$ (5 × 75 mL), $KHSO_4$ 10% (v/v, 3 × 75 mL), sat. $NaHCO_3$ (3 × 75 mL), and sat. NaCl (3 × 75 mL), dried over Na_2SO_4, and evaporated to dryness to give 7 as a beige-colored solid (4.41 g, 13.65 mmol, 90%). R_f = 0.75 (hexane/EE 1:1); ^{1}H NMR (400 MHz, $CDCl_3$): δ (ppm) 9.66 (s, 1H), 7.77

https://doi.org/10.1021/acs.jmedchem.0c02170
J. Med. Chem. 2021, 64, 4034−4058

(d, J = 7.49 Hz, 2H), 7.61 (d, J = 7.40 Hz, 2H), 7.51−7.37 (m, 4H), 5.40 (s, 1H), 4.48−4.43 (m, 2H), 4.35 (dd, J = 4.34, 8.02 Hz, 1H), 4.24 (t, J = 6.98 Hz, 1H), 2.32 (m, 1H), 2.32 (q, J = 6.26 Hz, 1H), 1.04 (d, J = 6.87 Hz, 3H), 0.97 (d, J = 6.97 Hz, 3H). ^{13}C NMR (100 MHz, $CDCl_3$): δ (ppm) 199.8, 156.5, 143.9, 141.5, 127.9, 127.2, 125.2, 120.1, 67.2, 65.2, 47.3, 29.2, 19.1, 17.7. HRMS (ESI) calcd for $C_{20}H_{21}NO_3$: 324.1594 $[M + H]^+$, 346.1414 $[M + Na]^+$; found 324.1590 $[M + H]^+$, 346.1414 $[M + Na]^+$.

General Procedure for the Synthesis of Fmoc-L-Thz-(L-Val)-OH (8). *N*-α-(9-Fluorenylmethyloxycarbonyl)-L-valinal 7 (4.41 g, 13.65 mmol) and H-L-Cys-OH (4.94 g, 40.8 mmol, 3 equiv) were suspended in MeOH/H_2O (2:1, 100 mL + 50 mL). The resulting suspension was heated to 65 °C and stirred for 20 h. During the reaction, a white precipitate was formed. Methanol was removed *in vacuo*, water (100 mL) was added, and the suspension was stored at 4 °C overnight. The white precipitate was filtered and washed with an excess of water (1 L). Residual water inside the wet solid was evaporated and vacuum-dried for 48 h. The resulting solid was slurried in toluene/pentane (3:1; 45 mL + 15 mL), $CHCl_3$/THF (1:1; 30 mL + 30 mL), and IPA/acetone/pentane (1:1:1; 20 mL + 20 mL + 20 mL) and dried under a vacuum to give 8 as a white solid (4.57 g, 10.7 mmol, 79%). ^{1}H NMR (400 MHz, DMSO-d_6/TFA-d 90:10): δ (ppm) 7.85 (d, J = 7.35 Hz, 2H), 7.72 (d, J = 7.77 Hz, 2H), 7.48−7.31 (m, 4H), 4.93 (d, J = 7.10 Hz, 2H), 4.84 (m, 1H), 4.21 (q, J = 4.33 Hz, 1H), 4.01 (t, J = 6.37 Hz, 1H), 3.49−3.32 (m, 1H), 3.28−3.18 (m, 1H), 1.79 (q, J = 6.23 Hz, 1H), 0.85 (d, J = 6.87 Hz, 3H), 0.78 (d, J = 6.84 Hz, 3H). ^{13}C NMR (100 MHz, DMSO-d_6/TFA-d 90:10): δ (ppm) 168.2, 157.2, 144.3, 141.2, 128.0, 127.4, 125.7, 120.4, 66.3, 66.2, 63.0, 57.3, 47.2, 35.2, 30.2, 20.0, 17.4. HRMS (ESI) calcd for $C_{23}H_{25}N_2O_4S$: 427.1686 $[M + H]^+$, 853.3299 $[2M + Na]^+$; found 427.1689 $[M + H]^+$, 853.3269 $[2M + Na]^+$.

Solid-Phase Peptide Synthesis (SPPS). *Deprotection*: The resin was treated with a solution of 2% DBU/10% morpholine (v/v) in DMF (2 mL) for 3 and 12 min and washed with DMF (3 × 2 mL), DCM (3 × 2 mL), and DMF (3 × 2 mL). *General amino acid coupling*: A preactivated solution of protected amino acid (6 equiv), HATU (6 equiv), HOBt (6 equiv), and *N*-methylmorpholine (NMM, 8 equiv) in DMF was added to the resin and reacted for 30−45 min. The procedure was repeated using PyBOP instead of HATU as a coupling reagent. Postcoupling washing was performed with DMF (3 × 2 mL), DCM (3 × 2 mL), and DMF (3 × 2 mL). Note: The first D-Val → L-Val coupling proceeded in DMF/DCM (1:1, 2 mL) due to better resin-swelling properties of DCM and HOAt instead of HOBt to attempted higher yields. *Capping*: Pyridine/Ac_2O/DMF (1:3:6 v/v/v, 2 mL) was added to the resin and reacted for 30 min. *Cleavage*: A mixture of TFA/TIPS/H_2O (90:5:5 v/v/v, 2 mL) was added to the resin for 1 h. The procedure was repeated twice.

Solid-Phase Peptide Synthesis of Linear Lugdunin 9 and Analogues. Fmoc-D-Val AC TG resin (loading: 0.23 mmol g^{-1}; 150 mg; 34.5 μmol scale) was swollen in DMF (2 mL) for 30 min. The Fmoc group was removed by treatment with a solution of 2% DBU/10% morpholine (v/v) in DMF (2 mL) for 3 min and an additional 12 min. The resin was washed with DMF (3 × 2 mL), DCM (3 × 2 mL), and DMF (3 × 2 mL). For the first consecutive Val → Val coupling, a solution of Fmoc-L-Val-OH (6 equiv), HATU (6 equiv), HOAt (6 equiv), and NMM (8 equiv) in DMF/DCM (2 mL) was added to the resin and agitated for 30−45 min. Double-coupling was performed with PyBOP (6 equiv) for 30−45 min. The resin was washed with DMF (3 × 2 mL), DCM (3 × 2 mL), and DMF (3 × 2 mL), and unreacted resin-bound amino groups were capped by treatment with pyridine/Ac_2O/DMF (1:3:6 v/v/v, 2 mL) for 30 min. The resin was washed with DMF (3 × 2 mL), DCM (3 × 2 mL), IPA (3 × 2 mL), and DMF (3 × 2 mL). The resin-bound residue was submitted to an iterative peptide assembly (Fmoc-SPPS) using 2% DBU/10% morpholine (v/v) in DMF (2 mL, 3 and 12 min) for Fmoc deprotection and Fmoc-D/L-AA-OH (6 equiv), HATU + PyBOP (6 equiv), HOBt (6 equiv), and NMM (8 equiv) in DMF (2 mL) for 2 × 30−45 min to double-couple each amino acid. Amino acid coupling sequence: Fmoc-D-Leu-OH, Fmoc-L-Trp(Boc)-OH, Fmoc-D-Val-OH, Fmoc-L-Thz(L-Val)-OH. After full assembly of the lugdunin sequence on the solid support, the final Fmoc-protecting group was removed and the resin was washed with DMF (3 × 2 mL), DCM (3 × 2 mL), toluene (3 × 2 mL), IPA (3 × 2 mL), and Et_2O (3 × 2 mL) and dried under reduced pressure for 3 h. The peptide was cleaved by treatment with TFA/TIPS/H_2O (90:5:5 v/v/v, 2 mL) for 3 × 1 h and one washing step with TFA (2 mL) for 10 min. The solvent was removed under reduced pressure, and the linear peptides were lyophilized using tBuOH/H_2O (1:1 v/v, 10 mL). The lyophilized linear peptide 9 (26.3 mg, 25.6 μM, 74%) was subsequently used for macrolactamization without further purification.

Solid-Phase Peptide Synthesis of Linear D-Trp^6-Lugdunin Analogues. Fmoc-D-Trp(Boc) AC TG resin (loading: 0.23 mmol g^{-1}; 150 mg; 34.5 μmol scale) was swollen in DMF (2 mL) for 30 min. The Fmoc group was removed by treatment with a solution of 2% DBU/10% morpholine (v/v) in DMF (2 mL) for 3 min and an additional 12 min. The resin-bound residue was submitted to an iterative peptide assembly (Fmoc-SPPS) using 2% DBU/10% morpholine (v/v) in DMF (2 mL, 3 + 12 min) for Fmoc deprotection and Fmoc-D/L-AA_x-OH (6 equiv), HATU + PyBOP (6 equiv), HOBt (6 equiv), and NMM (8 equiv) in DMF (2 mL) for 2 × 30−45 min to double-couple each amino acid. No capping step was included in the protocol. After full assembly of linear D-Trp^6-lugdunin analogues on the solid support, the resin was washed with DMF (3 × 2 mL), DCM (3 × 2 mL), toluene (3 × 2 mL), IPA (3 × 2 mL), and Et_2O (3 × 2 mL) and dried under reduced pressure for 3 h. The peptide was cleaved by treatment with TFA/TIPS/H_2O (95:5:5 v/v/v, 2 mL) for 3 × 1 h and one washing step with TFA (2 mL) for 10 min. The solvents were removed under reduced pressure, and the linear peptides were lyophilized using *tert*-butanol/water (1:1 v/v, 10 mL). The lyophilized linear peptides were subsequently used for macrolactamization without further purification.

Macrolactamization. To a stirred solution of linear lugdunin 9 (26.3 mg, 0.026 mmol, bis-TFA salt) in DMF (10 mL) were added HOAt (21.0 mg, 0.156 mmol, 6 equiv) and DIPEA (34 μL, 0.2 mmol, 8 equiv) at room temperature. HATU (38 mg, 0.1 mmol, 4 equiv) was dissolved in DMF (3 mL) and added over 1 h to the solution containing the linear peptide. The final concentration of the linear peptide was 2 mM. The yellow solution was stirred for 24 h at room temperature. To the reaction mixture were added chloroform (20 mL), *n*-butanol (5 mL), water (30 mL), and sat. NaCl (5 mL). After phase separation, the aqueous phase was extracted with chloroform (2 × 20 mL). The combined organic extracts were washed with $KHSO_4$ (10% v/v, 4 × 35 mL), sat. $NaHCO_3$ (3 × 35 mL), ACN/H_2O (10% v/v, 2 × 35 mL), and sat. NaCl (3 × 35 mL). The solvent was removed under reduced pressure and lyophilized with *tert*-butanol/water (1:1 v/v, 10 mL). Lugdunin 4 was obtained as a white, fluffy powder (17.3 mg, 22.0 μM, 84%). ^{1}H NMR (600 MHz, DMSO-d_6): δ (ppm) 10.82 (d, J = 2.35 Hz, 1H), 10.79 (d, J = 2.39 Hz, 1H), 8.83 (d, J = 8.45 Hz, 2H), 8.62 (d, J = 8.42 Hz, 1H), 8.57−8.52 (m, 2H), 8.26 (d, J = 8.56 Hz, 1H), 8.18 (d, J = 8.48 Hz, 1H), 8.05 (d, J = 7.88 Hz, 1H), 8.01 (d, J = 9.25 Hz, 1H), 7.80 (d, J = 11.00 Hz, 1H), 7.71 (d, J = 9.35 Hz, 1H), 7.67 (d, J = 7.95 Hz, 1H), 7.59 (d, J = 8.40 Hz, 1H), 7.51 (d, J = 7.84 Hz, 1H), 7.45 (d, J = 9.36 Hz, 1H), 7.30 (d, J = 8.16 Hz, 1H), 7.28 (d, J = 8.08 Hz, 1H), 7.20 (d, J = 2.34 Hz, 1H), 7.15 (d, J = 7.39 Hz, 1H), 7.07−6.98 (m, 2H), 6.95 (dd, J = 5.82, 7.86 Hz, 2H), 4.73 (d, J = 2.17 Hz, 1H), 4.71 (d, J = 2.33 Hz, 1H), 4.61 (dd, J = 8.66, 10.61 Hz, 1H), 4.58 (t, J = 5.49 Hz, 1H), 4.54−4.45 (m, 2H), 4.43 (s, 1H), 4.42 (s, 1H), 4.41 (s, 1H), 4.39 (s, 1H), 4.24 (t, J = 9.14 Hz, 1H), 4.17 (dd, J = 8.31, 9.48 Hz, 1H), 4.09 (d, J = 8.10 Hz, 1H), 4.08−4.06 (m, 2H), 4.05 (d, J = 8.28 Hz, 1H), 4.03 (d, J = 8.44 Hz, 1H), 3.76−3.74 (m, 2H), 3.72 (d, J = 2.48 Hz, 1H), 3.71 (q, J = 1.23, 1.72 Hz, 1H), 3.69 (s, 1H), 3.68 (d, J = 6.27 Hz, 1H), 3.66 (d, J = 8.36 Hz, 1H), 3.49−3.47 (m, 1H), 3.42 (d, J = 8.37 Hz, 1H), 3.36 (td, J = 1.59, 3.83, 4.52 Hz, 1H), 3.34 (d, J = 4.47 Hz, 1H), 3.29 (s, 1H), 3.25 (s, 1H), 3.20−3.14 (m, 1H), 3.06 (dd, J = 6.35, 9.89 Hz, 1H), 3.03 (s, 3H), 2.92 (d, J = 6.52 Hz, 1H), 2.90 (s, 1H), 2.90−2.87 (m, 1H), 2.87−2.85 (m, 1H), 2.84 (s, 2H), 2.83 (s, 2H), 2.80 (s, 2H), 2.73 (d, J = 0.63 Hz, 2H), 2.69 (s, 1H), 2.62−2.61 (m, 1H), 2.59−2.55 (m, 1H), 2.55 (s, 1H), 2.54 (s, 2H), 2.53 (d, J = 2.36 Hz, 1H), 2.38 (s, 1H), 2.08 (s, 1H), 2.07 (s, 1H), 2.06−2.04 (m, 2H), 2.04−

https://doi.org/10.1021/acs.jmedchem.0c02170
J. Med. Chem. 2021, 64, 4034−4058

1.94 (m, 3H), 1.42−1.34 (m, 2H), 1.30−1.28 (m, 2H), 1.27−1.20 (m, 3H), 1.01 (q, J = 2.43 Hz, 1H), 0.98 (d, J = 6.96 Hz, 3H), 0.92 (d, J = 6.66 Hz, 3H), 0.89−0.80 (m, 30H), 0.79 (s, 3H), 0.63 (d, J = 6.65 Hz, 3H), 0.51 (d, J = 6.75 Hz, 3H), 0.45 (d, J = 6.71 Hz, 3H). ^{13}C NMR (150 MHz, DMSO-d_6): δ (ppm) 171.6, 171.6, 171.5, 171.4, 171.0, 170.8, 170.5, 170.4, 170.2, 170.1, 169.8, 169.7, 151.8, 136.1, 136.0, 129.4, 127.1, 126.9, 124.2, 123.7, 121.3, 120.7, 120.5, 118.6, 118.1, 118.0, 111.2, 111.0, 110.2, 109.5, 72.3, 72.1, 72.0, 69.7, 68.5, 65.3, 63.6, 60.5, 59.1, 57.4, 57.3, 56.9, 56.5, 54.4, 53.5, 52.8, 52.2, 50.7, 41.3, 41.1, 40.4, 38.3, 38.2, 37.6, 32.6, 32.0, 31.2, 30.7, 29.8, 29.2, 29.0, 28.5, 28.0, 26.5, 24.1, 23.9, 23.0, 22.3, 22.0, 21.7, 20.8, 19.8, 19.7, 19.5, 19.3, 19.2, 19.1, 18.7, 18.5, 18.5, 18.3, 18.1, 18.0, 17.8, 17.4, 15.2, 12.0. HRMS (ESI) calcd for $C_{40}H_{62}N_8O_6S$: 783.4586 $[M + H]^+$; found 783.4596 $[M + H]^+$. HPLC purity 98.8%, t_r = 17.2/17.7 min.

Δ^2-[D-*allo*-Ile]-lugdunin (10). Yield: 19.9 mg (72%). ^{1}H NMR (600 MHz, DMSO-d_6): δ (ppm) 10.80 (d, J = 2.29 Hz, 1H), 10.77 (d, J = 2.34 Hz, 1H), 8.83 (d, J = 8.45 Hz, 1H), 8.62 (d, J = 8.39 Hz, 1H), 8.50 (d, J = 8.30 Hz, 1H), 8.42 (d, J = 7.63 Hz, 1H), 8.21 (d, J = 8.42 Hz, 1H), 8.12 (d, J = 9.54 Hz, 1H), 8.02 (d, J = 8.25 Hz, 1H), 7.80−7.77 (m, 2H), 7.74 (d, J = 9.39 Hz, 1H), 7.69−7.65 (m, 2H), 7.52 (d, J = 7.93 Hz, 1H), 7.47 (d, J = 9.34 Hz, 1H), 7.35−7.26 (m, 3H), 7.14 (d, J = 7.34 Hz, 1H), 7.08−7.00 (m, 2H), 6.95 (d, J = 7.35 Hz, 1H), 4.74 (d, J = 4.20 Hz, 1H), 4.72 (d, J = 4.37 Hz, 1H), 4.70 (d, J = 5.28 Hz, 1H), 4.59 (dd, J = 8.70, 10.79 Hz, 1H), 4.56−4.46 (m, 2H), 4.44−4.38 (m, 2H), 4.37−4.32 (m, 2H), 4.25 (d, J = 8.97 Hz, 2H), 4.07 (td, J = 6.18, 8.00, 9.50 Hz, 2H), 3.89 (ddd, J = 6.12, 8.26, 11.57 Hz, 1H), 3.76 (td, J = 5.26, 7.23, 7.87 Hz, 1H), 3.74−3.65 (m, 2H), 3.45 (t, J = 6.13 Hz, 1H), 3.41 (dd, J = 5.11, 10.30 Hz, 1H), 3.36 (d, J = 4.26 Hz, 1H), 3.34 (d, J = 4.02 Hz, 1H), 3.25 (s, 1H), 3.19−3.13 (m, 1H), 3.08−3.03 (m, 1H), 3.02 (s, 4H), 3.00 (d, J = 6.30 Hz, 1H), 2.98 (d, J = 5.33 Hz, 1H), 2.94−2.86 (m, 2H), 2.85−2.78 (m, 2H), 2.63−2.60 (m, 2H), 2.59 (s, 1H), 2.56 (d, J = 3.57 Hz, 1H), 2.53 (s, 1H), 2.09−2.04 (m, 1H), 1.98 (d, J = 3.91 Hz, 1H), 1.93−1.86 (m, 2H), 1.55 (d, J = 6.61 Hz, 1H), 1.50−1.43 (m, 2H), 1.40 (d, J = 16.22 Hz, 1H), 1.36−1.28 (m, 2H), 1.05−1.00 (m, 2H), 0.99 (s, 3H), 0.98 (s, 3H), 0.93 (dd, J = 3.85, 6.98 Hz, 6H), 0.90−0.75 (m, 26H), 0.73 (d, J = 6.84 Hz, 3H), 0.63−0.56 (m, 9H). ^{13}C NMR (150 MHz, DMSO-d_6): δ (ppm) 171.7, 171.6, 171.5, 171.4, 171.0, 170.9, 170.6, 170.4, 170.2, 169.9, 169.8, 151.8, 136.1, 136.0, 129.4, 127.1, 126.9, 124.2, 123.7, 121.2, 120.7, 120.5, 118.6, 118.1, 118.0, 117.9, 111.2, 111.0, 110.2, 109.5, 72.3, 72.1, 72.0, 69.7, 68.5, 65.4, 63.6, 60.3, 60.2, 59.4, 59.0, 57.5, 57.2, 56.9, 56.5, 55.9, 54.5, 53.5, 52.8, 52.2, 50.7, 41.3, 41.1, 40.4, 38.2, 38.2, 37.6, 37.0, 34.9, 32.6, 32.0, 31.2, 29.8, 29.2, 29.1, 28.0, 26.4, 25.6, 25.0, 24.8, 24.1, 24.0, 23.0, 22.3, 21.7, 20.8, 19.8, 19.7, 19.5, 19.2, 19.1, 18.6, 18.3, 18.0, 17.8, 17.4, 15.2, 15.1, 14.3, 12.0, 11.2, 11.1. HRMS m/z: 797.4760 $[M + H]^+$. HPLC purity 98.7%, t_r = 17.2/17.8 min.

Δ^2-[D-Leu]-lugdunin (11). Yield: 22.1 mg (80%). ^{1}H NMR (600 MHz, DMSO-d_6): δ (ppm) 10.79 (d, J = 2.22 Hz, 1H), 8.56 (d, J = 8.30 Hz, 1H), 8.48 (d, J = 8.77 Hz, 1H), 8.21−8.10 (m, 2H), 8.06−8.01 (m, 2H), 7.83−7.76 (m, 1H), 7.70 (d, J = 8.96 Hz, 1H), 7.63 (d, J = 7.99 Hz, 1H), 7.60 (d, J = 9.26 Hz, 1H), 7.53 (d, J = 7.87 Hz, 1H), 7.46 (d, J = 9.26 Hz, 1H), 7.30 (d, J = 7.97 Hz, 1H), 7.20 (s, 1H), 7.11 (d, J = 7.98 Hz, 1H), 7.07−6.99 (m, 2H), 6.99−6.91 (m, 2H), 4.73 (d, J = 6.77 Hz, 1H), 4.66 (q, J = 3.37, 6.02 Hz, 1H), 4.53 (t, J = 9.74 Hz, 1H), 4.46 (t, J = 7.50 Hz, 1H), 4.42−4.38 (m, 2H), 4.26 (t, J = 9.12 Hz, 1H), 4.15 (s, 1H), 4.06 (d, J = 8.08 Hz, 1H), 3.98−3.93 (m, 1H), 3.86 (d, J = 7.36, 1H), 3.76 (s, 1H), 3.73−3.59 (m, 2H), 3.45−3.40 (m, 1H), 3.16 (d, J = 9.30 Hz, 1H), 3.03 (d, J = 4.95, Hz, 1H), 2.99 (d, J = 5.13 Hz, 1H), 2.92 (d, J = 9.80 Hz, 1H), 2.86−2.78 (m, 1H), 2.67−2.58 (m, 1H), 2.12−2.06 (m, 1H), 2.03−1.87 (m, 3H), 1.55 (d, J = 6.66 Hz, 1H), 1.32 (d, J = 7.13, Hz, 1H), 1.20−1.14 (m, 2H), 1.03 (d, J = 6.49 Hz, 3H), 0.92 (d, J = 6.71 Hz, 3H), 0.88−0.84 (m, 12H), 0.82 (d, J = 8.24 Hz, 3H), 0.79 (d, J = 5.17 Hz, 3H), 0.76 (d, J = 6.30 Hz, 3H), 0.74 (s, 3H), 0.72 (s, 3H), 0.69 (d, J = 9.71 Hz, 3H), 0.55 (d, J = 6.69 Hz, 3H). ^{13}C NMR (150 MHz, DMSO-d_6): δ (ppm) 172.1, 171.8, 171.5, 171.5, 171.0, 170.8, 170.4, 170.2, 170.2, 169.7, 136.1, 136.0, 127.2, 126.9, 123.9, 123.4, 120.7, 120.6, 118.5, 118.1, 118.0, 111.2, 111.0, 110.5, 109.6, 74.5, 72.1, 72.1, 66.9, 65.3, 64.7, 63.7, 59.0, 57.4, 57.2, 56.9, 56.8, 54.4, 53.7, 52.9, 52.8, 52.2, 50.8, 50.3, 41.4, 41.2, 41.1, 37.8, 37.6, 32.6, 32.0, 31.3, 31.0, 29.8, 29.4, 29.1, 26.3, 24.1, 24.0, 23.7, 23.0, 22.5, 22.4, 22.3, 22.1, 21.9, 21.7, 20.8, 19.8, 19.7, 19.4, 19.2, 19.1, 18.6, 18.3, 17.9, 17.5, 15.2. HRMS m/z: 797.4743 $[M + H]^+$. HPLC purity 98.1%, t_r = 17.2/17.7 min.

Δ^2-[D-homo Leu]-lugdunin (12). Yield: 17.2 mg (61%). ^{1}H NMR (700 MHz, DMSO-d_6): δ (ppm) 10.82 (d, J = 2.32 Hz, 1H), 10.78 (d, J = 2.89 Hz, 1H), 8.54 (d, J = 8.51 Hz, 1H), 8.50 (d, J = 8.85 Hz, 1H), 8.37 (d, J = 8.78 Hz, 1H), 8.27 (d, J = 9.11 Hz, 1H), 8.10 (d, J = 9.71 Hz, 1H), 8.04 (d, J = 7.57 Hz, 1H), 7.90 (d, J = 8.16 Hz, 1H), 7.86 (d, J = 9.36 Hz, 1H), 7.83 (d, J = 8.17 Hz, 1H), 7.72 (d, J = 8.79 Hz, 1H), 7.65 (d, J = 7.82 Hz, 1H), 7.59 (d, J = 9.25 Hz, 1H), 7.54−7.47 (m, 3H), 7.29 (d, J = 6.73 Hz, 1H), 7.21−7.17 (m, 1H), 7.15 (d, J = 7.82 Hz, 1H), 7.10 (d, J = 7.68 Hz, 1H), 7.08−7.00 (m, 2H), 6.99−6.90 (m, 1H), 4.75 (d, J = 8.54 Hz, 1H), 4.73−4.63 (m, 2H), 4.59−4.49 (m, 2H), 4.46 (d, J = 9.92 Hz, 1H), 4.33−4.29 (m, 1H), 4.28 (s, 1H), 4.27−4.21 (m, 1H), 4.18−4.11 (m, 1H), 4.08 (d, J = 8.37 Hz, 1H), 4.06−3.97 (m, 3H), 3.92−3.86 (m, 1H), 3.83 (d, J = 5.22 Hz, 1H), 3.77 (d, J = 6.40 Hz, 2H), 3.26−3.21 (m, 1H), 3.18−3.14 (m, 1H), 3.11−3.07 (m, 2H), 3.02 (d, J = 6.55 Hz, 1H), 2.95 (d, J = 7.86 Hz, 1H), 2.91 (q, J = 7.08 Hz, 2H), 2.88−2.81 (m, 1H), 2.73 (s, 1H), 2.69 (s, 1H), 2.61 (p, J = 1.87 Hz, 1H), 2.47−2.39 (m, 1H), 2.38 (dt, J = 4.79, 5.48 Hz, 1H), 2.18 (t, J = 7.35 Hz, 1H), 2.08 (d, J = 7.45 Hz, 1H), 1.94 (d, J = 6.95 Hz, 1H), 1.75 (s, 1H), 1.73−1.69 (m, 1H), 1.64 (q, J = 5.74 Hz, 1H), 1.58−1.52 (m, 1H), 1.47 (d, J = 5.29 Hz, 1H), 1.43−1.38 (m, 2H), 1.35−1.31 (m, 2H), 1.28 (d, J = 9.39 Hz, 1H), 1.18 (d, J = 6.91 Hz, 3H), 1.16 (d, J = 3.36 Hz, 3H), 1.15 (s, 3H), 1.10 (d, J = 4.61 Hz, 2H), 1.06 (d, J = 6.96 Hz, 3H), 1.03 (d, J = 7.09 Hz, 3H), 0.98 (d, J = 6.90 Hz, 3H), 0.94−0.91 (m, 9H), 0.86−0.84 (m, 24H), 0.83−0.78 (m, 12H), 0.78−0.76 (m, 6H), 0.75 (d, J = 6.43 Hz, 3H), 0.75−0.73 (m, 3H), 0.73−0.71 (m, 3H), 0.71−0.69 (m, 3H), 0.66 (d, J = 6.86 Hz, 3H), 0.61 (d, J = 6.09 Hz, 3H), 0.49 (d, J = 6.52 Hz, 3H). HRMS m/z: 811.4893 $[M + H]^+$. HPLC purity 93.7%, t_r = 16.0/16.4 min.

Δ^2-[D-Nva]-lugdunin (13). Yield: 19.3 mg (71%). ^{1}H NMR (600 MHz, DMSO-d_6): δ (ppm) 10.78 (d, J = 2.25 Hz, 1H), 8.51 (d, J = 8.30 Hz, 1H), 8.46 (d, J = 7.66 Hz, 1H), 8.19 (d, J = 8.12 Hz, 1H), 8.16 (d, J = 8.54 Hz, 1H), 8.12 (d, J = 8.93 Hz, 1H), 8.05−7.97 (m, 1H), 7.80 (d, J = 9.26 Hz, 1H), 7.70 (d, J = 9.44 Hz, 1H), 7.65 (t, J = 8.40 Hz, 1H), 7.58 (d, J = 8.07 Hz, 1H), 7.53 (d, J = 7.91 Hz, 1H), 7.45 (d, J = 9.35 Hz, 1H), 7.30 (d, J = 7.98 Hz, 1H), 7.24 (d, J = 7.49 Hz, 1H), 7.12 (d, J = 8.39 Hz, 1H), 7.07−7.00 (m, 1H), 6.99−6.92 (m, 1H), 4.74 (d, J = 7.11 Hz, 1H), 4.72 (d, J = 6.15 Hz, 1H), 4.66 (d, J = 8.90 Hz, 1H), 4.57 (d, J = 8.74 Hz, 1H), 4.54 (s, 1H), 4.53−4.52 (m, 1H), 4.51−4.50 (m, 1H), 4.49−4.46 (m, 1H), 4.45 (d, J = 5.42 Hz, 1H), 4.43 (d, J = 6.05 Hz, 1H), 4.42 (s, 1H), 4.40 (t, J = 2.45 Hz, 1H), 4.39−4.37 (m, 1H), 4.35−4.33 (m, 1H), 4.26 (t, J = 9.05 Hz, 1H), 4.15 (s, 1H), 4.09−4.04 (m, 1H), 4.03 (s, 1H), 3.93 (d, J = 7.31 Hz, 1H), 3.87 (ddd, J = 6.46, 7.96, 11.41 Hz, 1H), 3.76 (s, 1H), 3.72 (d, J = 2.59 Hz, 1H), 3.71 (d, J = 7.69 Hz, 1H), 3.69 (d, J = 6.53 Hz, 1H), 3.66 (q, J = 2.26 Hz, 1H), 3.64 (s, 1H), 3.64−3.58 (m, 1H), 3.49 (d, J = 2.02 Hz, 1H), 3.43−3.41 (m, 2H), 3.38 (d, J = 2.92 Hz, 1H), 3.36 (d, J = 4.31 Hz, 1H), 3.34 (d, J = 4.45 Hz, 1H), 3.17 (d, J = 3.95 Hz, 1H), 3.15 (d, J = 3.57 Hz, 1H), 3.14 (s, 1H), 3.06 (s, 1H), 3.04 (s, 1H), 3.02 (d, J = 3.31 Hz, 1H), 3.01 (s, 1H), 2.99 (d, J = 5.19 Hz, 1H), 2.95 (s, 1H), 2.93 (d, J = 2.46 Hz, 1H), 2.92 (s, 1H), 2.90 (d, J = 5.14 Hz, 1H), 2.88 (s, 1H), 2.83 (s, 1H), 2.81 (d, J = 4.25 Hz, 1H), 2.79 (s, 1H), 2.65 (dd, J = 8.09, 9.85 Hz, 1H), 2.56 (s, 1H), 2.54 (d, J = 3.14 Hz, 1H), 2.52 (s, 1H), 2.38 (p, J = 1.88 Hz, 1H), 2.30 (s, 1H), 2.03−1.94 (m, 1H), 1.93−1.86 (m, 1H), 1.54 (dd, J = 6.72, 8.76 Hz, 1H), 1.49−1.44 (m, 1H), 1.42−1.30 (m, 3H), 1.06−0.97 (m, 4H), 0.92 (d, J = 6.71 Hz, 3H), 0.88 (d, J = 3.95 Hz, 3H), 0.88−0.86 (m, 9H), 0.86 (d, J = 3.72 Hz, 3H), 0.84−0.83 (m, 6H), 0.83 (d, J = 3.69 Hz, 3H), 0.81 (d, J = 3.80 Hz, 3H), 0.81−0.78 (m, 6H), 0.78 (d, J = 1.39 Hz, 3H), 0.77 (s, 3H), 0.76 (s, 3H), 0.73 (d, J = 4.18 Hz, 3H), 0.72 (d, J = 4.46 Hz, 3H), 0.70 (d, J = 2.06 Hz, 3H), 0.69 (s, 3H), 0.55 (d, J = 6.49 Hz, 3H). ^{13}C NMR (150 MHz, DMSO-d_6): δ (ppm) 172.0, 171.7, 171.5, 170.9, 170.9, 170.4, 170.2, 170.2, 170.1, 169.7, 136.1, 136.0, 128.8, 128.1, 127.2, 127.0, 124.0, 123.5, 120.7,

https://doi.org/10.1021/acs.jmedchem.0c02170
J. Med. Chem. 2021, 64, 4034−4058

120.6, 118.5, 118.1, 118.0, 111.2, 111.0, 110.4, 109.5, 74.5, 72.3, 72.1, 66.9, 65.3, 63.7, 60.3, 60.2, 59.0, 57.3, 57.1, 56.9, 56.8, 54.4, 54.2, 53.5, 52.8, 52.2, 51.5, 50.8, 41.1, 37.7, 37.5, 34.6, 32.6, 32.5, 31.9, 31.3, 31.0, 29.8, 29.4, 29.2, 28.0, 26.3, 24.1, 23.9, 23.0, 22.3, 22.0, 21.7, 20.8, 19.8, 19.7, 19.4, 19.2, 19.1, 18.5, 18.3, 18.1, 17.9, 17.5, 15.2, 13.6, 13.5. HRMS m/z: 783.4578 $[M + H]^+$. HPLC purity 97.8%, t_r = 16.6/17.4 min.

Δ^2-[D-Ile]-lugdunin (14). Yield: 15.8 mg (58%). ^{1}H NMR (700 MHz, DMSO-d_6): δ (ppm) 10.82 (d, J = 2.36 Hz, 1H), 10.79 (s, 1H), 10.77−10.75 (m, 1H), 10.74 (d, J = 2.20 Hz, 1H), 8.49 (t, J = 6.58 Hz, 1H), 8.40 (s, 1H), 8.34 (d, J = 8.08 Hz, 1H), 8.28 (d, J = 8.96 Hz, 1H), 8.10 (d, J = 8.85 Hz, 1H), 8.07 (d, J = 9.24 Hz, 1H), 7.84 (d, J = 4.13 Hz, 1H), 7.82 (d, J = 7.52 Hz, 1H), 7.77 (s, 1H), 7.71 (d, J = 8.49 Hz, 1H), 7.64−7.57 (m, 2H), 7.55 (d, J = 8.18 Hz, 1H), 7.51 (d, J = 8.05 Hz, 1H), 7.39 (s, 1H), 7.30 (d, J = 8.06 Hz, 2H), 7.29−7.25 (m, 1H), 7.19 (s, 1H), 7.17 (d, J = 8.34 Hz, 1H), 7.16 (d, J = 7.30 Hz, 1H), 7.13 (d, J = 8.32 Hz, 1H), 7.10 (s, 1H), 7.08 (s, 1H), 7.07−7.00 (m, 2H), 6.96 (d, J = 6.88 Hz, 1H), 4.72 (d, J = 6.25 Hz, 1H), 4.60−4.54 (m, 2H), 4.46−4.37 (m, 1H), 4.37−4.30 (m, 2H), 4.25 (d, J = 6.73 Hz, 1H), 4.21−4.13 (m, 1H), 4.13−4.05 (m, 2H), 4.01 (d, J = 7.49 Hz, 1H), 3.89−3.85 (m, 1H), 3.77 (dd, J = 5.67, 9.35 Hz, 2H), 3.42−3.37 (m, 1H), 3.36 (d, J = 8.03 Hz, 1H), 3.32 (d, J = 6.42 Hz, 1H), 3.23 (t, J = 9.79 Hz, 1H), 3.18−3.13 (m, 1H), 3.10 (dd, J = 4.80, 7.28 Hz, 1H), 3.06 (s, 1H), 3.06−3.03 (m, 2H), 3.01 (q, J = 5.54, 6.21 Hz, 1H), 2.96 (dd, J = 7.91 Hz, 1H), 2.92 (s, 1H), 2.87 (d, J = 4.25 Hz, 1H), 2.85 (d, J = 6.76 Hz, 1H), 2.82 (s, 1H), 2.63−2.59 (m, 1H), 2.43−2.39 (m, 1H), 2.39−2.37 (m, 1H), 2.18 (t, J = 7.39 Hz, 1H), 2.09 (d, J = 6.63 Hz, 1H), 2.06 (d, J = 1.71 Hz, 1H), 2.01 (d, J = 7.08 Hz, 1H), 1.94 (d, J = 7.13 Hz, 1H), 1.90−1.85 (m, 1H), 1.75 (s, 1H), 1.68−1.60 (m, 1H), 1.57−1.51 (m, 1H), 1.46−1.43 (m, 1H), 1.43−1.39 (m, 1H), 1.39−1.34 (m, 3H), 1.33 (s, 1H), 1.30−1.28 (m, 1H), 1.27 (d, J = 9.85 Hz, 1H), 1.18 (d, J = 7.33 Hz, 1H), 1.16 (s, 1H), 1.06 (d, J = 6.96 Hz, 3H), 1.03 (d, J = 6.99 Hz, 3H), 1.01 (s, 3H), 1.00 (d, J = 6.10 Hz, 3H), 0.98 (d, J = 7.68 Hz, 3H), 0.97 (d, J = 6.90 Hz, 3H), 0.94 (s, 3H), 0.93 (d, J = 6.80 Hz, 3H), 0.91 (s, 3H), 0.90 (dd, J = 2.37, 5.01 Hz, 3H), 0.87 (s, 3H), 0.86 (d, J = 6.67 Hz, 6H), 0.83 (dd, J = 3.39, 6.33 Hz, 6H), 0.81 (d, J = 7.17 Hz, 3H), 0.79 (d, J = 7.51 Hz, 3H), 0.76−0.71 (m, 6H), 0.69 (d, J = 5.78 Hz, 3H), 0.65 (t, J = 7.39 Hz, 3H), 0.59 (t, J = 7.26 Hz, 3H), 0.53 (d, J = 6.75 Hz, 3H), 0.46 (d, J = 6.74 Hz, 3H), 0.37 (d, J = 6.80 Hz, 3H), 0.34 (d, J = 6.80 Hz, 3H). HRMS m/z: 797.4746 $[M + H]^+$. HPLC purity 96.1%, t_r = 16.6/17.9 min.

Δ^2-[D-Tle]-lugdunin (15). Yield: 20.1 mg (73%). ^{1}H NMR (600 MHz, DMSO-d_6): δ (ppm) 10.82 (d, J = 2.32 Hz, 1H), 10.78 (d, J = 2.36 Hz, 1H), 8.83 (d, J = 8.45 Hz, 1H), 8.62 (d, J = 8.43 Hz, 1H), 8.44 (d, J = 8.02 Hz, 1H), 8.34 (d, J = 8.49 Hz, 1H), 8.30 (d, J = 9.87 Hz, 1H), 8.19 (d, J = 5.43 Hz, 1H), 8.15−8.11 (m, 1H), 7.98 (d, J = 9.37 Hz, 1H), 7.80 (d, J = 9.41 Hz, 1H), 7.76 (d, J = 9.00 Hz, 1H), 7.68 (d, J = 7.78 Hz, 1H), 7.64 (d, J = 9.40 Hz, 1H), 7.62−7.56 (m, 1H), 7.51 (d, J = 7.90 Hz, 1H), 7.41 (d, J = 9.41 Hz, 1H), 7.30 (d, J = 8.09 Hz, 1H), 7.18 (d, J = 2.49 Hz, 1H), 7.15 (d, J = 7.31 Hz, 1H), 7.06−6.99 (m, 3H), 6.98−6.92 (m, 3H), 4.72 (d, J = 7.97 Hz, 1H), 4.70 (d, J = 2.37 Hz, 1H), 4.68 (d, J = 4.66 Hz, 1H), 4.66 (d, J = 2.55 Hz, 1H), 4.64 (s, 1H), 4.56 (d, J = 4.11 Hz, 1H), 4.55−4.53 (m, 1H), 4.52 (d, J = 5.41 Hz, 1H), 4.50 (s, 1H), 4.49 (d, J = 3.90 Hz, 1H), 4.47 (dd, J = 2.66, 3.94 Hz,1H), 4.46 (d, J = 4.12 Hz, 1H), 4.43 (s, 1H), 4.41 (d, J = 5.74 Hz, 2H), 4.32 (d, J = 9.91 Hz, 1H), 4.23 (t, J = 9.30 Hz, 1H), 4.13 (d, J = 5.37 Hz, 1H), 4.10−4.05 (m, 1H), 4.01 (t, J = 7.99 Hz, 1H), 3.84 (d, J = 5.71 Hz, 1H), 3.82 (d, J = 5.51 Hz, 1H), 3.80 (d, J = 5.65 Hz, 1H), 3.75 (d, J = 2.78 Hz, 1H), 3.71 (d, J = 2.38 Hz, 1H), 3.69 (d, J = 2.11 Hz, 1H), 3.67 (d, J = 2.53 Hz, 1H), 3.66 (d, J = 3.93 Hz, 1H), 3.41 (d, J = 5.44 Hz, 1H), 3.36 (d, J = 4.25 Hz, 1H), 3.30 (s, 1H), 3.25 (s, 1H), 3.24 (d, J = 3.55 Hz, 1H), 3.22 (s, 1H), 3.16 (d, J = 5.18 Hz, 1H), 3.05 (dd, J = 5.73, 8.54 Hz, 1H), 3.02 (s, 1H), 3.00 (d, J = 5.45 Hz, 1H), 2.98−2.96 (m, 1H), 2.89 (s, 1H), 2.87 (d, J = 4.69 Hz, 1H), 2.84 (q, J = 3.09, 4.33 Hz, 1H), 2.82 (d, J = 3.93 Hz, 1H), 2.80−2.79 (m, 1H), 2.73 (s, 1H), 2.62−2.59 (m, 2H), 2.57 (s, 1H), 2.55 (s, 1H), 2.54 (d, J = 2.31 Hz, 1H), 2.53−2.52 (m, 1H), 2.38 (t, J = 1.84 Hz, 1H), 2.08 (s, 1H), 2.07 (s, 1H), 2.05 (s, 1H), 2.03−1.94 (m, 3H), 1.90 (dd, J = 4.65, 6.93 Hz, 2H), 1.57 (dd, J = 1.89, 6.72 Hz, 1H), 1.55−1.52 (m, 1H), 1.43−1.33 (m, 3H), 1.33−1.26 (m, 3H), 1.23 (s, 3H), 1.15 (d, J = 5.36 Hz, 3H), 1.11 (s, 3H), 1.04−1.00 (m, 6H), 0.98 (d, J = 7.00 Hz, 3H), 0.92 (d, J = 6.69 Hz, 3H), 0.88 (d, J = 6.43 Hz, 9H), 0.87−0.85 (m, 9H), 0.83 (d, J = 7.04 Hz, 6H), 0.81 (d, J = 1.45 Hz, 3H), 0.79 (dd, J = 1.66, 6.58 Hz, 6H), 0.76 (s, 3H), 0.75 (d, J = 2.18 Hz, 12H), 0.71 (d, J = 1.93 Hz, 3H), 0.69 (d, J = 6.34 Hz, 3H), 0.65 (d, J = 4.72 Hz, 3H), 0.63 (s, 3H), 0.61 (s, 6H). ^{13}C NMR (150 MHz, DMSO-d_6): δ (ppm) 172.1, 172.0, 171.9, 171.6, 171.4, 171.4, 171.3, 170.8, 170.7, 170.6, 170.3, 169.4, 152.3, 139.2, 136.6, 136.5, 135.1, 127.4, 126.9, 124.9, 124.3, 121.8, 121.2, 121.0, 119.2, 118.5, 118.4, 111.7, 111.5, 110.7, 110.1, 72.8, 72.6, 72.4, 69.0, 65.8, 63.8, 63.1, 60.7, 59.8, 58.0, 57.8, 57.2, 56.7, 54.9, 54.2, 53.3, 52.7, 51.0, 42.9, 42.0, 41.6, 38.7, 38.1, 35.2, 34.8, 33.1, 32.7, 32.0, 31.8, 30.3, 29.4, 28.4, 27.1, 26.9, 26.7, 26.7, 24.6, 24.4, 23.5, 22.8, 22.5, 22.1, 21.4, 20.4, 20.2, 19.7, 19.6, 19.1, 18.9, 18.4, 18.3, 17.8, 15.7, 12.6. HRMS m/z: 797.4744 $[M + H]^+$. HPLC purity 96.1%, t_r = 17.1/18.0 min.

Δ^2-[L-Phe]-lugdunin (16). Yield: 21.4 mg (75%). ^{1}H NMR (700 MHz, DMSO-d_6): δ (ppm) 10.78 (d, J = 2.43 Hz, 1H), 8.74 (s, 1H), 8.70 (s, 1H), 8.64 (s, 1H), 8.56 (d, J = 8.75 Hz, 1H), 8.35 (s, 1H), 8.27 (d, J = 8.78 Hz, 1H), 8.14 (s, 1H), 8.11 (d, J = 7.79 Hz, 1H), 7.91 (d, J = 9.44 Hz, 1H), 7.74 (s, 1H), 7.62 (s, 1H), 7.60 (d, J = 9.31 Hz, 1H), 7.42 (d, J = 7.93 Hz, 1H), 7.37 (s, 1H), 7.36−7.35 (m, 1H), 7.34 (d, J = 8.42 Hz, 1H), 7.31−7.27 (m, 3H), 7.26−7.24 (m, 1H), 7.23 (d, J = 2.08 Hz, 1H), 7.23 (t, J = 7.32 Hz, 1H), 7.21−7.17 (m, 2H), 7.12 (s, 1H), 7.11 (s, 1H), 7.10 (s, 1H), 7.06 (d, J = 2.33 Hz, 1H), 7.05 (d, J = 7.08 Hz, 1H), 7.04 (t, J = 7.20 Hz, 1H), 7.03 (s, 1H), 7.02 (s, 1H), 7.01 (s, 1H), 6.95 (d, J = 6.93 Hz, 1H), 6.94−6.91 (m, 1H), 6.89 (d, J = 9.11 Hz, 1H), 6.54 (s, 1H), 6.44 (s, 1H), 6.35 (s, 1H), 4.80−4.69 (m, 1H), 4.70 (s, 1H), 4.29 (s, 1H), 4.25−4.18 (m, 1H), 4.18−4.08 (m, 1H), 4.05 (t, J = 9.55 Hz, 1H), 3.89−3.78 (m, 1H), 3.69−3.59 (m, 1H), 3.54 (s, 1H), 3.47−3.41 (m, 1H), 3.42−3.37 (m, 2H), 3.31−3.28 (m, 1H), 3.27−3.19 (m, 1H), 3.17 (d, J = 5.31 Hz, 1H), 3.12 (s, 1H), 3.12−3.02 (m, 1H), 2.92 (d, J = 3.99 Hz, 1H), 2.78 (d, J = 7.49 Hz, 1H), 2.74 (s, 1H), 2.55 (d, J = 6.53 Hz, 1H), 2.47−2.44 (m, 1H), 2.28−2.17 (m, 2H), 2.07 (s, 1H), 1.99 (s, 1H), 1.91 (s, 1H), 1.85 (d, J = 7.32 Hz, 1H), 1.76 (d, J = 7.01 Hz, 1H), 1.60−1.53 (m, 1H), 1.52 (d, J = 5.82 Hz, 1H), 1.41 (d, J = 6.71 Hz, 1H), 1.35−1.29 (m, 1H), 1.25 (d, J = 7.03 Hz, 1H), 1.19−1.12 (m, 1H), 1.09 (s, 9H), 0.93 (d, J = 6.74 Hz, 3H), 0.89 (d, J = 6.75 Hz, 6H), 0.87 (d, J = 6.57 Hz, 3H), 0.85 (s, 3H), 0.85−0.83 (m, 3H), 0.81 (d, J = 6.42 Hz, 3H), 0.78 (d, J = 6.87 Hz, 3H), 0.75 (d, J = 6.48 Hz, 3H), 0.73−0.71 (m, 9H), 0.72−0.68 (m, 3H), 0.66 (d, J = 6.84 Hz, 3H), 0.58 (d, J = 6.66 Hz, 3H), 0.54 (d, J = 6.81 Hz, 3H), 0.40 (d, J = 6.86 Hz, 3H). HRMS m/z: 831.4603 $[M + H]^+$. HPLC purity 91.8%, t_r = 17.4/17.6 min.

Δ^2-[D-Trp]-lugdunin (17). Yield: 16.9 mg (56%). ^{1}H NMR (700 MHz, DMSO-d_6): δ (ppm) 10.83−10.78 (m, 1H), 10.76 (s, 1H), 10.70 (s, 1H), 8.49 (d, J = 7.65 Hz, 1H), 8.44 (d, J = 8.27 Hz, 1H), 8.29 (d, J = 8.33 Hz, 1H), 8.22 (d, J = 9.14 Hz, 1H), 8.07 (d, J = 8.33 Hz, 1H), 8.02 (d, J = 9.07 Hz, 1H), 7.95 (d, J = 8.05 Hz, 1H), 7.89 (d, J = 9.20 Hz, 1H), 7.81 (d, J = 9.03 Hz, 1H), 7.77 (d, J = 9.32 Hz, 1H), 7.70 (d, J = 9.45 Hz, 1H), 7.60 (d, J = 7.88 Hz, 1H), 7.52 (d, J = 8.24 Hz, 1H), 7.47 (d, J = 7.92 Hz, 1H), 7.34 (d, J = 8.04 Hz, 1H), 7.32−7.26 (m, 1H), 7.16 (d, J = 7.39 Hz, 1H), 7.11 (d, J = 7.38 Hz, 1H), 7.08−6.99 (m, 2H), 6.99−6.88 (m, 2H), 4.71 (d, J = 8.68 Hz, 1H), 4.61 (q, J = 7.69 Hz, 1H), 4.54 (s, 1H), 4.54−4.50 (m, 1H), 4.50 (s, 1H), 4.48 (d, J = 3.20 Hz, 1H), 4.46 (d, J = 3.48 Hz, 1H), 4.45 (d, J = 2.63 Hz, 1H), 4.41 (d, J = 2.62 Hz, 1H), 4.40 (d, J = 2.43 Hz, 1H), 4.38 (s, 1H), 4.30 (s, 1H), 4.29 (d, J = 2.40 Hz, 1H), 4.28 (d, J = 2.84 Hz, 1H), 4.26 (s, 1H), 4.25 (s, 1H), 4.16 (q, J = 7.47 Hz, 1H), 4.07 (t, J = 9.28 Hz, 1H), 3.72 (d, J = 7.90 Hz, 1H), 3.68−3.61 (m, 1H), 3.10 (d, J = 5.40 Hz, 1H), 3.08 (d, J = 5.23 Hz, 1H), 3.02 (d, J = 6.25 Hz, 1H), 3.00 (s, 1H), 2.99 (d, J = 4.01 Hz, 1H), 2.97 (d, J = 3.27 Hz, 1H), 2.96 (s, 1H), 2.91 (d, J = 6.73 Hz, 1H), 2.89 (s, 1H), 2.87 (s, 1H), 2.86 (s, 1H), 2.85 (s, 1H), 2.84 (d, J = 3.94 Hz, 1H), 2.80 (s, 1H), 2.78 (s, 1H), 2.76 (dd, J = 3.11, 6.34 Hz, 2H), 2.74 (d, J = 5.54 Hz, 1H), 2.72 (d, J = 4.82 Hz, 1H), 2.70 (s, 1H), 2.61 (p, J = 1.88 Hz, 1H), 2.43 (s, 1H), 2.42 (s, 1H), 2.40 (s, 1H), 2.38 (p, J = 1.94 Hz, 1H), 2.24 (s, 1H), 2.20−2.12 (m, 1H), 2.11 (s, 1H), 2.10 (s,

https://doi.org/10.1021/acs.jmedchem.0c02170
J. Med. Chem. 2021, 64, 4034−4058

1H), 2.08 (s, 1H), 2.06 (s, 1H), 2.02 (d, J = 7.00 Hz, 1H), 1.99 (q, J = 6.71, 7.26 Hz, 1H), 1.94 (s, 1H), 1.93 (s, 1H), 1.91 (d, J = 2.13 Hz, 1H), 1.88 (s, 1H), 1.87 (s, 1H), 1.86 (s, 1H), 1.85 (s, 1H), 1.83−1.77 (m, 1H), 1.55−1.50 (m, 1H), 1.35 (s, 1H), 1.33 (s, 1H), 1.32−1.25 (m, 1H), 1.23 (s, 3H), 1.18 (d, J = 7.13 Hz, 3H), 1.14 (d, J = 6.15 Hz, 3H), 1.11 (s, 3H), 0.92 (d, J = 6.69 Hz, 3H), 0.86 (s, 3H), 0.85 (d, J = 1.29 Hz, 3H), 0.83 (d, J = 2.66 Hz, 3H), 0.82 (d, J = 2.35 Hz, 3H), 0.81 (s, 3H), 0.79 (dd, J = 2.96, 6.85 Hz, 6H), 0.77 (d, J = 3.30 Hz, 3H), 0.73 (dd, J = 4.20, 6.25 Hz, 6H), 0.70 (d, J = 6.93 Hz, 3H). HRMS m/z: 870.4691 $[M + H]^+$. HPLC purity 98.6%, t_r = 17.0/17.1 min.

$\Delta^{2,4}$-[D-Leu^2-D-Val^4]-lugdunin (18). Yield: 17.4 mg (64%). ^{1}H NMR (700 MHz, DMSO-d_6): δ (ppm) 10.79 (s, 1H), 10.77 (s, 1H), 8.58 (d, J = 8.39 Hz, 1H), 8.42 (s, 1H), 8.26 (d, J = 7.37 Hz, 1H), 8.15 (s, 1H), 7.93 (d, J = 8.89 Hz, 1H), 7.81 (d, J = 9.58 Hz, 2H), 7.72 (d, J = 9.64 Hz, 1H), 7.65 (s, 1H), 7.54 (d, J = 8.17 Hz, 1H), 7.38 (s, 1H), 7.37 (d, J = 7.83 Hz, 1H), 7.35 (d, J = 7.92 Hz, 2H), 7.34 (d, J = 7.20 Hz, 2H), 7.32 (d, J = 6.39 Hz, 1H), 7.31 (s, 1H), 7.25 (t, J = 7.35 Hz, 1H), 7.23 (d, J = 7.27 Hz, 1H), 7.22 (t, J = 7.34 Hz, 1H), 7.20 (d, J = 7.59 Hz, 2H), 7.19 (t, J = 7.32 Hz, 3H), 6.53 (s, 3H), 6.43 (s, 2H), 4.73 (d, J = 2.35 Hz, 1H), 4.71 (s, 2H), 4.48 (s, 1H), 4.45 (s, 1H), 4.44 (s, 1H), 4.31 (s, 1H), 4.29 (d, J = 8.44 Hz, 1H), 4.06 (s, 1H), 4.05 (s, 1H), 4.00 (s, 1H), 3.50 (s, 1H), 3.29−3.25 (m, 1H), 3.22 (d, J = 9.56 Hz, 1H), 3.13 (d, J = 2.96 Hz, 1H), 3.05 (d, J = 5.18 Hz, 1H), 3.01 (s, 1H), 2.94 (s, 3H), 2.61 (d, J = 4.85 Hz, 1H), 2.59−2.56 (m, 1H), 2.54 (s, 2H), 2.38 (d, J = 3.85 Hz, 1H), 2.08 (s, 1H), 1.98 (d, J = 7.25 Hz, 1H), 1.90 (s, 1H), 1.26 (s, 1H), 1.23 (s, 1H), 1.14 (s, 2H), 0.98 (d, J = 7.11 Hz, 3H), 0.93 (d, J = 6.77 Hz, 3H), 0.91 (d, J = 6.40 Hz, 3H), 0.90−0.85 (m, 18H), 0.85−0.83 (m, 6H), 0.82 (d, J = 6.15 Hz, 3H), 0.81 (s, 3H), 0.80 (d, J = 6.32 Hz, 3H), 0.79 (d, J = 6.45 Hz, 3H), 0.77 (d, J = 6.68 Hz, 3H), 0.74 (d, J = 6.86 Hz, 3H), 0.72 (d, J = 6.69 Hz, 3H), 0.69−0.66 (m, 3H), 0.64 (d, J = 6.69 Hz, 3H), 0.60 (d, J = 6.44 Hz, 3H). HRMS m/z: 783.4591 $[M + H]^+$. HPLC purity 92.1%, t_r = 16.8/17.1 min.

Δ^3-[L-Phe]-lugdunin (19). Yield: 22.1 mg (86%). ^{1}H NMR (600 MHz, DMSO-d_6): δ (ppm) 8.55 (d, J = 8.64 Hz, 1H), 8.48 (d, J = 5.43 Hz, 1H), 8.31 (d, J = 8.79 Hz, 1H), 8.17 (t, J = 8.60 Hz, 1H), 8.03 (d, J = 7.72 Hz, 1H), 7.82 (d, J = 8.97 Hz, 1H), 7.77 (d, J = 9.41 Hz, 1H), 7.70 (d, J = 9.28 Hz, 1H), 7.45 (d, J = 9.38 Hz, 1H), 7.29−7.19 (m, 2H), 7.18−7.12 (m, 2H), 4.74 (d, J = 2.19 Hz, 1H), 4.72 (d, J = 2.18 Hz, 1H), 4.60 (d, J = 8.55 Hz, 1H), 4.56−4.47 (m, 2H), 4.45−4.36 (m, 2H), 4.30 (t, J = 5.17 Hz, 1H), 4.24 (t, J = 9.19 Hz, 1H), 4.14 (t, 1H), 4.09−4.02 (m, 2H), 3.90−3.84 (m, 1H), 3.75 (d, J = 7.11 Hz, 1H), 3.71−3.62 (m, 3H), 3.42 (d, J = 5.41 Hz, 1H), 3.40−3.36 (m, 2H), 3.27 (d, J = 4.13 Hz, 1H), 3.24 (d, J = 4.15 Hz, 1H), 3.19−3.13 (m, 1H), 3.06 (d, J = 7.75 Hz, 1H), 2.93 (d, J = 5.65 Hz, 1H), 2.91−2.86 (m, 1H), 2.85 (d, J = 4.79 Hz, 1H), 2.75 (s, 1H), 2.73 (d, J = 3.28 Hz, 1H), 2.71 (s, 1H), 2.69 (s, 1H), 2.67 (s, 1H), 2.65 (d, J = 2.79 Hz, 1H), 2.63 (s, 1H), 2.58−2.52 (m, 2H), 1.98 (dd, J = 4.62, 9.60 Hz, 2H), 1.93−1.84 (m, 1H), 1.69 (dd, J = 6.69, 8.96 Hz, 2H), 1.63−1.58 (m, 1H), 1.54 (dd, J = 6.69, 8.68 Hz, 1H), 1.40 (dd, J = 4.22, 8.77 Hz, 1H), 1.37−1.30 (m, 2H), 1.30 (s, 1H), 1.25 (d, J = 3.64 Hz, 3H), 1.03 (dd, J = 3.69, 5.53, Hz, 6H), 0.98 (d, J = 6.76 Hz, 3H), 0.92 (d, J = 6.71 Hz, 3H), 0.89−0.85 (m, 15H), 0.85−0.83 (m, 6H), 0.82 (d, J = 5.02 Hz, 3H), 0.80 (d, J = 5.96 Hz, 3H), 0.77 (d, J = 5.95 Hz, 3H), 0.75 (d, J = 6.96 Hz, 3H), 0.62 (d, J = 6.82 Hz, 3H), 0.46 (d, J = 6.75 Hz, 3H), 0.42 (d, J = 6.72 Hz, 3H). ^{13}C NMR (150 MHz, DMSO-d_6): δ (ppm) 171.7, 171.6, 171.5, 171.4, 171.0, 170.6, 170.4, 170.3, 170.2, 169.8, 169.8, 169.7, 151.8, 138.2, 137.6, 129.4, 129.0, 128.0, 127.8, 126.1, 121.3, 72.3, 72.1, 68.5, 65.4, 63.6, 60.6, 60.3, 59.1, 57.5, 57.4, 57.3, 56.8, 56.5, 54.4, 54.2, 53.5, 52.3, 50.6, 41.4, 41.1, 38.3, 37.9, 37.6, 36.2, 34.7, 32.6, 32.1, 31.3, 30.7, 29.8, 29.1, 28.6, 24.1, 24.0, 23.1, 22.4, 22.0, 21.7, 20.9, 19.8, 19.7, 19.5, 19.4, 19.2, 19.1, 19.1, 18.6, 18.6, 18.4, 18.3, 18.2, 18.0, 17.8, 17.4, 15.2, 13.8, 12.1. HRMS m/z: 744.4476 $[M + H]^+$. HPLC purity 96.3%, t_r = 17.3/17.9 min.

Δ^3-[L-Tyr]-lugdunin (20). Yield: 15.8 mg (60%). ^{1}H NMR (600 MHz, DMSO-d_6): δ (ppm) 9.22 (s, 1H), 9.17 (s, 1H), 8.58 (d, J = 5.44 Hz, 1H), 8.54 (d, J = 8.53 Hz, 1H), 8.25 (d, J = 8.70 Hz, 1H), 8.18 (d, J = 9.46 Hz, 1H), 8.11 (d, J = 8.47 Hz, 1H), 8.02 (t, J = 6.71 Hz, 1H), 7.81 (d, J = 9.15 Hz, 1H), 7.76 (d, J = 8.07 Hz, 1H), 7.69 (d, J = 9.29 Hz, 1H), 7.52−7.38 (m, 1H), 7.06−6.99 (m, 2H), 6.68−6.57 (m, 2H), 4.73 (d, J = 2.19 Hz, 1H), 4.71 (d, J = 2.23 Hz, 1H), 4.63−4.58 (m, 1H), 4.52 (d, J = 4.60 Hz, 1H), 4.50 (d, J = 4.50 Hz, 1H), 4.47 (d, J = 5.15 Hz, 1H), 4.43 (s, 1H), 4.39 (dd, J = 7.73, 9.36 Hz, 2H), 4.34 (t, J = 5.17 Hz, 1H), 4.23 (t, J = 9.15 Hz, 1H), 4.18 (d, J = 2.02 Hz, 1H), 4.16 (s, 1H), 4.14 (s, 1H), 4.06 (d, J = 4.88 Hz, 2H), 3.95 (d, J = 5.67 Hz, 1H), 3.88 (q, J = 8.46, 9.05 Hz, 1H), 3.75 (d, J = 6.48 Hz, 1H), 3.73−3.71 (m, 1H), 3.68 (dd, J = 4.08, 9.83 Hz, 2H), 3.62 (dd, J = 4.09, 5.74 Hz, 2H), 3.48 (s, 1H), 3.44 (d, J = 6.17 Hz, 1H), 3.41 (d, J = 5.39 Hz, 1H), 3.37 (dd, J = 4.97, 6.56 Hz, 1H), 3.30 (s, 1H), 3.20 (s, 1H), 3.18 (d, J = 3.43 Hz, 1H), 3.17 (s, 1H), 3.14 (d, J = 3.49 Hz, 1H), 3.12 (d, J = 4.15 Hz, 1H), 3.10 (d, J = 3.96 Hz, 1H), 3.07 (d, J = 6.50 Hz, 1H), 3.05 (s, 1H), 3.00 (s, 1H), 2.98 (s, 1H), 2.94−2.92 (m, 1H), 2.89 (dd, J = 5.57, 9.02 Hz, 1H), 2.84 (d, J = 3.32 Hz, 1H), 2.82 (dd, J = 3.72, 6.35 Hz, 1H), 2.79 (d, J = 1.61 Hz, 1H), 2.76 (d, J = 5.28 Hz, 1H), 2.73 (d, J = 5.17 Hz, 1H), 2.71 (d, J = 6.43 Hz, 1H), 2.69 (s, 1H), 2.68−2.65 (m, 1H), 2.64 (s, 1H), 2.61 (d, J = 3.89 Hz, 1H), 2.59 (d, J = 5.61 Hz, 1H), 2.57 (d, J = 3.21 Hz, 1H), 2.54 (d, J = 6.15 Hz, 1H), 2.54−2.52 (m, 1H), 2.38 (d, J = 3.86 Hz, 1H), 2.10 (s, 1H), 2.07 (s, 1H), 2.05 (d, J = 3.08 Hz, 1H), 2.02 (t, J = 1.43 Hz, 1H), 2.02−1.99 (m, 1H), 1.96 (s, 1H), 1.93 (d, J = 1.86 Hz, 1H), 1.92 (d, J = 2.15 Hz, 1H), 1.91 (d, J = 2.23 Hz, 1H), 1.89 (d, J = 6.85 Hz, 1H), 1.73 (dd, J = 6.72, 8.78 Hz, 2H), 1.69−1.63 (m, 1H), 1.55 (dd, J = 6.60, 8.74 Hz, 1H), 1.46 (d, J = 4.02 Hz, 1H), 1.42−1.36 (m, 1H), 1.36 (s, 1H), 1.25 (s, 1H), 1.17−1.13 (m, 2H), 1.11 (s, 2H), 1.07 (d, J = 6.63 Hz, 3H), 1.02−1.00 (m, 3H), 0.98 (d, J = 6.97 Hz, 3H), 0.92 (d, J = 6.70 Hz, 3H), 0.89−0.82 (m, 15H), 0.82 (d, J = 2.45 Hz, 3H), 0.81 (d, J = 1.90 Hz, 3H), 0.79 (t, J = 2.98 Hz, 3H), 0.73 (d, J = 6.03 Hz, 3H), 0.65 (d, J = 6.75 Hz, 3H), 0.62 (d, J = 6.81 Hz, 3H), 0.54 (d, J = 6.76 Hz, 3H), 0.51 (d, J = 6.77 Hz, 3H). ^{13}C NMR (150 MHz, DMSO-d_6): δ (ppm) 171.7, 171.5, 171.5, 171.5, 171.0, 170.5, 170.4, 170.2, 169.9, 169.8, 169.8, 155.7, 130.3, 130.1, 130.1, 130.0, 129.8, 129.6, 128.1, 127.5, 114.8, 114.8, 114.7, 114.6, 105.1, 98.9, 74.5, 72.3, 72.1, 72.0, 69.5, 68.8, 65.3, 63.6, 60.6, 60.3, 60.1, 59.0, 57.4, 57.3, 57.3, 56.8, 56.5, 54.6, 54.4, 52.2, 50.6, 41.3, 41.1, 38.2, 37.6, 37.2, 35.4, 35.1, 34.6, 32.6, 32.0, 31.3, 30.7, 29.7, 29.1, 28.6, 24.1, 23.9, 23.2, 23.1, 22.4, 21.9, 21.6, 20.8, 19.8, 19.7, 19.5, 19.4, 19.2, 19.1, 18.6, 18.3, 18.1, 18.0, 17.8, 17.4, 15.2, 13.9, 13.8, 12.0. HRMS m/z: 760.4424 $[M + H]^+$. HPLC purity 95.2%, t_r = 15.7/16.5 min.

Δ^3-[L-Phg]-lugdunin (21). Yield: 18.6 mg (74%). ^{1}H NMR (600 MHz, DMSO-d_6): δ (ppm) 8.75 (d, J = 7.77 Hz, 1H), 8.70 (d, J = 8.24 Hz, 1H), 8.62 (d, J = 8.52 Hz, 1H), 8.56 (d, J = 8.56 Hz, 1H), 8.49 (d, J = 8.67 Hz, 1H), 8.44 (d, J = 7.99 Hz, 1H), 8.31 (d, J = 9.50 Hz, 1H), 8.24 (d, J = 9.29 Hz, 1H), 8.06 (d, J = 8.30 Hz, 1H), 8.05 (d, J = 8.24 Hz, 1H), 7.77 (d, J = 9.19 Hz, 1H), 7.65 (d, J = 9.59 Hz, 1H), 7.59 (d, J = 9.38 Hz, 1H), 7.48 (d, J = 7.86 Hz, 2H), 7.46−7.42 (m, 2H), 7.34 (d, J = 7.83 Hz, 2H), 7.33−7.26 (m, 2H), 7.24 (d, J = 7.25 Hz, 1H), 7.22−7.19 (m, 1H), 7.16 (d, J = 8.89 Hz, 1H), 5.57 (d, J = 7.65 Hz, 1H), 5.48 (d, J = 7.79 Hz, 1H), 5.42 (d, J = 8.45 Hz, 1H), 4.73 (d, J = 4.71 Hz, 1H), 4.71 (s, 2H), 4.69 (d, J = 2.37 Hz, 1H), 4.68−4.66 (m, 1H), 4.65 (s, 1H), 4.53 (d, J = 6.57 Hz, 1H), 4.49−4.45 (m, 2H), 4.43−4.35 (m, 2H), 4.29−4.20 (m, 2H), 4.20−4.20 (m, 1H), 4.20 (s, 2H), 4.15−4.07 (m, 3H), 3.98−3.93 (m, 3H), 3.80−3.75 (m, 2H), 3.72 (dd, J = 3.19, 7.31 Hz, 2H), 3.66 (q, J = 5.93 Hz, 2H), 3.46−3.40 (m, 2H), 3.40−3.36 (m, 3H), 3.24−3.19 (m, 2H), 3.17 (d, J = 5.71 Hz, 1H), 3.14−3.09 (m, 3H), 3.02 (t, J = 1.94 Hz, 1H), 2.94 (s, 1H), 2.81−2.78 (m, 1H), 2.61 (t, 3H), 2.46 (s, 1H), 2.44 (d, J = 4.36 Hz, 1H), 2.38 (d, J = 4.45 Hz, 1H), 2.19 (d, J = 6.72 Hz, 1H), 2.12−2.08 (m, 2H), 2.06 (d, J = 6.73 Hz, 1H), 2.04 (s, 1H), 2.01 (d, J = 9.16 Hz, 1H), 1.98 (s, 1H), 1.95 (d, J = 7.05 Hz, 1H), 1.94−1.83 (m, 2H), 1.66−1.62 (m, 1H), 1.57 (dd, J = 3.44, 6.56 Hz, 2H), 1.43 (d, J = 5.61 1H), 1.35 (d, J = 7.19 Hz, 1H), 1.29 (d, J = 6.70 Hz, 2H), 1.27 (s, 3H), 1.24 (dd, J = 2.27, 4.60 Hz, 2H), 1.20 (d, J = 6.36 Hz, 1H), 1.14 (dd, J = 5.33, 7.48 Hz, 2H), 1.07 (s, 1H), 1.05−1.03 (m, 1H), 1.02 (d, J = 3.87 Hz, 3H), 1.01 (s, 9H), 0.96 (d, J = 6.86 Hz, 3H), 0.95−0.93 (m, 9H), 0.92 (d, J = 7.77 Hz, 3H), 0.91 (s, 3H), 0.89 (d, J = 6.61 Hz, 3H), 0.88 (d, J = 6.17 Hz, 3H), 0.87 (d, J = 7.32 Hz, 3H), 0.86 (d, J = 7.13 Hz, 12H), 0.85−0.84 (m, 3H),

https://doi.org/10.1021/acs.jmedchem.0c02170
J. Med. Chem. 2021, 64, 4034−4058

0.83 (d, J = 6.18 Hz, 3H), 0.81 (d, J = 6.05 Hz, 3H), 0.80 (d, J = 7.86 Hz, 3H), 0.79 (d, J = 7.65 Hz, 6H), 0.78 (s, 3H), 0.76 (d, J = 6.14 Hz, 3H), 0.75 (d, J = 7.36 Hz, 3H), 0.67 (d, J = 6.14 Hz, 3H). ^{13}C NMR (150 MHz, DMSO-d_6): δ (ppm) 172.4, 171.9, 171.7, 171.5, 171.2, 170.9, 170.9, 170.8, 170.7, 170.5, 170.4, 170.3, 170.2, 169.4, 169.0, 168.7, 138.6, 137.6, 128.2, 128.1, 128.1, 127.9, 127.6, 127.4, 127.2, 127.1, 126.6, 76.3, 76.3, 74.6, 74.6, 74.5, 74.5, 74.5, 74.4, 72.3, 72.1, 72.1, 72.1, 66.5, 65.9, 65.3, 65.2, 64.7, 64.6, 63.8, 63.7, 61.5, 60.3, 60.2, 59.6, 58.9, 58.3, 58.2, 58.0, 57.7, 57.4, 57.3, 57.1, 57.0, 56.7, 56.4, 56.3, 55.1, 54.5, 54.5, 52.5, 51.5, 41.5, 40.4, 38.2, 37.4, 37.3, 34.6, 32.8, 32.4, 32.1, 31.2, 30.8, 30.5, 30.1, 29.9, 29.8, 29.6, 29.1, 28.6, 27.7, 24.1, 24.1, 24.0, 22.8, 22.7, 22.3, 22.2, 21.5, 21.1, 20.8, 20.4, 20.2, 19.9, 19.8, 19.7, 19.6, 19.5, 19.2, 19.1, 19.0, 18.8, 18.4, 18.4, 18.2, 18.2, 18.1, 18.0, 17.8, 17.5, 17.2, 16.9, 15.2. HRMS m/z: 730.4312 [M + H]$^+$. HPLC purity 82.6%, t_r = 17.0/17.6 min.

Δ^3-[L-DOPA]-Lugdunin (22). Yield: 16.3 mg (61%). ^{1}H NMR (700 MHz, DMSO-d_6): δ (ppm) 8.61 (s, 1H), 8.59 (s, 1H), 8.57 (s, 1H), 8.51 (s, 1H), 8.48 (d, J = 7.05 Hz, 1H), 8.46 (s, 1H), 8.29 (d, J = 8.83 Hz, 1H), 8.21 (d, J = 9.42 Hz, 1H), 8.06 (d, J = 8.90 Hz, 1H), 7.85 (d, J = 9.02 Hz, 1H), 7.79 (d, J = 9.37 Hz, 1H), 7.75 (d, J = 9.64 Hz, 1H), 7.72 (d, J = 9.31 Hz, 1H), 7.48 (d, J = 9.43 Hz, 1H), 6.66 (d, J = 7.95 Hz, 1H), 6.60 (d, J = 7.08 Hz, 1H), 6.56 (s, 1H), 6.55 (s, 1H), 6.54 (s, 1H), 6.53 (s, 1H), 6.52 (d, J = 8.00 Hz, 1H), 6.50 (d, J = 7.89 Hz, 1H), 6.48 (d, J = 6.07 Hz, 1H), 6.47 (d, J = 7.12 Hz, 1H), 4.74 (d, J = 2.23 Hz, 1H), 4.72 (d, J = 2.28 Hz, 1H), 4.60 (s, 1H), 4.58 (dd, J = 4.74, 9.35 Hz, 1H), 4.55 (d, J = 4.30 Hz, 1H), 4.53 (d, J = 4.27 Hz, 1H), 4.49 (dd, J = 5.10, 9.00 Hz, 1H), 4.44 (s, 1H), 4.42 (d, J = 2.28 Hz, 1H), 4.41 (d, J = 2.44 Hz, 1H), 4.40 (s, 1H), 4.38 (d, J = 6.13 Hz, 2H), 4.36 (d, J = 4.36 Hz, 1H), 4.24 (t, J = 9.18 Hz, 1H), 4.16 (t, J = 9.00 Hz, 1H), 4.09 (d, J = 2.22 Hz, 1H), 4.07 (d, J = 2.49 Hz, 1H), 4.06–4.05 (m, 2H), 4.05 (s, 1H), 3.70 (s, 1H), 3.70 (s, 1H), 3.69 (s, 1H), 3.67 (dd, J = 2.99, 5.76 Hz, 1H), 3.66 (s, 1H), 3.65 (s, 1H), 3.17 (s, 1H), 3.16 (d, J = 3.57 Hz, 1H), 3.14 (s, 1H), 3.08 (s, 1H), 3.07–3.05 (m, 1H), 3.04 (d, J = 4.07 Hz, 1H), 2.68 (d, J = 5.03 Hz, 1H), 2.65 (d, J = 5.15 Hz, 1H), 2.61 (p, J = 1.86 Hz, 1H), 2.55 (s, 2H), 2.44 (s, 1H), 2.43–2.41 (m, 1H), 2.38 (p, J = 1.86 Hz, 1H), 2.26 (s, 1H), 2.24 (s, 1H), 2.18 (s, 1H), 2.11 (s, 1H), 2.10 (s, 1H), 2.08 (s, 1H), 2.06 (d, J = 2.74 Hz, 1H), 2.02 (d, J = 2.38 Hz, 1H), 2.01 (d, J = 2.35 Hz, 1H), 2.00 (s, 1H), 1.98 (s, 1H), 1.97 (s, 1H), 1.96 (d, J = 2.76 Hz, 1H), 1.91 (d, J = 2.34 Hz, 1H), 1.89 (d, J = 2.54 Hz, 1H), 1.88 (d, J = 2.50 Hz, 1H), 1.87 (s, 1H), 1.75 (d, J = 3.58 Hz, 1H), 1.73 (s, 1H), 1.64–1.62 (m, 1H), 1.46–1.38 (m, 1H), 1.35 (s, 1H), 1.34 (d, J = 3.25 Hz, 1H), 1.32 (s, 1H), 1.31 (t, J = 4.43 Hz, 1H), 1.29 (s, 1H), 1.23 (d, J = 4.50 Hz, 2H), 1.15 (d, J = 4.14 Hz, 1H), 1.14 (d, J = 7.97 Hz, 3H), 1.11 (s, 3H), 0.92 (d, J = 6.69 Hz, 3H), 0.89–0.83 (m, 18H), 0.82 (d, J = 7.88 Hz, 3H), 0.81–0.79 (m, 6H), 0.76 (dd, J = 6.47, 8.03 Hz, 9H), 0.65 (d, J = 6.75 Hz, 3H), 0.56 (d, J = 6.73 Hz, 3H), 0.51 (d, J = 6.68 Hz, 3H). HRMS m/z: 776.4381 [M + H]$^+$. HPLC purity 98.1%, t_r = 15.4/16.0 min.

Δ^3-[L-His]-lugdunin (23). Yield: 18.6 mg (74%). ^{1}H NMR (700 MHz, DMSO-d_6): δ (ppm) 14.19 (s, 1H), 9.04 (d, J = 8.76 Hz, 1H), 9.02–8.92 (m, 2H), 8.70 (t, J = 6.67 Hz, 1H), 8.63–8.49 (m, 1H), 8.36 (d, J = 8.41 Hz, 1H), 8.18 (d, J = 9.26 Hz, 1H), 8.12 (d, J = 9.54 Hz, 1H), 8.06 (d, J = 7.88 Hz, 1H), 7.92 (d, J = 8.88 Hz, 1H), 7.89 (s, 1H), 7.85–7.77 (m, 1H), 7.74 (d, J = 9.34 Hz, 1H), 7.52 (d, J = 9.41 Hz, 1H), 7.40 (s, 1H), 7.32 (d, J = 6.39 Hz, 1H), 7.31 (d, J = 6.38 Hz, 1H), 7.29 (d, J = 7.35 Hz, 1H), 7.28 (d, J = 7.65 Hz, 1H), 7.25 (t, J = 6.34 Hz, 1H), 7.24–7.23 (m, 1H), 7.23–7.18 (m, 1H), 7.13 (d, J = 5.65 Hz, 1H), 7.04 (d, J = 6.73 Hz, 1H), 4.80 (s, 1H), 4.78 (d, J = 8.12 Hz, 1H), 4.75 (q, J = 4.88 Hz, 1H), 4.75–4.69 (m, 1H), 4.63 (d, J = 10.98 Hz, 1H), 4.58 (d, J = 7.41 Hz, 1H), 4.56 (d, J = 4.16 Hz, 1H), 4.54 (s, 1H), 4.44 (s, 1H), 4.43 (d, J = 2.13 Hz, 1H), 4.41 (d, J = 2.48 Hz, 1H), 4.40 (d, J = 2.24 Hz, 1H), 4.39 (d, J = 2.28 Hz, 1H), 4.38 (s, 1H), 4.25 (t, J = 9.13 Hz, 1H), 4.22 (t, J = 8.96 Hz, 1H), 4.07 (d, J = 8.00 Hz, 2H), 3.85 (d, J = 9.01 Hz, 1H), 3.74 (s, 1H), 3.69 (d, J = 6.20 Hz, 1H), 3.63 (dd, J = 5.27, 8.96 Hz, 1H), 3.48 (d, J = 5.42 Hz, 1H), 3.41 (d, J = 5.39 Hz, 1H), 3.32 (d, J = 2.90 Hz, 1H), 3.30 (d, J = 2.58 Hz, 1H), 3.28 (d, J = 5.17 Hz, 1H), 3.26 (d, J = 4.91 Hz, 1H), 3.18 (dd, J = 5.87, 9.48 Hz, 1H), 3.03 (d, J = 4.14 Hz, 1H), 3.01 (t, J = 7.30 Hz, 1H), 2.92 (d, J = 7.58 Hz, 1H), 2.85 (t, J = 4.10 Hz, 1H), 2.83 (d, J = 4.32 Hz, 1H), 2.81 (s, 1H), 2.61 (d, J = 3.82 Hz, 1H), 2.56 (d, J = 2.54 Hz, 1H), 2.52 (d, J = 3.92 Hz, 1H), 2.38 (d, J = 6.94 Hz, 1H), 2.18 (t, J = 7.38 Hz, 1H), 2.09 (d, J = 6.45 Hz, 1H), 2.06 (s, 1H), 2.04 (d, J = 2.25 Hz, 1H), 2.03 (d, J = 2.20 Hz, 1H), 2.02 (d, J = 2.27 Hz, 1H), 2.01 (s, 1H), 2.00–1.95 (m, 1H), 1.95–1.92 (m, 1H), 1.87 (d, J = 6.78 Hz, 1H), 1.81–1.71 (m, 1H), 1.64 (d, J = 5.79 Hz, 1H), 1.55 (dd, J = 6.66, 8.82 Hz, 1H), 1.45 (s, 1H), 1.37–1.29 (m, 2H), 1.29 (s, 1H), 1.29–1.28 (m, 1H), 1.27 (s, 1H), 1.26 (d, J = 4.01 Hz, 1H), 1.25 (s, 1H), 1.21 (s, 1H), 1.20–1.16 (m, 1H), 1.06 (d, J = 6.93 Hz, 3H), 1.03 (d, J = 7.03 Hz, 3H), 1.00 (d, J = 7.02 Hz, 3H), 0.99 (s, 3H), 0.93 (d, J = 6.70 Hz, 3H), 0.86 (d, J = 5.80 Hz, 3H), 0.83 (d, J = 7.38 Hz, 3H), 0.82 (d, J = 7.15 Hz, 3H), 0.81 (t, J = 1.32 Hz, 3H), 0.79 (d, J = 6.34 Hz, 3H), 0.78 (d, J = 5.18 Hz, 3H), 0.77 (d, J = 4.23 Hz, 3H), 0.76 (d, J = 2.97 Hz, 3H), 0.75 (d, J = 3.82 Hz, 3H), 0.73 (s, 3H), 0.64 (d, J = 6.71 Hz, 3H), 0.57 (d, J = 6.73 Hz, 3H). HRMS m/z: 734.4371 [M + H]$^+$. HPLC purity 98.1%, t_r = 15.5/15.7 min.

Δ^3-[L-Phe(4-chloro)]-lugdunin (24). Yield: 21.1 mg (79%). ^{1}H NMR (700 MHz, DMSO-d_6): δ (ppm) 8.41 (d, J = 9.51 Hz, 1H), 8.08 (d, J = 9.83 Hz, 1H), 8.01 (d, J = 8.63 Hz, 1H), 7.99–7.92 (m, 1H), 7.88 (d, J = 6.72 Hz, 1H), 7.86 (s, 1H), 7.71 (d, J = 9.58 Hz, 1H), 7.44–7.34 (m, 1H), 7.33–7.24 (m, 1H), 7.24 (s, 1H), 7.18 (t, J = 8.45 Hz, 1H), 7.00 (d, J = 8.19 Hz, 1H), 6.87 (s, 1H), 6.63 (s, 1H), 6.58 (d, J = 2.42 Hz, 1H), 6.56–6.49 (m, 1H), 6.41 (d, J = 2.43 Hz, 1H), 6.40 (d, J = 2.45 Hz, 1H), 5.32 (d, J = 2.40, Hz, 1H), 5.23 (d, J = 5.43 Hz, 1H), 4.92 (d, J = 4.97 Hz, 1H), 4.90 (d, J = 4.88 Hz, 1H), 4.79 (d, J = 4.59 Hz, 1H), 4.72 (d, J = 3.04 Hz, 1H), 4.71 (d, J = 2.06 Hz, 1H), 4.69 (d, J = 5.33 Hz, 1H), 4.68 (s, 1H), 4.66 (d, J = 4.28 Hz, 1H), 4.64 (d, J = 4.57 Hz, 1H), 4.60 (d, J = 5.82 Hz, 1H), 4.57–4.54 (m, 1H), 4.54 (s, 1H), 4.53 (s, 1H), 4.51 (d, J = 8.29 Hz, 1H), 4.47 (s, 1H), 4.41 (d, J = 3.38 Hz, 1H), 4.40–4.38 (m, 1H), 4.35 (d, J = 9.68 Hz, 1H), 4.32 (d, J = 6.08 Hz, 1H), 4.27 (t, J = 3.32 Hz, 1H), 4.24 (d, J = 3.00 Hz, 1H), 4.24–4.22 (m, 1H), 4.21 (d, J = 4.15 Hz, 1H), 4.21–4.19 (m, 1H), 4.11 (d, J = 8.66 Hz, 1H), 4.06 (d, J = 4.17 Hz, 1H), 3.97 (d, J = 6.18 Hz, 1H), 3.84 (d, J = 7.39 Hz, 1H), 3.78 (d, J = 3.67 Hz, 1H), 3.77 (d, J = 4.06 Hz, 1H), 3.73 (d, J = 3.55 Hz, 1H), 3.60 (d, J = 5.84 Hz, 1H), 3.48 (d, J = 5.40 Hz, 1H), 3.45 (t, J = 6.04 Hz, 1H), 3.41 (d, J = 5.39 Hz, 1H), 3.40 (s, 1H), 3.29 (d, J = 5.94 Hz, 1H), 3.28 (s, 1H), 3.16 (d, J = 4.79 Hz, 1H), 2.95 (d, J = 3.08 Hz, 1H), 2.94 (d, J = 2.70 Hz, 1H), 2.90 (s, 1H), 2.79 (s, 1H), 2.60 (d, J = 5.85 Hz, 1H), 2.56 (d, J = 4.57 Hz, 1H), 2.54 (s, 1H), 2.52–2.51 (m, 1H), 2.27 (d, J = 7.44 Hz, 1H), 2.18 (t, J = 7.39 Hz, 1H), 2.13 (s, 1H), 2.08 (d, J = 8.03 Hz, 1H), 2.02 (d, J = 3.37 Hz, 1H), 2.02–1.99 (m, 1H), 1.99–1.96 (m, 1H), 1.96 (d, J = 6.57 Hz, 1H), 1.94 (d, J = 6.97 Hz, 1H), 1.91 (d, J = 2.49 Hz, 2H), 1.85 (s, 1H), 1.83 (d, J = 6.63 Hz, 2H), 1.45 (t, J = 7.01 Hz, 1H), 1.35 (s, 1H), 1.29 (s, 1H), 1.14 (s, 1H), 1.02 (d, J = 6.51 Hz, 3H), 0.92 (d, J = 6.94 Hz, 3H), 0.89 (d, J = 7.05 Hz, 3H), 0.88 (s, 3H), 0.86–0.84 (m, 3H), 0.83 (s, 12H), 0.82–0.81 (m, 6H), 0.80 (d, J = 6.59 Hz, 3H), 0.79–0.77 (m, 9H), 0.77 (s, 3H), 0.74 (s, 3H), 0.66 (d, J = 6.87 Hz, 3H), 0.65–0.64 (m, 3H), 0.61 (d, J = 6.95 Hz, 3H). ^{13}C NMR (175 MHz, DMSO-d_6): δ (ppm) 174.3, 172.3, 171.0, 170.6, 170.6, 170.3, 169.1, 167.8, 162.9, 157.9, 157.1, 149.2, 149.1, 132.0, 130.3, 129.6, 128.5, 124.6, 118.2, 105.1, 99.0, 72.3, 69.5, 68.8, 67.7, 67.1, 67.0, 62.6, 60.2, 57.4, 57.3, 55.4, 55.2, 55.1, 53.5, 53.4, 48.5, 41.1, 38.2, 36.9, 35.1, 35.1, 31.3, 30.6, 29.9, 29.1, 29.0, 28.8, 28.7, 28.5, 26.5, 25.1, 24.3, 24.1, 23.0, 22.9, 22.8, 22.4, 22.1, 21.8, 21.7, 19.3, 19.2, 19.1, 18.2, 17.8, 17.6, 15.2, 15.1, 13.9. HRMS m/z: 778.4091 [M + H]$^+$. HPLC purity 95.4%, t_r = 17.7/18.6 min.

Δ^3-[L-Phe(3-nitro)]-lugdunin (25). Yield: 20.4 mg (75%). ^{1}H NMR (600 MHz, DMSO-d_6): δ (ppm) 8.76 (d, J = 7.52 Hz, 1H), 8.53 (d, J = 8.63 Hz, 1H), 8.46 (d, J = 5.49 Hz, 1H), 8.43 (d, J = 7.29 Hz, 1H), 8.37 (d, J = 8.88 Hz, 2H), 8.22 (d, J = 9.22 Hz, 2H), 8.16 (d, J = 8.61 Hz, 2H), 8.08 (d, J = 9.36 Hz, 1H), 8.03 (d, J = 7.96 Hz, 1H), 7.90 (t, J = 7.63 Hz, 1H), 7.85 (d, J = 8.85 Hz, 2H), 7.81 (d, J = 9.31 Hz, 1H), 7.78 (d, J = 8.95 Hz, 1H), 7.74 (d, J = 8.65 Hz, 1H), 7.49 (d, J = 9.43 Hz, 1H), 5.76 (s, 1H), 4.81 (d, J = 4.58 Hz, 1H), 4.74 (d, J = 4.94 Hz, 1H), 4.61 (d, J = 3.79 Hz, 1H), 4.60–4.53 (m, 1H), 4.51 (d, J = 4.55 Hz, 1H), 4.42 (d, J = 9.06 Hz, 1H), 4.34 (d, J = 8.29 Hz, 1H), 4.27 (t, J = 9.08 Hz, 1H), 4.21–4.17 (m, 1H), 4.13 (d,

https://doi.org/10.1021/acs.jmedchem.0c02170
J. Med. Chem. 2021, 64, 4034−4058

J = 9.98 Hz, 1H), 4.05 (d, J = 7.30 Hz, 1H), 3.98 (d, J = 7.89 Hz, 1H), 3.93−3.84 (m, 2H), 3.78−3.71 (m, 2H), 3.70 (s, 1H), 3.61 (d, J = 8.64 Hz, 2H), 3.46 (d, J = 4.68 Hz, 1H), 3.42 (d, J = 5.17 Hz, 1H), 3.25−3.13 (m, 1H), 3.07 (d, J = 7.51 Hz, 2H), 2.99−2.87 (m, 1H), 2.87 (s, 1H), 2.76−2.70 (m, 2H), 2.67 (t, J = 4.44 Hz, 2H), 2.61 (d, J = 12.85 Hz, 1H), 2.58−2.53 (m, 1H), 2.41 (s, 1H), 2.34 (s, 1H), 2.07 (d, J = 4.65 Hz, 1H), 1.99 (d, J = 5.66 Hz, 1H), 1.90 (d, J = 8.12 Hz, 6H), 1.72 (d, J = 7.25 Hz, 1H), 1.62 (d, J = 7.31 Hz, 2H), 1.57 (s, 2H), 1.48−1.37 (m, 1H), 1.35−1.27 (m, 1H), 1.24 (s, 1H), 1.22−1.15 (m, 1H), 1.07 (d, J = 7.00 Hz, 3H), 0.99 (d, J = 7.38 Hz, 3H), 0.93 (d, J = 6.79 Hz, 12H), 0.82 (d, J = 6.13 Hz, 6H), 0.70 (d, J = 6.31 Hz, 6H), 0.64 (d, J = 6.65 Hz, 6H), 0.62 (s, 3H), 0.50 (d, J = 6.84 Hz, 9H), 0.44 (d, J = 6.78 Hz, 3H). ^{13}C NMR (150 MHz, DMSO-d_6): δ (ppm) 170.0, 169.9, 169.9, 169.7, 169.3, 168.9, 168.7, 168.6, 168.5, 168.1, 167.8, 135.5, 135.0, 129.7, 129.5, 129.4, 129.3, 129.2, 126.3, 126.1, 70.7, 70.5, 63.7, 58.8, 58.6, 57.2, 55.8, 55.8, 55.6, 55.1, 54.8, 53.3, 52.8, 52.3, 51.7, 50.5, 49.4, 48.8, 46.9, 39.8, 39.6, 38.4, 35.9, 35.6, 34.1, 31.0, 30.6, 29.7, 29.6, 29.1, 28.3, 27.7, 27.6, 27.4, 27.0, 26.8, 22.5, 22.4, 21.5, 21.4, 20.8, 20.4, 20.4, 20.0, 19.3, 18.4, 18.2, 18.1, 17.9, 17.7, 17.5, 17.5, 17.4, 17.0, 16.8, 16.6, 16.5, 16.4, 16.2, 16.0, 15.7, 13.5. HRMS m/z: 789.4339 [M + H]$^+$. HPLC purity 94.8%, t_r = 16.7/17.2 min.

Δ^3-[L-Phe(F_5)]-lugdunin (26). Yield: 18.8 mg (65%). ^{1}H NMR (600 MHz, DMSO-d_6): δ (ppm) 9.46 (s, 1H), 9.43 (d, J = 5.11 Hz, 1H), 9.06−8.97 (m, 1H), 8.84 (s, 1H), 8.75 (d, J = 6.36 Hz, 1H), 8.62 (d, J = 9.00 Hz, 1H), 8.53 (t, J = 3.19, Hz, 1H), 8.40 (d, J = 7.94 Hz, 2H), 8.32 (d, J = 8.97 Hz, 1H), 8.26 (d, J = 8.25 Hz, 1H), 8.20 (d, J = 9.10 Hz, 1H), 8.14 (d, J = 9.31 Hz, 1H), 8.10 (d, J = 9.28 Hz, 1H), 8.02−7.98 (m, 1H), 7.95 (d, J = 9.27 Hz, 1H), 7.91 (d, J = 8.24 Hz, 1H), 7.80 (d, J = 9.40 Hz, 1H), 7.76 (d, J = 8.97 Hz, 1H), 7.73 (t, J = 2.89 Hz, 1H), 7.70 (s, 1H), 7.58 (t, J = 8.23 Hz, 1H), 7.52 (d, J = 4.42 Hz, 1H), 7.50 (d, J = 4.43 Hz, 1H), 7.37 (d, J = 4.97 Hz, 3H), 7.32 (dd, J = 3.02, 6.70 Hz, 1H), 7.21 (d, J = 8.87 Hz, 1H), 7.01 (d, J = 8.33 Hz, 1H), 6.89 (s, 1H), 5.76 (s, 1H), 5.06 (s, 1H), 4.80−4.74 (m, 1H), 4.73 (s, 1H), 4.71 (d, J = 2.69 Hz, 1H), 4.70 (s, 1H), 4.68 (s, 1H), 4.59 (dd, J = 6.51, 10.57 Hz, 2H), 4.51−4.50 (m, 2H), 4.49−4.47 (m, 2H), 4.47−4.45 (m, 1H), 4.45 (s, 1H), 4.43 (d, J = 2.88 Hz, 2H), 4.42 (s, 1H), 4.40 (d, J = 3.02 Hz, 1H), 4.40−4.34 (m, 3H), 4.29 (t, J = 8.93 Hz, 1H), 4.24 (t, J = 8.82 Hz, 1H), 4.18 (t, J = 7.48 Hz, 1H), 4.07 (t, J = 2.39, 9.03 Hz, 1H), 3.93 (d, J = 8.65 Hz, 1H), 3.75 (d, J = 6.36 Hz, 1H), 3.73 (s, 1H), 3.71 (dd, J = 2.99, 6.91 Hz, 2H), 3.69 (d, J = 2.68 Hz, 1H), 3.67 (d, J = 6.19 Hz, 1H), 3.63 (d, J = 3.76 Hz, 2H), 3.59 (s, 1H), 3.45 (t, J = 6.05 Hz, 1H), 3.41 (t, J = 5.30 Hz, 1H), 3.25 (s, 1H), 3.24 (d, J = 4.09 Hz, 1H), 3.22 (s, 1H), 3.16 (s, 2H), 3.15−3.13 (m, 2H), 3.11 (s, 1H), 3.10 (d, J = 4.07 Hz, 2H), 3.08 (d, J = 3.25 Hz, 1H), 3.06 (t, J = 4.16 Hz, 1H), 3.02 (d, J = 3.36 Hz, 1H), 3.00 (d, J = 2.32 Hz, 1H), 2.93 (d, J = 5.13 Hz, 3H), 2.92−2.90 (m, 2H), 2.88 (d, J = 5.92 Hz, 3H), 2.86 (d, J = 3.95 Hz, 2H), 2.82 (d, J = 2.60 Hz, 1H), 2.64 (s, 1H), 2.63−2.59 (m, 2H), 2.54 (d, J = 2.89 Hz, 2H), 2.46 (s, 1H), 2.40−2.38 (m, 1H), 2.34 (s, 1H), 2.18 (t, J = 7.33 Hz, 1H), 2.07−2.05 (m, 2H), 1.99−1.89 (m, 1H), 1.88−1.76 (m, 1H), 1.55 (dd, J = 6.81, 9.02 Hz, 2H), 1.40 (d, J = 2.80 Hz, 1H), 1.39 (d, J = 7.18 Hz, 2H), 1.34 (d, J = 9.57 Hz, 2H), 1.30 (d, J = 2.20 Hz, 1H), 1.29 (d, J = 2.70 Hz, 1H), 1.26 (s, 1H), 1.23 (s, 1H), 1.19 (t, J = 7.31 Hz, 2H), 1.11 (s, 1H), 1.09 (d, J = 5.95 Hz, 2H), 1.04−0.99 (m, 12H), 0.97 (d, J = 7.00 Hz, 9H), 0.92 (d, J = 6.70 Hz, 6H), 0.88−0.85 (m, 6H), 0.85 (d, J = 6.50 Hz, 3H), 0.83 (d, J = 6.93 Hz, 3H), 0.81 (d, J = 7.04 Hz, 3H), 0.81−0.77 (m, 3H), 0.77 (s, 3H), 0.76 (d, J = 6.30 Hz, 3H), 0.75 (s, 3H), 0.73 (s, 3H), 0.70 (d, J = 6.86 Hz, 3H), 0.66 (d, J = 6.71 Hz, 3H). ^{13}C NMR (150 MHz, DMSO-d_6): δ (ppm) 171.6, 171.6, 171.5, 171.0, 170.9, 170.7, 170.6, 170.5, 170.4, 170.4, 170.3, 169.6, 169.4, 169.1, 168.9, 168.6, 151.0, 145.9, 144.3, 140.0, 139.6, 139.0, 138.3, 137.5, 135.8, 134.6, 130.3, 129.6, 128.7, 128.3, 127.8, 127.6, 124.0, 120.6, 73.1, 72.3, 72.1, 69.5, 68.8, 67.2, 66.3, 65.5, 65.0, 63.7, 60.3, 60.2, 58.2, 57.8, 57.4, 57.3, 57.2, 56.8, 56.6, 55.2, 54.5, 53.4, 52.0, 51.9, 51.8, 51.2, 50.8, 50.5, 41.3, 41.3, 41.2, 39.1, 37.5, 36.9, 35.1, 34.4, 32.6, 32.0, 31.2, 30.9, 30.5, 30.4, 30.0, 29.7, 29.7, 29.5, 29.0, 28.9, 28.6, 28.5, 25.7, 24.4, 24.1, 24.0, 22.9, 22.8, 22.2, 22.0, 21.5, 21.5, 21.1, 20.8, 20.0, 19.8, 19.7, 19.2, 19.2, 18.9, 18.7, 18.4, 18.2, 18.0, 17.9, 17.7, 17.2, 17.2, 15.2, 13.9, 12.9, 10.9. HRMS m/z: 834.4010 [M + H]$^+$. HPLC purity 96.9%, t_r = 18.1/18.8 min.

Δ^3-[L-Ala(4-pyridyl)]-lugdunin (27). Yield: 20.3 mg (79%). ^{1}H NMR (700 MHz, DMSO-d_6): δ (ppm) 8.76 (d, J = 7.52 Hz, 1H), 8.53 (d, J = 8.63 Hz, 1H), 8.46 (d, J = 5.49 Hz, 1H), 8.43 (d, J = 7.29 Hz, 1H), 8.37 (d, J = 8.88 Hz, 2H), 8.22 (d, J = 9.22 Hz, 2H), 8.16 (d, J = 8.61 Hz, 2H), 8.08 (d, J = 9.36 Hz, 1H), 8.03 (d, J = 7.96 Hz, 1H), 7.90 (t, J = 7.63 Hz, 1H), 7.85 (d, J = 8.85 Hz, 2H), 7.81 (d, J = 9.31 Hz, 1H), 7.78 (d, J = 8.95 Hz, 1H), 7.74 (d, J = 8.65 Hz, 1H), 7.49 (d, J = 9.43 Hz, 1H), 5.76 (s, 1H), 4.81 (d, J = 4.58 Hz, 1H), 4.74 (d, J = 4.94 Hz, 1H), 4.61 (d, J = 3.79 Hz, 1H), 4.60−4.53 (m, 1H), 4.51 (d, J = 4.55 Hz, 1H), 4.42 (d, J = 9.06 Hz, 1H), 4.34 (d, J = 8.29 Hz, 1H), 4.27 (t, J = 9.08 Hz, 1H), 4.21−4.17 (m, 1H), 4.13 (d, J = 9.98 Hz, 1H), 4.05 (d, J = 7.30 Hz, 1H), 3.98 (d, J = 7.89 Hz, 1H), 3.93−3.84 (m, 2H), 3.78−3.71 (m, 2H), 3.70 (s, 1H), 3.61 (d, J = 8.64 Hz, 2H), 3.46 (d, J = 4.68 Hz, 1H), 3.42 (d, J = 5.17 Hz, 1H), 3.25−3.13 (m, 1H), 3.07 (d, J = 7.51 Hz, 2H), 2.99−2.87 (m, 1H), 2.87 (s, 1H), 2.76−2.70 (m, 2H), 2.67 (t, J = 4.44 Hz, 2H), 2.61 (d, J = 12.85 Hz, 1H), 2.58−2.53 (m, 1H), 2.41 (s, 1H), 2.34 (s, 1H), 2.07 (d, J = 4.65 Hz, 1H), 1.99 (d, J = 5.66 Hz, 1H), 1.90 (d, J = 8.12 Hz, 6H), 1.72 (d, J = 7.25 Hz, 1H), 1.62 (d, J = 7.31 Hz, 2H), 1.57 (s, 2H), 1.48−1.37 (m, 1H), 1.35−1.27 (m, 1H), 1.24 (s, 1H), 1.22−1.15 (m, 1H), 1.07 (d, J = 7.00 Hz, 3H), 0.99 (d, J = 7.38 Hz, 3H), 0.93 (d, J = 6.79 Hz, 12H), 0.82 (d, J = 6.13 Hz, 6H), 0.70 (d, J = 6.31 Hz, 6H), 0.64 (d, J = 6.65 Hz, 6H), 0.62 (s, 3H), 0.50 (d, J = 6.84 Hz, 9H), 0.44 (d, J = 6.78 Hz, 3H). ^{13}C NMR (175 MHz, DMSO-d_6): δ (ppm) 170.0, 169.9, 169.9, 169.7, 169.3, 168.9, 168.7, 168.6, 168.5, 168.1, 167.8, 135.5, 135.0, 129.7, 129.5, 129.4, 129.3, 129.2, 126.3, 126.1, 70.7, 70.5, 63.7, 58.8, 58.6, 57.2, 55.8, 55.8, 55.6, 55.1, 54.8, 53.3, 52.8, 52.3, 51.7, 50.5, 49.4, 48.8, 46.9, 39.8, 39.6, 38.4, 35.9, 35.6, 34.1, 31.0, 30.6, 29.7, 29.6, 29.1, 28.3, 27.7, 27.6, 27.4, 27.0, 26.8, 22.5, 22.4, 21.5, 21.4, 20.8, 20.4, 20.4, 20.0, 19.3, 18.4, 18.2, 18.1, 17.9, 17.7, 17.5, 17.5, 17.4, 17.0, 16.8, 16.6, 16.5, 16.4, 16.2, 16.0, 15.7, 13.5. HRMS m/z: 745.4437 [M + H]$^+$. HPLC purity 93.8%, t_r = 14.4/15.0 min.

Δ^3-[L-Ala(4-thiazolyl)]-lugdunin (28). Yield: 19.7 mg (76%). ^{1}H NMR (600 MHz, DMSO-d_6): δ (ppm) 8.99 (d, J = 4.00 Hz, 1H), 8.97 (d, J = 4.96 Hz, 1H), 8.59 (d, J = 8.51 Hz, 1H), 8.56 (d, J = 5.05 Hz, 1H), 8.37 (d, J = 8.58 Hz, 1H), 8.25 (d, J = 9.41 Hz, 1H), 8.05 (d, J = 7.42 Hz, 1H), 8.03 (s, 1H), 7.96 (d, J = 8.29 Hz, 1H), 7.79 (d, J = 9.00 Hz, 1H), 7.75 (d, J = 9.52 Hz, 1H), 7.72 (d, J = 9.62 Hz, 1H), 7.65 (d, J = 9.32 Hz, 1H), 7.43 (d, J = 9.53 Hz, 1H), 7.36 (dd, J = 2.05, 3.84 Hz, 2H), 5.07 (s, 1H), 4.83 (dd, J = 5.92, 8.87 Hz, 1H), 4.75 (d, J = 2.00 Hz, 1H), 4.73 (d, J = 2.07 Hz, 1H), 4.70 (d, J = 3.83 Hz, 1H), 4.69 (t, J = 3.35 Hz, 1H), 4.67 (d, J = 3.99 Hz, 1H), 4.62 (dd, J = 8.59, 10.75 Hz, 1H), 4.51 (d, J = 4.56 Hz, 1H), 4.49 (d, J = 4.60 Hz, 1H), 4.43 (s, 1H), 4.41 (d, J = 5.78 Hz, 1H), 4.40−4.38 (m, 1H), 4.37 (d, J = 2.94 Hz, 1H), 4.36 (s, 1H), 4.28 (t, J = 5.15 Hz, 1H), 4.22 (t, J = 9.24 Hz, 1H), 4.17 (dd, J = 8.07, 9.47 Hz, 1H), 4.07 (dd, J = 2.17, 8.99 Hz, 1H), 3.99 (t, J = 8.15 Hz, 1H), 3.92−3.87 (m, 1H), 3.75 (d, J = 7.12 Hz, 1H), 3.73 (d, J = 2.45 Hz, 1H), 3.72 (d, J = 2.66 Hz, 1H), 3.70 (d, J = 2.19 Hz, 1H), 3.70−3.64 (m, 1H), 3.57 (dd, J = 5.01, 9.11 Hz, 1H), 3.46−3.43 (m, 1H), 3.42−3.39 (m, 1H), 3.38 (dd, J = 2.65, 3.95 Hz, 1H), 3.21−3.16 (m, 1H), 3.12−3.03 (m, 2H), 3.02 (d, J = 3.92 Hz, 1H), 3.01−2.98 (m, 1H), 2.97 (d, J = 9.15 Hz, 1H), 2.94 (d, J = 2.39 Hz, 1H), 2.92 (d, J = 3.32 Hz, 1H), 2.91−2.89 (m, 1H), 2.83 (dd, J = 3.23, 6.42 Hz, 1H), 2.62−2.58 (m, 1H), 2.57−2.54 (m, 1H), 2.54 (d, J = 1.52 Hz, 1H), 2.41−2.37 (m, 1H), 2.08 (s, 1H), 2.08−2.05 (m, 1H), 2.03−2.01 (m, 1H), 1.99 (d, J = 7.17 Hz, 1H), 1.96 (d, J = 6.72 Hz, 1H), 1.92−1.85 (m, 2H), 1.75−1.66 (m, 2H), 1.54 (d, J = 6.76 Hz, 1H), 1.43−1.32 (m, 3H), 1.31−1.27 (m, 1H), 1.25 (d, J = 8.49 Hz, 3H), 1.15 (d, J = 5.64 Hz, 3H), 1.04 (d, J = 5.70 Hz, 3H), 1.02−1.00 (m, 3H), 0.99 (d, J = 7.03 Hz, 18H), 0.93 (dd, J = 2.68, 6.70 Hz, 6H), 0.91 (d, J = 6.18 Hz, 1H), 0.91 (s, 3H), 0.90 (d, J = 7.13 Hz, 3H), 0.88 (d, J = 2.60 Hz, 3H), 0.87 (dd, J = 2.32, 4.40 Hz, 3H), 0.86 (s, 3H), 0.85 (s, 3H), 0.83 (d, J = 2.59 Hz, 3H), 0.82 (d, J = 3.29 Hz, 3H), 0.81−0.80 (m, 3H), 0.79 (d, J = 6.47 Hz, 3H), 0.76 (d, J = 6.95 Hz, 3H), 0.68−0.66 (m, 6H), 0.54 (d, J = 6.70 Hz, 3H), 0.47 (d, J = 6.75 Hz, 3H). ^{13}C NMR (150 MHz, DMSO-d_6): δ (ppm) 172.1, 172.0, 172.0, 171.9, 171.5, 171.2,

https://doi.org/10.1021/acs.jmedchem.0c02170
J. Med. Chem. 2021, 64, 4034−4058

170.9, 170.7, 170.4, 170.4, 170.0, 154.0, 153.7, 153.4, 116.3, 116.1, 72.8, 72.6, 72.5, 65.9, 64.1, 61.4, 60.8, 60.7, 59.9, 57.9, 57.7, 57.4, 57.0, 54.9, 53.1, 52.9, 52.3, 51.2, 42.1, 41.6, 38.8, 38.3, 35.2, 33.9, 33.1, 32.5, 32.4, 31.7, 31.3, 30.1, 29.7, 29.3, 28.9, 24.6, 24.5, 23.6, 22.8, 22.4, 22.2, 21.4, 20.4, 20.2, 20.0, 19.7, 19.6, 19.1, 19.0, 18.7, 18.6, 18.5, 17.9, 15.7, 14.3. HRMS m/z: 751.4001 $[M + H]^+$. HPLC purity 95.8%, t_r = 16.0/16.9 min.

Δ^3-[L-Ala(2-furyl)]-lugdunin (29). Yield: 12.3 mg (49%). ^{1}H NMR (600 MHz, DMSO-d_6): δ (ppm) 8.63 (d, J = 8.52 Hz, 1H), 8.58 (d, J = 5.25 Hz, 1H), 8.32 (d, J = 8.43 Hz, 1H), 8.23 (d, J = 9.47 Hz, 1H), 8.10 (d, J = 8.36 Hz, 1H), 8.06 (d, J = 9.04 Hz, 1H), 8.01 (d, J = 7.76 Hz, 1H), 7.79 (dd, J = 5.07, 9.33 Hz, 2H), 7.75 (d, J = 9.26 Hz, 1H), 7.70 (d, J = 9.32 Hz, 1H), 7.48–7.43 (m, 3H), 6.31 (dd, J = 5.89, 8.19 Hz, 1H), 6.29 (dd, J = 6.90, 9.13 Hz, 1H), 6.14 (t, J = 3.34 Hz, 2H), 4.75 (d, J = 2.20 Hz, 1H), 4.73 (d, J = 2.22 Hz, 1H), 4.64–4.58 (m, 1H), 4.57 (d, J = 4.03 Hz, 1H), 4.56 (dd, J = 2.46, 4.03 Hz, 1H), 4.54 (d, J = 4.09 Hz, 1H), 4.51 (d, J = 4.78 Hz, 1H), 4.49 (d, J = 4.80 Hz, 1H), 4.47 (d, J = 9.34 Hz, 1H), 4.40 (d, J = 9.04 Hz, 2H), 4.38 (d, J = 2.85 Hz, 1H), 4.36 (s, 1H), 4.24 (d, J = 9.12 Hz, 1H), 4.21 (d, J = 4.63 Hz, 1H), 4.19 (d, J = 1.27 Hz, 1H), 4.18 (s, 1H), 4.09–4.04 (m, 1H), 4.03 (t, J = 8.02 Hz, 1H), 3.96 (d, J = 5.27 Hz, 1H), 3.92–3.88 (m, 1H), 3.76 (dd, J = 2.89, 4.51 Hz, 1H), 3.73–3.71 (m, 1H), 3.70 (s, 1H), 3.69 (t, J = 2.74 Hz, 1H), 3.67 (s, 1H), 3.67–3.65 (m, 1H), 3.64 (d, J = 3.72 Hz, 1H), 3.63 (s, 1H), 3.46–3.40 (m, 3H), 3.40–3.36 (m, 1H), 3.26 (d, J = 4.25 Hz, 1H), 3.23 (d, J = 3.77 Hz, 1H), 3.19 (s, 1H), 3.18 (d, J = 3.47 Hz, 1H), 3.17 (s, 1H), 3.10 (s, 1H), 3.08 (d, J = 3.24 Hz, 1H), 3.07 (s, 1H), 2.95 (dd, J = 2.89, 6.00 Hz, 1H), 2.92 (d, J = 5.49 Hz, 1H), 2.89 (d, J = 5.64 Hz, 1H), 2.84 (d, J = 9.18 Hz, 1H), 2.83–2.82 (m, 1H), 2.81 (d, J = 3.43 Hz, 1H), 2.78 (d, J = 4.37 Hz, 1H), 2.76 (s, 1H), 2.61 (d, J = 4.83 Hz, 1H), 2.58 (dd, J = 8.46, 9.77 Hz, 1H), 2.55 (s, 1H), 2.53 (d, J = 3.83 Hz, 1H), 2.38 (d, J = 4.87 Hz, 2H), 2.08 (s, 1H), 2.07 (s, 1H), 2.04 (s, 1H), 2.01 (s, 1H), 2.00 (d, J = 2.45 Hz, 1H), 1.98–1.97 (m, 9H), 1.96 (s, 1H), 1.95 (d, J = 1.92 Hz, 1H), 1.92 (s, 1H), 1.91 (s, 1H), 1.90–1.88 (m, 1H), 1.88 (d, J = 7.38 Hz, 1H), 1.83–1.73 (m, 2H), 1.58–1.53 (m, 1H), 1.49–1.46 (m, 1H), 1.44–1.39 (m, 1H), 1.39–1.36 (m, 1H), 1.35 (d, J = 4.09 Hz, 1H), 1.34–1.32 (m, 1H), 1.31–1.27 (m, 1H), 1.27–1.25 (m, 1H), 1.15 (dd, J = 4.31, 7.85 Hz, 2H), 1.10–1.06 (m, 3H), 1.05 (s, 12H), 1.02 (d, J = 3.98 Hz, 3H), 1.01 (s, 3H), 0.93 (d, J = 6.72 Hz, 3H), 0.90 (d, J = 6.62 Hz, 3H), 0.88 (dd, J = 2.51, 4.43 Hz, 9H), 0.86 (dd, J = 1.26, 6.78 Hz, 6H), 0.85–0.83 (m, 3H), 0.82 (d, J = 3.39 Hz, 3H), 0.82–0.80 (m, 3H), 0.79 (d, J = 7.09 Hz, 3H), 0.77 (d, J = 7.08 Hz, 3H), 0.75 (s, 1H), 0.74–0.72 (m, 3H), 0.71 (d, J = 6.82 Hz, 3H), 0.69 (d, J = 6.94 Hz, 3H), 0.65 (d, J = 6.85 Hz, 3H), 0.64 (d, J = 6.84 Hz, 3H). ^{13}C NMR (150 MHz, DMSO-d_6): δ (ppm) 171.6, 171.5, 171.4, 171.3, 171.0, 170.6, 170.4, 170.2, 169.9, 169.9, 169.7, 169.2, 151.8, 151.2, 141.6, 141.5, 110.2, 110.2, 107.1, 106.8, 76.3, 76.3, 74.5, 74.5, 72.3, 72.1, 72.0, 65.3, 65.2, 64.7, 63.6, 60.8, 59.2, 57.4, 57.3, 56.8, 56.5, 54.4, 52.4, 51.7, 50.9, 50.7, 41.4, 41.1, 38.2, 37.7, 32.6, 32.0, 31.2, 30.8, 30.6, 29.6, 29.3, 29.0, 29.0, 28.5, 24.1, 24.0, 23.0, 22.3, 22.0, 21.7, 20.8, 20.3, 19.8, 19.7, 19.5, 19.1, 18.8, 18.6, 18.5, 18.4, 18.1, 18.0, 17.8, 17.4, 17.2, 17.2, 15.2. HRMS m/z: 734.4277 $[M + H]^+$. HPLC purity 96.1%, t_r = 16.7/17.7 min.

Δ^3-[L-Ala(2-thienyl)]-lugdunin (30). Yield: 15.4 mg (60%). ^{1}H NMR (600 MHz, DMSO-d_6): δ (ppm) 8.61 (d, J = 8.57 Hz, 1H), 8.54 (d, J = 6.39 Hz, 1H), 8.27 (d, J = 8.58 Hz, 1H), 8.19 (d, J = 8.77 Hz, 1H), 8.17 (d, J = 8.67 Hz, 1H), 8.06 (d, J = 9.17 Hz, 1H), 8.00 (d, J = 7.89 Hz, 1H), 7.80 (d, J = 5.28 Hz, 1H), 7.79 (d, J = 7.79 Hz, 1H), 7.72 (d, J = 9.38 Hz, 1H), 7.70 (d, J = 9.41 Hz, 1H), 7.47 (d, J = 9.37 Hz, 1H), 7.30 (d, J = 7.03 Hz, 1H), 7.28 (d, J = 7.98 Hz, 1H), 6.93–6.91 (m, 1H), 6.90 (s, 1H), 6.89 (d, J = 7.67 Hz, 1H), 6.89–6.88 (m, 1H), 6.87 (d, J = 8.67 Hz, 1H), 6.86 (s, 1H), 4.74 (d, J = 2.21 Hz, 1H), 4.72 (d, J = 2.24 Hz, 1H), 4.59 (dd, J = 4.80, 6.72 Hz, 1H), 4.50 (d, J = 7.65 Hz, 2H), 4.40 (d, J = 4.10 Hz, 2H), 4.24 (t, J = 9.11 Hz, 1H), 4.19 (dd, J = 8.02, 9.51 Hz, 1H), 4.10–4.03 (m, 3H), 3.96 (t, J = 4.97 Hz, 1H), 3.76 (d, J = 5.89 Hz, 1H), 3.68 (dd, J = 6.25, 9.63 Hz, 2H), 3.46–3.40 (m, 3H), 3.17 (dd, J = 5.66, 9.40 Hz, 1H), 3.08 (dd, J = 2.64, 7.12 Hz, 1H), 3.06 (d, J = 5.40 Hz, 1H), 3.02 (d, J = 9.15 Hz, 1H), 2.99 (d, J = 4.41 Hz, 1H), 2.96 (d, J = 4.31 Hz, 1H), 2.94 (s, 1H), 2.91 (dd, J = 8.83, 11.75 Hz, 1H), 2.62–2.59 (m, 1H), 2.58 (s, 1H), 2.55 (s, 1H), 2.54–2.52 (m, 1H), 2.39–2.37 (m, 1H), 2.08 (s, 1H), 2.07 (s, 1H), 2.04 (s, 1H), 2.01 (d, J = 5.56 Hz, 1H), 1.98–1.96 (m, 1H), 1.96–1.94 (m, 1H), 1.93–1.86 (m, 2H), 1.81–1.77 (m, 1H), 1.77–1.72 (m, 1H), 1.57–1.53 (m, 1H), 1.51–1.45 (m, 1H), 1.45–1.40 (m, 1H), 1.38–1.32 (m, 2H), 1.29 (d, J = 6.81 Hz, 1H), 1.26 (dd, J = 2.10, 5.61 Hz, 1H), 1.23 (t, J = 3.46 Hz, 1H), 1.19 (d, J = 7.14 Hz, 1H), 1.15 (td, J = 2.60, 6.56 Hz, 1H), 1.07 (t, J = 5.56 Hz, 2H), 1.02 (d, J = 6.94 Hz, 3H), 1.01 (s, 3H), 0.93 (d, J = 6.65 Hz, 3H), 0.88 (s, 3H), 0.88 (d, J = 7.68 Hz, 3H), 0.87 (d, J = 6.08 Hz, 6H), 0.86 (d, J = 7.06 Hz, 3H), 0.85 (d, J = 6.22 Hz, 1H), 0.83 (d, J = 7.64 Hz, 3H), 0.82 (d, J = 6.18 Hz, 3H), 0.81 (d, J = 6.59 Hz, 6H), 0.79 (s, 3H), 0.78 (s, 3H), 0.74 (d, J = 6.87 Hz, 3H), 0.68 (d, J = 6.84 Hz, 3H), 0.62 (d, J = 6.79 Hz, 3H), 0.57 (d, J = 6.73 Hz, 3H). ^{13}C NMR (150 MHz, DMSO-d_6): δ (ppm) 171.6, 171.6, 171.5, 171.3, 170.9, 170.6, 170.4, 170.2, 169.9, 169.9, 169.8, 169.2, 140.1, 139.1, 126.6, 126.6, 126.5, 126.2, 124.3, 124.1, 76.3, 76.3, 74.6, 74.5, 74.5, 74.5, 74.4, 72.3, 72.1, 72.1, 65.3, 65.2, 64.7, 63.7, 60.6, 59.0, 57.4, 57.3, 57.2, 56.8, 56.6, 54.4, 53.4, 52.3, 50.7, 41.4, 41.1, 38.1, 37.6, 32.6, 32.1, 32.0, 31.1, 30.6, 29.7, 29.3, 29.1, 28.6, 24.1, 24.0, 23.1, 22.4, 22.0, 21.7, 20.8, 20.3, 20.2, 19.8, 19.7, 19.5, 19.3, 19.2, 19.1, 18.7, 18.6, 18.4, 18.3, 18.0, 18.0, 17.4, 17.2, 15.2. HRMS m/z: 750.4041 $[M + H]^+$. HPLC purity 97.4%, t_r = 17.1/17.9 min.

Δ^3-[L-Ala(2-benzothiazolyl)]-lugdunin (31). Yield: 19.3 mg (70%). ^{1}H NMR (600 MHz, DMSO-d_6): δ (ppm) 8.91 (d, J = 8.64 Hz, 1H), 8.71 (d, J = 5.04 Hz, 1H), 8.54 (d, J = 8.45 Hz, 1H), 8.28 (d, J = 9.40 Hz, 1H), 8.17 (d, J = 8.28 Hz, 1H), 8.07 (d, J = 7.90 Hz, 2H), 8.05 (s, 1H), 8.04–8.01 (m, 2H), 7.94 (d, J = 7.92 Hz, 1H), 7.89 (d, J = 8.24 Hz, 1H), 7.80 (d, J = 9.17 Hz, 1H), 7.76 (d, J = 9.39 Hz, 1H), 7.69 (d, J = 9.33 Hz, 1H), 7.49–7.43 (m, 2H), 7.39 (d, J = 7.02 Hz, 1H), 5.04 (t, J = 7.91 Hz, 1H), 5.00 (d, J = 6.54 Hz, 1H), 4.90 (d, J = 4.22 Hz, 1H), 4.89 (d, J = 4.19 Hz, 1H), 4.87 (d, J = 4.25 Hz, 1H), 4.73 (d, J = 2.13 Hz, 1H), 4.71 (d, J = 2.22 Hz, 1H), 4.64 (d, J = 2.47 Hz, 1H), 4.63–4.61 (m, 1H), 4.60 (d, J = 5.42 Hz, 1H), 4.56 (d, J = 8.13 Hz, 1H), 4.51–4.48 (m, 1H), 4.48 (s, 1H), 4.43 (s, 1H), 4.41 (s, 1H), 4.36 (d, J = 7.85 Hz, 1H), 4.24 (d, J = 4.28 Hz, 1H), 4.21 (d, J = 8.98 Hz, 1H), 4.20–4.17 (m, 1H), 4.12 (d, J = 8.93 Hz, 1H), 4.09–4.06 (m, 1H), 4.06 (s, 1H), 4.04–4.03 (m, 1H), 4.01 (d, J = 8.03 Hz, 1H), 3.97 (d, J = 8.64 Hz, 1H), 3.92 (d, J = 6.28 Hz, 1H), 3.75 (d, J = 2.23 Hz, 1H), 3.74–3.72 (m, 1H), 3.70 (d, J = 4.54 Hz, 1H), 3.67–3.65 (m, 1H), 3.58 (d, J = 3.64 Hz, 1H), 3.48 (d, J = 5.42 Hz, 1H), 3.45–3.43 (m, 1H), 3.41–3.41 (m, 1H), 3.39 (d, J = 7.17 Hz, 1H), 3.36–3.34 (m, 1H), 3.30 (s, 1H), 3.30–3.27 (m, 1H), 3.25 (s, 1H), 3.24–3.21 (m, 1H), 3.20 (d, J = 3.43 Hz, 1H), 3.19 (s, 1H), 3.17–3.15 (m, 2H), 3.09 (s, 1H), 3.08 (dd, J = 3.17, 6.56 Hz, 2H), 3.04 (d, J = 4.88 Hz, 1H), 3.02 (d, J = 3.06 Hz, 1H), 2.99 (d, J = 2.67 Hz, 1H), 2.97 (s, 1H), 2.96–2.91 (m, 1H), 2.89 (s, 1H), 2.83 (dd, J = 3.23, 4.72 Hz, 1H), 2.82–2.78 (m, 1H), 2.73 (s, 1H), 2.69 (s, 1H), 2.63–2.59 (m, 1H), 2.60–2.56 (m, 1H), 2.54 (s, 1H), 2.41 (d, J = 9.82 Hz, 1H), 2.38 (d, J = 3.68 Hz, 1H), 2.32–2.30 (m, 1H), 2.18 (t, J = 7.30 Hz, 1H), 2.08 (d, J = 6.03 Hz, 1H), 2.05 (d, J = 3.52 Hz, 1H), 2.02 (d, J = 2.69 Hz, 1H), 2.00 (s, 1H), 1.97 (dd, J = 4.83, 7.08 Hz, 1H), 1.94 (s, 1H), 1.93–1.92 (m, 1H), 1.91 (dd, J = 2.35, 3.56 Hz, 1H), 1.90 (d, J = 1.31 Hz, 1H), 1.74 (dd, J = 6.84, 8.94 Hz, 2H), 1.56–1.50 (m, 1H), 1.39 (dd, J = 3.37, 6.40 Hz, 2H), 1.36 (s, 1H), 1.33–1.28 (m, 1H), 1.23 (s, 1H), 1.04–0.99 (m, 9H), 0.98 (d, J = 6.91 Hz, 3H), 0.92 (d, J = 7.07 Hz, 3H), 0.87 (d, J = 4.00 Hz, 3H), 0.87 (s, 6H), 0.85 (d, J = 3.19 Hz, 3H), 0.83 (d, J = 1.85 Hz, 3H), 0.82 (d, J = 1.78 Hz, 3H), 0.81 (d, J = 6.48 Hz, 3H), 0.80–0.80 (m, 3H), 0.79 (d, J = 2.21 Hz, 3H), 0.79 (d, J = 2.10 Hz, 3H), 0.78–0.76 (m, 3H), 0.75 (d, J = 3.15 Hz, 3H), 0.73 (d, J = 7.25 Hz, 3H), 0.64 (d, J = 6.79 Hz, 3H), 0.51 (d, J = 6.45 Hz, 3H), 0.43 (d, J = 6.74 Hz, 3H). ^{13}C NMR (150 MHz, DMSO-d_6): δ (ppm) 171.6, 171.5, 171.4, 170.9, 170.7, 170.5, 170.4, 170.2, 170.1, 170.0, 169.1, 168.8, 168.0, 166.9, 152.5, 135.0, 135.0, 134.9, 126.0, 125.9, 125.8, 125.8, 124.8, 124.8, 122.1, 122.1, 122.0, 121.9, 121.9, 72.3, 72.1, 71.9, 69.7, 69.5, 66.9, 65.2, 63.7, 60.9, 60.3, 60.1, 59.1, 57.4, 57.3, 57.3, 57.0, 56.7, 54.4, 52.6, 52.5, 51.9, 50.9, 41.4, 41.0, 38.2, 38.1, 37.7, 36.1, 35.1, 34.8, 34.6, 32.5, 32.4, 31.9, 31.3, 31.0, 30.6, 29.3, 29.0, 28.5, 28.3, 24.0, 22.9, 22.9, 22.3, 21.8, 21.6, 20.8, 19.9, 19.8, 19.7, 19.4, 19.2,

https://doi.org/10.1021/acs.jmedchem.0c02170
J. Med. Chem. 2021, 64, 4034−4058

19.1, 18.9, 18.6, 18.6, 18.4, 18.2, 18.0, 17.8, 17.5, 15.3, 15.2, 13.9, 13.8. HRMS m/z: 801.4159 $[M + H]^+$. HPLC purity 95.2%, t_r = 17.3/17.9 min.

Δ^3-[L-Ala(3-benzothienyl)]-lugdunin (32). Yield: 18.9 mg (69%). ^{1}H NMR (600 MHz, DMSO-d_6): δ (ppm) 8.83 (d, J = 7.38 Hz, 1H), 8.82 (d, J = 7.32 Hz, 1H), 8.78 (d, J = 8.44 Hz, 1H), 8.63 (d, J = 7.37 Hz, 1H), 8.61 (d, J = 8.31 Hz, 1H), 8.43 (d, J = 8.83 Hz, 1H), 8.36 (d, J = 8.64 Hz, 1H), 8.23 (d, J = 9.43 Hz, 1H), 8.10–8.08 (m, 1H), 8.03 (d, J = 8.01 Hz, 1H), 7.97–7.95 (m, 1H), 7.91 (d, J = 7.13 Hz, 1H), 7.89 (d, J = 6.35 Hz, 1H), 7.87 (s, 1H), 7.86 (d, J = 7.02 Hz, 1H), 7.84–7.83 (m, 1H), 7.82 (s, 1H), 7.80 (d, J = 9.35 Hz, 1H), 7.74 (d, J = 9.28 Hz, 2H), 7.58 (d, J = 7.40 Hz, 1H), 7.57 (d, J = 8.50 Hz, 2H), 7.55 (d, J = 7.37 Hz, 1H), 7.52 (s, 2H), 7.50 (s, 2H), 7.48 (s, 1H), 7.45 (d, J = 9.30 Hz, 1H), 7.43 (d, J = 8.00 Hz, 2H), 7.41 (d, J = 7.86 Hz, 1H), 7.39 (d, J = 7.19 Hz, 1H), 7.38–7.32 (m, 4H), 4.85 (t, J = 5.22 Hz, 1H), 4.76 (d, J = 5.41 Hz, 1H), 4.73 (d, J = 2.21 Hz, 1H), 4.72 (s, 1H), 4.71 (d, J = 2.23 Hz, 1H), 4.65 (s, 1H), 4.62 (d, J = 4.91 Hz, 1H), 4.60 (s, 1H), 4.57 (d, J = 5.49 Hz, 2H), 4.53–4.52 (m, 2H), 4.50 (t, J = 4.09 Hz, 1H), 4.49 (s, 1H), 4.45 (d, J = 5.00 Hz, 1H), 4.43 (d, J = 4.45 Hz, 1H), 4.37 (d, J = 4.27 Hz, 1H), 4.34 (d, J = 7.46 Hz, 2H), 4.25 (t, J = 9.13 Hz, 1H), 4.09–4.08 (m, 3H), 4.03 (d, J = 8.04 Hz, 1H), 3.89–3.82 (m, 1H), 3.75 (d, J = 6.82 Hz, 2H), 3.71 (s, 1H), 3.71–3.66 (m, 3H), 3.64 (s, 1H), 3.48 (d, J = 4.84 Hz, 1H), 3.47–3.45 (m, 1H), 3.42 (d, J = 5.38 Hz, 1H), 3.40 (d, J = 6.11 Hz, 1H), 3.29 (s, 1H), 3.27 (d, J = 2.25 Hz, 2H), 3.25 (s, 1H), 3.20 (s, 1H), 3.17 (s, 1H), 3.16 (d, J = 5.24 Hz, 1H), 3.11 (d, J = 5.28 Hz, 2H), 3.09 (s, 1H), 3.08 (d, J = 4.05 Hz, 1H), 3.06 (d, J = 3.23 Hz, 1H), 3.05–3.04 (m, 1H), 3.02 (d, J = 3.82 Hz, 3H), 2.93–2.91 (m, 2H), 2.91–2.86 (m, 1H), 2.85–2.82 (m, 1H), 2.75 (d, J = 2.88 Hz, 2H), 2.73 (s, 1H), 2.69 (s, 1H), 2.65 (s, 1H), 2.63 (d, J = 3.22 Hz, 1H), 2.53 (d, J = 6.83 Hz, 1H), 2.38 (d, J = 7.87 Hz, 1H), 2.32 (d, J = 3.26 Hz, 1H), 2.08 (d, J = 7.30 Hz, 1H), 2.05 (d, J = 3.28 Hz, 2H), 2.03 (d, J = 2.67 Hz, 1H), 2.01 (d, J = 7.17 Hz, 2H), 1.99–1.97 (m, 2H), 1.96 (s, 1H), 1.96 (d, J = 2.06 Hz, 1H), 1.94 (dd, J = 2.00, 6.68 Hz, 2H), 1.93–1.90 (m, 1H), 1.70 (dd, J = 6.75, 8.81 Hz, 2H), 1.61–1.52 (m, 2H), 1.49–1.41 (m, 4H), 1.38 (dd, J = 4.56, 7.99 Hz, 2H), 1.32 (dd, J = 4.89, 7.07 Hz, 2H), 1.23 (s, 1H), 1.15 (d, J = 5.35 Hz, 1H), 1.12–1.09 (m, 1H), 1.01 (t, J = 3.45 Hz, 3H), 0.98 (d, J = 6.90 Hz, 9H), 0.93–0.90 (m, 12H), 0.90 (s, 3H), 0.83 (d, J = 6.84 Hz, 3H), 0.82 (d, J = 7.71 Hz, 3H), 0.80 (d, J = 7.90 Hz, 3H), 0.79 (s, 3H), 0.75 (d, J = 6.89 Hz, 3H), 0.73 (d, J = 7.11 Hz, 6H), 0.72 (d, J = 7.05 Hz, 6H), 0.70 (d, J = 7.03 Hz, 3H), 0.65 (d, J = 7.79 Hz, 3H), 0.63 (d, J = 6.92 Hz, 3H), 0.61 (d, J = 6.71 Hz, 3H), 0.58 (d, J = 6.87 Hz, 3H), 0.51 (d, J = 6.71 Hz, 3H), 0.41 (d, J = 6.71 Hz, 3H). ^{13}C NMR (150 MHz, DMSO-d_6): δ (ppm) 171.7, 171.6, 171.5, 171.3, 171.1, 171.0, 170.9, 170.7, 170.7, 170.3, 170.3, 170.2, 169.8, 169.7, 169.6, 169.4, 151.8, 139.6, 138.5, 138.4, 138.3, 132.2, 131.6, 130.8, 129.4, 124.7, 124.2, 124.1, 124.0, 123.9, 123.9, 123.8, 122.9, 122.7, 122.6, 122.1, 121.8, 121.8, 121.5, 121.3, 72.3, 72.1, 72.0, 69.5, 68.9, 68.5, 65.3, 63.5, 60.7, 60.3, 60.1, 59.2, 57.6, 57.5, 57.4, 57.3, 56.8, 56.4, 56.1, 54.4, 52.5, 52.3, 51.6, 51.1, 50.6, 48.5, 41.4, 41.1, 40.4, 38.5, 38.2, 37.6, 34.6, 32.6, 32.3, 32.1, 31.3, 31.2, 30.9, 30.8, 30.7, 29.8, 29.3, 28.9, 28.5, 24.2, 24.0, 23.9, 23.8, 23.0, 22.3, 22.0, 21.7, 20.9, 20.8, 20.0, 19.8, 19.7, 19.5, 19.4, 19.2, 19.2, 19.1, 19.0, 18.7, 18.6, 18.6, 18.4, 18.3, 18.2, 18.1, 18.0, 17.8, 17.8, 17.7, 17.6, 17.3, 15.2, 13.9, 13.8. HRMS m/z: 800.4195 $[M + H]^+$. HPLC purity 97.1%, t_r = 17.9/19.0 min.

Δ^3-[L-Bip]-lugdunin (33). Yield: 21.8 mg (77%). ^{1}H NMR (700 MHz, DMSO-d_6): δ (ppm) 8.56 (d, J = 8.68 Hz, 1H), 8.46 (s, 1H), 8.40 (d, J = 8.49 Hz, 1H), 8.20 (t, J = 9.23 Hz, 2H), 8.09 (d, J = 9.38 Hz, 1H), 8.05 (d, J = 7.75 Hz, 1H), 7.86 (d, J = 8.93 Hz, 1H), 7.83 (d, J = 9.77 Hz, 1H), 7.75 (d, J = 9.44 Hz, 1H), 7.60 (d, J = 7.77 Hz, 4H), 7.55–7.51 (m, 3H), 7.50 (d, J = 7.72 Hz, 2H), 7.44 (t, J = 7.40 Hz, 3H), 7.35 (d, J = 8.88 Hz, 2H), 7.29 (d, J = 7.57 Hz, 1H), 7.26 (d, J = 7.09 Hz, 1H), 7.20 (d, J = 7.52 Hz, 1H), 6.52 (s, 1H), 6.43 (s, 1H), 4.74 (s, 1H), 4.72 (s, 1H), 4.62 (d, J = 9.94 Hz, 1H), 4.53 (s, 1H), 4.43 (s, 1H), 4.26 (s, 1H), 4.25 (s, 1H), 4.14 (d, J = 9.07 Hz, 1H), 4.09 (d, J = 9.88 Hz, 2H), 3.85 (s, 1H), 3.72–3.61 (m, 2H), 3.17 (d, J = 5.27 Hz, 1H), 3.05 (s, 2H), 2.94 (s, 1H), 2.90 (d, J = 9.06 Hz, 1H), 2.18 (s, 1H), 1.99 (s, 1H), 1.90 (d, J = 6.26 Hz, 1H), 1.69 (s, 1H), 1.31 (s, 1H), 1.24 (s, 2H), 1.15 (s, 1H), 0.92 (d, J = 6.68 Hz, 3H), 0.88 (s, 3H), 0.87 (d, J = 7.09 Hz, 3H), 0.86 (s, 3H), 0.85 (s, 6H), 0.84 (d, J = 7.32 Hz, 3H), 0.83 (s, 3H), 0.83–0.81 (m, 12H), 0.80 (d, J = 6.71 Hz, 3H), 0.78 (d, J = 6.53 Hz, 3H), 0.76 (d, J = 6.85 Hz, 3H), 0.74 (d, J = 6.91 Hz, 3H), 0.62 (d, J = 6.76 Hz, 3H), 0.48 (d, J = 6.78 Hz, 3H), 0.42 (d, J = 6.71 Hz, 3H). HRMS m/z: 820.4781 $[M + H]^+$. HPLC purity 92.7%, t_r = 18.4/19.0 min.

Δ^3-[L-Dip]-lugdunin (34). Yield: 16.7 mg (59%). ^{1}H NMR (700 MHz, DMSO-d_6): δ (ppm) 8.49 (d, J = 9.25 Hz, 1H), 8.36 (s, 1H), 8.24 (d, J = 9.36 Hz, 1H), 8.20 (s, 1H), 8.14 (s, 2H), 8.03 (d, J = 9.63 Hz, 1H), 7.95 (s, 1H), 7.85 (d, J = 9.18 Hz, 1H), 7.80 (s, 1H), 7.79 (s, 1H), 7.73 (s, 1H), 7.72 (s, 1H), 7.69 (s, 1H), 7.67 (s, 1H), 7.50 (d, J = 7.81 Hz, 1H), 7.47 (d, J = 7.47 Hz, 2H), 7.39 (d, J = 7.36 Hz, 1H), 7.31 (d, J = 7.46 Hz, 2H), 7.17 (d, J = 7.73 Hz, 1H), 7.09 (d, J = 6.74 Hz, 1H), 6.52 (s, 1H), 5.40 (d, J = 6.56 Hz, 1H), 4.81 (s, 1H), 4.78 (s, 1H), 4.69 (s, 1H), 4.66 (s, 1H), 4.65 (s, 1H), 4.63 (s, 1H), 4.61 (s, 1H), 4.55 (s, 1H), 4.52 (s, 1H), 4.51 (s, 1H), 4.45 (d, J = 4.90 Hz, 1H), 4.43 (s, 1H), 4.38 (s, 1H), 4.34 (t, J = 5.10 Hz, 1H), 4.27 (s, 1H), 4.25 (s, 1H), 4.21 (s, 1H), 4.10 (s, 1H), 4.09 (d, J = 5.22 Hz, 2H), 4.08 (s, 1H), 4.05 (d, J = 4.60 Hz, 1H), 4.04 (d, J = 4.69 Hz, 1H), 4.03 (d, J = 4.90 Hz, 1H), 4.02 (d, J = 3.69 Hz, 1H), 4.01 (d, J = 3.87 Hz, 1H), 3.84 (s, 1H), 3.69 (s, 1H), 3.45 (s, 1H), 3.44 (d, J = 3.92 Hz, 1H), 3.43 (d, J = 4.83 Hz, 1H), 3.42 (s, 1H), 3.17 (d, J = 5.22 Hz, 1H), 3.05 (s, 1H), 2.99 (s, 1H), 2.97 (s, 1H), 2.96 (s, 1H), 2.89 (s, 2H), 2.83 (s, 1H), 2.73 (d, J = 3.67 Hz, 2H), 2.71 (s, 1H), 2.69 (s, 2H), 2.59 (s, 1H), 2.57 (s, 1H), 2.30 (s, 1H), 2.20 (s, 1H), 2.18 (d, J = 3.08 Hz, 1H), 2.13 (d, J = 2.83 Hz, 1H), 2.08 (s, 1H), 2.07 (s, 1H), 1.99 (s, 1H), 1.91 (s, 1H), 1.86 (s, 1H), 1.37 (s, 1H), 1.23 (s, 2H), 1.22 (s, 2H), 1.17 (t, J = 7.11 Hz, 1H), 1.15 (s, 1H), 1.14 (d, J = 5.08 Hz, 1H), 1.05 (t, J = 7.03 Hz, 3H), 1.03 (s, 3H), 1.00 (s, 3H), 0.99 (d, J = 7.19 Hz, 3H), 0.95 (d, J = 3.85 Hz, 3H), 0.94 (d, J = 6.62 Hz, 3H), 0.91 (d, J = 6.88 Hz, 3H), 0.86 (d, J = 6.79 Hz, 12H), 0.85–0.82 (m, 3H), 0.82–0.81 (m, 3H), 0.80 (d, J = 6.71 Hz, 3H), 0.78 (d, J = 6.70 Hz, 3H), 0.76 (d, J = 6.84 Hz, 6H), 0.68 (s, 3H), 0.62 (d, J = 6.55 Hz, 3H), 0.55 (d, J = 7.31 Hz, 3H), 0.53 (d, J = 7.12 Hz, 3H). HRMS m/z: 820.4793 $[M + H]^+$. HPLC purity 91.2%, t_r = 18.4/18.9 min.

Δ^3-[L-pBpa]-lugdunin (35). Yield: 18.7 mg (64%). ^{1}H NMR (700 MHz, DMSO-d_6): δ (ppm) 8.64 (d, J = 8.90 Hz, 1H), 8.55 (s, 1H), 8.39 (d, J = 8.66 Hz, 1H), 8.28 (d, J = 8.59 Hz, 1H), 8.25 (d, J = 9.40 Hz, 1H), 8.17 (d, J = 9.15 Hz, 1H), 8.01 (d, J = 9.07 Hz, 1H), 7.94 (d, J = 8.19 Hz, 1H), 7.88 (t, J = 9.75 Hz, 1H), 7.80 (d, J = 8.78 Hz, 1H), 7.75 (d, J = 9.62 Hz, 1H), 7.62 (d, J = 9.44 Hz, 1H), 7.41 (d, J = 4.26 Hz, 1H), 7.32 (d, J = 5.19 Hz, 1H), 4.79–4.74 (m, 1H), 4.71 (d, J = 5.01 Hz, 2H), 4.59 (d, J = 6.19 Hz, 1H), 4.51–4.45 (m, 1H), 4.43 (d, J = 9.06 Hz, 1H), 4.38 (d, J = 7.69 Hz, 1H), 4.30 (t, J = 9.00 Hz, 1H), 4.24 (d, J = 8.68 Hz, 1H), 4.21 (d, J = 7.73 Hz, 1H), 4.07 (t, J = 9.58 Hz, 1H), 3.91 (t, J = 8.85 Hz, 1H), 3.74 (d, J = 7.45 Hz, 2H), 3.71–3.66 (m, 2H), 3.62–3.58 (m, 1H), 3.23 (d, J = 6.03 Hz, 1H), 3.14 (t, J = 8.07 Hz, 1H), 3.11 (d, J = 3.95 Hz, 1H), 3.09 (d, J = 5.34 Hz, 1H), 3.07 (d, J = 7.43 Hz, 1H), 2.91 (d, J = 7.83 Hz, 2H), 2.81 (d, J = 7.04 Hz, 1H), 2.59 (t, J = 8.96 Hz, 1H), 2.45 (s, 1H), 2.43 (s, 1H), 2.18 (t, J = 7.04 Hz, 1H), 2.04 (d, J = 6.40 Hz, 2H), 2.04–1.99 (m, 1H), 1.97 (s, 1H), 1.91 (d, J = 6.75 Hz, 1H), 1.81 (d, J = 7.00 Hz, 2H), 1.54 (d, J = 7.16 Hz, 1H), 1.45 (d, J = 6.21 Hz, 1H), 1.38–1.33 (m, 2H), 1.14 (d, J = 6.76 Hz, 3H), 1.11 (d, J = 7.37 Hz, 3H), 1.01 (d, J = 6.56 Hz, 3H), 0.96 (d, J = 7.35 Hz, 3H), 0.92 (d, J = 6.48 Hz, 3H), 0.89–0.69 (m, 15H), 0.66 (d, J = 6.75 Hz, 3H). HRMS m/z: 848.4730 $[M + H]^+$. HPLC purity 90.9%, t_r = 17.4/18.0 min.

Δ^3-[L-Ala(1-naphthyl)]-lugdunin (36). Yield: 24.3 mg (89%). ^{1}H NMR (600 MHz, DMSO-d_6): δ (ppm) 8.73 (d, J = 8.48 Hz, 1H), 8.55 (d, J = 5.31 Hz, 1H), 8.44 (d, J = 8.92 Hz, 2H), 8.27 (t, J = 8.17 Hz, 2H), 8.19 (d, J = 9.70 Hz, 2H), 8.17–8.13 (m, 1H), 8.07 (d, J = 9.35 Hz, 1H), 7.91 (d, J = 8.13 Hz, 1H), 7.88 (d, J = 8.05 Hz, 1H), 7.81 (d, J = 9.36 Hz, 1H), 7.79–7.75 (m, 3H), 7.74 (s, 1H), 7.70 (d, J = 9.24 Hz, 1H), 7.62–7.58 (m, 1H), 7.57 (d, J = 7.97 Hz, 1H), 7.54–7.52 (m, 1H), 7.50 (dd, J = 6.78, 9.83 Hz, 2H), 7.46 (d, J = 6.81 Hz, 1H), 7.42 (d, J = 9.32 Hz, 1H), 7.35 (d, J = 8.06 Hz, 2H), 5.08 (d, J = 6.91 Hz, 1H), 4.95 (dd, J = 5.66, 8.80 Hz, 1H), 4.87 (dd, J = 5.22, 9.02 Hz, 1H), 4.83–4.78 (m, 1H), 4.76–4.70 (m, 1H), 4.69–4.66

https://doi.org/10.1021/acs.jmedchem.0c02170
J. Med. Chem. 2021, 64, 4034–4058

(m, 1H), 4.63 (d, J = 8.51, 1H), 4.54 (dd, J = 3.61, 8.85 Hz, 2H), 4.50−4.44 (m, 2H), 4.44−4.37 (m, 2H), 4.26 (t, J = 9.27 Hz, 1H), 4.15 (t, J = 9.01 Hz, 2H), 4.07 (d, J = 8.97 Hz, 1H), 4.00 (t, J = 8.10 Hz, 1H), 3.96 (d, J = 5.23 Hz, 1H), 3.93 (d, J = 3.56 Hz, 1H), 3.90 (d, J = 3.32 Hz, 1H), 3.88−3.82 (m, 1H), 3.66 (d, J = 3.87 Hz, 2H), 3.45−3.40 (m, 2H), 3.35−3.31 (m, 2H), 3.26−3.24 (m, 1H), 3.23−3.20 (m, 1H), 3.19−3.14 (m, 2H), 3.06 (dd, J = 6.33, 9.74 Hz, 1H), 3.02 (s, 1H), 3.00 (d, J = 3.28 Hz, 1H), 2.93−2.84 (m, 2H), 2.63−2.59 (m, 1H), 2.57 (s, 1H), 2.54 (dd, J = 5.07, 9.96 Hz, 2H), 2.41−2.37 (m, 1H), 2.08 (s, 1H), 2.04 (s, 1H), 2.01 (d, J = 6.02 Hz, 2H), 1.98−1.94 (m, 2H), 1.92−1.86 (m, 2H), 1.63 (dd, J = 6.65, 9.31 Hz, 1H), 1.58−1.48 (m, 2H), 1.47−1.39 (m, 2H), 1.30 (d, J = 5.80 Hz, 1H), 1.27−1.25 (m, 2H), 1.24 (d, J = 6.57 Hz, 2H), 1.22−1.17 (m, 1H), 1.15 (d, J = 5.57 Hz, 2H), 1.10−0.98 (m, 21H), 0.92 (d, J = 6.69 Hz, 3H), 0.89 (d, J = 4.06 Hz, 3H), 0.88 (d, J = 1.73 Hz, 3H), 0.86 (d, J = 6.45 Hz, 6H), 0.85−0.83 (m, 6H), 0.82 (d, J = 7.97 Hz, 3H), 0.80 (s, 1H), 0.80−0.77 (m, 3H), 0.76 (d, J = 6.88 Hz, 3H), 0.58 (d, J = 6.72 Hz, 3H). ^{13}C NMR (150 MHz, DMSO-d_6): δ (ppm) 171.7, 171.5, 171.5, 171.3, 171.1, 170.7, 170.3, 170.3, 170.2, 169.8, 169.7, 169.7, 134.0, 133.4, 133.3, 133.2, 131.6, 131.1, 128.7, 128.3, 128.1, 127.6, 127.0, 126.9, 126.2, 125.9, 125.5, 125.3, 125.1, 125.1, 124.1, 123.2, 76.3, 76.3, 74.6, 74.5, 74.5, 74.5, 74.4, 74.3, 73.1, 73.0, 72.3, 72.3, 72.1, 72.1, 72.0, 65.3, 65.2, 64.7, 63.9, 63.5, 60.9, 59.4, 57.5, 57.3, 57.3, 56.8, 56.4, 54.4, 53.7, 52.6, 52.5, 50.7, 41.4, 41.1, 38.4, 37.7, 35.0, 33.6, 32.6, 32.1, 31.3, 30.7, 29.9, 29.2, 28.8, 28.3, 24.2, 24.0, 23.0, 22.2, 22.1, 21.7, 20.9, 20.2, 19.8, 19.7, 19.5, 19.1, 19.1, 18.7, 18.7, 18.6, 18.5, 18.2, 18.0, 17.3, 17.3, 17.2, 16.9, 16.9, 15.2. HRMS m/z: 794.4631 $[M + H]^+$. HPLC purity 96.2%, t_r = 18.0/19.4 min.

Δ^3-[L-Ala-3-(9-anth)]-lugdunin (37). Yield: 21.0 mg (72%). ^{1}H NMR (600 MHz, DMSO-d_6): δ (ppm) 8.76 (d, J = 8.95 Hz, 1H), 8.57 (d, J = 8.95 Hz, 1H), 8.50 (d, J = 6.68 Hz, 1H), 8.49 (s, 1H), 8.45 (d, J = 8.89 Hz, 1H), 8.38 (d, J = 8.52 Hz, 1H), 8.20 (d, J = 9.26 Hz, 1H), 8.07−8.03 (m, 2H), 8.01 (d, J = 8.75 Hz, 1H), 7.90−7.86 (m, 1H), 7.82 (d, J = 8.27 Hz, 1H), 7.73−7.69 (m, 1H), 7.69−7.66 (m, 1H), 7.58−7.52 (m, 2H), 7.50 (d, J = 6.23 Hz, 1H), 4.94 (q, J = 7.91 Hz, 1H), 4.77 (dd, J = 4.24, 8.92 Hz, 1H), 4.72 (d, J = 2.47 Hz, 1H), 4.70 (d, J = 2.48 Hz, 1H), 4.66 (d, J = 8.80 Hz, 1H), 4.54 (t, J = 5.48 Hz, 1H), 4.49 (dd, J = 4.58, 9.12 Hz, 1H), 4.47 (s, 1H), 4.45 (d, J = 1.91 Hz, 1H), 4.44−4.42 (m, 1H), 4.35 (s, 1H), 4.34 (d, J = 2.45 Hz, 1H), 4.33 (s, 1H), 4.31 (s, 1H), 4.30 (s, 1H), 4.29 (d, J = 9.15 Hz, 1H), 4.26 (d, J = 4.55 Hz, 1H), 4.15−4.10 (m, 2H), 4.06 (d, J = 9.07 Hz, 1H), 3.98 (d, J = 8.24 Hz, 1H), 3.87−3.83 (m, 1H), 3.82 (d, J = 5.41 Hz, 1H), 3.79 (d, J = 7.02 Hz, 1H), 3.77 (s, 1H), 3.76 (s, 1H), 3.75 (s, 1H), 3.74−3.71 (m, 1H), 3.70 (d, J = 2.62 Hz, 1H), 3.69−3.67 (m, 1H), 3.66 (t, J = 3.00 Hz, 1H), 3.63 (s, 1H), 3.61 (s, 1H), 3.60 (d, J = 3.80 Hz, 1H), 3.58 (s, 1H), 3.48 (s, 1H), 3.47 (s, 1H), 3.45 (s, 1H), 3.42 (d, J = 5.35 Hz, 1H), 3.40 (s, 1H), 3.40−3.36 (m, 1H), 3.28 (s, 1H), 3.25 (s, 1H), 3.17 (d, J = 5.20 Hz, 1H), 3.13 (dd, J = 6.06, 9.36 Hz, 1H), 3.10 (s, 1H), 3.09 (d, J = 3.35 Hz, 1H), 3.07 (s, 1H), 3.06−3.04 (m, 2H), 3.02 (d, J = 4.20 Hz, 1H), 2.96−2.92 (m, 1H), 2.91 (d, J = 4.53 Hz, 1H), 2.89 (s, 1H), 2.85−2.83 (m, 1H), 2.81 (dd, J = 3.41, 8.27 Hz, 1H), 2.73 (s, 1H), 2.61 (d, J = 4.87 Hz, 1H), 2.57 (s, 1H), 2.57−2.55 (m, 1H), 2.54 (s, 1H), 2.53−2.51 (m, 1H), 2.39−2.37 (m, 1H), 2.11 (s, 1H), 2.08 (s, 1H), 2.07 (s, 1H), 2.06 (s, 1H), 2.00 (dd, J = 4.07, 6.97 Hz, 1H), 1.91 (s, 1H), 1.90−1.86 (m, 1H), 1.69 (dd, J = 4.52, 8.48, 2H), 1.54 (dd, J = 6.67, 9.28 Hz, 2H), 1.33−1.27 (m, 1H), 1.26 (s, 1H), 1.25 (s, 1H), 1.24 (d, J = 5.01 Hz, 2H), 1.16−1.10 (m, 1H), 1.10−1.05 (m, 1H), 1.01 (d, J = 6.77 Hz, 3H), 0.92 (d, J = 6.72 Hz, 3H), 0.89 (d, J = 6.90 Hz, 3H), 0.88 (d, J = 7.91 Hz, 3H), 0.87 (s, 3H), 0.85 (d, J = 6.72 Hz, 3H), 0.85 (s, 3H), 0.84 (s, 3H), 0.84 (s, 3H), 0.83 (s, 3H), 0.81 (d, J = 6.22 Hz, 6H), 0.80 (d, J = 6.03 Hz, 3H), 0.78 (d, J = 6.64 Hz, 3H), 0.77 (s, 3H), 0.76 (s, 3H), 0.71 (d, J = 6.32 Hz, 3H), 0.70−0.68 (m, 6H), 0.63 (d, J = 6.80 Hz, 3H), 0.59 (d, J = 6.44 Hz, 3H), 0.52 (d, J = 6.33 Hz, 3H), 0.35 (d, J = 6.70 Hz, 3H). ^{13}C NMR (150 MHz, DMSO-d_6): δ (ppm) 172.1, 172.0, 171.7, 171.6, 171.5, 171.2, 171.0, 170.8, 170.6, 170.3, 170.2, 170.2, 168.2, 167.4, 158.4, 157.6, 141.2, 135.0, 132.2, 132.0, 131.5, 131.4, 130.7, 130.3, 129.8, 129.4, 129.3, 129.1, 128.1, 127.5, 127.2, 126.9, 126.7, 126.2, 126.2, 125.4, 125.4, 125.3, 120.5, 118.7, 105.6, 99.5, 72.8, 72.6, 72.5, 70.2, 70.0, 69.3, 68.3, 67.7, 65.5, 64.2, 61.3, 60.7, 59.1, 58.0, 57.9, 57.8, 57.4, 57.0, 55.7, 55.3, 55.0, 54.0, 52.7, 51.3, 41.5, 41.4, 38.2, 36.9, 33.5, 33.1, 32.4, 32.0, 31.6, 31.1, 30.9, 30.2, 29.9, 29.8, 29.4, 28.8, 26.2, 24.5, 24.3, 23.1, 22.6, 22.5, 22.4, 21.3, 20.3, 20.2, 19.8, 19.7, 19.7, 19.2, 18.5, 18.4, 17.8, 15.7, 14.7, 14.3. HRMS m/z: 844.4795 $[M + H]^+$. HPLC purity 98.4%, t_r = 19.0/19.7 min.

Δ^3-[L-Trp(1-Me)]-lugdunin (38). Yield: 14.3 mg (52%). ^{1}H NMR (600 MHz, DMSO-d_6): δ (ppm) 8.58−8.52 (m, 1H), 8.25 (d, J = 8.67 Hz, 1H), 8.20 (d, J = 8.41 Hz, 1H), 8.18 (d, J = 9.41 Hz, 1H), 8.05−8.03 (m, 1H), 7.79 (d, J = 9.32 Hz, 1H), 7.69 (d, J = 8.11 Hz, 1H), 7.53 (d, J = 8.02 Hz, 1H), 7.45 (d, J = 9.40 Hz, 1H), 7.34 (d, J = 8.38 Hz, 1H), 7.33−7.31 (m, 1H), 7.13−7.08 (m, 2H), 7.00 (dd, J = 4.67, 7.04 Hz, 1H), 4.73 (d, J = 2.23 Hz, 1H), 4.70 (d, J = 2.42 Hz, 1H), 4.61 (d, J = 3.54 Hz, 1H), 4.60−4.59 (m, 1H), 4.59−4.57 (m, 1H), 4.51 (d, J = 4.38 Hz, 1H), 4.50−4.49 (m, 1H), 4.48 (d, J = 4.26 Hz, 1H), 4.43 (d, J = 5.14 Hz, 1H), 4.41 (d, J = 2.44 Hz, 1H), 4.39 (d, J = 2.60 Hz, 1H), 4.38 (s, 1H), 4.24 (t, J = 9.11 Hz, 1H), 4.17 (t, J = 8.98 Hz, 1H), 4.09−4.03 (m, 1H), 3.91−3.87 (m, 1H), 3.85 (t, J = 4.04 Hz, 1H), 3.75 (d, J = 6.65 Hz, 2H), 3.71−3.69 (m, 1H), 3.62 (dd, J = 4.87, 9.43 Hz, 1H), 3.45−3.42 (m, 1H), 3.42−3.40 (m, 1H), 3.40−3.37 (m, 1H), 3.36−3.34 (m, 1H), 3.29 (s, 1H), 3.29−3.26 (m, 1H), 3.25 (s, 1H), 3.19 (s, 1H), 3.17 (d, J = 3.42 Hz, 1H), 3.16 (t, J = 2.64 Hz, 1H), 3.05 (dd, J = 4.45, 7.22 Hz, 1H), 3.03−3.01 (m, 1H), 2.99 (d, J = 5.40 Hz, 1H), 2.97 (s, 1H), 2.92 (s, 1H), 2.90 (d, J = 2.22 Hz, 1H), 2.88 (d, J = 4.89 Hz, 1H), 2.86 (d, J = 4.96 Hz, 1H), 2.84 (d, J = 4.16 Hz, 1H), 2.81 (t, J = 2.92 Hz, 1H), 2.79 (d, J = 6.63 Hz, 1H), 2.62−2.60 (m, 1H), 2.59 (s, 1H), 2.58−2.55 (m, 1H), 2.54 (d, J = 3.17 Hz, 1H), 2.52 (d, J = 3.90 Hz, 1H), 2.38 (d, J = 3.58 Hz, 1H), 2.27 (d, J = 7.34 Hz, 1H), 2.18 (t, J = 7.36 Hz, 1H), 2.07 (s, 1H), 2.05 (d, J = 2.88 Hz, 1H), 2.03−1.94 (m, 2H), 1.93−1.88 (m, 1H), 1.71 (dd, J = 2.27, 6.68 Hz, 1H), 1.54 (dd, J = 6.68, 8.88 Hz, 2H), 1.41 (dd, J = 4.40, 8.87 Hz, 1H), 1.33−1.26 (m, 1H), 1.03−0.97 (m, 6H), 0.92 (d, J = 6.66 Hz, 3H), 0.89−0.81 (m, 18H), 0.81 (s, 3H), 0.78 (d, J = 6.87 Hz, 3H), 0.75 (d, J = 5.97 Hz, 3H), 0.71 (d, J = 6.98 Hz, 3H), 0.70−0.69 (m, 3H), 0.64 (d, J = 6.78 Hz, 3H), 0.63−0.61 (m, 3H), 0.50 (d, J = 6.84 Hz, 3H), 0.46 (d, J = 6.80 Hz, 3H). ^{13}C NMR (150 MHz, DMSO-d_6): δ (ppm) 171.7, 171.5, 171.5, 171.4, 171.0, 170.7, 170.5, 170.4, 170.2, 170.0, 169.9, 169.6, 136.5, 136.4, 128.7, 128.3, 127.5, 127.2, 120.9, 120.8, 118.3, 109.7, 109.4, 109.1, 108.9, 72.3, 72.1, 72.0, 69.5, 68.8, 65.3, 63.6, 60.6, 60.3, 60.1, 59.0, 57.4, 57.4, 57.3, 56.9, 56.5, 55.4, 55.2, 54.4, 53.4, 52.7, 52.2, 50.7, 41.3, 41.1, 40.4, 38.2, 38.2, 37.6, 35.1, 34.6, 32.6, 32.1, 32.0, 31.2, 31.1, 30.6, 29.7, 29.3, 29.0, 28.9, 28.6, 28.5, 26.2, 24.1, 23.9, 23.0, 22.3, 22.0, 20.8, 19.8, 19.7, 19.5, 19.4, 19.2, 19.1, 18.5, 18.4, 18.3, 18.1, 18.0, 17.8, 17.4, 15.1, 13.9. HRMS m/z: 797.4738 $[M + H]^+$. HPLC purity 87.5%, t_r = 17.5/18.3 min.

Δ^3-[L-Tic]-lugdunin (39). Yield: 21.7 mg (83%). ^{1}H NMR (600 MHz, DMSO-d_6): δ (ppm) 8.61 (d, J = 7.91 Hz, 1H), 8.44 (d, J = 9.15 Hz, 1H), 8.37 (d, J = 7.04 Hz, 1H), 8.35 (d, J = 8.31 Hz, 1H), 8.30 (d, J = 7.73 Hz, 1H), 8.23 (d, J = 8.96 Hz, 1H), 8.19 (d, J = 8.34 Hz, 1H), 8.11 (d, J = 8.08 Hz, 1H), 8.07 (d, J = 8.33 Hz, 1H), 7.78 (d, J = 9.43 Hz, 1H), 7.69 (d, J = 8.90 Hz, 1H), 7.65 (d, J = 9.17 Hz, 1H), 7.60 (d, J = 8.47 Hz, 1H), 7.58−7.55 (m, 2H), 7.54 (d, J = 8.26 Hz, 1H), 7.35 (d, J = 7.60 Hz, 2H), 7.31−7.20 (m, 2H), 7.20−7.08 (m, 2H), 5.41 (d, J = 2.19 Hz, 2H), 5.41 (d, J = 2.34 Hz, 1H), 5.17−5.14 (m, 2H), 5.13 (s, 1H), 5.09−5.07 (m, 1H), 4.98 (d, J = 1.69 Hz, 1H), 4.95 (s, 1H), 4.94−4.89 (m, 3H), 4.84 (d, J = 4.57 Hz, 1H), 4.77 (dd, J = 4.54, 6.26 Hz, 2H), 4.73 (t, J = 1.41 Hz, 1H), 4.54 (s, 1H), 4.51 (d, J = 2.33 Hz, 1H), 4.47−4.36 (m, 3H), 4.24−4.22 (m, 1H), 4.22−4.20 (m, 1H), 4.18−4.06 (m, 2H), 4.01 (t, J = 8.90 Hz, 1H), 3.80−3.76 (m, 2H), 3.69 (d, J = 3.19 Hz, 1H), 3.68−3.66 (m, 1H), 3.43−3.41 (m, 2H), 3.38 (d, J = 2.04 Hz, 2H), 3.24 (dd, J = 5.47, 9.88 Hz, 1H), 3.17 (d, J = 4.91 Hz, 2H), 3.05 (d, J = 5.93 Hz, 1H), 3.03 (s, 1H), 2.89−2.84 (m, 1H), 2.83 (d, J = 3.71 Hz, 2H), 2.80 (d, J = 4.27 Hz, 1H), 2.72−2.66 (m, 2H), 2.67−2.60 (m, 2H), 2.46 (t, J = 9.88 Hz, 1H), 2.38 (d, J = 2.05, 4.56 Hz, 2H), 2.06 (s, 1H), 2.00 (d, J = 4.62 Hz, 1H), 1.96−1.87 (m, 2H), 1.66−1.58 (m, 2H), 1.54 (dd, J = 2.03, 5.94 Hz, 2H), 1.53−1.51 (m, 1H), 1.51−1.44 (m, 2H), 1.36 (dd, J = 2.73, 5.12 Hz, 2H), 1.23 (d, J = 4.81 Hz, 1H),

https://doi.org/10.1021/acs.jmedchem.0c02170
J. Med. Chem. 2021, 64, 4034−4058

1.15 (s, 1H), 1.06–1.02 (m, 18H), 1.02 (s, 3H), 0.97 (s, 3H), 0.95 (d, J = 6.72 Hz, 3H), 0.93 (d, J = 3.09 Hz, 3H), 0.92–0.90 (m, 12H), 0.90 (d, J = 6.74 Hz, 3H), 0.89 (s, 3H), 0.87 (s, 3H), 0.86 (d, J = 6.87 Hz, 3H), 0.84 (d, J = 6.50 Hz, 3H), 0.82–0.80 (m, 3H), 0.79 (s, 3H), 0.77 (d, J = 6.49 Hz, 3H), 0.68 (d, J = 6.58 Hz, 3H), 0.59 (d, J = 6.80 Hz, 3H), 0.52 (d, J = 6.42 Hz, 3H). ^{13}C NMR (150 MHz, DMSO-d_6): δ (ppm) 172.5, 172.1, 171.4, 171.2, 170.6, 169.5, 167.8, 135.4, 134.9, 127.5, 126.8, 126.5, 125.7, 72.2, 66.9, 63.2, 58.6, 56.5, 55.9, 54.9, 49.7, 44.9, 38.8, 35.5, 31.9, 31.5, 31.3, 31.0, 29.8, 24.2, 24.1, 22.7, 22.0, 22.0, 21.8, 20.1, 19.9, 19.6, 19.0, 18.9, 18.0. HRMS m/z: 756.4479 [M + H]$^+$. HPLC purity 96.7%, t_r = 17.1/17.4 min.

Δ^{3}-[L-Pra]-lugdunin (40). Yield: 16.2 mg (68%). ^{1}H NMR (600 MHz, DMSO-d_6): δ (ppm) 8.74 (d, J = 7.31 Hz, 1H), 8.71 (d, J = 8.40 Hz, 1H), 8.35 (d, J = 8.62 Hz, 1H), 8.28 (d, J = 9.37 Hz, 1H), 8.17 (d, J = 9.95 Hz, 1H), 8.09 (d, J = 9.05 Hz, 1H), 7.97 (d, J = 7.89 Hz, 1H), 7.80 (d, J = 9.25 Hz, 1H), 7.72 (d, J = 9.31 Hz, 1H), 7.47 (s, 1H), 4.73 (d, J = 2.15 Hz, 1H), 4.71 (d, J = 2.22 Hz, 1H), 4.65 (s, 1H), 4.64 (d, J = 3.60 Hz, 1H), 4.62 (s, 1H), 4.60 (d, J = 5.55 Hz, 1H), 4.56–4.52 (m, 1H), 4.49 (d, J = 3.58, 7.32 Hz, 2H), 4.43 (d, J = 4.07 Hz, 1H), 4.42–4.40 (m, 1H), 4.40 (d, J = 4.33 Hz, 1H), 4.37 (s, 1H), 4.35 (d, J = 2.84 Hz, 1H), 4.34 (d, J = 4.77 Hz, 1H), 4.33 (d, J = 2.59 Hz, 1H), 4.25–4.23 (m, 1H), 4.22 (d, J = 2.51 Hz, 1H), 4.21 (d, J = 2.42 Hz, 1H), 4.08 (d, J = 2.11 Hz, 1H), 4.07–4.05 (m, 1H), 4.04 (s, 1H), 4.03 (s, 1H), 3.75 (d, J = 2.08 Hz, 1H), 3.75 (d, J = 3.64 Hz, 1H), 3.74 (d, J = 3.97 Hz, 1H), 3.72 (t, J = 1.56 Hz, 1H), 3.71 (s, 1H), 3.70 (d, J = 4.05 Hz, 1H), 3.66 (d, J = 3.39 Hz, 1H), 3.49–3.42 (m, 1H), 3.41 (d, J = 5.37 Hz, 1H), 3.38–3.36 (m, 1H), 3.25 (s, 1H), 3.21 (dd, J = 6.00, 9.34 Hz, 1H), 3.16 (d, J = 5.20 Hz, 1H), 3.12–3.07 (m, 1H), 3.06–3.03 (m, 1H), 3.02 (d, J = 3.17 Hz, 1H), 3.00 (s, 1H), 2.95 (d, J = 3.32 Hz, 1H), 2.93–2.90 (m, 1H), 2.84 (dd, J = 3.08, 4.78 Hz, 1H), 2.80 (t, J = 2.60 Hz, 1H), 2.76 (t, J = 2.65 Hz, 1H), 2.74 (d, J = 3.79 Hz, 1H), 2.71 (dd, J = 2.69, 4.46 Hz, 1H), 2.63–2.57 (m, 1H), 2.55 (s, 1H), 2.54 (s, 1H), 2.43 (d, J = 3.74 Hz, 1H), 2.39–2.38 (m, 1H), 2.34 (d, J = 3.12 Hz, 1H), 2.08 (d, J = 6.59 Hz, 1H), 2.05 (s, 1H), 2.02 (d, J = 2.39 Hz, 1H), 1.97 (d, J = 3.32 Hz, 1H), 1.95–1.84 (m, 3H), 1.61 (d, J = 6.54 Hz, 1H), 1.58–1.52 (m, 1H), 1.48 (dd, J = 4.54, 9.09 Hz, 1H), 1.44–1.33 (m, 2H), 1.01 (d, J = 6.54 Hz, 6H), 0.95 (d, J = 6.75 Hz, 3H), 0.93 (s, 3H), 0.87 (d, J = 6.46 Hz, 3H), 0.86 (d, J = 3.60 Hz, 3H), 0.85 (d, J = 6.61 Hz, 3H), 0.83 (d, J = 6.79 Hz, 3H), 0.82 (d, J = 6.60 Hz, 3H), 0.81 (d, J = 6.32 Hz, 3H), 0.80 (d, J = 7.60 Hz, 3H), 0.79 (d, J = 6.22 Hz, 3H), 0.76 (s, 3H), 0.70 (d, J = 6.67 Hz, 3H). ^{13}C NMR (150 MHz, DMSO-d_6): δ (ppm) 171.7, 171.5, 171.4, 171.3, 171.0, 170.6, 170.2, 170.0, 169.1, 168.6, 81.0, 80.4, 72.5, 72.3, 72.1, 71.9, 65.2, 63.7, 60.7, 60.3, 60.1, 59.0, 57.4, 57.3, 56.9, 56.7, 54.4, 52.4, 51.8, 51.0, 50.8, 41.3, 41.1, 38.2, 37.6, 34.6, 32.6, 31.9, 31.2, 31.1, 30.6, 29.6, 29.0, 28.5, 24.1, 24.0, 23.0, 22.3, 22.0, 21.7, 20.8, 20.5, 19.8, 19.7, 19.6, 19.5, 19.2, 19.1, 18.9, 18.5, 18.3, 18.2, 18.0, 17.8, 17.8, 17.5, 15.3, 13.8, 11.4. HRMS m/z: 692.4163 [M + H]$^+$. HPLC purity 95.9%, t_r = 16.0/16.7 min.

Δ^{6}-[D-Trp]-lugdunin (41). Yield: 18.1 mg (60%). ^{1}H NMR (600 MHz, DMSO-d_6): δ (ppm) 10.77 (d, J = 2.47 Hz, 1H), 10.74 (d, J = 2.39 Hz, 1H), 8.47 (d, J = 8.38 Hz, 1H), 8.44 (d, J = 5.74 Hz, 1H), 8.27 (d, J = 8.03 Hz, 1H), 8.22 (d, J = 8.50 Hz, 1H), 8.17 (d, J = 8.73 Hz, 1H), 8.01 (d, J = 9.35 Hz, 1H), 7.92 (d, J = 9.32 Hz, 1H), 7.84 (d, J = 9.34 Hz, 1H), 7.67 (d, J = 7.60 Hz, 2H), 7.60 (d, J = 9.52 Hz, 1H), 7.50 (d, J = 7.85 Hz, 1H), 7.31–7.26 (m, 2H), 7.24 (d, J = 6.32 Hz, 1H), 7.15 (d, J = 6.36 Hz, 1H), 7.14 (d, J = 6.40 Hz, 1H), 7.12 (d, J = 6.46 Hz, 1H), 7.06–7.00 (m, 2H), 6.95 (d, J = 6.93 Hz, 2H), 4.90 (dd, J = 6.07, 8.74 Hz, 1H), 4.74–4.69 (m, 1H), 4.64 (s, 1H), 4.62 (d, J = 1.79 Hz, 1H), 4.61 (dd, J = 2.31, 5.71 Hz, 1H), 4.59 (d, J = 1.18 Hz, 1H), 4.48 (dd, J = 5.47, 9.11 Hz, 1H), 4.41 (d, J = 5.99, 8.51 Hz, 1H), 4.29 (dd, J = 6.81, 9.38 Hz, 1H), 4.20–4.15 (m, 1H), 4.05 (dd, J = 2.39, 9.19 Hz, 1H), 3.94 (d, J = 7.38 Hz, 1H), 3.76 (s, 1H), 3.72 (s, 1H), 3.69 (s, 1H), 3.68 (s, 1H), 3.67 (d, J = 2.38 Hz, 1H), 3.65 (s, 1H), 3.48 (d, J = 6.08 Hz, 1H), 3.41 (t, J = 5.29 Hz, 1H), 3.30 (s, 1H), 3.12 (dd, J = 5.99, 9.40 Hz, 1H), 3.08 (d, J = 6.15 Hz, 1H), 3.06 (d, J = 6.38 Hz, 1H), 3.05 (d, J = 2.96 Hz, 1H), 3.04 (d, J = 2.83 Hz, 1H), 3.02 (d, J = 5.91 Hz, 1H), 2.98 (d, J = 5.59 Hz, 1H), 2.97 (s, 1H), 2.92 (s, 1H), 2.92–2.89 (m, 1H), 2.89 (q, J = 2.75 Hz, 1H), 2.87 (d, J = 4.69 Hz, 1H), 2.85 (s, 1H), 2.80 (s, 1H), 2.78 (d, J = 4.55 Hz, 1H), 2.76 (s, 1H), 2.69 (s, 1H), 2.59 (d, J = 3.74 Hz, 1H), 2.58 (d, J = 4.83 Hz, 1H), 2.57 (s, 1H), 2.40 (d, J = 4.95 Hz, 1H), 2.08–2.07 (m, 1H), 2.06 (s, 1H), 1.88 (d, J = 6.93 Hz, 1H), 1.71 (d, J = 6.75 Hz, 1H), 1.64–1.58 (m, 1H), 1.50–1.43 (m, 1H), 1.42–1.38 (m, 1H), 1.37–1.33 (m, 1H), 1.33–1.24 (m, 1H), 1.24–1.18 (m, 3H), 1.02 (d, J = 7.35 Hz, 3H), 0.99–0.96 (m, 3H), 0.85 (d, J = 6.71 Hz, 3H), 0.82 (d, J = 6.61 Hz, 3H), 0.81 (d, J = 6.50 Hz, 3H), 0.77 (d, J = 6.24 Hz, 3H), 0.74 (d, J = 6.38 Hz, 3H), 0.67 (d, J = 6.58 Hz, 3H), 0.61 (d, J = 6.68 Hz, 6H), 0.55 (d, J = 6.86 Hz, 3H), 0.53 (d, J = 6.72 Hz, 3H), 0.49 (d, J = 6.77 Hz, 3H), 0.45 (d, J = 6.72 Hz, 3H). ^{13}C NMR (150 MHz, DMSO-d_6): δ (ppm) 172.1, 171.6, 171.5, 171.4, 171.3, 170.9, 170.8, 170.5, 170.2, 170.1, 169.9, 169.7, 136.1, 136.0, 136.0, 127.3, 127.2, 127.0, 124.3, 124.1, 123.8, 123.7, 120.8, 120.7, 120.6, 118.7, 118.7, 118.2, 118.1, 118.0, 111.2, 111.0, 110.2, 109.8, 109.7, 109.6, 72.3, 72.1, 66.9, 65.2, 63.7, 60.3, 57.4, 57.2, 57.2, 56.5, 54.5, 53.8, 53.3, 52.7, 52.1, 50.6, 41.3, 41.0, 40.4, 38.3, 38.1, 37.5, 32.6, 31.2, 30.9, 29.9, 29.7, 28.7, 28.1, 27.1, 26.8, 24.1, 24.0, 23.0, 22.3, 22.1, 21.7, 20.4, 19.6, 19.5, 19.3, 19.1, 18.7, 18.6, 18.3, 18.2, 17.6, 15.0. HRMS m/z: 870.4690 [M + H]$^+$. HPLC purity 97.4%, t_r = 16.6/17.3 min.

$\Delta^{2,6}$-[D-Nva^2-D-Trp^6]-lugdunin (42). Yield: 22.3 mg (74%). ^{1}H NMR (600 MHz, DMSO-d_6): δ (ppm) 10.82 (d, J = 2.49 Hz, 1H), 10.80 (d, J = 2.80 Hz, 1H), 10.77 (d, J = 2.41 Hz, 1H), 8.62 (d, J = 8.40 Hz, 1H), 8.54–8.47 (m, 1H), 8.23 (d, J = 8.19 Hz, 1H), 8.20–8.15 (m, 1H), 8.14 (d, J = 7.72 Hz, 1H), 8.12 (s, 1H), 7.95 (d, J = 9.23 Hz, 1H), 7.84 (d, J = 9.14 Hz, 1H), 7.79 (d, J = 9.38 Hz, 1H), 7.67–7.65 (m, 1H), 7.65–7.62 (m, 1H), 7.60 (d, J = 4.40 Hz, 1H), 7.58 (d, J = 4.40 Hz, 1H), 7.55 (s, 1H), 7.54–7.53 (m, 1H), 7.52–7.50 (m, 1H), 7.31 (d, J = 7.90 Hz, 1H), 7.31–7.29 (m, 1H), 7.28 (d, J = 6.27 Hz, 1H), 7.23 (d, J = 7.37 Hz, 1H), 7.13 (d, J = 2.57 Hz, 1H), 7.12 (d, J = 2.40 Hz, 1H), 7.05–7.03 (m, 1H), 7.03–7.02 (m, 2H), 7.02–7.00 (m, 1H), 6.98–6.91 (m, 1H), 5.09 (s, 1H), 4.89–4.80 (m, 1H), 4.72 (d, J = 2.20 Hz, 1H), 4.70 (d, J = 2.23 Hz, 1H), 4.66 (dd, J = 5.35, 8.72 Hz, 1H), 4.61–4.57 (m, 1H), 4.56–4.53 (m, 1H), 4.49 (dd, J = 4.26, 8.28 Hz, 1H), 4.43 (d, J = 2.78 Hz, 1H), 4.41 (s, 1H), 4.37 (d, J = 6.04 Hz, 1H), 4.31 (t, J = 5.15 Hz, 1H), 4.26 (dd, J = 6.72, 9.28 Hz, 1H), 4.21–4.14 (m, 1H), 4.03 (dd, J = 2.21, 9.19 Hz, 1H), 3.97–3.90 (m, 1H), 3.75 (d, J = 7.16 Hz, 1H), 3.74–3.66 (m, 1H), 3.66–3.63 (m, 1H), 3.49–3.46 (m, 1H), 3.42 (d, J = 5.37 Hz, 1H), 3.40–3.37 (m, 1H), 3.29 (s, 1H), 3.24 (t, J = 5.74 Hz, 1H), 3.16 (d, J = 5.36 Hz, 1H), 3.14 (d, J = 3.50 Hz, 1H), 3.13 (s, 1H), 3.09 (d, J = 6.28 Hz, 1H), 3.05 (d, J = 5.63 Hz, 1H), 3.04–3.01 (m, 1H), 3.00 (dd, J = 2.49, 5.17 Hz, 2H), 2.98 (s, 1H), 2.95 (s, 1H), 2.91 (dd, J = 3.87, 6.54 Hz, 2H), 2.89 (s, 1H), 2.84 (s, 1H), 2.81 (d, J = 4.28 Hz, 1H), 2.79 (d, J = 2.42 Hz, 1H), 2.73 (d, J = 4.65 Hz, 1H), 2.71 (d, J = 5.14 Hz, 1H), 2.63–2.60 (m, 1H), 2.39 (d, J = 4.93 Hz, 1H), 2.08 (s, 1H), 2.02 (d, J = 7.69 Hz, 1H), 1.93–1.89 (m, 1H), 1.85 (dd, J = 3.53, 6.89 Hz, 1H), 1.79–1.72 (m, 1H), 1.68–1.65 (m, 1H), 1.61 (d, J = 5.07 Hz, 1H), 1.51–1.40 (m, 2H), 1.39–1.30 (m, 3H), 1.30 (s, 1H), 1.23 (s, 1H), 1.16 (s, 1H), 1.08 (s, 3H), 1.06–1.01 (m, 9H), 0.94–0.92 (m, 3H), 0.90 (s, 2H), 0.88 (d, J = 6.11 Hz, 3H), 0.86 (d, J = 7.04 Hz, 3H), 0.84 (s, 3H), 0.80 (d, J = 6.01 Hz, 3H), 0.78–0.73 (m, 3H), 0.72 (d, J = 7.23 Hz, 3H), 0.70 (s, 3H), 0.66 (d, J = 7.04 Hz, 3H), 0.64 (d, J = 6.83 Hz, 3H), 0.62 (d, J = 8.97 Hz, 3H), 0.60 (s, 3H), 0.57 (d, J = 6.81 Hz, 3H), 0.54 (d, J = 6.81 Hz, 3H). ^{13}C NMR (150 MHz, DMSO-d_6): δ (ppm) 171.9, 171.9, 171.7, 171.5, 171.4, 170.9, 170.7, 170.3, 170.3, 170.2, 170.0, 170.0, 165.3, 151.8, 136.0, 130.3, 129.6, 129.4, 127.2, 127.0, 124.0, 123.7, 123.5, 121.2, 120.7, 120.6, 118.6, 118.1, 117.9, 111.2, 111.0, 110.3, 109.8, 109.6, 109.5, 72.3, 72.1, 71.9, 68.5, 65.2, 63.9, 60.3, 60.2, 57.3, 57.2, 56.7, 55.2, 54.4, 54.2, 53.8, 53.4, 53.3, 53.0, 52.9, 52.2, 51.5, 50.8, 47.8, 40.9, 38.2, 37.5, 34.6, 34.6, 32.4, 31.4, 31.3, 30.8, 29.8, 29.7, 29.0, 28.0, 27.0, 25.9, 24.1, 23.9, 22.3, 22.0, 21.7, 20.3, 19.5, 19.4, 19.1, 18.9, 18.6, 18.2, 18.1, 17.8, 17.6, 15.2, 13.6, 12.0. HRMS m/z: 870.4698 [M + H]$^+$. HPLC purity 98.9%, t_r = 16.6/17.0 min.

$\Delta^{2,6}$-[D-AllylGly^2-D-Trp^6]-lugdunin (43). Yield: 20.1 mg (67%). ^{1}H NMR (600 MHz, DMSO-d_6): δ (ppm) 10.81 (d, J = 2.98 Hz, 1H), 10.79–10.75 (m, 1H), 8.83 (d, J = 8.45 Hz, 1H), 8.62 (d, J = 8.44 Hz, 1H), 8.54 (d, J = 8.13 Hz, 1H), 8.52 (d, J = 8.28 Hz, 1H), 8.19 (d, J = 8.05 Hz, 1H), 8.17–8.13 (m, 1H), 8.08 (d, J = 8.53 Hz,

https://doi.org/10.1021/acs.jmedchem.0c02170
J. Med. Chem. 2021, 64, 4034–4058

1H), 7.96−7.91 (m, 1H), 7.87 (d, J = 9.10 Hz, 1H), 7.77 (d, J = 9.40 Hz, 1H), 7.66 (d, J = 7.79 Hz, 1H), 7.64−7.56 (m, 1H), 7.55−7.50 (m, 1H), 7.34−7.26 (m, 2H), 7.22 (d, J = 7.38 Hz, 1H), 7.16−7.08 (m, 1H), 7.06−6.99 (m, 2H), 6.98−6.90 (m, 2H), 5.50−5.32 (m, 1H), 4.94 (d, J = 7.15 Hz, 1H), 4.87−4.82 (m, 1H), 4.72 (d, J = 3.00 Hz, 1H), 4.69−4.56 (m, 1H), 4.56−4.50 (m, 1H), 4.46 (dd, J = 5.90, 7.92 Hz, 2H), 4.39 (d, J = 6.73 Hz, 1H), 4.30 (t, J = 5.17 Hz, 1H), 4.24 (dd, J = 6.80, 9.24 Hz, 1H), 4.20−4.13 (m, 1H), 4.09−4.01 (m, 1H), 3.97 (d, J = 5.68 Hz, 1H), 3.78−3.67 (m, 1H), 3.66−3.60 (m, 1H), 3.46−3.40 (m, 1H), 3.17 (d, J = 5.22 Hz, 1H), 3.12 (dd, J = 6.02, 9.55 Hz, 1H), 3.09−3.06 (m, 1H), 3.05−2.98 (m, 1H), 2.93 (dd, J = 5.12, 9.29 Hz, 1H), 2.91−2.85 (m, 1H), 2.83−2.78 (m, 1H), 2.73−2.71 (m, 1H), 2.27−2.10 (m, 2H), 2.07−1.95 (m, 1H), 1.84 (dd, J = 2.82, 6.86 Hz, 1H), 1.75 (d, J = 6.55 Hz, 1H), 1.50−1.42 (m, 1H), 1.39 (dd, J = 3.66, 6.78 Hz, 1H), 1.34−1.28 (m, 1H), 1.26 (s, 1H), 1.07 (d, J = 6.62 Hz, 3H), 1.05−1.03 (m, 6H), 1.03−1.00 (m, 9H), 0.99 (d, J = 6.77 Hz, 3H), 0.87 (d, J = 7.35 Hz, 3H), 0.84 (t, J = 6.22 Hz, 3H), 0.82 (d, J = 6.35 Hz, 3H), 0.79 (d, J = 6.20 Hz, 3H), 0.75 (d, J = 6.03 Hz, 3H), 0.68−0.65 (m, 3H), 0.65−0.62 (m, 3H), 0.60 (d, J = 6.89 Hz, 3H), 0.57 (d, J = 6.81 Hz, 3H), 0.54 (d, J = 6.83 Hz, 3H). ^{13}C NMR (150 MHz, DMSO-d_6): δ (ppm) 172.0, 171.7, 171.4, 171.3, 171.2, 170.8, 170.7, 170.2, 170.2, 170.1, 170.0, 169.6, 151.8, 138.7, 136.1, 136.0, 134.6, 133.6, 133.2, 129.4, 127.2, 127.1, 124.0, 123.8, 123.7, 123.4, 121.2, 120.6, 118.1, 117.9, 117.7, 117.2, 111.2, 111.0, 110.2, 109.6, 109.5, 74.5, 72.3, 72.1, 71.9, 68.5, 66.9, 65.2, 64.7, 63.9, 60.3, 60.2, 57.2, 57.1, 56.8, 54.5, 53.9, 53.7, 53.3, 53.1, 53.0, 52.1, 51.2, 50.9, 40.9, 38.2, 37.4, 37.1, 36.8, 34.8, 34.6, 32.5, 31.3, 30.7, 29.8, 29.5, 29.0, 28.6, 27.9, 27.2, 26.6, 24.0, 24.0, 22.9, 22.3, 22.0, 21.6, 20.3, 19.5, 19.5, 19.1, 18.1, 17.8, 17.6, 17.2, 15.1. HRMS m/z: 868.4797 $[M + H]^+$. HPLC purity 97.3%, t_r = 16.5/16.9 min.

$\Delta^{2,6}$-[D-Pra^2-D-Trp^6]-lugdunin (44). Yield: 22.8 mg (76%). ^{1}H NMR (600 MHz, DMSO-d_6): δ (ppm) 10.81−10.78 (m, 1H), 10.78 (d, J = 2.37 Hz, 1H), 10.76 (d, J = 2.38 Hz, 1H), 8.90 (d, J = 8.05 Hz, 1H), 8.64 (d, J =8.71 Hz, 1H), 8.50 (d, J = 7.30 Hz, 1H), 8.42 (d, J = 8.95 Hz, 1H), 8.31 (d, J = 8.37 Hz, 1H), 8.20−8.15 (m, 1H), 8.14 (d, J = 8.32 Hz, 1H), 8.03−7.97 (m, 1H), 7.89 (d, J = 9.38 Hz, 1H), 7.76 (d, J = 9.39 Hz, 1H), 7.72−7.68 (m, 1H), 7.65 (dd, J = 1.08, 7.83 Hz, 1H), 7.58 (d, J = 7.65 Hz, 1H), 7.52−7.49 (m, 1H), 7.31−7.23 (m, 2H), 7.22 (d, J = 7.38 Hz, 1H), 7.14 (d, J = 7.38 Hz, 1H), 7.08−7.00 (m, 2H), 6.95 (d, J = 8.13 Hz, 1H), 5.11 (s, 1H), 4.86 (d, J = 8.71 Hz, 1H), 4.73 (d, J = 2.56 Hz, 1H), 4.71 (d, J = 2.54 Hz, 1H), 4.70−4.66 (m, 1H), 4.66 (s, 1H), 4.65−4.63 (m, 1H), 4.62 (d, J = 2.97 Hz, 1H), 4.62 (d, J = 2.20 Hz, 1H), 4.61−4.59 (m, 1H), 4.42 (s, 1H), 4.40 (d, J = 8.22 Hz, 1H), 4.27 (s, 1H), 4.25 (d, J = 2.43 Hz, 1H), 4.24 (d, J = 6.21 Hz, 1H), 4.23 (d, J = 4.40 Hz, 1H), 4.21 (d, J = 2.47 Hz, 1H), 4.20 (d, J = 1.46 Hz, 1H), 4.19 (s, 1H), 4.08 (d, J = 2.50 Hz, 1H), 4.07 (d, J = 2.52 Hz, 1H), 4.05 (d, J = 2.57 Hz, 1H), 3.95−3.91 (m, 2H), 3.76 (s, 1H), 3.75 (d, J = 1.17 Hz, 1H), 3.71 (d, J = 2.59 Hz, 1H), 3.70−3.69 (m, 1H), 3.68 (d, J = 2.83 Hz, 1H), 3.66 (s, 1H), 3.65−3.62 (m, 1H), 3.62 (s, 1H), 3.45 (d, J = 6.13 Hz, 1H), 3.40 (d, J = 4.66 Hz, 1H), 3.31 (s, 1H), 3.23 (d, J = 6.01 Hz, 1H), 3.21 (d, J = 5.91 Hz, 1H), 3.17 (d, J = 5.06 Hz, 1H), 3.12−3.08 (m, 1H), 3.08 (d, J = 5.58 Hz, 1H), 3.05 (d, J = 5.84 Hz, 1H), 3.04−3.03 (m, 1H), 3.02 (dd, J = 3.31, 6.47 Hz, 2H), 2.99 (d, J = 3.56 Hz, 1H), 2.96 (d, J = 2.80 Hz, 1H), 2.94 (d, J = 2.96 Hz, 1H), 2.90 (d, J = 9.13 Hz, 1H), 2.88 (d, J = 9.10 Hz, 1H), 2.84 (d, J = 4.20 Hz, 1H), 2.82 (d, J = 6.12 Hz, 1H), 2.81 (s, 1H), 2.77 (t, J = 2.60 Hz, 1H), 2.71 (s, 1H), 2.70 (d, J = 2.60 Hz, 1H), 2.68 (d, J = 2.10 Hz, 1H), 2.67 (t, J = 2.61 Hz, 1H), 2.56 (d, J = 9.77 Hz, 1H), 2.46 (s, 1H), 2.44 (s, 1H), 2.40 (ddd, J = 2.59, 6.58, 9.73 Hz, 1H), 2.27−2.24 (m, 1H), 2.07 (s, 1H), 2.05 (d, J = 4.18 Hz, 1H), 2.02−2.00 (m, 1H), 1.98 (d, J = 5.89 Hz, 1H), 1.68 (d, J = 6.94 Hz, 1H), 1.48 (d, J = 4.17 Hz, 1H), 1.34 (d, J = 1.57 Hz, 1H), 1.32−1.31 (m, 1H), 1.30−1.29 (m, 1H), 1.28 (d, J = 7.29 Hz, 1H), 1.25−1.22 (m, 2H), 1.17 (s, 1H), 1.15 (s, 1H), 1.15−1.13 (m, 1H), 1.11 (s, 1H), 0.98 (d, J = 7.19 Hz, 3H), 0.87 (d, J = 6.69 Hz, 3H), 0.85−0.83 (m, 15H), 0.81 (d, J = 6.63 Hz, 3H), 0.78 (d, J = 6.23 Hz, 3H), 0.75 (d, J = 6.54 Hz, 3H), 0.73−0.68 (m, 3H), 0.63 (d, J = 6.87 Hz, 3H), 0.59 (d, J = 6.76 Hz, 3H), 0.56 (d, J = 6.77 Hz, 3H), 0.49 (d, J = 6.75 Hz, 3H), 0.34 (d, J = 6.67 Hz, 3H). ^{13}C NMR (150 MHz, DMSO-d_6): δ (ppm) 172.8, 172.1, 171.9, 171.5, 171.0, 170.9, 170.8, 170.7, 170.6, 170.6, 170.5, 169.0, 136.5, 136.5, 136.4, 130.1, 127.8, 127.7, 124.6, 124.3, 123.9, 121.2, 121.1, 119.3, 118.7, 118.6, 118.4, 111.6, 111.5, 110.5, 110.3, 110.2, 109.9, 80.7, 80.4, 73.7, 73.1, 72.7, 72.5, 65.6, 64.3, 57.6, 57.1, 55.0, 53.9, 53.8, 53.6, 53.3, 52.2, 51.2, 50.9, 41.5, 41.4, 40.9, 38.2, 37.7, 33.1, 31.8, 31.4, 30.5, 30.3, 29.5, 29.3, 28.5, 28.1, 27.6, 24.5, 23.4, 22.7, 22.6, 22.1, 21.1, 20.9, 20.1, 19.5, 18.1, 15.6, 14.4, 12.5. HRMS m/z: 866.4373 $[M + H]^+$. HPLC purity 97.6%, t_r = 16.0/16.5 min.

$\Delta^{2,6}$-[D-Leu^2-D-Trp^6]-lugdunin (45). Yield: 18.4 mg (60%). ^{1}H NMR (600 MHz, DMSO-d_6): δ (ppm) 10.88 (d, J = 2.84 Hz, 1H), 8.83 (d, J = 8.47 Hz, 1H), 8.62 (d, J = 8.40 Hz, 1H), 8.47 (d, J = 6.50 Hz, 1H), 8.44−8.40 (m, 1H), 8.25 (d, J = 8.36 Hz, 1H), 7.96 (s, 1H), 7.73−7.54 (m, 2H), 7.53−7.46 (m, 1H), 7.35−7.25 (m, 2H), 7.20 (d, J = 7.35 Hz, 1H), 7.16 (d, J = 7.37 Hz, 1H), 7.12 (d, J = 7.31 Hz, 1H), 7.09 (d, J = 7.32 Hz, 1H), 7.07−6.98 (m, 2H), 6.99−6.88 (m, 2H), 5.10 (s, 1H), 4.73−4.57 (m, 1H), 4.53 (t, J = 7.24 Hz, 1H), 4.48 (dd, J = 3.46, 7.89, Hz, 1H), 4.43 (s, 1H), 4.39 (d, J = 5.34 Hz, 1H), 4.36 (d, J = 7.12 Hz, 1H), 4.34 (s, 1H), 4.22 (dd, J = 4.85, 9.30 Hz, 1H), 4.18 (s, 1H), 3.98−3.88 (m, 1H), 3.76−3.71 (m, 2H), 3.70−3.64 (m, 1H), 3.44−3.39 (m, 1H), 3.25 (s, 1H), 3.19−3.13 (m, 2H), 3.12 (d, J = 5.02 Hz, 1H), 3.08 (d, J = 5.87 Hz, 1H), 3.01 (dd, J = 3.46, 6.86 Hz, 1H), 2.97 (s, 1H), 2.96−2.93 (m, 1H), 2.92−2.86 (m, 1H), 2.84 (d, J = 3.20 Hz, 1H), 2.65−2.57 (m, 1H), 2.54 (s, 1H), 2.46−2.35 (m, 1H), 2.25−2.14 (m, 1H), 2.14−2.08 (m, 1H), 2.08 (d, J = 6.54 Hz, 1H), 2.05 (d, J = 2.89 Hz, 1H), 2.04−1.98 (m, 1H), 1.94 (d, J = 7.04 Hz, 1H), 1.91 (s, 1H), 1.82 (d, J = 6.49 Hz, 1H), 1.74−1.71 (m, 1H), 1.68 (s, 1H), 1.54 (d, J = 4.35 Hz, 1H), 1.49−1.41 (m, 2H), 1.39−1.35 (m, 2H), 1.35−1.27 (m, 1H), 1.16−1.14 (m, 1H), 1.07 (d, J = 5.31 Hz, 2H), 0.98 (d, J = 6.94 Hz, 3H), 0.86 (d, J = 6.71 Hz, 6H), 0.84 (t, J = 6.36 Hz, 3H), 0.78 (d, J = 6.27 Hz, 3H), 0.74 (s, 3H), 0.72 (d, J = 6.49 Hz, 3H), 0.71−0.68 (m, 12H), 0.67 (d, J = 6.41 Hz, 3H), 0.66−0.63 (m, 6H), 0.61 (d, J = 5.71 Hz, 3H). ^{13}C NMR (150 MHz, DMSO-d_6): δ (ppm) 171.9, 171.7, 171.4, 171.3, 171.2, 171.0, 170.7, 170.6, 170.2, 169.5, 152.3, 151.8, 138.7, 136.1, 136.0, 134.6, 129.4, 127.2, 127.2, 127.1, 123.8, 123.5, 123.3, 121.3, 120.7, 120.6, 118.3, 118.1, 118.0, 111.3, 111.1, 110.9, 109.9, 109.8, 109.3, 72.3, 71.0, 68.8, 68.5, 66.9, 66.4, 65.6, 60.1, 59.2, 58.8, 56.8, 54.5, 53.5, 51.9, 51.1, 50.4, 45.8, 45.8, 41.5, 38.2, 37.6, 31.3, 30.5, 30.4, 29.7, 29.0, 28.6, 27.2, 25.9, 24.1, 24.0, 23.8, 23.0, 22.9, 22.7, 22.6, 22.2, 22.0, 22.0, 21.8, 20.8, 20.1, 19.7, 19.5, 19.2, 18.3, 17.8, 17.0, 16.6, 15.2, 13.9, 12.0. HRMS m/z: 884.4835 $[M + H]^+$. HPLC purity 98.7%, t_r = 17.1/17.6 min.

$\Delta^{2,6}$-[D-Met^2-D-Trp^6]-lugdunin (46). Yield: 22.9 mg (74%). ^{1}H NMR (600 MHz, DMSO-d_6): δ (ppm) 10.88−10.84 (m, 1H), 10.80 (d, J = 2.45 Hz, 1H), 8.83 (d, J = 8.42 Hz, 1H), 8.71 (d, J = 8.77 Hz, 1H), 8.68 (d, J = 8.40 Hz, 1H), 8.62 (d, J = 8.38 Hz, 1H), 8.56 (d, J = 8.53 Hz, 1H), 8.50 (d, J = 8.79 Hz, 1H), 8.40 (d, J = 8.27 Hz, 1H), 8.38−8.30 (m, 1H), 8.26 (d, J = 7.99 Hz, 1H), 8.17 (d, J = 7.80 Hz, 1H), 8.05 (s, 1H), 7.97 (d, J = 8.48 Hz, 1H), 7.93 (d, J = 9.29 Hz, 1H), 7.88 (d, J = 8.72 Hz, 1H), 7.78 (d, J = 9.60 Hz, 1H), 7.75 (d, J = 7.80 Hz, 1H), 7.66 (t, J = 7.89 Hz, 1H), 7.61−7.56 (m, 1H), 7.52 (t, J = 8.50 Hz, 1H), 7.30 (d, J = 7.68 Hz, 1H), 7.22 (d, J = 7.37 Hz, 1H), 7.20 (d, J = 7.38 Hz, 1H), 7.17−7.11 (m, 1H), 7.10 (d, J = 2.28 Hz, 1H), 7.03 (d, J = 9.33 Hz, 1H), 6.98−6.91 (m, 1H), 4.86−4.77 (m, 1H), 4.76 (s, 1H), 4.72 (s, 1H), 4.70 (d, J = 2.06 Hz, 1H), 4.68 (s, 1H), 4.60−4.57 (m, 1H), 4.55−4.52 (m, 1H), 4.48 (dd, J = 4.00, 7.80 Hz, 1H), 4.43 (s, 1H), 4.38 (d J = 7.37 Hz, 1H), 4.28−4.21 (m, 1H), 4.18 (d, J = 6.39 Hz, 1H), 4.08−4.00 (m, 1H), 3.98 (d, J = 4.77 Hz, 1H), 3.96−3.91 (m, 1H), 3.88 (d, J = 6.69 Hz, 1H), 3.77−3.74 (m, 1H), 3.70 (d, J = 6.16 Hz, 1H), 3.45 (s, 1H), 3.41 (t, J = 5.31 Hz, 1H), 3.38 (d, J = 3.58 Hz, 1H), 3.36 (d, J = 3.56 Hz, 1H), 3.30 (s, 1H), 3.25 (s, 1H), 3.22−3.14 (m, 1H), 3.09 (d, J = 5.71 Hz, 1H), 3.05 (d, J = 6.79 Hz, 1H), 3.02 (d, J = 4.93 Hz, 1H), 3.00 (s, 1H), 2.97 (d, J = 3.45 Hz, 1H), 2.96 (s, 1H), 2.95−2.90 (m, 1H), 2.84 (s, 1H), 2.72 (dd, J = 5.89, 9.45 Hz, 1H), 2.62−2.61 (m, 1H), 2.38 (d, J = 3.96 Hz, 1H), 2.36 (s, 1H), 2.34 (s, 1H), 2.31 (d, J = 4.49 Hz, 1H), 2.27−2.24 (m, 1H), 2.23 (s, 1H), 2.21 (s, 1H), 2.16 (dd, J = 6.55, 9.44 Hz, 2H), 2.11−2.04 (m, 1H), 2.02 (dd, J = 2.33, 6.60 Hz, 2H), 1.98 (d, J = 6.31 Hz, 1H), 1.95−1.93 (m, 1H), 1.90 (s, 1H), 1.84 (s,

https://doi.org/10.1021/acs.jmedchem.0c02170
J. Med. Chem. 2021, 64, 4034−4058

1H), 1.78 (d, J = 6.84 Hz, 1H), 1.73 (d, J = 3.59 Hz, 1H), 1.68 (d, J = 4.84 Hz, 1H), 1.66 (d, J = 7.85 Hz, 1H), 1.54 (d, J = 4.33 Hz, 1H), 1.46 (dd, J = 4.10, 8.61 Hz, 1H), 1.37 (d, J = 4.54 Hz, 1H), 1.31 (s, 1H), 1.23 (s, 1H), 1.15 (d, J = 5.21 Hz, 1H), 1.01 (d, J = 5.21 Hz, 1H), 0.98 (d, J = 7.02 Hz, 3H), 0.87 (d, J = 6.92 Hz, 3H), 0.84 (d, J = 6.87 Hz, 3H), 0.82 (s, 3H), 0.80–0.77 (m, 9H), 0.77–0.73 (m, 6H), 0.73–0.71 (m, 6H), 0.68 (d, J = 6.58 Hz, 3H), 0.66–0.61 (m, 3H), 0.61 (s, 3H), 0.59–0.57 (m, 3H), 0.55 (d, J = 6.90 Hz, 3H). ^{13}C NMR (150 MHz, DMSO-d_6): δ (ppm) 172.0, 171.9, 171.7, 171.6, 171.4, 171.1, 170.8, 170.7, 170.5, 170.4, 170.4, 170.3, 170.1, 169.8, 169.7, 164.5, 157.9, 151.8, 138.7, 136.0, 130.3, 129.4, 128.0, 127.1, 126.4, 124.0, 123.7, 123.5, 123.3, 121.3, 120.7, 118.1, 111.2, 110.9, 110.3, 109.8, 109.6, 109.2, 105.1, 98.9, 72.3, 71.9, 69.5, 68.8, 68.5, 67.2, 66.9, 66.3, 66.1, 66.0, 65.7, 65.1, 64.0, 60.1, 58.8, 57.2, 55.2, 54.5, 53.7, 53.5, 52.1, 52.0, 51.3, 50.9, 40.9, 40.4, 38.2, 37.4, 32.5, 32.1, 31.3, 30.6, 30.2, 29.1, 28.9, 28.6, 27.1, 26.6, 24.0, 23.9, 23.0, 22.6, 22.3, 22.0, 21.9, 21.6, 20.8, 20.1, 19.5, 18.3, 18.0, 17.8, 17.0, 16.6, 15.3, 15.2, 14.5, 13.9, 12.2, 12.0. HRMS m/z: 902.4426 [M + H]$^+$. HPLC purity 89.1%, t_r = 16.6/17.1 min.

Δ^4-[D-Ile]-lugdunin (47). Yield: 14.9 mg (55%). ^{1}H NMR (700 MHz, DMSO-d_6): δ (ppm) 10.82 (d, J = 2.30 Hz, 1H), 10.75 (d, J = 2.51 Hz, 1H), 8.48 (d, J = 8.19 Hz, 1H), 8.44 (d, J = 8.82 Hz, 1H), 8.38 (d, J = 8.73 Hz, 1H), 8.35 (d, J = 8.79 Hz, 1H), 8.25 (d, J = 7.89 Hz, 1H), 8.15 (d, J = 9.07 Hz, 1H), 8.06 (d, J = 9.49 Hz, 1H), 7.95 (s, 1H), 7.92 (d, J = 9.10 Hz, 1H), 7.86 (d, J = 9.16 Hz, 1H), 7.82 (d, J = 9.06 Hz, 1H), 7.77 (d, J = 8.22 Hz, 1H), 7.70 (d, J = 7.90 Hz, 1H), 7.64 (t, J = 8.65 Hz, 1H), 7.58 (s, 1H), 7.53 (d, J = 7.82 Hz, 1H), 7.48 (d, J = 7.92 Hz, 1H), 7.43 (d, J = 9.14 Hz, 1H), 7.31–7.26 (m, 2H), 7.18 (d, J = 7.33 Hz, 1H), 7.16 (d, J = 7.53 Hz, 1H), 7.12 (d, J = 7.33 Hz, 1H), 7.09 (d, J = 7.26 Hz, 1H), 7.06–6.99 (m, 2H), 4.80 (t, J = 6.76 Hz, 1H), 4.75–4.70 (m, 1H), 4.66 (d, J = 7.54 Hz, 1H), 4.64 (s, 1H), 4.62 (d, J = 8.31 Hz, 1H), 4.58 (d, J = 5.06 Hz, 1H), 4.52 (dd, J = 5.77, 9.16 Hz, 1H), 4.44 (d, J = 9.97 Hz, 1H), 4.41 (d, J = 7.14 Hz, 1H), 4.35 (d, J = 8.40 Hz, 1H), 4.33 (d, J = 3.31 Hz, 1H), 4.30 (d, J = 8.95 Hz, 1H), 4.29–4.23 (m, 1H), 4.19 (d, J = 8.97 Hz, 1H), 4.17 (d, J = 5.09 Hz, 1H), 4.15 (d, J = 3.14 Hz, 1H), 4.13 (d, J = 9.77 Hz, 1H), 4.11 (s, 1H), 4.09 (d, J = 2.33 Hz, 1H), 4.07 (dd, J = 2.78, 6.95 Hz, 1H), 3.98 (t, J = 9.27 Hz, 1H), 3.90–3.86 (m, 1H), 3.80 (s, 1H), 3.78 (d, J = 2.92 Hz, 1H), 3.77 (d, J = 5.10 Hz, 1H), 3.67 (s, 1H), 3.32 (d, J = 4.71 Hz, 1H), 3.30 (d, J = 4.75 Hz, 1H), 3.15 (s, 1H), 3.14 (d, J = 3.41 Hz, 1H), 3.13 (s, 1H), 2.99 (d, J = 5.04 Hz, 1H), 2.97 (d, J = 5.21 Hz, 1H), 2.92 (d, J = 7.61 Hz, 1H), 2.90 (s, 1H), 2.89 (d, J = 3.47 Hz, 1H), 2.86 (s, 1H), 2.81 (s, 1H), 2.79 (d, J = 4.51 Hz, 1H), 2.76 (d, J = 5.41 Hz, 1H), 2.73 (s, 1H), 2.69 (s, 1H), 2.62 (d, J = 4.99 Hz, 1H), 2.61 (q, J = 1.92 Hz, 1H), 2.59 (s, 1H), 2.52–2.51 (m, 1H), 2.46–2.42 (m, 1H), 2.38 (d, J = 3.85 Hz, 1H), 2.20–2.16 (m, 1H), 2.08 (s, 1H), 2.06 (s, 1H), 2.03–2.01 (m, 1H), 2.00 (s, 1H), 1.97 (d, J = 6.93 Hz, 1H), 1.96–1.88 (m, 1H), 1.84 (s, 1H), 1.75 (s, 1H), 1.59–1.52 (m, 1H), 1.33 (dd, J = 3.42, 7.59 Hz, 2H), 1.23 (s, 2H), 1.20 (d, J = 8.61 Hz, 1H), 1.18 (d, J = 3.79 Hz, 1H), 1.14 (d, J = 6.75 Hz, 1H), 1.11 (s, 1H), 1.05 (s, 1H), 0.99 (d, J = 6.86 Hz, 3H), 0.94 (d, J = 6.66 Hz, 3H), 0.90 (s, 3H), 0.90–0.83 (m, 12H), 0.80 (d, J = 10.01 Hz, 3H), 0.76 (s, 3H), 0.74 (d, J = 3.20 Hz, 3H), 0.68 (s, 3H), 0.67–0.64 (m, 6H), 0.63 (d, J = 7.45 Hz, 3H), 0.61 (d, J = 6.76 Hz, 3H), 0.55 (d, J = 6.70 Hz, 3H), 0.48 (d, J = 6.83 Hz, 3H), 0.41 (d, J = 6.65 Hz, 3H). HRMS m/z: 783.4579 [M + H]$^+$. HPLC purity 96.8%, t_r = 16.1/16.3 min.

$\Delta^{4,6}$-[D-*allo*-Ile^4-D-Trp^6]-lugdunin (48). Yield: 21.8 mg (73%). ^{1}H NMR (600 MHz, DMSO-d_6): δ (ppm) 10.99 (d, J = 2.39 Hz, 1H), 10.96 (d, J = 2.62 Hz, 1H), 10.88 (d, J = 2.82 Hz, 1H), 8.65 (d, J = 8.79 Hz, 1H), 8.50 (d, J = 7.20 Hz, 1H), 8.31 (d, J = 8.65 Hz, 1H), 8.23 (d, J = 9.49 Hz, 1H), 8.21 (d, J = 8.65 Hz, 1H), 8.00 (d, J = 8.98 Hz, 1H), 7.98 (d, J = 9.31 Hz, 1H), 7.86 (d, J = 9.77 Hz, 1H), 7.79 (d, J = 9.20 Hz, 1H), 7.75 (t, J = 8.10 Hz, 1H), 7.53 (d, J = 7.89 Hz, 1H), 7.43 (d, J = 9.32 Hz, 1H), 7.35–7.28 (m, 4H), 7.24 (d, J = 7.34 Hz, 1H), 7.17 (d, J = 7.37 Hz, 1H), 7.07–7.01 (m, 2H), 6.98 (d, J = 8.05 Hz, 1H), 4.92 (d, J = 6.02 Hz, 1H), 4.83–4.80 (m, 1H), 4.76 (d, J = 6.31 Hz, 1H), 4.72–4.67 (m, 1H), 4.62 (d, J = 5.80 Hz, 2H), 4.47–4.41 (m, 1H), 4.40 (t, J = 5.16 Hz, 1H), 4.34 (dd, J = 6.38, 9.28 Hz, 1H), 4.27 (t, J = 8.94 Hz, 1H), 4.23–4.18 (m, 2H), 4.08–4.02 (m, 1H), 4.01 (d, J = 7.22 Hz, 1H), 3.70 (d, J = 7.03 Hz, 1H), 3.41 (t, J = 5.31 Hz, 1H), 3.30 (d, J = 3.99 Hz, 1H), 3.26–3.15 (m, 2H), 3.08–2.97 (m, 1H), 2.93 (d, J = 7.61 Hz, 1H), 2.86 (d, J = 5.67 Hz, 1H), 2.78 (d, J = 5.67 Hz, 1H), 2.62 (d, J = 4.02 Hz, 1H), 2.60–2.56 (m, 2H), 2.48–2.41 (m, 1H), 2.25 (s, 1H), 2.12 (s, 1H), 2.03 (d, J = 2.69 Hz, 1H), 1.90 (d, J = 6.86 Hz, 1H), 1.88–1.69 (m, 4H), 1.64 (d, J = 2.47 Hz, 1H), 1.54–1.46 (m, 2H), 1.38–1.31 (m, 1H), 1.15–1.08 (m, 2H), 1.07 (s, 3H), 0.98–0.93 (m, 6H), 0.91–0.86 (m, 12H), 0.84 (d, J = 6.65 Hz, 3H), 0.81 (d, J = 7.32 Hz, 3H), 0.77–0.72 (m, 3H), 0.71 (d, J = 6.71 Hz, 3H), 0.72–0.67 (m, 9H), 0.65 (d, J = 6.69 Hz, 3H), 0.55 (d, J = 6.82 Hz, 3H), 0.52 (d, J = 6.79 Hz, 3H), 0.45 (d, J = 6.72 Hz, 3H). ^{13}C NMR (150 MHz, DMSO-d_6): δ (ppm) 171.7, 171.6, 171.4, 171.3, 171.1, 170.7, 170.6, 170.5, 170.5, 170.1, 169.9, 169.8, 164.6, 162.3, 136.1, 136.1, 136.0, 127.3, 127.2, 126.9, 124.3, 124.1, 123.8, 123.7, 120.7, 120.7, 120.6, 120.6, 118.7, 118.6, 118.1, 118.0, 117.9, 117.9, 111.2, 111.1, 111.0, 110.2, 109.8, 109.6, 109.5, 72.3, 72.2, 72.0, 69.8, 65.3, 63.7, 60.3, 60.3, 60.2, 58.5, 57.5, 57.2, 57.2, 56.6, 55.6, 54.4, 54.1, 53.5, 52.7, 52.7, 42.7, 40.4, 38.0, 37.6, 36.8, 36.6, 35.8, 34.7, 31.3, 31.0, 30.7, 30.3, 29.9, 29.7, 29.0, 28.7, 28.2, 26.7, 25.5, 25.1, 22.1, 20.4, 19.6, 19.5, 19.3, 19.1, 18.7, 18.6, 18.5, 18.4, 18.2, 17.5, 15.1, 14.8, 14.4, 14.0, 13.9, 12.1, 11.4, 10.9. HRMS m/z: 870.4672 [M + H]$^+$. HPLC purity 98.8%, t_r = 16.3/16.8 min.

$\Delta^{4,6}$-[D-Tle^4-D-Trp^6]-lugdunin (49). Yield: 22.4 mg (75%). ^{1}H NMR (600 MHz, DMSO-d_6): δ (ppm) 10.88 (s, 1H), 10.84 (d, J = 2.77 Hz, 1H), 8.25 (d, J = 8.60 Hz, 1H), 8.23 (d, J = 6.32 Hz, 1H), 8.21–8.19 (m, 1H), 8.15 (d, J = 7.61 Hz, 1H), 7.97 (d, J = 9.27 Hz, 1H), 7.94 (d, J = 7.69 Hz, 1H), 7.88 (d, J = 9.48 Hz, 1H), 7.85 (d, J = 9.07 Hz, 1H), 7.75 (d, J = 9.84 Hz, 1H), 7.72 (d, J = 7.15 Hz, 1H), 7.70 (d, J = 8.55 Hz, 1H), 7.54 (d, J = 7.94 Hz, 1H), 7.51 (d, J = 9.44 Hz, 1H), 7.48–7.42 (m, 1H), 7.37–7.31 (m, 1H), 7.28 (d, J = 7.47 Hz, 1H), 7.23 (t, J = 6.07 Hz, 1H), 7.19 (d, J = 6.37 Hz, 1H), 7.07 (d, J = 6.73 Hz, 1H), 6.98 (d, J = 6.94 Hz, 1H), 5.08–4.99 (m, 1H), 4.76 (s, 1H), 4.72 (d, J = 7.95 Hz, 1H), 4.71 (d, J = 2.74 Hz, 1H), 4.75 (d, J = 3.06 Hz, 1H), 4.68 (s, 1H), 4.67 (s, 1H), 4.53 (d, J = 9.41 Hz, 1H), 4.45 (s, 1H), 4.42 (d, J = 4.87 Hz, 1H), 4.35 (d, J = 9.60 Hz, 1H), 4.27 (dd, J = 7.73, 9.13 Hz, 2H), 4.27–4.19 (m, 1H), 4.17–4.13 (m, 1H), 4.07 (d, J = 9.48 Hz, 1H), 4.08 (d, J = 5.58 Hz, 1H), 3.98 (d, J = 6.42 Hz, 1H), 3.87 (d, J = 4.56 Hz, 1H), 3.82–3.77 (m, 1H), 3.72 (d, J = 6.27 Hz, 1H), 3.46 (d, J = 4.51 Hz, 2H), 3.41 (d, J = 2.67 Hz, 1H), 3.40 (d, J = 5.88 Hz, 1H), 3.39–3.23 (m, 1H), 3.21 (s, 1H), 3.15 (dd, J = 5.91, 9.61 Hz, 1H), 3.16 (d, J = 4.98 Hz, 1H), 3.07–3.05 (m, 1H), 3.04 (d, J = 5.18 Hz, 1H), 3.01 (d, J = 5.45 Hz, 1H), 2.97 (dd, J = 5.64, 9.20 Hz, 1H), 2.87 (d, J = 6.10 Hz, 1H), 2.65–2.61 (m, 1H), 2.15 (s, 1H), 2.16–2.05 (m, 1H), 2.05 (d, J = 2.38 Hz, 1H), 2.06 (d, J = 3.58 Hz, 1H), 2.02–1.97 (m, 1H), 1.77 (d, J = 7.36 Hz, 1H), 1.65–1.61 (m, 1H), 1.57 (d, J = 4.63 Hz, 1H), 1.57–1.42 (m, 1H), 1.37 (d, J = 6.75 Hz, 1H), 1.35–1.25 (m, 1H), 1.23–1.21 (m, 1H), 1.13 (d, J = 6.48 Hz, 3H), 1.11 (d, J = 6.43 Hz, 3H), 1.07 (s, 6H), 1.01 (d, J = 6.15 Hz, 3H), 0.97 (d, J = 6.73 Hz, 3H), 0.88 (s, 3H), 0.78 (d, J = 6.63 Hz, 3H), 0.73 (s, 3H), 0.71 (d, J = 6.99 Hz, 3H), 0.66 (d, J = 6.75 Hz, 3H), 0.62 (d, J = 6.84 Hz, 3H), 0.62 (d, J = 6.74 Hz, 3H), 0.60 (d, J = 6.77 Hz, 3H), 0.49 (d, J = 6.76 Hz, 3H). ^{13}C NMR (150 MHz, DMSO-d_6): δ (ppm) 172.1, 171.5, 171.1, 170.9, 170.8, 170.3, 170.1, 169.9, 169.7, 169.7, 169.4, 169.4, 136.1, 127.2, 127.2, 127.1, 124.3, 124.1, 123.7, 120.6, 120.6, 118.8, 118.7, 118.7, 118.3, 118.0, 117.9, 117.8, 111.0, 111.0, 109.9, 109.8, 109.7, 109.6, 76.3, 76.3, 74.6, 74.5, 74.5, 73.1, 73.0, 72.3, 72.1, 72.1, 65.3, 65.2, 64.7, 63.8, 63.5, 60.4, 60.2, 59.2, 59.2, 59.1, 57.3, 57.1, 56.9, 56.2, 54.5, 53.1, 52.5, 52.4, 36.9, 34.3, 34.1, 32.7, 31.5, 30.7, 30.0, 29.9, 29.4, 29.3, 28.9, 28.6, 28.4, 28.0, 27.7, 26.7, 26.5, 22.0, 20.5, 20.3, 19.6, 19.5, 19.3, 19.2, 18.8, 18.6, 18.1, 18.1, 17.3, 17.2, 17.2, 16.9, 15.1, 13.9, 11.3. HRMS m/z: 870.4696 [M + H]$^+$. HPLC purity 95.2%, t_r = 16.6/17.2 min.

$\Delta^{4,6}$-[D-Nva^4-D-Trp^6]-lugdunin (50). Yield: 24.2 mg (82%). ^{1}H NMR (600 MHz, DMSO-d_6): δ (ppm) 10.96 (s, 1H), 10.86 (d, J = 2.60 Hz, 1H), 8.56 (d, J = 8.35 Hz, 1H), 8.56 (d, J = 8.80 Hz, 1H), 8.35 (d, J = 8.49 Hz, 1H), 8.23 (d, J = 7.70 Hz, 1H), 8.21 (d, J = 8.80 Hz, 1H), 8.17 (d, J = 8.66 Hz, 1H), 8.13 (s, 1H), 7.98 (d, J = 7.19 Hz, 1H), 7.93 (s, 1H), 7.91 (d, J = 9.26 Hz, 1H), 7.77 (s, 1H), 7.72 (d, J =

https://doi.org/10.1021/acs.jmedchem.0c02170
J. Med. Chem. 2021, 64, 4034−4058

7.89 Hz, 1H), 7.70 (d, J = 7.92 Hz, 1H), 7.67 (d, J = 9.42 Hz, 1H), 7.54 (d, J = 7.88 Hz, 1H), 7.52 (d, J = 7.72 Hz, 1H), 7.38−7.34 (m, 1H), 7.27 (d, J = 6.37 Hz, 1H), 7.15 (d, J = 7.51 Hz, 1H), 7.14−7.11 (m, 1H), 7.10−7.07 (m, 1H), 7.03−6.98 (m, 1H), 5.18 (s, 1H), 4.99 (dd, J = 5.82, 8.60 Hz, 1H), 4.75 (d, J = 5.55 Hz, 1H), 4.73−4.56 (m, 1H), 4.47−4.44 (m, 1H), 4.36−4.33 (m, 1H), 4.31 (d, J = 7.27 Hz, 1H), 4.25 (s, 1H), 4.23 (t, J = 8.85 Hz, 1H), 4.03 (d, J = 9.26 Hz, 1H), 4.01 (d, J = 7.57 Hz, 1H), 3.85 (s, 1H), 3.83 (d, J = 3.30 Hz, 1H), 3.77 (d, J = 5.72 Hz, 1H), 3.55 (s, 1H), 3.44−3.42 (m, 1H), 3.40 (d, J = 6.86 Hz, 1H), 3.36 (s, 1H), 3.33 (d, J = 4.84 Hz, 1H), 3.26 (s, 1H), 3.23 (s, H), 3.21 (d, J = 5.20 Hz, 1H), 3.17 (dd, J = 5.97, 9.40 Hz, 2H), 3.14 (d, J = 6.03 Hz, 1H), 3.12 (s, 1H), 3.08 (d, J = 2.17 Hz, 1H), 3.07 (d, J = 2.13 Hz, 1H), 3.02 (s, 1H), 3.06−3.03 (m, 1H), 2.95 (d, J = 6.96 Hz, 1H), 2.93 (s, 1H), 2.91 (s, 1H), 2.86 (s, 1H), 2.85−2.82 (m, 1H), 2.81 (s, 1H), 2.67−2.64 (m, 1H), 2.63 (s, 1H), 2.56 (s, 2H), 2.57 (s, 1H), 2.55 (s, 1H), 2.45 (s, 1H), 2.43 (d, J = 5.87 Hz, 1H), 2.25 (s, 1H), 2.12 (s, 1H), 2.10 (d, J = 3.16 Hz, 1H), 2.08 (d, J = 7.83 Hz, 1H), 2.0 (d, J = 5.78 Hz, 1H), 1.97−1.85 (m, 2H), 1.82−1.77 (m, 2H), 1.74−1.68 (m, 1H), 1.58 (dd, J = 6.80, 9.11 Hz, 1H), 1.42 (d, J = 6.74 Hz, 1H), 1.36 (d, J = 2.10 Hz, 1H), 1.33 (s, 1H), 1.31 (s, 1H), 1.27 (s, 1H), 1.16 (s, 1H), 1.08 (d, J = 4.74 Hz, 1H), 1.0−1.0 (m, 1H), 1.0 (d, J = 7.04 Hz, 1H), 0.9 (s, 1H), 0.9−0.8 (m, 1H), 0.8 (d, J = 6.62 Hz, 1H), 0.8 (s, 1H), 0.86 (d, J = 7.57 Hz, 3H), 0.76 (d, J = 7.48 Hz, 6H), 0.73 (d, J = 6.68 Hz, 3H), 0.72 (d, J = 6.71 Hz, 3H), 0.67 (d, J = 6.96 Hz, 3H), 0.58 (d, J = 7.33 Hz, 3H), 0.54 (d, J = 6.76 Hz, 3H), 0.52 (d, J = 6.71 Hz, 3H). ^{13}C NMR (150 MHz, DMSO-d_6): δ (ppm) 172.1, 171.4, 171.4, 171.1, 170.9, 170.7, 170.5, 170.4, 170.1, 169.9, 169.8, 164.6, 162.3, 136.1, 136.0, 127.3, 127.2, 127.0, 124.2, 124.1, 123.8, 123.7, 120.7, 120.7, 120.6, 118.7, 118.7, 118.1, 117.9, 111.2, 111.0, 110.1, 109.8, 109.7, 109.6, 72.3, 72.2, 72.0, 65.2, 63.7, 60.3, 60.2, 57.4, 57.2, 56.6, 54.5, 53.7, 53.3, 53.2, 52.8, 52.7, 51.9, 38.0, 37.5, 35.8, 34.7, 34.5, 34.1, 32.6, 31.3, 31.0, 30.8, 29.8, 29.7, 29.0, 28.7, 28.0, 27.2, 26.8, 22.1, 20.4, 19.6, 19.3, 19.1, 18.7, 18.6, 18.6, 18.3, 18.2, 18.1, 17.8, 17.6, 15.0, 14.0, 13.9, 13.7, 13.5, 12.1. HRMS m/z: 856.4509 [M + H]$^+$. HPLC purity 95.9%, t_r = 16.1/16.5 min.

Δ^{4,6}-[D-AllylGly^4-D-Trp^6]-lugdunin (51). Yield: 22.9 mg (78%). ^{1}H NMR (600 MHz, DMSO-d_6): δ (ppm) 10.89−10.78 (m, 1H), 8.56 (d, J = 8.47 Hz, 1H), 8.45 (d, J = 7.64 Hz, 1H), 8.23 (d, J = 8.50 Hz, 1H), 8.23 (d, J = 7.52 Hz, 1H), 8.15 (d, J = 8.57 Hz, 1H), 7.95 (d, J = 9.18 Hz, 1H), 7.91 (d, J = 9.23 Hz, 1H), 7.85 (d, J = 9.41 Hz, 1H), 7.75−7.63 (m, 1H), 7.55 (d, J = 7.85 Hz, 1H), 7.35−7.32 (m, 1H), 7.24 (d, J = 7.37 Hz, 1H), 7.15−7.13 (m, 1H), 7.11−6.98 (m, 2H), 5.6 (dd, J = 6.89 Hz, 1H), 5.5 (d, J = 7.04 Hz, 1H), 5.05−5.02 (m, 1H), 5.05 (dd, J = 6.70 Hz, 1H), 4.95 (d, J = 3.66 Hz, 1H), 4.97−4.85 (m, 1H), 4.7 (d, J = 5.46 Hz, 1H), 4.75 (s, 1H), 4.72 (t, J = 4.47 Hz, 1H), 4.64−4.61 (m, 2H), 4.55 (dd, J = 5.90, 8.08 Hz, 1H), 4.45−4.41 (m, 1H), 4.40 (dd, J = 6.75, 8.82 Hz, 1H), 4.33 (dd, J = 6.79, 9.44 Hz, 1H), 4.24−4.12 (m, 1H), 4.04 (d, J = 9.41 Hz, 1H), 4.02−3.95 (m, 1H), 3.74−3.6 2(m, 2H), 3.55−3.48 (m, 1H), 3.43−3.40 (m, 1H), 3.21−3.16 (m, 1H), 3.17−3.08 (m, 1H), 2.95 (d, J = 8.81 Hz, 1H), 2.87 (d, J = 4.75 Hz, 1H), 2.75 (s, 1H), 2.64−2.62 (m, 1H), 2.61−2.58 (m, 1H), 2.45 (d, J = 4.88 Hz, 1H), 2.22 (d, J = 7.20 Hz, 1H), 2.14−1.98 (m, 1H), 1.95 (t, J = 7.42 Hz, 1H), 1.84−1.75 (m, 1H), 1.65 (d, J = 5.56 Hz, 1H), 1.54−1.45 (m, 1H), 1.44−1.42 (m, 1H), 1.35−1.25 (m, 2H), 1.25 (d, J = 6.71 Hz, 1H), 1.15−0.98 (m, 12H), 0.93−0.87 (m, 9H), 0.78 (d, J = 6.63 Hz, 3H), 0.74 (d, J = 6.78 Hz, 3H), 0.65−0.62 (m, 3H), 0.54 (d, J = 6.59 Hz, 3H), 0.51 (d, J = 6.74 Hz, 3H). ^{13}C NMR (150 MHz, DMSO-d_6): δ (ppm) 172.1, 171.4, 171.3, 170.8, 170.6, 170.5, 170.4, 170.4, 170.2, 170.1, 169.9, 151.8, 136.1, 136.1, 134.1, 133.8, 129.4, 127.2, 127.2, 127.1, 127.0, 124.1, 124.0, 123.7, 123.6, 121.2, 120.7, 120.6, 118.7, 118.6, 118.5, 118.1, 117.9, 117.9, 117.7, 117.2, 111.2, 111.0, 110.1, 109.8, 109.6, 109.6, 76.3, 76.3, 74.6, 74.5, 74.5, 72.3, 72.1, 72.1, 72.0, 68.5, 65.3, 65.2, 64.7, 63.7, 60.3, 60.2, 60.2, 57.3, 57.2, 57.1, 56.7, 54.5, 53.7, 53.5, 53.1, 52.8, 52.7, 51.7, 45.8, 39.1, 38.2, 37.9, 37.4, 36.7, 36.6, 34.6, 32.5, 31.3, 30.8, 30.7, 29.7, 29.6, 28.9, 28.7, 27.8, 27.2, 26.7, 25.8, 22.0, 20.4, 20.2, 19.5, 19.2, 19.1, 18.7, 18.5, 18.2, 18.0, 17.8, 17.6, 17.2, 17.1, 15.0, 13.9, 13.8, 12.0. HRMS m/z: 854.4633 [M + H]$^+$. HPLC purity 97.7%, t_r = 16.1/16.4 min.

Δ^{4,6}-[D-Pra^4-D-Trp^6]-lugdunin (52). Yield: 23.2 mg (79%). ^{1}H NMR (600 MHz, DMSO-d_6): δ (ppm) 10.98 (s, 1H), 10.93 (s, 1H), 10.88 (s, 1H), 8.55−8.42 (m, 1H), 8.35 (d, J = 8.51 Hz, 1H), 8.35 (d, J = 8.54 Hz, 1H), 8.31 (d, J = 9.47 Hz, 1H), 8.22 (d, J = 8.56 Hz, 1H), 8.14 (d, J = 8.25 Hz, 1H), 8.12 (d, J = 9.24 Hz, 1H), 8.04 (d, J = 9.50 Hz, 1H), 7.95 (d, J = 9.40 Hz, 1H), 7.87 (d, J = 7.87 Hz, 1H), 7.65 (d, J = 7.87 Hz, 1H), 7.54 (d, J = 7.93 Hz, 1H), 7.37−7.29 (m, 1H), 7.22 (d, J = 0.38 Hz, 1H), 7.18 (d, J = 6.02 Hz, 1H), 7.15 (d, J = 7.39 Hz, 1H), 7.08 (d, J = 7.57 Hz, 1H), 6.95 (d, J = 6.87 Hz, 1H), 4.85 (d, J = 8.42 Hz, 1H), 4.75 (dd, J = 5.14, 9.91 Hz, 1H), 4.65 (d, J = 7.73 Hz, 1H), 4.55−4.42 (m, 1H), 4.25 (dd, J = 6.87, 9.34 Hz, 1H), 4.21 (t, J = 8.74 Hz, 1H), 4.12 (d, J = 9.60 Hz, 1H), 3.95 (d, J = 5.85 Hz, 1H), 3.85 (t, J = 7.32 Hz, 1H), 3.82−3.75 (m, 1H), 3.25−3.18 (m, 1H), 3.15−3.07 (m, 1H), 2.96 (dd, J = 4.06, 9.99 Hz, 1H), 2.95−2.88 (m, 1H), 2.86 (t, J = 4.64 Hz, 1H), 2.78 (t, J = 2.61 Hz, 1H), 2.65−2.55 (m, 1H), 2.46−2.38 (m, 1H), 2.25 (dd, J = 3.68, 7.26 Hz, 1H), 2.05 (d, J = 5.65 Hz, 1H), 1.90 (s, 1H), 1.85 (d, J = 7.13 Hz, 1H), 1.75 (d, J = 7.23 Hz, 1H), 1.67 (dd, J = 6.52, 9.31 Hz, 1H), 1.54−1.47 (m, 1H), 1.15−1.06 (m, 2H), 0.96 (d, J = 6.63 Hz, 3H), 0.85 (d, J = 6.72 Hz, 3H), 0.83 (s, 3H), 0.78 (d, J = 6.72 Hz, 3H), 0.65 (d, J = 6.86 Hz, 3H), 0.61 (d, J = 6.74 Hz, 3H), 0.55 (d, J = 6.75 Hz, 3H), 0.53 (d, J = 6.77 Hz, 3H), 0.51 (d, J = 6.75 Hz, 3H). ^{13}C NMR (150 MHz, DMSO-d_6): δ (ppm) 174.3, 172.8, 171.5, 171.0, 170.9, 170.8, 170.3, 170.0, 170.0, 169.7, 169.4, 169.0, 136.1, 136.0, 136.0, 129.6, 127.2, 127.2, 127.2, 124.3, 124.1, 123.9, 123.6, 120.7, 120.6, 119.0, 118.7, 118.6, 118.3, 118.0, 118.0, 117.9, 117.8, 111.1, 111.1, 111.0, 109.8, 109.8, 109.7, 109.6, 80.5, 80.5, 72.7, 72.5, 72.3, 72.0, 72.0, 64.8, 63.8, 60.1, 59.5, 57.2, 57.2, 57.0, 56.9, 54.7, 53.1, 52.9, 52.6, 52.5, 52.3, 51.2, 40.4, 38.2, 37.0, 35.1, 32.6, 31.9, 31.3, 31.1, 30.7, 30.0, 29.7, 29.5, 29.1, 28.7, 28.6, 28.1, 27.7, 27.6, 26.6, 26.6, 25.1, 22.1, 21.6, 20.5, 19.8, 19.6, 19.1, 19.0, 18.8, 18.8, 18.1, 17.9, 17.7, 15.2, 14.0, 12.1. HRMS m/z: 852.4225 [M + H]$^+$. HPLC purity 98.9%, t_r = 15.9 min.

Δ4,6-[D-Pro^4-D-Trp^6]-lugdunin (53). Yield: 17.0 mg (58%). ^{1}H NMR (700 MHz, DMSO-d_6): δ (ppm) 11.07 (s, 1H), 10.96 (d, J = 2.25 Hz, 1H), 8.85 (d, J = 8.41 Hz, 1H), 8.62 (d, J = 8.38 Hz, 1H), 8.60 (d, J = 8.37 Hz, 1H), 8.43 (d, J = 8.61 Hz, 1H), 8.38 (d, J = 7.00 Hz, 1H), 8.33 (d, J = 7.07 Hz, 1H), 8.06 (d, J = 9.38 Hz, 1H), 7.95 (d, J = 8.20 Hz, 1H), 7.84 (d, J = 9.21 Hz, 1H), 7.76 (d, J = 9.46 Hz, 1H), 7.71 (d, J = 9.50 Hz, 1H), 7.70−7.65 (m, 1H), 7.63 (d, J = 8.38 Hz, 1H), 7.55 (d, J = 7.94 Hz, 1H), 7.52 (d, J = 7.94 Hz, 1H), 7.51 (d, J = 7.92 Hz, 1H), 7.47 (d, J = 9.30 Hz, 1H), 7.34 (d, J = 8.01 Hz, 2H), 7.32−7.27 (m, 2H), 7.25 (d, J = 7.51 Hz, 1H), 7.17 (d, J = 7.75 Hz, 1H), 7.15 (d, J = 6.27 Hz, 1H), 7.13 (d, J = 7.33 Hz, 1H), 7.11−6.97 (m, 4H), 5.18 (s, 1H), 4.97−4.94 (m, 1H), 4.85−4.83 (m, 1H), 4.78 (d, J = 2.50 Hz, 1H), 4.74 (d, J = 2.47 Hz, 1H), 4.71 (d, J = 7.12 Hz, 1H), 4.67−4.64 (m, 1H), 4.62 (s, 1H), 4.58 (t, J = 10.00 Hz, 1H), 4.37−4.34 (m, 2H), 4.27−4.23 (m,1H), 4.12−4.05 (m, 2H), 4.07 (d, J = 8.95 Hz, 1H), 3.98 (t, J = 7.37 Hz, 1H), 3.88 (d, J = 8.17 Hz, 1H), 3.77 (d, J = 9.94 Hz, 1H), 3.74 (dd, J = 6.28, 9.47 Hz, 1H), 3.58−3.56 (m, 1H), 3.44−3.42 (m, 1H), 3.37 (s, 1H), 3.25 (s, 1H), 3.25 (d, J = 5.22 Hz, 1H), 3.19 (d, J = 6.66 Hz, 1H), 3.17 (d, J = 6.56 Hz, 1H), 3.14 (d, J = 6.25 Hz, 1H), 3.07 (d, J = 3.1 Hz, 1H), 3.05 (s, 1H), 3.03 (s, 1H), 3.01 (t, J = 3.40 Hz, 1H), 2.98 (s, 1H), 2.95 (d, J = 4.31 Hz, 1H), 2.94 (s, 1H), 2.92 (d, J = 4.58 Hz, 1H), 2.90 (d, J = 5.55 Hz, 1H), 2.88 (s, 1H), 2.61 (d, J = 5.84 Hz, 1H), 2.58 (d, J = 4.03 Hz, 1H), 2.47 (t, J = 3.90 Hz, 1H), 2.24−2.21 (m, 1H), 2.06 (d, J = 3.15 Hz, 1H), 1.98 (dd, J = 6.89, 9.69 Hz, 2H), 1.87 (dd, J = 6.07, 9.98 Hz, 1H), 1.75 (d, J = 5.32 Hz, 1H), 1.57 (d, J = 5.91 Hz, 1H), 1.55−1.47 (m, 1H), 1.24 (s, 3H), 1.16 (s, 1H), 1.08−1.05 (m, 6H), 1.03 (d, J = 7.20 Hz, 6H), 0.98−0.92 (m, 3H), 0.90−0.85 (m, 9H), 0.82 (d, J = 6.74 Hz, 3H), 0.78 (d, J = 6.77 Hz, 3H), 0.72 (s, 3H), 0.70 (d, J = 6.73 Hz, 6H), 0.66 (d, J = 6.71 Hz, 6H), 0.64 (d, J = 6.83 Hz, 3H), 0.61 (d, J = 6.89 Hz, 3H), 0.58 (d, J = 6.78 Hz, 3H). ^{13}C NMR (175 MHz, DMSO-d_6): δ (ppm) 171.9, 171.7, 171.5, 171.3, 171.2, 170.6, 170.4, 170.2, 170.1, 169.9, 164.6, 151.9, 138.7, 136.1, 136.0, 134.6, 129.5, 128.1, 127.2, 127.0, 126.4, 124.3, 123.4, 121.3, 120.9, 120.7, 118.4, 118.0, 111.4, 111.1, 109.7, 109.5, 108.9, 72.3, 72.1, 71.7, 69.8, 68.6, 65.1, 64.1, 60.3, 60.2, 59.3, 57.6, 57.4, 56.9, 55.0, 53.3, 53.0, 51.9, 50.6, 46.8, 46.4, 42.7, 42.4, 42.0, 40.4, 36.8,

32.1, 31.3, 31.2, 30.5, 30.4, 29.7, 29.5, 29.2, 29.0, 28.8, 28.4, 27.2, 23.8, 22.1, 20.3, 19.8, 19.6, 19.4, 19.0, 17.7, 15.1, 12.1. HRMS *m/z*: 854.4400 $[M + H]^+$. HPLC purity 98.4%, t_r = 16.2/16.4 min.

$\Delta^{4,6}$-[D-Met^4-D-Trp^6]-lugdunin (54). Yield: 16.8 mg (55%). ^{1}H NMR (600 MHz, DMSO-d_6): δ (ppm) 10.98−10.76 (m, 1H), 8.55 (d, J = 8.19 Hz, 1H), 8.52 (d, J = 8.56 Hz, 1H), 8.35−8.27 (m, 1H), 8.25 (d, J = 7.64 Hz, 1H), 8.22 (d, J = 9.35 Hz, 1H), 8.15 (d, J = 8.74 Hz, 1H), 7.98−7.95 (m, 1H), 7.88 (d, J = 9.41 Hz, 1H), 7.84−7.78 (m, 1H), 7.64 (d, J = 7.52 Hz, 1H), 7.61 (d, J = 9.41 Hz, 1H), 7.57−7.54 (m, 1H), 7.39−7.35 (m, 1H), 7.24 (d, J = 7.43 Hz, 1H), 7.22−7.17 (m, 1H), 7.15−6.98 (m, 2H), 5.18 (s, 1H), 4.97 (d, J = 8.05 Hz, 1H), 4.79−4.75 (m, 1H), 4.67 (d, J = 5.93, 9.17 Hz, 1H), 4.67 (d, J = 5.51 Hz, 1H), 4.58−4.49 (m, 1H), 4.47 (s, 1H), 4.37 (dd, J = 6.86, 9.36 Hz, 1H), 4.27−4.25 (m, 1H), 4.17 (d, J = 5.66 Hz, 1H), 4.15 (d, J = 9.30 Hz, 1H), 4.08−4.02 (m, 1H), 3.87−3.75 (m, 1H), 3.72 (s, 1H), 3.68 (t, J = 4.86 Hz, 1H), 3.45 (t, J = 5.33 Hz, 1H), 3.45−3.41 (m, 1H), 3.38 (s, 1H), 3.28−3.16 (m, 1H), 3.15 (d, J = 6.03 Hz, 1H), 3.12−3.08 (m, 1H), 2.95−2.92 (m, 1H), 2.91 (s, 1H), 2.90−2.88 (m, 1H), 2.85 (s, 1H), 2.82 (s, 1H), 2.75 (d, J = 4.96 Hz, 1H), 2.72 (s, 1H), 2.65−2.62 (m, 1H), 2.55 (s, 1H), 2.53 (s, 1H), 2.44 (s, 1H), 2.40 (d, J = 4.34 Hz, 1H), 2.29 (d, J = 5.29 Hz, 1H), 2.23 (s, 1H), 2.21 (d, J = 4.13 Hz, 1H), 2.20 (d, J = 4.84 Hz, 1H), 2.17 (s, 1H), 2.12 (d, J = 3.16 Hz, 1H), 2.06 (d, J = 4.97 Hz, 1H), 1.88−1.76 (m, 1H), 1.73−1.68 (m, 1H), 1.62 (d, J = 5.17 Hz, 1H), 1.55 (d, J = 4.50 Hz, 1H), 1.51−1.47 (m, 1H), 1.42 (d, J = 4.91 Hz, 1H), 1.40−1.29 (m, 2H), 1.08 (s, 2H), 1.05 (d, J = 7.04 Hz, 3H), 0.97−0.89 (m, 12H), 0.86 (d, J = 6.11 Hz, 3H), 0.82 (s, 3H), 0.78 (d, J = 6.61 Hz, 3H), 0.74 (d, J = 6.62 Hz, 3H), 0.65 (d, J = 6.68 Hz, 3H), 0.62 (d, J = 6.47 Hz, 3H), 0.59 (d, J = 6.73 Hz, 3H), 0.55 (d, J = 6.79 Hz, 3H). ^{13}C NMR (150 MHz, DMSO-d_6): δ (ppm) 172.1, 171.5, 171.3, 171.1, 170.7, 170.6, 170.1, 169.9, 166.9, 136.1, 136.1, 136.0, 131.7, 131.5, 128.6, 127.2, 127.2, 127.1, 126.9, 124.0, 123.7, 120.7, 120.6, 118.7, 118.5, 118.1, 117.9, 111.2, 111.1, 110.1, 109.8, 109.6, 109.5, 72.3, 72.1, 71.9, 69.5, 68.8, 68.5, 67.8, 65.2, 63.8, 60.3, 60.2, 57.4, 57.3, 57.1, 56.7, 55.2, 54.5, 53.7, 53.4, 52.8, 51.7, 37.5, 36.4, 33.0, 32.5, 31.8, 30.6, 29.3, 28.7, 25.7, 22.0, 20.3, 19.5, 19.3, 19.1, 18.7, 18.5, 18.2, 17.8, 15.2, 15.1, 14.6, 14.3, 14.1, 13.8, 12.0. HRMS *m/z*: 888.4259 $[M + H]^+$. HPLC purity 94.8%, t_r = 16.3/16.8 min.

$\Delta^{4,6}$-[D-Phe^4-D-Trp^6]-lugdunin (55). Yield: 19.5 mg (63%). ^{1}H NMR (600 MHz, DMSO-d_6): δ (ppm) 10.87 (d, J = 2.47 Hz, 1H), 10.85 (d, J = 2.43 Hz, 1H), 10.84 (d, J = 2.37 Hz, 1H), 10.79 (d, J = 2.38 Hz, 1H), 8.56 (t, J = 7.59 Hz, 2H), 8.38 (d, J = 7.53 Hz, 1H), 8.26 (d, J = 8.72 Hz, 1H), 8.24 (d, J = 9.59 Hz, 1H), 8.16 (d, J = 8.69 Hz, 1H), 8.13 (t, J = 9.61 Hz, 2H), 7.99 (t, J = 8.99 Hz, 2H), 7.78−7.67 (m, 3H), 7.59−7.57 (m, 1H), 7.39 (d, J = 7.93 Hz, 1H), 7.37−7.35 (m, 3H), 7.39 (d, J = 7.08 Hz, 1H), 7.27 (d, J = 7.30 Hz, 1H), 7.24 (q, J = 7.58 Hz, 3H), 7.18 (d, J = 7.13 Hz, 2H), 7.15 (s, 1H), 7.14 (d, J = 7.40 Hz, 1H), 7.13 (d, J = 7.45 Hz, 1H), 7.12 (d, J = 7.09 Hz, 1H), 7.06 (d, J = 7.00 Hz, 2H), 7.05 (d, J = 7.08 Hz, 1H), 7.04−7.02 (m, 1H), 7.01 (d, J = 7.87 Hz, 1H), 7.00 (d, J = 7.04 Hz, 1H), 6.98 (d, J = 7.02 Hz, 1H), 6.96 (d, J = 7.00 Hz, 1H), 4.99 (d, J = 6.30 Hz, 1H), 4.88−4.77 (m, 2H), 4.76 (s, 1H), 4.75−4.68 (m, 1H), 4.65 (s, 1H), 4.64 (d, J = 1.70 Hz, 1H), 4.62 (d, J = 4.68 Hz, 1H), 4.61−4.58 (m, 1H), 4.37−4.35 (m, 1H), 4.28 (d, J = 9.47 Hz, 1H), 4.24 (s, 1H), 4.15−4.13 (m, 1H), 4.12−4.06 (m, 1H), 3.94 (d, J = 7.36 Hz, 1H), 3.87−3.77 (m, 2H), 3.76 (dd, J = 2.47, 9.39 Hz, 1H), 3.45 (d, J = 5.40 Hz, 1H), 3.44−3.43 (m, 1H), 3.26 (d, J = 4.71 Hz, 1H), 3.24−3.23 (m, 1H), 3.24 (s, 1H), 3.15 (d, J = 3.27 Hz, 1H), 3.13 (s, 1H), 3.12 (d, J = 6.03 Hz, 1H), 3.11 (d, J = 5.93 Hz, 1H), 2.96 (d, J = 2.67 Hz, 1H), 2.95−2.93 (m, 1H), 2.92−2.90 (m, 1H), 2.88 (d, J = 3.78 Hz, 2H), 2.86 (d, J = 8.75 Hz, 1H), 2.75−2.74 (m, 1H), 2.68 (s, 1H), 2.65−2.63 (m, 3H), 2.62−2.55 (m, 1H), 2.53 (d, J = 3.23 Hz, 1H), 2.49−2.46 (m, 1H), 2.14 (s, 1H), 2.12 (s, 1H), 2.09 (d, J = 7.13, Hz, 1H), 1.88 (d, J = 6.86 Hz, 1H), 1.85−1.68 (m, 3H), 1.65 (d, J = 3.16 Hz, 1H), 1.64−1.57 (m, 1H), 1.55 (d, J = 6.60 Hz, 1H), 1.45−1.43 (m, 1H), 1.37−1.34 (m, 1H), 1.28 (s, 3H), 1.25 (s, 1H), 1.04 (d, J = 7.04 Hz, 6H), 0.87 (d, J = 6.68 Hz, 6H), 0.79 (d, J = 6.56 Hz, 3H), 0.67−0.58 (m, 12H), 0.55 (d, J = 6.70 Hz, 3H), 0.52 (d, J = 6.76 Hz, 6H), 0.47 (d, J = 6.66 Hz, 3H). ^{13}C NMR (150 MHz, DMSO-d_6): δ (ppm) 172.2, 171.4, 171.2, 171.0, 170.8, 170.7, 170.5, 170.3, 170.2, 170.1, 170.0, 169.8, 164.6, 137.9, 137.6, 136.1, 136.0, 129.6, 129.2, 128.1, 127.7, 127.3, 127.2, 127.1, 127.0, 126.1, 126.0, 124.3, 124.1, 123.7, 123.6, 120.8, 120.7, 120.6, 118.7, 118.1, 118.0, 117.9, 111.2, 111.0, 111.0, 110.2, 109.8, 109.7, 72.3, 72.3, 72.0, 66.9, 65.3, 63.6, 60.4, 60.3, 60.2, 57.3, 57.2, 57.2, 56.6, 55.4, 54.6, 53.7, 53.5, 53.0, 52.7, 52.7, 40.4, 34.7, 32.6, 31.3, 31.1, 30.7, 30.0, 29.9, 29.0, 28.8, 28.7, 27.6, 27.3, 26.7, 22.1, 20.4, 19.6, 19.3, 19.0, 18.9, 18.7, 18.6, 18.2, 17.9, 17.7, 15.0, 14.0, 13.9, 12.1. HRMS *m/z*: 904.4514 $[M + H]^+$. HPLC purity 98.4%, t_r = 16.4/16.9 min.

$\Delta^{4,6}$-[D-Trp^4-D-Trp^6]-lugdunin (56). Yield: 16.4 mg (50%). ^{1}H NMR (600 MHz, DMSO-d_6): δ (ppm) 10.87 (d, J = 2.64 Hz, 1H), 10.83 (d, J =2.25 Hz, 1H), 10.72 (d, J = 2.36 Hz, 1H), 8.64−8.58 (m, 2H), 8.56 (d, J = 8.45 Hz, 1H), 8.48 (d, J = 7.33 Hz, 1H), 8.29 (d, J = 8.98 Hz, 1H), 8.17 (d, J = 8.70 Hz, 1H), 8.16−8.05 (m, 1H), 7.98 (d, J = 7.49 Hz, 1H), 7.76 (d, J = 7.96 Hz, 1H), 7.75−7.64 (m, 3H), 7.57−7.55 (m, 2H), 7.46−7.29 (m, 2H), 7.17 (dd, J = 2.31, 5.44 Hz, 1H), 7.15 (d, J = 2.35 Hz, 1H), 7.04 (d, J = 9.61 Hz, 3H), 7.02−6.95 (m, 2H), 4.97 (dd, J = 6.22, 8.51 Hz, 1H), 4.75 (d, J = 2.40 Hz, 1H), 4.74 (d, J = 2.43 Hz, 1H), 4.73−4.71 (m, 1H), 4.63 (d, J = 7.22 Hz, 1H), 4.60 (s, 1H), 4.69−4.65 (m, 1H), 4.65−4.57 (m, 1H), 4.47−4.39 (m, 1H), 4.28−4.25 (m, 1H), 4.16−4.13 (m, 1H), 4.12−4.06 (m, 1H), 4.04 (d, J = 5.85 Hz, 1H), 3.84−3.77 (m, 2H), 3.75 (d, J = 2.25 Hz, 1H), 3.54 (s, 1H), 3.47 (d, J = 4.91 Hz, 1H), 3.44−3.42 (m, 1H), 3.36 (s, 1H), 3.34 (d, J = 4.22 Hz, 1H), 3.24−3.16 (m, 1H), 3.13 (d, J = 6.14 Hz, 1H), 3.05 (d, J = 7.84 Hz, 1H), 3.06−2.96 (m, 2H), 2.94 (d, J = 4.50 Hz, 1H), 2.92 (s, 1H), 2.90 (d, J = 2.94 Hz, 1H), 2.90−2.87 (m, 1H), 2.85 (d, J = 5.36 Hz, 1H), 2.77−2.74 (m, 1H), 2.73 (s, 1H), 2.69 (s, 1H), 2.66 (s, 1H), 2.65−2.58 (m, 3H), 2.46−2.39 (m, 1H), 2.17 (s, 1H), 2.08−2.05 (m, 1H), 1.99−1.87 (m, 1H), 1.88−1.66 (m, 3H), 1.65 (s, 1H), 1.64−1.58 (m, 1H), 1.56 (dd, J = 3.75, 6.83 Hz, 1H), 1.48−1.45 (m, 1H), 1.38−1.35 (m, 1H), 1.18 (d, J = 2.36 Hz, 1H), 1.06 (d, J = 6.95 Hz, 12H), 0.99−0.96 (m, 3H), 0.95−0.88 (m, 6H), 0.77 (d, J = 6.62 Hz, 3H), 0.65 (d, J = 6.72 Hz, 3H), 0.64−0.58 (m, 12H), 0.56 (d, J = 6.80 Hz, 3H), 0.45 (d, J = 6.72 Hz, 3H). ^{13}C NMR (150 MHz, DMSO-d_6): δ (ppm) 172.2, 171.6, 171.3, 171.2, 171.0, 171.0, 170.7, 170.6, 170.5, 170.1, 170.0, 169.7, 164.6, 136.1, 136.0, 135.9, 127.4, 127.3, 127.2, 127.1, 126.9, 124.3, 124.1, 123.8, 123.7, 120.8, 120.7, 120.7, 120.6, 118.9, 118.7, 118.1, 118.1, 118.0, 118.0, 111.3, 111.2, 111.1, 111.0, 111.0, 110.2, 110.1, 109.8, 109.7, 109.6, 72.3, 72.3, 72.0, 65.4, 63.7, 60.5, 60.3, 60.2, 57.4, 57.2, 56.6, 54.8, 54.5, 54.0, 53.3, 53.1, 52.8, 52.6, 42.7, 37.6, 34.7, 32.6, 31.3, 31.1, 30.7, 30.0, 29.9, 29.8, 29.0, 28.7, 28.6, 28.2, 27.7, 27.0, 26.6, 26.6, 25.1, 22.1, 20.4, 19.6, 19.6, 19.4, 19.0, 18.8, 18.7, 18.6, 18.3, 18.1, 17.6, 15.0, 14.0, 13.9, 12.1. HRMS *m/z*: 943.4515 $[M + H]^+$. HPLC purity 96.2%, t_r = 16.2 min.

$\Delta^{4,6}$-[ACPC^4-D-Trp^6]-lugdunin (57). Yield: 20.7 mg (72%). ^{1}H NMR (600 MHz, DMSO-d_6): δ (ppm) 11.07 (s, 1H), 10.97 (d, J = 2.38 Hz, 1H), 10.96−10.88 (m, 1H), 10.84−10.81 (m, 1H), 8.94 (s, 1H), 8.85 (d, J = 8.45 Hz, 1H), 8.67 (d, J = 7.38 Hz, 1H), 8.65 (d, J = 7.39 Hz, 1H), 8.63 (s, 1H), 8.60 (d, J = 7.41 Hz, 1H), 8.48 (s, 1H), 8.25 (d, J = 6.60 Hz, 1H), 7.87 (d, J = 9.43 Hz, 1H), 7.66 (d, J = 7.13 Hz, 1H), 7.58−7.54 (m, 1H), 7.47−7.39 (m, 1H), 7.27 (d, J = 7.50 Hz, 2H), 7.24 (d, J = 7.44 Hz, 2H), 7.17 (d, J = 2.49 Hz, 1H), 7.15 (s, 1H), 7.14 (s, 1H), 7.12 (d, J = 7.40 Hz, 1H), 7.07 (d, J = 7.20 Hz, 1H), 7.05−7.02 (m, 1H), 7.01−6.98 (m, 2H), 4.86 (d, J = 2.30 Hz, 1H), 4.75 (d, J = 2.31 Hz, 1H), 4.67 (d, J = 5.76 Hz, 1H), 4.68 (t, J = 5.49 Hz, 1H), 4.59−4.48 (m, 2H), 4.46−4.43 (m, 1H), 4.27−4.17 (m, 2H), 4.13−3.96 (m, 1H), 3.93−3.8 (m, 1H), 3.88−3.75 (m, 1H), 3.73 (d, J = 4.06 Hz, 1H), 3.46−3.43 (m, 1H), 3.42−3.40 (m, 1H), 3.29 (d, J = 4.55 Hz, 1H), 3.27−3.25 (m, 3H), 3.24−3.23 (m, 1H), 3.22 (d, J = 7.11 Hz, 1H), 3.19 (d, J = 6.78 Hz, 1H), 3.17−3.15 (m, 2H), 3.07−3.05 (m, 2H), 2.99−2.86 (m, 1H), 2.84−2.77 (m, 1H), 2.75 (t, J = 6.30 Hz, 1H), 2.46 (t, J = 9.79 Hz, 1H), 2.14−2.08 (m, 1H), 1.95−1.87 (m, 1H), 1.85 (d, J = 7.10 Hz, 1H), 1.27−1.14 (m, 1H), 1.13−1.12 (m, 2H), 1.10−1.06 (m, 9H), 1.04−1.02 (m, 9H), 1.00 (d, J = 6.72 Hz, 6H), 0.98 (d, J = 6.72 Hz, 3H), 0.86−0.67 (m, 12H), 0.58 (d, J = 6.80 Hz, 3H). ^{13}C NMR (150 MHz, DMSO-d_6): δ (ppm) 172.9, 172.3, 172.3, 171.9, 171.6, 171.6, 171.3, 170.9, 170.9, 151.8, 136.1, 136.0, 136.0, 135.9, 129.4, 127.3, 127.1, 127.0, 127.0, 123.9, 123.6, 121.3, 120.8, 120.7, 120.6, 118.5, 118.4, 118.1, 118.1,

https://doi.org/10.1021/acs.jmedchem.0c02170
J. Med. Chem. 2021, 64, 4034−4058

118.0, 111.2, 111.1, 110.0, 109.8, 109.7, 76.3, 76.3, 74.5, 72.1, 71.6, 70.8, 69.7, 68.5, 66.9, 66.5, 65.3, 65.2, 64.9, 64.7, 59.6, 59.4, 58.4, 57.7, 56.1, 55.0, 54.7, 53.6, 53.2, 39.9, 39.8, 39.7, 39.5, 39.4, 39.2, 39.1, 38.2, 36.9, 34.0, 34.0, 32.2, 32.0, 31.3, 31.1, 29.6, 28.6, 27.8, 26.5, 26.4, 26.4, 26.2, 25.8, 20.3, 19.8, 19.6, 19.5, 19.1, 18.6, 18.4, 17.8, 17.2, 16.9, 16.6, 16.3, 15.7, 12.0. HRMS m/z: 840.4475 $[M + H]^+$. HPLC purity 96.9%, t_r = 15.8/16.8 min.

$\Delta^{2,3,6}$-[D-*allo*-Ile^2-L-Ala-3-(9-Anth)^3-D-Trp^6]-lugdunin (58). Yield: 23.2 mg (71%). ^{1}H NMR (600 MHz, DMSO-d_6): δ (ppm) 10.76 (s, 1H), 10.73 (d, J = 2.43 Hz, 1H), 8.73 (d, J = 8.96 Hz, 1H), 8.54 (d, J = 9.01 Hz, 1H), 8.50 (s, 2H), 8.45 (d, J = 8.88 Hz, 1H), 8.39 (d, J = 5.81 Hz, 1H), 8.26 (d, J = 8.44 Hz, 1H), 8.19 (d, J = 7.81 Hz, 1H), 8.13 (d, J = 9.41 Hz, 1H), 8.11–8.01 (m, 2H), 7.97 (t, J = 8.81 Hz, 1H), 7.86 (d, J = 8.81 Hz, 1H), 7.79 (d, J = 9.32 Hz, 1H), 7.67 (d, J = 7.96 Hz, 1H), 7.64 (t, J = 8.53 Hz, 1H), 7.61–7.44 (m, 1H), 7.33–7.25 (m, 2H), 7.23 (d, J = 2.37 Hz, 1H), 7.13 (d, J = 2.35 Hz, 1H), 7.07–6.99 (m, 2H), 6.97–6.89 (m, 1H), 4.94 (d, J = 7.84 Hz, 1H), 4.82 (d, J = 9.14 Hz, 1H), 4.78 (d, J = 3.94 Hz, 1H), 4.76 (d, J = 4.18 Hz, 1H), 4.71 (d, J = 2.55 Hz, 1H), 4.70–4.66 (m, 1H), 4.66 (s, 1H), 4.64–4.58 (m, 1H), 4.54 (t, J = 5.46 Hz, 1H), 4.51–4.45 (m, 1H), 4.43 (s, 1H), 4.41–4.40 (m, 1H), 4.32–4.25 (m, 1H), 4.24–4.21 (m, 1H), 4.21 (s, 1H), 4.19 (d, J = 3.36 Hz, 1H), 4.17 (d, J = 2.96 Hz, 1H), 4.15 (s, 1H), 4.08 (d, J = 5.12 Hz, 1H), 4.06 (d, J = 2.33 Hz, 1H), 4.04 (d, J = 9.26 Hz, 1H), 3.98–3.94 (m, 1H), 3.93 (d, J = 6.97 Hz, 1H), 3.83 (s, 1H), 3.81–3.77 (m, 1H), 3.76 (s, 1H), 3.75–3.72 (m, 1H), 3.71–3.69 (m, 1H), 3.68–3.62 (m, 2H), 3.60 (d, J = 6.09 Hz, 1H), 3.59 (s, 1H), 3.45 (s, 1H), 3.42 (t, J = 5.29 Hz, 1H), 3.41–3.36 (m, 1H), 3.26–3.24 (m, 1H), 3.23–3.20 (m, 1H), 3.17 (d, J = 4.99 Hz, 1H), 3.08 (d, J = 5.65 Hz, 2H), 3.02–2.83 (m, 1H), 2.69 (s, 1H), 2.61 (d, J = 3.69 Hz, 1H), 2.41–2.35 (m, 1H), 2.09–2.04 (m, 1H), 2.04 (s, 1H), 2.03–1.99 (m, 1H), 1.98 (s, 1H), 1.96–1.90 (m, 1H), 1.45 (d, J = 7.57 Hz, 2H), 1.33–1.28 (m, 1H), 1.26 (d, J = 6.66 Hz, 1H), 1.24 (d, J = 6.89 Hz, 1H), 1.20 (t, J = 7.37 Hz, 1H), 1.17 (s, 1H), 1.09–1.06 (m, 2H), 1.05 (s, 9H), 1.04–1.03 (m, 12H), 1.03 (s, 3H), 1.03 (s, 3H), 1.02 (s, 6H), 1.01 (s, 3H), 0.85 (d, J = 6.72 Hz, 3H), 0.74 (d, J = 6.62 Hz, 3H), 0.69 (s, 3H), 0.67–0.61 (m, 3H), 0.59 (d, J = 6.83 Hz, 3H), 0.55 (d, J = 6.05 Hz, 3H), 0.53 (d, J = 6.80 Hz, 3H), 0.47 (d, J = 6.75 Hz, 3H). ^{13}C NMR (150 MHz, DMSO-d_6): δ (ppm) 172.1, 171.6, 171.5, 171.1, 171.1, 170.7, 170.7, 170.2, 170.0, 169.9, 169.8, 169.8, 167.7, 157.9, 157.1, 136.0, 131.0, 130.3, 130.2, 129.8, 129.2, 128.8, 128.8, 127.2, 127.2, 126.4, 125.7, 124.9, 124.8, 124.0, 123.8, 120.6, 117.9, 111.0, 109.8, 109.7, 105.1, 98.9, 76.3, 76.3, 74.6, 74.5, 74.5, 72.3, 72.1, 69.5, 68.8, 67.3, 67.2, 66.9, 65.3, 65.2, 64.7, 63.8, 63.8, 62.6, 60.2, 59.8, 57.5, 57.2, 56.7, 55.9, 55.2, 54.7, 54.5, 53.7, 53.5, 52.8, 52.2, 50.9, 48.5, 38.2, 37.9, 37.6, 36.8, 34.7, 32.5, 30.7, 29.6, 29.5, 27.2, 25.1, 24.0, 23.8, 22.8, 22.5, 22.1, 22.0, 20.4, 20.2, 19.6, 19.5, 19.1, 19.0, 18.4, 17.8, 17.6, 17.3, 17.2, 17.2, 16.9, 15.2, 15.0, 14.2, 11.2. HRMS m/z: 945.5043 $[M + H]^+$. HPLC purity 98.5%, t_r = 19.1/19.6 min.

$\Delta^{3,4,5,6}$-[L-Val^3-D-Val^4-L-Leu^5-D-Trp^6]-lugdunin (59). Yield: 19.8 mg (73%). ^{1}H NMR (700 MHz, DMSO-d_6): δ (ppm) 10.77 (d, J = 2.21 Hz, 1H), 8.36 (d, J = 6.00 Hz, 1H), 8.28 (d, J = 7.76 Hz, 1H), 8.18 (d, J = 9.40 Hz, 1H), 8.12 (d, J = 8.62 Hz, 1H), 8.05 (d, J = 8.93 Hz, 1H), 7.99 (d, J = 8.71 Hz, 1H), 7.94 (d, J = 8.56 Hz, 1H), 7.86 (d, J = 9.63 Hz, 1H), 7.84 (d, J = 9.78 Hz, 1H), 7.70–7.67 (m, 1H), 7.65 (d, J = 7.90 Hz, 1H), 7.60 (d, J = 9.49 Hz, 1H), 7.51 (d, J = 8.12 Hz, 1H), 7.28 (d, J = 8.16 Hz, 1H), 7.23 (d, J = 7.37 Hz, 1H), 7.12 (d, J = 7.40 Hz, 1H), 7.05–7.03 (m, 1H), 7.03–7.01 (m, 1H), 6.95 (d, J = 7.88 Hz, 1H), 4.77 (d, J = 5.03 Hz, 1H), 4.74 (d, J = 2.67 Hz, 1H), 4.72 (d, J = 2.68 Hz, 1H), 4.63 (d, J = 8.97 Hz, 1H), 4.60–4.54 (m, 1H), 4.50–4.46 (m, 1H), 4.46 (d, J = 1.33 Hz, 1H), 4.45 (s, 1H), 4.36–4.33 (m, 1H), 4.32 (s, 1H), 4.30 (s, 1H), 4.26 (dd, J = 5.24, 8.18 Hz, 1H), 4.22 (dd, J = 7.11 Hz, 1H), 4.16 (s, 1H), 4.06 (d, J = 9.34 Hz, 1H), 4.04–4.03 (m, 1H), 4.02 (d, J = 4.62 Hz, 1H), 3.99 (d, J = 7.34 Hz, 1H), 3.78–3.74 (m, 1H), 3.73 (d, J = 4.52 Hz, 1H), 3.73–3.70 (m, 1H), 3.69 (s, 1H), 3.61 (d, J = 3.95 Hz, 1H), 3.45 (t, J = 5.99 Hz, 1H), 3.41 (d, J = 4.55 Hz, 1H), 3.19–3.16 (m, 1H), 3.12 (s, 1H), 3.11–3.09 (m, 1H), 3.08 (s, 1H), 3.08–3.06 (m, 1H), 3.06–3.04 (m, 1H), 3.00–2.94 (m, 1H), 2.90 (s, 1H), 2.89 (d, J = 5.22 Hz, 1H), 2.87 (d, J = 4.30 Hz, 1H), 2.86 (d, J = 4.71 Hz, 1H), 2.84 (s, 1H), 2.82 (s, 1H), 2.81 (s, 1H), 2.65 (d, J = 7.87 Hz, 1H), 2.58 (t, J = 9.71 Hz, 1H), 2.52–2.51 (m, 1H), 2.49 (s, 1H), 2.47 (s, 1H), 2.41–2.39 (m, 1H), 2.13 (d, J = 4.45 Hz, 1H), 2.06 (d, J = 8.87 Hz, 1H), 2.04 (d, J = 6.60 Hz, 1H), 2.01 (s, 1H), 1.99 (d, J = 3.47 Hz, 1H), 1.98 (d, J = 2.58 Hz, 1H), 1.97 (d, J = 2.57 Hz, 1H), 1.96 (d, J = 2.59 Hz, 1H), 1.95 (d, J = 2.86 Hz, 1H), 1.94–1.89 (m, 1H), 1.89 (d, J = 3.94 Hz, 1H), 1.88 (d, J = 2.18 Hz, 1H), 1.87–1.86 (m, 2H), 1.86 (s, 1H), 1.85 (d, J = 1.93 Hz, 1H), 1.84 (d, J = 2.15 Hz, 1H), 1.83 (d, J = 2.39 Hz, 1H), 1.82 (s, 1H), 1.51 (d, J = 6.62 Hz, 1H), 1.33–1.27 (m, 1H), 1.23 (d, J = 4.20 Hz, 1H), 1.21–1.16 (m, 1H), 1.15–1.12 (m, 1H), 1.09–1.04 (m, 6H), 1.04–0.99 (m, 9H), 0.96 (d, J = 6.68 Hz, 3H), 0.91 (d, J = 6.74 Hz, 3H), 0.88 (d, J = 6.53 Hz, 3H), 0.87 (d, J = 6.65 Hz, 3H), 0.85 (d, J = 6.79 Hz, 3H), 0.84 (s, 3H), 0.83 (s, 3H), 0.81 (s, 3H), 0.78 (d, J = 6.72 Hz, 3H), 0.76–0.74 (m, 3H), 0.73 (d, J = 7.57 Hz, 3H), 0.72 (d, J = 6.74 Hz, 3H), 0.71–0.69 (m, 3H), 0.68 (d, J = 6.96 Hz, 3H). ^{13}C NMR (175 MHz, DMSO-d_6): δ (ppm) 172.0, 171.8, 171.6, 171.5, 170.8, 170.6, 170.4, 170.2, 170.1, 170.0, 170.0, 136.0, 135.9, 127.3, 127.3, 124.1, 123.8, 120.6, 118.7, 118.6, 118.0, 117.9, 111.0, 109.8, 109.7, 72.3, 72.0, 66.9, 65.2, 63.7, 59.5, 59.1, 57.6, 57.4, 57.3, 57.3, 57.0, 54.5, 53.7, 53.1, 50.1, 41.2, 40.9, 40.4, 40.0, 37.9, 37.3, 32.6, 31.3, 30.7, 30.6, 29.8, 29.5, 29.3, 29.1, 27.1, 24.0, 23.9, 22.8, 22.8, 21.8, 21.6, 20.5, 19.6, 19.5, 19.3, 19.2, 19.1, 19.0, 19.0, 19.0, 18.9, 18.4, 18.2, 18.1, 17.8, 17.0, 15.2. HRMS m/z: 783.4583 $[M + H]^+$. HPLC purity 96.5%, t_r = 16.7/17.4 min.

Minimum Inhibitory Concentration (MIC) Assay. Antibacterial activities and MIC values of **4** and its analogues (**10**–**59**) were determined using a serial dilution method as previously described.[10] Therefore, a twofold serial dilution in microtiter plates (stock solution: 10 mg mL^{-1}) with various concentrations of lugdunin and its analogues in Mueller Hinton broth (MHB) was prepared. The microtiter plates were inoculated with *S. aureus* USA300 LAC from an overnight culture to a final density of 1×10^6 colony forming units (cfu) per mL. The inoculated microtiter plates were incubated at 37 °C for 21 h under continuous shaking at 160 rpm. The OD_{600} of each well was measured with a microtiter plate reader. The MIC value was defined as the lowest concentration where $OD_{600} < 0.1$ (a.u.). The tested MIC range was between 0.195 and 100 μg mL^{-1}. Growth control was 100% dimethyl sulfoxide (DMSO) in a culture without any additives. Positive controls were vancomycin (10 mg mL^{-1} in MilliQ-H_2O, MIC: 0.78 μg mL^{-1}), daptomycin (10 mg mL^{-1} in DMSO, MIC: 3.13–6.25 μg mL^{-1}; note: the used MHB nutrition medium was not calcium-adjusted with $CaCl_2$), and natural isolated lugdunin (10 mg mL^{-1} in DMSO, MIC: 3.13 μg mL^{-1}).

■ ASSOCIATED CONTENT

Supporting Information

The Supporting Information is available free of charge at https://pubs.acs.org/doi/10.1021/acs.jmedchem.0c02170.

Synthesis protocol, MS and MS/MS data, NMR spectra, extended biological data, supporting figures (PDF)

Molecular formula strings "SMILES" and antimicrobial data (CSV)

■ AUTHOR INFORMATION

Corresponding Author

Stephanie Grond − *Institute of Organic Chemistry and Cluster of Excellence EXC 2124 Controlling Microbes to Fight Infections, Eberhard Karls University Tuebingen, 72076 Tuebingen, Germany*; Phone: +49 (0)7071 29−72060; Email: Stephanie.grond@uni-tuebingen.de

Authors

Julian S. Saur − *Institute of Organic Chemistry, Eberhard Karls University Tuebingen, 72076 Tuebingen, Germany*

Sebastian N. Wirtz − *Institute of Organic Chemistry, Eberhard Karls University Tuebingen, 72076 Tuebingen, Germany*; orcid.org/0000-0002-8233-202X

https://doi.org/10.1021/acs.jmedchem.0c02170
J. Med. Chem. 2021, 64, 4034−4058

Nadine A. Schilling – *Institute of Organic Chemistry, Eberhard Karls University Tuebingen, 72076 Tuebingen, Germany*

Bernhard Krismer – *Interfaculty Institute of Microbiology and Infection Medicine, German Center for Infection Research (DZIF) and German Center for Infection Research (DZIF), Eberhard Karls University Tuebingen, 72076 Tuebingen, Germany; Cluster of Excellence EXC 2124 Controlling Microbes to Fight Infections, Eberhard Karls University Tuebingen, 72076 Tuebingen, Germany*

Andreas Peschel – *Interfaculty Institute of Microbiology and Infection Medicine, German Center for Infection Research (DZIF) and German Center for Infection Research (DZIF), Eberhard Karls University Tuebingen, 72076 Tuebingen, Germany; Cluster of Excellence EXC 2124 Controlling Microbes to Fight Infections, Eberhard Karls University Tuebingen, 72076 Tuebingen, Germany*

Complete contact information is available at: https://pubs.acs.org/10.1021/acs.jmedchem.0c02170

Author Contributions

J.S.S. designed the synthesis, planned and prepared the majority of the analogues, and wrote the manuscript. S.N.W. designed and synthesized the selected analogues and performed HPLC analytics. N.A.S. designed and synthesized the selected analogues. B.K. performed all antimicrobial experiments. A.P., B.K., and S.G. planned and supervised the project, provided critical input to the manuscript, and organized the financial support.

Notes

The authors declare the following competing financial interest(s): Eberhard Karls University Tuebingen holds a patent (EP3072899B1) covering the compound lugdunin, derivatives thereof, and the bacterial infection prevention by lugdunin producing bacteria. The patent has also been filed in the USA (US2018/0155397A1). Eberhard Karls University Tuebingen has also filed a provisional patent application that covers the described synthesis of lugdunin and derivatives thereof.

■ ACKNOWLEDGMENTS

The work of J.S.S. was supported by the state of Baden-Wuerttemberg (Promotionskolleg IPMB Reutlingen-Tuebingen) and the work of N.A.S. by the Institutional Strategy of the University of Tuebingen (DFG, ZUK63). This work was supported by grants from the German Center for Infection Research (DZIF) to B.K. and A.P. and the Deutsche Forschungsgemeinschaft (Cluster of Excellence EXC 2124 Controlling Microbes to Fight Infections, project ID 390838134 to B.K., A.P., and S.G. The authors thank M. C. Konnerth for valuable discussion, P. Rath for NMR measurements, J. M. Beltran for technical support, and P.-M. Geißler for synthetic work.

■ ABBREVIATIONS USED

Ac_2O, acetic anhydride; ACPC, 1-aminocyclopropane-1-carboxylic acid; AllylGly, allylglycine; Anth, anthracenyl; Bip, biphenylalanine; CDI, 1,1′-carbonyldiimidazole; DBU, 2,3,4,6,7,8,9,10-octahydropyrimido[1,2-*a*]azepine; Dip, diphenylalanine; DIPEA, *N*-ethyl-*N*-(propan-2-yl)propan-2-amine; DMP, Dess–Martin periodinane; HATU, 1-[bis(dimethylamino)methylene]-1*H*-1,2,3-triazolo[4,5-*b*]pyridinium 3-oxide hexafluorophosphate; HOAt, 3-hydroxytriazolo[4,5-*b*]pyridine; HOBt, benzotriazol-1-ol; MHMPA, 3-methoxy-4-(hydroxymethyl) phenoxyacetic acid; MIC, minimum inhibitory concentration; MOA, mechanism of action; *n*-BuOH, *n*-butanol; NMM, 4-methylmorpholine; Nva, norvaline; pBPA, 4-benzoyl-phenylalanine; Phg, phenylglycine; Pra, propargylglycine; PyBOP, (benzotriazol-1-yloxy)-tripyrrolidinophosphonium hexafluorophosphate; Pyr, pyridine; SPPS, solid-phase peptide synthesis; TFA, trifluoroacetic acid; Thz, thiazolidine; Tic, 1,2,3,4-tetrahydroisoquinoline-3-carboxylic acid; TIPS, triisopropylsilane; Tle, *tert*-leucine

■ REFERENCES

(1) Blaskovich, M. A. T. Unusual Amino Acids in Medicinal Chemistry. *J. Med. Chem.* **2016**, *59*, 10807–10836.

(2) Bojsen, R.; Torbensen, R.; Larsen, C. E.; Folkesson, A.; Regenberg, B. The synthetic amphipathic peptidomimetic LTX109 is a potent fungicide that disturbs plasma membrane integrity in a sphingolipid dependent manner. *PLoS One* **2013**, *8*, No. e69483.

(3) Abe, Y.; Kayakiri, H.; Satoh, S.; Inoue, T.; Sawada, Y.; Inamura, N.; Asano, M.; Aramori, I.; Hatori, C.; Sawai, H.; Oku, T.; Tanaka, H. A novel class of orally active non-peptide bradykinin B_2 receptor antagonists. 3. Discovering Bioisosteres of the Imidazo[1,2-a]pyridine Moiety. *J. Med. Chem.* **1998**, *41*, 4062.

(4) Okada, Y.; Takasawa, R.; Kubo, D.; Iwanaga, N.; Fujita, S.; Suzuki, K.; Suzuki, H.; Kamiya, H.; Chiba, K. Improved tag-assisted liquid-phase peptide synthesis: application to the synthesis of the bradykinin receptor antagonist Icatibant acetate. *Org. Process Res. Dev.* **2019**, *23*, 2576–2581.

(5) Zong, Y.; Fang, F.; Meyer, K. J.; Wang, L.; Ni, Z.; Gao, H.; Lewis, K.; Zhang, J.; Rao, Y. Gram-scale total synthesis of teixobactin promoting binding mode study and discovery of more potent antibiotics. *Nat. Comm.* **2019**, *10*, No. 3268.

(6) Wu, C.; Pan, Z.; Yao, G.; Wang, W.; Fang, L.; Su, W. Synthesis and structure–activity relationship studies of teixobactin analogues. *RSC Adv.* **2017**, *7*, 1923–1926.

(7) Guan, Q.; Huang, S.; Jin, Y.; Campagne, R.; Alezra, V.; Wan, Y. Recent advances in the exploration of therapeutic analogues of gramicidin S, an old but still potent antimicrobial peptide. *J. Med. Chem.* **2019**, *62*, 7603–7617.

(8) Lin, D.; Lam, H. Y.; Han, W.; Cotroneo, N.; Pandya, B. A.; Li, X. Structure-activity relationship of daptomycin analogues with substitution at (2S, 3R) 3-methyl glutamic acid position. *Bioorg. Med. Chem. Lett.* **2017**, *27*, 456–459.

(9) Zipperer, A.; Konnerth, M. C.; Laux, C.; Berscheid, A.; Janek, D.; Weidenmaier, C.; Burian, M.; Schilling, N. A.; Slavetinsky, C.; Marschal, M.; Willmann, M.; Kalbacher, H.; Schittek, B.; Brötz-Oesterhelt, H.; Grond, S.; Peschel, A.; Krismer, B. Human commensals producing a novel antibiotic impair pathogen colonization. *Nature* **2016**, *535*, 511–516.

(10) Schilling, N. A.; Berscheid, A.; Schumacher, J.; Saur, J. S.; Konnerth, M. C.; Wirtz, S. N.; Beltrán-Beleña, J. M.; Zipperer, A.; Krismer, B.; Peschel, A.; Kalbacher, H.; Brötz-Oesterhelt, H.; Steinem, C.; Grond, S. Synthetic lugdunin analogues reveal essential structural motifs for antimicrobial action and proton translocation capability. *Angew. Chem., Int. Ed.* **2019**, *58*, 9234–9238.

(11) Miteva, M.; Andersson, M.; Karshikoff, A.; Otting, G. Molecular electroporation: a unifying concept for the description of membrane pore formation by antibacterial peptides, exemplified with NK-lysin. *FEBS Lett.* **1999**, *462*, 155–158.

(12) Pokorny, A.; Almeida, P. F. F. Kinetics of dye efflux and lipid flip-flop induced by delta-lysin in phosphatidylcholine vesicles and the mechanism of graded release by amphipathic, alpha-helical peptides. *Biochemistry* **2004**, *43*, 8846–8857.

(13) (a) Mojsoska, B.; Jenssen, H. Peptides and peptidomimetics for antimicrobial drug design. *Pharmaceuticals* **2015**, *8*, 366–415. (b) Ageitos, J. M.; Sanchez-Perez, A.; Calo-Mata, P.; Villa, T. G. Antimicrobial peptides (AMPs): Ancient compounds that represent

novel weapons in the fight against bacteria. *Biochem. Pharmacol.* **2017**, *133*, 117−138.
(14) Wiesner, J.; Vilcinskas, A. Antimicrobial peptides: the ancient arm of the human immune system. *Virulence* **2010**, *1*, 440−464.
(15) Mansour, S. C.; Pena, O. M.; Hancock, R. E. Host defense peptides: front-line immunomodulators. *Trends Immunol.* **2014**, *35*, 443−450.
(16) Catte, A.; Wilson, M. R.; Walker, M.; Oganesyan, V. S. Antimicrobial action of the cationic peptide, chrysophsin-3: a coarse-grained molecular dynamics study. *Soft Matter* **2018**, *14*, 2796.
(17) Lyu, Y.; Chen, T.; Shang, L.; Yang, Y.; Li, Z.; Zhu, J.; Shan, A. Design of Trp-rich dodecapeptides with broad-spectrum antimicrobial potency and membrane-disruptive mechanism. *J. Med. Chem.* **2019**, *62*, 6941−6957.
(18) Ramamoorthy, A. Beyond NMR spectra of antimicrobial peptides: Dynamical images at atomic resolution and functional insights. *Solid State Nucl. Magn. Reson.* **2009**, *35*, 201−207.
(19) Dürr, U. H. N.; Sudheendra, U. S.; Ramamoorthy, A. LL-37, the only human member of the cathelicidin family of antimicrobial peptides. *Biochim. Biophys. Acta, Biomembr.* **2006**, *1758*, 1408−1425.
(20) Gottler, L. M.; Ramamoorthy, A. Structure, membrane orientation, mechanism, and function of pexiganan - A highly potent antimicrobial peptide designed from magainin. *Biochim. Biophys. Acta, Biomembr.* **2009**, *1788*, 1680−1686.
(21) Yau, W. M.; Wimley, W. C.; Gawrisch, K.; White, S. H. The preference of tryptophan for membrane interfaces. *Biochemistry* **1998**, *37*, 14713−14718.
(22) Persson, S.; Killian, J. A.; Lindblom, G. Molecular ordering of interfacially localized tryptophan analogs in ester- and ether-lipid bilayers studied by H-2-NMR. *Biophys. J.* **1998**, *75*, 1365−1371.
(23) Killian, J. A.; Salemink, I.; de Planque, M. R. R.; Lindblom, G.; Koeppe, R. E.; Greathouse, D. V. Induction of nonbilayer structures in diacylphosphatidylcholine model membranes by transmembrane alpha-helical peptides: Importance of hydrophobic mismatch and proposed role of tryptophans. *Biochemistry* **1996**, *35*, 1037−1045.
(24) Tew, G. N.; Scott, R. W.; Klein, M. L.; Degrado, W. F. De novo design of antimicrobial polymers, foldamers, and small molecules: from discovery to practical applications. *Acc. Chem. Res.* **2010**, *43*, 30−39.
(25) Epand, R. M.; Epand, R. F. Domains in bacterial membranes and the action of antimicrobial agents. *Mol. BioSyst.* **2009**, *5*, 580−587.
(26) Teixeira, V.; Feio, M. J.; Bastos, M. Role of lipids in the interaction of antimicrobial peptides with membranes. *Prog. Lipid Res.* **2012**, *51*, 149−177.
(27) Katragadda, M.; Magotti, P.; Sfyroera, G.; Lambris, J. D. Hydrophobic effect and hydrogen bonds account for the improved activity of a complement inhibitor compstatin. *J. Med. Chem.* **2006**, *49*, 4616−4622.
(28) Cardenas, A. E.; Shrestha, R.; Webb, L. J.; Elber, R. Membrane permeation of a peptide: it is better to be positive. *J. Phys. Chem. B* **2015**, *119*, 6412−6420.
(29) Henzler-Wildman, K. A.; Martinez, G. V.; Brown, M. F.; Ramamoorthy, A. Perturbation of the hydrophobic core of lipid bilayers by the human antimicrobial peptide LL-37. *Biochemistry* **2004**, *43*, 8459−8469.
(30) Mazze, F. M.; Fuzo, C. A.; Degreve, L. A new amphipathy scale I. Determination of the scale from molecular dynamics data. *Biochim. Biophys. Acta* **2005**, *1747*, 35−46.
(31) Dougherty, D. A. Cation-pi interactions in chemistry and biology: a new view of benzene Phe, Tyr, and Trp. *Science* **1996**, *271*, 163−168.
(32) Schweizer, S.; Reed, J. Effect of variation of the strength of the aromatic interactions of tryptophan on the cooperative structural refolding behavior of a peptide from HIV 1. *Biophys. J.* **2008**, *95*, 3381−3390.
(33) Chan, D. I.; Prenner, E. J.; Vogel, H. J. Tryptophan- and arginine-rich antimicrobial peptides: Structures and mechanisms of action. *Biochim. Biophys. Acta, Biomembr.* **2006**, *1758*, 1184−1202.
(34) Bi, X.; Wang, C.; Ma, L.; Sun, Y.; Shang, D. Investigation of the role of tryptophan residues in cationic antimicrobial peptides to determine the mechanism of antimicrobial action. *J. Appl. Microbiol.* **2013**, *115*, 663−672.
(35) Ryge, T. S.; Doisy, X.; Ifrah, D.; Olsen, J. E.; Hansen, P. R. New indolicidin analogues with potent antibacterial Activity. *J. Pept. Res.* **2004**, *64*, 171−185.
(36) Khandelia, H.; Kaznessis, Y. N. Cation-π interactions stabilize the structure of the antimicrobial peptide indolicidin near membranes: molecular dynamics simulations. *J. Phys. Chem. B* **2007**, *111*, 242−250.
(37) Haug, B. E.; Svendsen, J. S. The role of tryptophan in the antibacterial activity of a 15-residue bovine lactoferricin peptide. *J. Peptide Sci.* **2001**, *7*, 190−196.
(38) Hwang, S. H.; Blaskovich, M. A.; Kim, H. O. A convenient reduction of α-amino acids to 1,2-amino alcohols with retention of optical purity. *Open Org. Chem. J.* **2008**, *2*, 107−109.
(39) Myers, A. G.; Zhong, B.; Movassaghi, M.; Kung, D. W.; Lanman, B. A.; Kwon, S. Synthesis of highly epimerizable N-protected α-amino aldehydes of high enantiomeric excess. *Tetrahedron Lett.* **2000**, *41*, 1359−1362.
(40) Meyer, S. D.; Schreiber, S. L. Acceleration of the Dess−Martin oxidation by water. *J. Org. Chem.* **1994**, *59*, 7549−7552.
(41) Campiglia, P.; Gomez-Monterreyb, I.; Carotenutob, A.; Lamab, T.; Diumob, M. V.; Bertaminob, A.; Mazzonib, O.; Salab, M.; Novellinob, E.; Grieco, P. Design and synthesis of small libraries of peptidomimetics based on a thiazolidine moiety. *Lett. Org. Chem.* **2006**, *3*, 539−545.
(42) Sucholeiki, I. New developments in solid phase synthesis supports. In *Annual Reports in Combinatorial Chemistry and Molecular Diversity*; Springer: Dordrecht, 1999; Vol. 2, pp 9−14.
(43) Santini, R.; Griffith, M. G.; Qi, M. A measure of solvent effects on swelling of resins for solid phase organic synthesis. *Tetrahedron Lett.* **1998**, *39*, 8951−8954.
(44) Lawrenson, S.; North, M.; Peigneguy, F.; Routledge, A. Greener solvents for solid-phase synthesis. *Green Chem.* **2017**, *19*, 952.
(45) Bayer, E. Towards the chemical synthesis of proteins. *Angew. Chem., Int. Ed.* **1991**, *30*, 113−129.
(46) Renil, M.; Meldal, M. Synthesis and application of a PEGA polymeric support for high capacity continuous flow solid-phase peptide synthesis. *Tetrahedron Lett.* **1995**, *36*, 4647−4650.
(47) Paradís-Bas, M.; Tulla-Puche, J.; Albericio, F. The road to the synthesis of "difficult peptides". *Chem. Soc. Rev.* **2016**, *45*, 631−654.
(48) Malins, L. R.; de Gruyter, J. N.; Robbins, K. J.; Scola, P. M.; Eastgate, M. D.; Ghadiri, R. M.; Baran, P. S. Peptide macrocyclization inspired by non-ribosomal Imine natural products. *J. Am. Chem. Soc.* **2017**, *139*, 5233−5241.
(49) Strauß, L.; Stegger, M.; Akpaka, P. E.; Alabi, A.; Breurec, S.; Coombs, G.; Egyir, B.; Larsen, A. R.; Laurent, F.; Monecke, S.; Peters, G.; Skov, R.; Strommenger, B.; Vandenesch, F.; Schaumburg, F.; Mellmann, A. Origin, evolution, and global transmission of community-acquired *Staphylococcus aureus* ST8. *Proc. Natl. Acad. Sci. U.S.A.* **2017**, *114*, E10596−E10604.
(50) Jones, M. B.; Montgomery, C. P.; Boyle-Vavra, S.; Shatzkes, K.; Maybank, R.; Frank, B. C.; Peterson, S. N.; Daum, R. S. Genomic and transcriptomic differences in community acquired methicillin resistant *Staphylococcus aureus* USA300 and USA400 strains. *BMC Genomics* **2014**, *15*, 1145−1155.
(51) David, M. Z.; Rudolph, K. M.; Hennessy, T. W.; Boyle-Vavra, S.; Daum, R. S. Molecular epidemiology of methicillin-resistant *Staphylococcus aureus*, rural southwestern Alaska. *Emerging Infect. Dis.* **2008**, *14*, 1693−1699.
(52) King, J. M.; Kulhankova, K.; Stach, C. S.; Vu, B. G.; Salgado-Pabón, W. Phenotyps and virulence among Staphylococcus aureus USA100, USA200, USA300, USA400, and USA600 clonal lineages. *mSphere* **2016**, *1*, e00071−16.
(53) Haug, B. E.; Camilio, K. E.; Eliassen, L. T.; Stensen, W.; Svendsen, J. S.; Berg, K.; Mortensen, B.; Serin, G.; Mirjolet, J. F.; Bichat, F.; Rekdal, O. Discovery of a 9-mer cationic peptide (LTX-

315) as a potential first in class oncolytic peptide. *J. Med. Chem.* **2016**, *59*, 2918−2927.
(54) Sharma, R. K.; Sundriyal, S.; Wangoo, N.; Tegge, W.; Jain, R. New antimicrobial hexapeptides: synthesis, antimicrobial activities, cytotoxicity, and mechanistic studies. *ChemMedChem* **2010**, *5*, 86−95.
(55) Oliva, R.; Chino, M.; Pane, K.; Pistorio, V.; De Santis, A.; Pizzo, E.; D'Errico, G.; Pavone, V.; Lombardi, A.; Del Vecchio, P.; Notomista, E.; Nastri, F.; Petraccone, L. Exploring the role of unnatural amino acids in antimicrobial peptides. *Sci. Rep.* **2018**, *8*, No. 8888.
(56) Kyte, J.; Doolittle, R. F. A simple method for displaying the hydropathic character of a protein. *J. Mol. Biol.* **1982**, *157*, 105−132.
(57) Gfeller, D.; Michielin, O.; Zoete, V. SwissSidechain: a molecular and structural database of non-natural sidechains. *Nucleic Acids Res.* 2012, *41*, D327−D332, DOI: 10.1093/nar/gks991; Swiss Institute of Bioinformatics and Molecular Modelling. https://www.swisssidechain.ch (accessed Jan 28, 2020).

6.4 Manuscript 4, 2022

S.N. Wirtz, D. Ruppelt, M. Meixner, C. Huhn, C. Steinem, S. Grond, unpublished

Paper 4

Development of fluorescent derivatives as tools to validate the in vivo mode of action of the antibiotic lugdunin

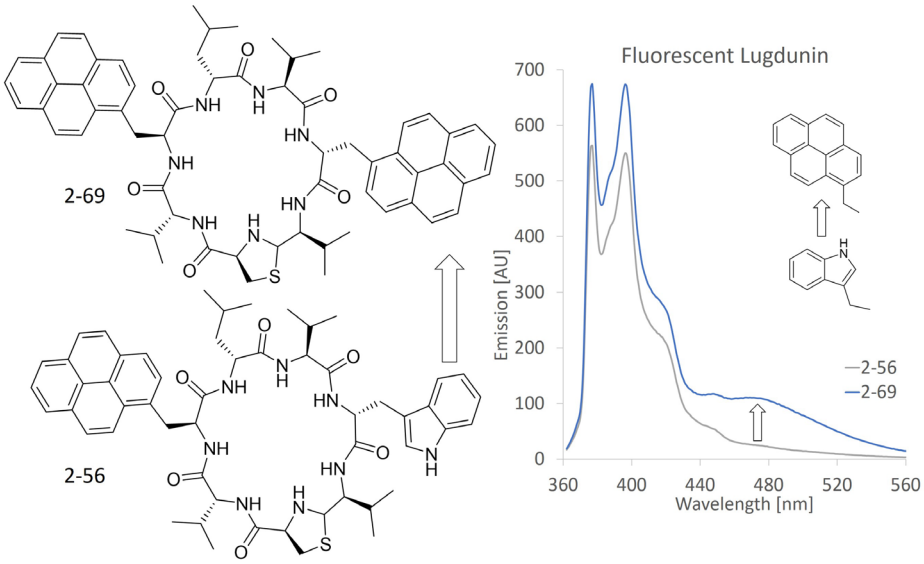

Development of fluorescent derivatives as tools to validate the *in vivo* mode of action of the antibiotic lugdunin

Sebastian N. Wirtz [a], Dominik Ruppelt [b], Martin Meixner [c], Carolin Huhn [c], Claudia Steinem [b] and Stephanie Grond* [a]

[a]	S. N. Wirtz, Prof. S. Grond Institute of Organic and Biomolecular Chemistry Eberhard Karls Universität Tübingen Auf der Morgenstelle 18 72076 Tübingen *Corresponding author e-mail: stephanie.grond@uni-tuebingen.de
[b]	D. Ruppelt, Prof. C. Steinem Institute for Organic and Biomolecular Chemistry Georg-August-Universität Göttingen 37077 Göttingen
[c]	M. Meixner, Prof. C. Huhn Institute for Physical und Theoretical Chemistry Eberhard Karls Universität Tübingen 72076 Tübingen

Abstract:

Lugdunin is a novel antimicrobial peptide with promising activity against a broad range of Gram-positive bacteria. Here we report the synthesis and characterization of lugdunin derivatives containing a pyrenylalanine as the fluorescent tag. These new fluorescent peptides display a wide range of antimicrobial activity against *Staphylococcus aureus*. Pyrene-excimer detection in combination with insights into the pK_a-values of lugdunin, membrane vesicle assays as well as preliminary modelling calculations enabled a deeper understanding of the way lugdunin interacts with a bacterial cell. We show the pK_a-value of lugdunin to be at 3.60-3.83, highlighting the environmental sensitivity of lugdunin. Membrane vesicle assays further demonstrate the sensitivity of lugdunin to its environment, and modelling calculation show the potential three-dimensional structure of lugdunin. These novel fluorescent lugdunins promise to be powerful tools to localize lugdunin in live cells and further investigate its mode of action.

Introduction:

The introduction of antibiotics into clinical use was arguably the greatest medical breakthrough of the 20th century[1]. However, in 2014, the WHO's assistant director general for health security stated that "a post-antibiotic era – in which common infections and minor injuries can kill – far from being an apocalyptic fantasy, is instead a very real possibility for the 21st century"[2]. This is due to the decreasing amount of novel antibiotics and the emergence of resistant bacteria which are becoming one of the leading public health threats of the 21st century[3]. As a result, it has been estimated that by 2050 antimicrobial resistance (AMR) could kill ten million people per year[4-5]. The need for novel antibiotics with a new mode-of-action (MOA) is thus one of the world's most pressing health issues[6]. One of these novel antimicrobial compounds is lugdunin (**I**).

This new, thiazolidine containing cyclic peptide is bactericidal against major gram-positive pathogens with low micro-molar activity against methicillin-resistant *Staphylococcus aureus* (MRSA) and vancomycin-resistant *Enterococcus faecium* (VRE)[7]. Lugdunin is a cyclic heptapeptide and the product of a non-ribosomal peptide synthetase (NRPS) with an unusual reductase activity resulting in the formation of an aldehyde and thus enabling the building of a thiazolidine ring[7]. We have previously carried out structure-activity-relationship (SAR) studies[8-9]. First, a basic stereo scan was carried out, where each amino acid was replaced by its analogue with a switched stereo-center at the side chain, thus demonstrating that the alternating D-L-amino acid backbone is crucial to activity[9]. Afterwards, an alanine scan was performed, where each amino acid was replaced by alanine in order to investigate the effect of each side chain on the activity[9]. We therefore identified 6-tryptophan-lugdunin as the only known derivative with a higher activity than natural lugdunin[9].

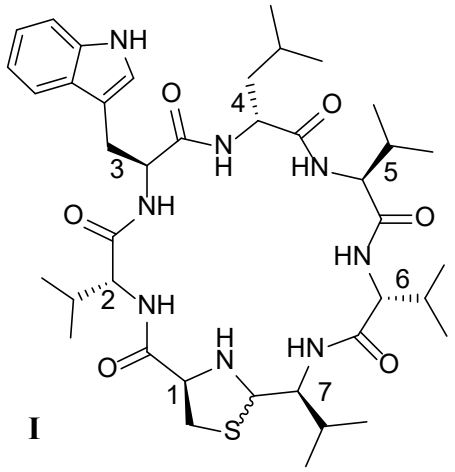

I

*Figure 37: Chemical structure of lugdunin (**I**) with highlighted amino acid numbering*

As previously shown, lugdunin is capable of equalizing pH gradients in artificial membrane vesicles without disrupting the membrane integrity[9]. We therefore propose two possible mechanisms by which lugdunin induces proton translocation: 1) lugdunin may

function as a proton carrier. Considering the inactivity of *N*-methylated thiazolidine lugdunin, it is possible that the secondary amine of the thiazolidine binds to a proton, traverses the membrane and then releases the proton on the other side of the membrane, thus equalizing the membrane potential. Due to the steric hinderance of tertiary residues (methyl or acetyl) the amine, although more basic than a secondary amine, might not be able to absorb a proton. This scenario has been previously envisaged and the postulated change in three-dimensional structure of lugdunin, whether protonated or not, does support this theory. However, we have not yet been able to confirm or reject the hypothesis of lugdunin as a proton carrier. In the second proposed mechanism multiple lugdunin molecules could form pore-like substructures within the membrane. In this scenario, multiple lugdunin molecules would arrange themselves, via intermolecular bonds, in such a three-dimensional structure that enables the translocation of positively charged cations. This second model has previously been reported by Ghadiri *et al.* for various other cyclic peptides that also had similar size and an alternating stereo configuration[10-11]. These compounds are able to participate in backbone-backbone intermolecular hydrogen bonding to produce a contiguous β-sheet structure, which results in amino acid side chains lying on the outside of the structure and display good ion transport properties[10, 12].

We aimed at gaining detailed chemical knowledge of the MOA of lugdunin in order to further optimize the structural elements of the peptide. We optimized the existing synthesis strategy according to the desired peptides. Since fluorescence microscopy is frequently used for MOA studies[13-14], the compounds required a fluorescent label. Here we report the synthesis of fluorescent derivatives of lugdunin and their characterization with respect to their physico-chemical properties and antibacterial activity.

Results and Discussion:

Chemical synthesis. The strategy behind the synthesis of these derivatives was a sequential replacement of L-trp^3 and D-val^6 in natural lugdunin with pyrenylalanine as the fluorescent tag. Furthermore, replacing D-val^2 with D-leu^2 was found to be beneficial to antimicrobial activity. We utilized our previously published strategy for lugdunin synthesis with pre-synthesized thiazolidine building blocks[8]. When numbering amino acids, we always used natural lugdunin as reference with cysteine at position one, L-trp^3 at position 3 and so on[7], see Figure 1.

For lugdunin derivatives with valine or tryptophan at position six, we also started at that position with commercially available, pre-loaded resins. As previously shown[8-9], this starting position increased coupling conditions, as well as the macrolactamization properties. For derivatives with pyrenylalanine at position six, we started on position four, due to the limited availability of pre-loaded resins. In contrast to conditions previously published by Saur *et al.*[8], the pyrenylalanine coupling was carried out with only a three times excess (compared to the usual six times excess) due to financial and availability aspects.

This resulted in a total of 13 peptides, shown in table 1. As a result, 3-pyrenylalanine-lugdunin **1** was the first derivative, which also showed promising bioactivity against MRSA at 25 µg*ml^{-1} (12.5 µM). 2-leucine-3-pyrenylalanine-lugdunin **2** followed with a less potent activity at 50 µg*ml^{-1} (50 µM), corresponding, however, to the activity of the derivative 2-leucine-lugdunin. 3-pyrenylalanine-6-tryptophan-lugdunin **3** also followed the trend of lugdunin, whereas the 6-tryptophan-derivatives were generally more active than their 6-valine counterparts. This is demonstrated in **3** with an antimicrobial activity of 3.13 µg*ml^{-1} (1.56 µM), the same as natural lugdunin. 6-pyrenylalanine-lugdunin **4** is the counterpart to **3**, in which the tryptophan at position six and pyrenylalanine at position three have been interchanged. While this change is not possible in 6-tryptophan-lugdunin

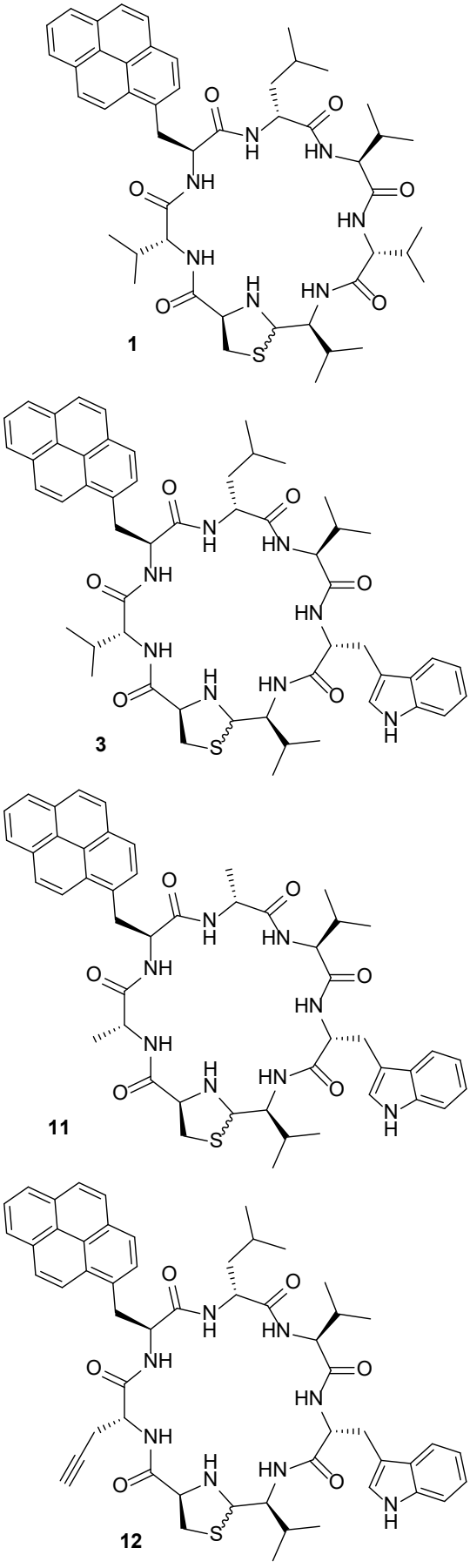

*Figure 38: Chemical structures of **1**, **3**, **11** and **12***

due to the identical amino acids at these positions, there is a noticeable change in activity, as **4** is only active against MRSA at 50 µg*ml^{-1} (50 µM). In contrast, 3-valine-6-pyrenylalanine-lugdunin **5** is slightly more active at 25 µg*ml^{-1} (25 µM) even though lugdunin derivatives with an additional tryptophan residue have mostly shown a higher activity. 2-leucine-3-valine-6-pyrenylalanine-lugdunin **6** is less active than the previously mentioned 6-pyrenylalanine derivatives at 50 µg*ml^{-1} (100 µM). 2-leucine-6-pyrenylalanine-lugdunin **7** and 2-leucine-3-pyrenylalanine-6 tryptophan-lugdunin **8** are also inactive (inactivity is hereby defined as an activity of more than 100 µg*ml^{-1} (100 µM)). This highlights again the 2-leucine derivatives to be less suitable than their 2-valine counterparts. 3-pyrenylalanine-6-pyrenylalanine-lugdunin **9** and 2-leucine-3-pyrenylalanine-6-pyrenylalanine-lugdunin **10** are the only two lugdunin derivatives with multiple pyrenylalanine moieties. Unfortunately, neither of these peptides showed activity against MRSA with MIC values of more than 100 µg*ml^{-1} (100 µM). 2-alanine-3-pyrenylalanine-4-alanine-6-tryptophan-lugdunin **11** was designed to be the negative control as previously all lugdunin-derivatives with an alanine-moiety in position 2 or 4 were inactive. Interestingly, **11** showed some, albeit low, activity at 50 µg*ml^{-1} (50 µM), suggesting that alanine-derivatization in lugdunin might need to be reconsidered in combination with other amino acids. 2-propagylglycine-3 pyrenylalanine-6-tryptophan-lugdunin **12** and 2-propagylglycine-3-pyrenylalanine-lugdunin **13** were designed to enable further reactions with the propagyl-residue, such as immobilization via click-chemistry or the addition of other click-fluorophores. These derivatives also show promising antimicrobial activity towards MRSA with 12.5 µg*ml^{-1} (12.5 µM) for **12** and 25 µg*ml^{-1} (12.5 µM) for **13**. Lugdunin **14** as well as 6-tryptophan-lugdunin **15** were also synthesized as controls and exhibited the previously reported activities of 3.13 µg*ml^{-1} (3.13 µM) and 1.56 µg*ml^{-1} (1.56 µM), respectively[8-9]. After being synthesized, each peptide was analyzed via ^{1}H-, ^{13}C- and ^{1}H,^{1}H-COSY-NMR, HR-ESI-MS with their respective MS/MS-sequencing. Furthermore, their antimicrobial activity was analyzed against methicillin-resistant *Staphylococcus aureus*, *Bacillus subtilis*, *Bacillus megaterium* and *Escherichia coli* at concentrations between 100 µg*ml^{-1} and 0.185 µg*ml^{-1} as well as from 100 µM to 0.185 µM (see supporting information). We defined antimicrobial activity as an OD_{600} value of >0.1 in the liquid MIC assay. All peptides are listed in Table 1 with their MICs in µg*ml^{-1} and µM against MRSA and their respective amino acids at position two, three, four and six as well as the numbers used for their individual analysis.

Table 3. Synthesized lugdunin analogues with their respective amino acids at positions two, three, four and six as well as their respective MIC values against methicillin-resistant *Staphylococcus aureus* USA300 LAC tested with serial dilution from 10 mg*ml^{-1} and 10 mM stock solutions in DMSO.

Nr.	AA at Pos. 2	AA at Pos. 3	AA at Pos. 4	AA at Pos. 6	Name	Nr.[c]	MIC[a] MIC[b]
1	D-Val	L-Pyr	D-Leu	D-Val	3-Pyrenylalanine-lugdunin	2-52	25[a] 12,5[b]
2	D-Leu	L-Pyr	D-Leu	D-Val	2-Leucine-3-pyrenylalanine-lugdunin	2-55	50[a] 50[b]
3	D-Val	L-Pyr	D-Leu	D-Trp	3-Pyrenylalanine-6-tryptophan-lugdunin	2-56	3,13[a] 1,56[b]
4	D-Val	L-Trp	D-Leu	D-Pyr	6-Pyrenylalanine-lugdunin	15-7	50[a] 50[b]
5	D-Val	L-Val	D-Leu	D-Pyr	3-Valine-6-pyrenylalanine-lugdunin	15-9	25[a] 25[b]
6	D-Leu	L-Val	D-Leu	D-Pyr	2-Leucine-3-valine-6-pyrenylalanine-lugdunin	2-66	50[a] >100[b]
7	D-Leu	L-Trp	D-Leu	D-Pyr	2-Leucine-6-pyrenylalanine-lugdunin	2-67	100[a] 100[b]
8	D-Leu	L-Pyr	D-Leu	D-Trp	2-Leucine-3-pyrenylalanine-6-tryptophan-lugdunin	2-68	100[a] >100[b]
9	D-Val	L-Pyr	D-Leu	D-Pyr	3-Pyrenylalanine-6-pyrenylalanine-lugdunin	2-69	>100[a] >100[b]
10	D-Leu	L-Pyr	D-Leu	D-Pyr	2-Leucine-3-pyrenylalanine-6-pyrenylalanine-lugdunin	2-70	>100[a] >100[b]
11	D-Ala	L-Pyr	D-Ala	D-Trp	2-Alanine-3-pyrenylalanine-4-alanine-6-tryptophan-lugdunin	2-71	50[a] 50[b]
12	D-Pra	L-Pyr	D-Leu	D-Trp	2-Propagylglycine-3-pyrenylalanine-6-tryptophan-lugdunin	2-72	12,5[a] 12,5[b]
13	D-Pra	L-Pyr	D-Leu	D-Val	2-Propagylglycine-3-pyrenylalanine-lugdunin	2-73	25[a] 12,5[b]
14	D-Val	L-Trp	D-Leu	D-Val	Lugdunin		3,13[a] 3,13[b]
15	D-Val	L-Trp	D-Leu	D-Trp	6-Tryptophan-lugdunin		1,56[a] 1,56[b]

[a] MRSA USA300 LAC (MIC in mg*mL^{-1}). [b] MRSA USA300 LAC (MIC in mM)

[c] Numbers used for each peptide in their respective analysis (e.g. HR-ESI-MS, NMR)

AA = amino acid, Ala = alanine, Leu = leucine, Trp = tryptophan, Pra = propargylglycine, Pyr = 1-pyrenylalanine. All structures shown in figure 7 of the supporting information.

pK_a-Value. As the main aim of this study was to further explore lugdunin's MOA, we are now focusing on the pK_a-value. In order to get a deeper understanding of lugdunin's response to environmental changes in pH-value, we focused on the unusual thiazolidine moiety. We have previously shown that the free secondary amine is crucial for activity, with methylated- or acetylated thiazolidine lugdunin derivatives being inactive[9]. Different combinations of valine and cysteine (peptide bond, linear peptide or homocysteine) also resulted in inactive peptides. We therefore synthesized two thiazolidine derivatives with only the secondary amine available and other functional groups inactivated through methylation, as shown in Figure 3.

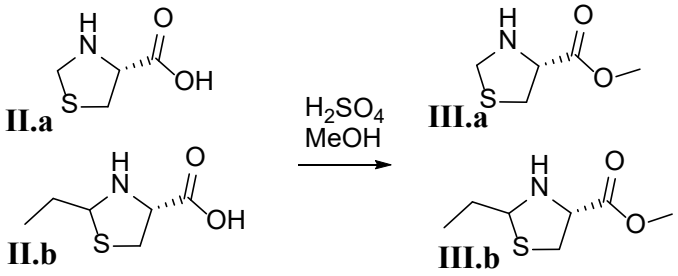

Figure 39: Acid catalyzed methylation of thiazolidine controls II.a and II.b

Thiazolidine-4-carboxylic acid methyl ester (**III.a**) and 2-ethyl-thiazolidine-4-carboxylic acid methyl ester (**III.b**) were then subjected to a capillary electrophoresis (CE) mass spectrometry (MS)-based screening method for the determination of pI-values. CE-MS proved to be the most suitable analysis for distinct reasons: the effective electrophoretic mobility of compounds in solution at pH-values close to their pK_a- or pI-value exhibit a strong pH-dependence [15]. In literature, CE-UV methods for the automated determination of electrophoretic mobility curves are well-established[15-16]. Not only automation but also high accuracy for single compounds can be achieved, and measurement times are minimized by pressure-assisted separations[17]. Another advantage of this technique is that CO_2-absorption into buffers of high pH is minimized, increasing the accuracy in this pH-range[16]. But even with standard CE devices, fast approaches were described[18] based on curve fitting from two pH-values. However, this approach is limited to compounds of low acidity / basicity and requires reference materials with comparable pI-values. CE-MS is an alternative for pI determination of mixtures, of non-UV-active samples or with low solubility. CE-MS hyphenation offers up to 10-fold higher sensitivities compared to conventional CE-UV, as published by Wan *et al.*[17]. Robustness was demonstrated with regard to the presence of DMSO and elevated ionic strength (25 to 150 mmol/l) in the sample with only minor changes in pK_a-values by

0.06 pH-units. The calculation of pK_a-values based on the pH-dependence of the effective electrophoretic mobility in the pH-titration curve is well described in several publications[19-20] and is based on previously reported processes such as enzyme digestion[21]. To compare our results with literature we initially tested various amino acids using citric acid (pK_a = 3.13, 4.76, 6.40) and ammonium (pK_a = 9.24) granting a pH range from 2.1 to 7.4, which enabled us to confirm the suitability of the method for our task. Subsequently, lugdunin and the two thiazolidine references were analyzed in the same conditions. Interestingly, pH-dependent speciation occurred exclusively for natural lugdunin, an effect that we were able to confirm using LC-MS and NMR analysis. The thiazolidine reference **III.b** was unfortunately poorly detected and only showed an estimated pI-value of 5.00 - 6.02. However, **III.a** was clearly detected and showed a similar pI-value of ≤6.02. Due to the two peaks of lugdunin that formed during the analysis we calculated an average pI-value of 3.60 – 3.83, demonstrating the importance and impact of the unusual thiazolidine connection in the peptide backbone. All results are shown in Table 1 of the supporting information.

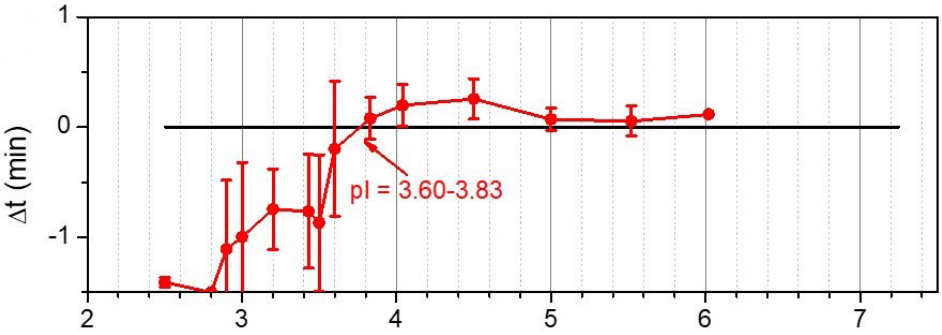

Figure 40: pI-value determination. The Δt-values were plotted by taking the average values of the first and the second peak into consideration.

UV analysis. Due to the different effects of concentration as well as pH-values that we observed, we measured all transmission spectra at various concentrations, as well as various pH-values (by addition of NaOH and HCl). Fluorescence spectra were measured at various excitation wavelengths and all samples were dissolved in MeOH. All available spectra are shown in the supporting information. While at different concentrations certain differences in the transmission spectra were observed, those differences can be attributed to suboptimal conditions for the measurement and do not result from differences in the compounds. There is no shift in transmission wavelength between derivatives with one or two pyrenylalanine moieties. However, there is an additional local absorption maximum for **9** and **10** at 375 nm, potentially corresponding to an intramolecular interaction between the two pyrenes. All fluorescent lugdunins have

local absorption maxima at 342 nm, 326 nm, 312 nm, 299 nm, 275 nm, 265 nm, 255 nm, 243 nm and 224 nm, although for wavelengths <300 nm the values might be inaccurate due to very strong absorption in that area. The change in pH did have an effect on the absorption, however the acidic/basic conditions did not uniformly impact all peptides. All transmission spectra of compounds **1**-**13** are shown in Figure 5. Any values over 100% transmission result from air in the sample/cuvette during analysis and can be disregarded. All spectra are shown in a stacked view to highlight the unity among all samples.

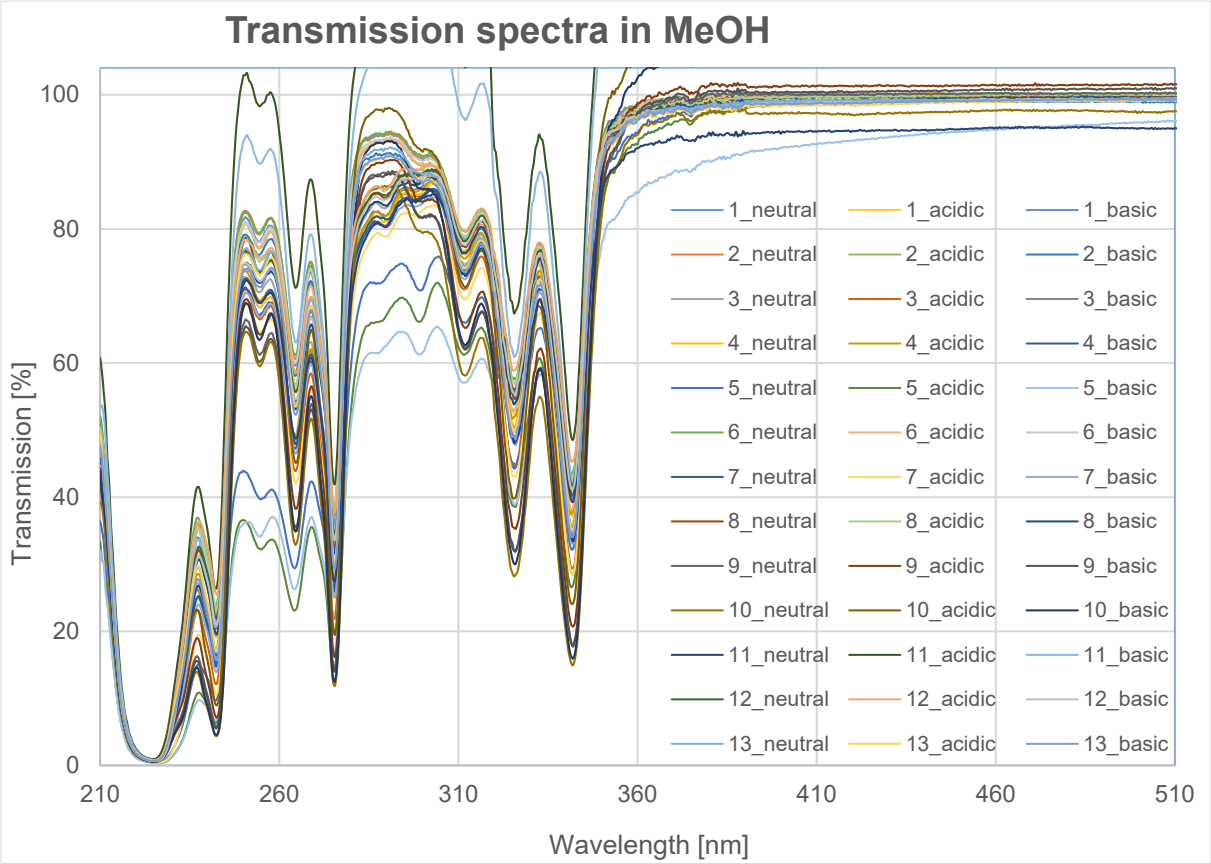

*Figure 41: Measured transmission spectra of compounds **1-13** in MeOH at a concentration of 0.0125 mg*ml^{-1}.*

As a result, we chose 311 nm, 325 nm, 342 nm and 374 nm as excitation wavelengths for fluorescence analysis. The results for compounds **1**-**13** were similar compared to the transmission spectra and are shown in Figure 6. All peptides had local maxima at 376 nm, 396 nm, a shoulder at 420 nm as well as a small shoulder at 450 nm. However, there were noticeable differences for derivatives **9** and **10**, i.e., those peptides with two pyrenylalanines, which exhibited an additional broad maximum at 475 nm for excitation wavelengths of 325 nm and 342 nm. This suggests the existence of pyrene excimers due to the close proximity of the two pyrenes within the peptide[22-29].

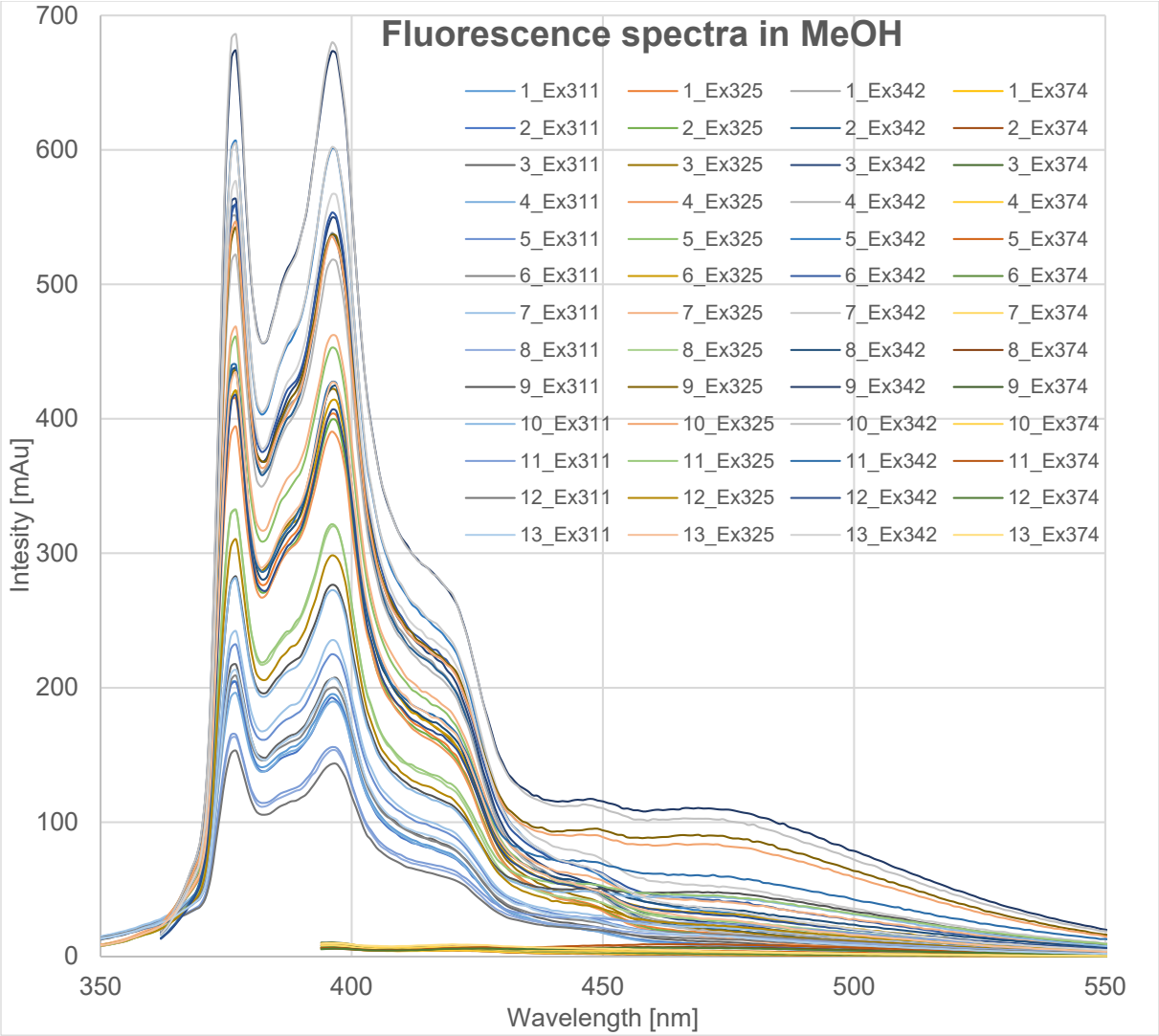

*Figure 42: Measured fluorescence spectra of compounds **1-13** in MeOH at a concentration of 0.0125 mg*ml^{-1}. Excitation was at 311 nm, 325 nm, 342 nm and 374 nm for each compound. Fluorescence was measured 20 nm after the excitation wavelength (e.g., for excitation at 311 nm, fluorescence was recorded for 331 nm - 800 nm)*

This is in accordance to previous modelling attempts, suggesting a three-dimensional structure with the two pyrenylalanines in **9** and **10** folding over / below the peptide backbone[30]. Similar to the transmission spectra, the addition of acid or base did not have a significant impact on the fluorescence.

This suggests that, contrary to previous assumptions, the protonation-state of lugdunin does not impact the three-dimensional structure enough for a significant impact on fluorescence. However, a more accurate statement of the three-dimensional structure can only be made via x-ray structure analysis. Since the excimer fluorescence is only poorly detected in the derivatives with a single pyrenylalanine, we hypothesize that intermolecular excimers do not form in solution. As a result, the fluorescence of lugdunin can be used as a powerful tool to investigate the MOA of lugdunin in bacterial cells. If lugdunin forms channels, the proximity of the pyrenes should be close enough for

the formation of excimers, resulting in a distinct fluorescence increase at 475 nm. On the contrary, if lugdunin functions as a carrier, the first proposed MOA, excimers should not form.

Artificial vesicle assay. To more closely investigate the MOA of lugdunin in a simplified model system, we exposed the fluorescent lugdunin derivatives to artificial vesicles, simulating a bacterial membrane. Compared to bacterial cells, the use of an *in vitro* vesicle assay enabled us to measure fluorescence of the compounds in the presence of various concentrations of the artificial lipid. For lipids, a POPC (1-palmitoyl-2-oleoyl-sn-glycero-3-phosphocholine) solution (2 mg total lipid mass in chloroform) was used to create large unilamellar vesicles (LUVs). Compounds were used as 2-Propanol stock solutions and diluted in HEPES buffer to a final concentration of 10 µM. Lipids were added stepwise for concentrations of 0 µM to 100 µM, 500 µM and 1000 µM. Interestingly, compound **1** showed decent excimer fluorescence with 0 µM lipid concentration, which shifted drastically towards pure monomer fluorescence with increased lipid concentration. This strongly suggests that lugdunin acts as a cation carrier rather than by forming a channel. This is also supported by other derivatives, such as **3**, **4** and **11**. While these four peptides all have one pyrenylalanine in their respective amino acid sequence, the remaining amino acids, with exception of the thiazolidine ring, differ throughout. They are, however, all antimicrobially active between 3 µM and 50 µM, unlike peptides **9** and **10** with two pyrene moieties.

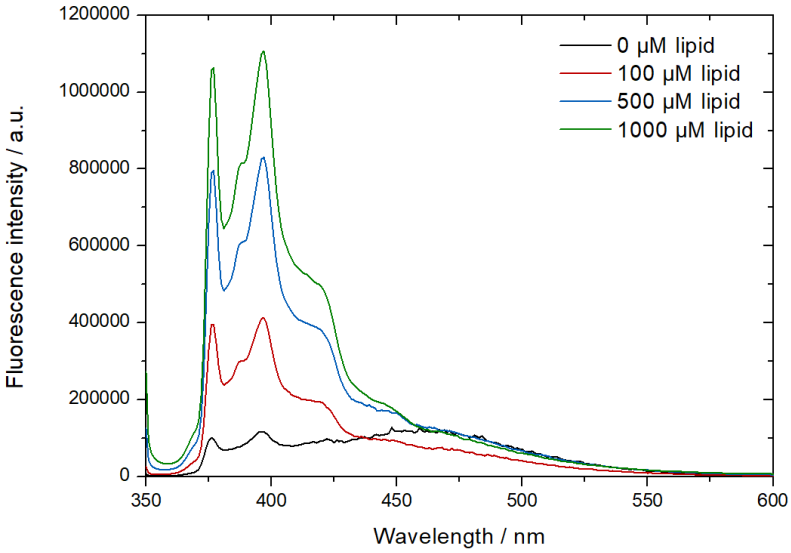

*Figure 43: Fluorescence spectroscopy of **1** in water in the presence of various lipid concentrations*

Derivative **9** was subjected to the same experiment, however, the excimer fluorescence was still detectable in high concentrations of lipids (green curve, Figure 8). While this is the only derivative with this trend, it is also the only derivative tested with two pyrene-moieties as well as the only peptide without a measurable activity in our antimicrobial assays. As a result, we expected the excimer fluorescence in presence of the vesicles. But this may also be due to the inability of derivative 9 to permeate the artificial membrane, resulting in most of the compound remaining in the aqueous phase, which might also explain the antibacterial inactivity. Another reason might be the size of the pyrene rings interfering with the spatial availability of the secondary amine in the thiazolidine ring. Due to the previously mentioned arrangement of the pyrenes over and underneath the thiazolidine ring, the crucial amine might be sterically hindered, rendering the peptide inactive.

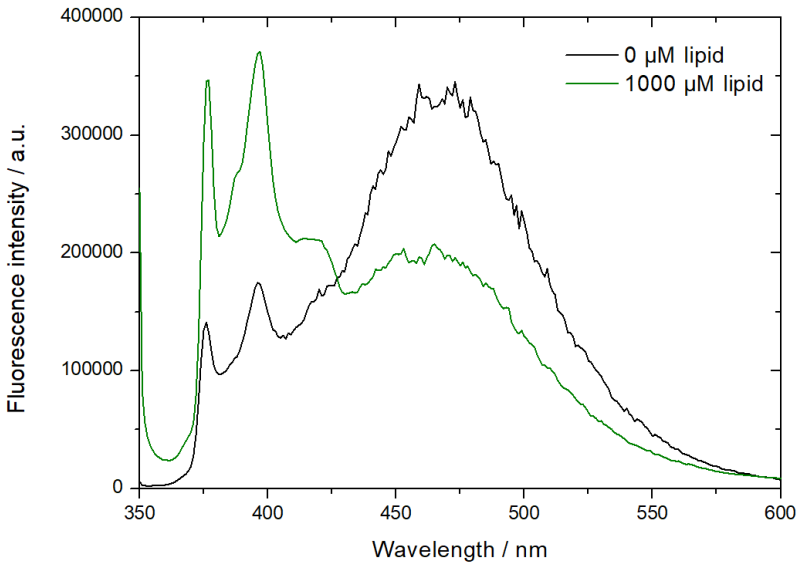

*Figure 44: Fluorescence spectroscopy of derivative **9** in water in the absence or presence of artificial lipids*

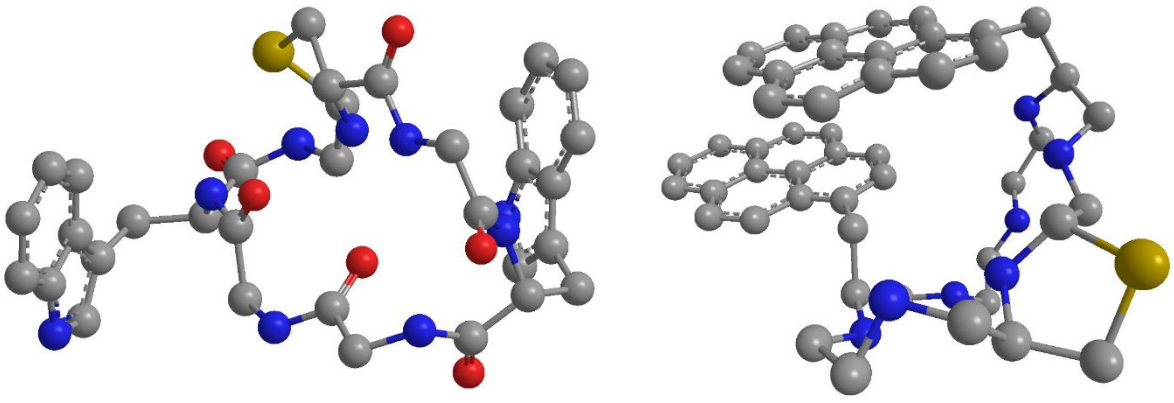

*Figure 45: Potential three-dimensional structures of 6-tryptophan-lugdunin (**15**, shown on the left side) and 3-pyrenylalanine-6-pyrenylalanine-lugdunin (**9**, shown on the right side), calculated via MM2 in Chem3D*

As shown on the left side of Figure 9, it is possible for the two tryptophan residues to be on either side of the thiazolidine ring, allowing for cation-π-interactions and thus stabilizing the potentially charged amine. This could explain the improved activity of **15** compared to **14**. On the right side of Figure 9, a potential three-dimensional structure of **9** is shown, with the two pyrene moieties in close proximity of each other. This could

explain the excimer-fluorescence as well as the drastically declined activity due to the reduced electron density in the pyrene-rings and thus fewer stabilizing effects onto the thiazolidine amine. However, while the predicted structures might explain certain trends, they remain speculative and need to be confirmed.

Conclusion:

In summary, we report the development of novel pyrenyl-derivatives of lugdunin, which allow for fluorescence-based studies of the mode of action of lugdunin. Among the 13 newly synthesized compounds, nine retain antimicrobial activity at a concentration below 100 µg*ml^{-1}. We have also shown the environmental sensitivity of pyrene excimers, enabling further MOA studies. The pK_a-values of lugdunin have also not been previously shown and the unexpectedly low pK_a of 3.6-3.8 might be an interesting property for further structure optimization. While these new derivatives are definitely a step in the right direction for identifying the MOA of lugdunin, additional ones with more optimized properties such as improved quantum yields, higher absorption wavelengths and stronger antimicrobial activities might be required.

Experimental Section:

Detailed experimental procedures are provided in the appendix.

Acknowledgements:

The work of S.N.W. and S.G. was supported by SFB 766. M.M. and C.H. acknowledge support from Karl & Anna Buck Stiftung and the Excellence Initiative, organized by the German Research Foundation (DFG). We further acknowledge Taulant Dema and Pascal Rath for NMR measurements and Bernhard Krismer for biological activity assays.

Conflict of interest:

Eberhard Karls University Tübingen holds a patent for lugdunin (EP3072899B1) covering lugdunin itself, derivatives thereof and the bacterial infection prevention by lugdunin producing bacteria as well as lugdunin derivatives of bacterial origin. The patent has also been filed in the USA (US2018/0155397A1).

Keywords: fluorescent antibiotic • methicillin-resistant *Staphylococcus aureus* • proton translocation • artificial membrane interaction • mode-of-action microscopy

References:

[1] L. Katz, R. H. Baltz, Natural product discovery: past, present, and future, *Journal of Industrial Microbiology and Biotechnology* **2016**, *43*, 155-176.

[2] S. Reardon, WHO warns against 'post-antibiotic' era, *Nature* **2014**.

[3] C. J. L. Murray, K. S. Ikuta, F. Sharara*, et al.*, Global burden of bacterial antimicrobial resistance in 2019: a systematic analysis, *The Lancet* **2022**, *399*, 629-655.

[4] J. O'Neill, *Antimicrobial Resistance: Tackling a Crisis for the Health and Wealth of Nations: December 2014*, Review on antimicrobial resistance, **2014**.

[5] J. O'Neill, *Tackling drug-resistant infections globally: final report and recommendations*, Government of the United Kingdom, **2016**.

[6] M. S. Butler, D. L. Paterson, Antibiotics in the clinical pipeline in October 2019, *The Journal of Antibiotics* **2020**, *73*, 329-364.

[7] A. Zipperer, M. C. Konnerth, C. Laux*, et al.*, Human commensals producing a novel antibiotic impair pathogen colonization, *Nature* **2016**, *535*, 511-516.

[8] J. S. Saur, S. N. Wirtz, N. A. Schilling*, et al.*, Distinct Lugdunins from a New Efficient Synthesis and Broad Exploitation of Its MRSA-Antimicrobial Structure, *Journal of Medicinal Chemistry* **2021**, *64*, 4034-4058.

[9] N. A. Schilling, A. Berscheid, J. Schumacher*, et al.*, Synthetic lugdunin analogues reveal essential structural motifs for antimicrobial action and proton translocation capability, *Angew. Chem., Int. Ed.* **2019**, *58*, 9234.

[10] M. R. Ghadiri, J. R. Granja, R. A. Milligan*, et al.*, Self-assembling organic nanotubes based on a cyclic peptide architecture, *Nature* **1993**, *366*, 324-327.

[11] D. T. Bong, T. D. Clark, J. R. Granja*, et al.*, Self-Assembling Organic Nanotubes, *Angew. Chem. Int. Ed.* **2001**, *40*, 988-1011.

[12] J. D. Hartgerink, J. R. Granja, R. A. Milligan*, et al.*, Self-Assembling Peptide Nanotubes, *Journal of the American Chemical Society* **1996**, *118*, 43-50.

[13] R. Velleste, H. Teugjas, P. Väljamäe, Reducing end-specific fluorescence labeled celluloses for cellulase mode of action, *Cellulose* **2010**, *17*, 125-138.

[14] T. A. Perkins, D. E. Wolf, J. Goodchild, Fluorescence Resonance Energy Transfer Analysis of Ribozyme Kinetics Reveals the Mode of Action of a Facilitator Oligonucleotide, *Biochemistry* **1996**, *35*, 16370-16377.

[15] S. K. Poole, S. Patel, K. Dehring*, et al.*, Determination of acid dissociation constants by capillary electrophoresis, *J. Chromatogr. A* **2004**, *1037*, 445-454.

[16] M. Lowry, S. O. Fakayode, M. L. Geng*, et al.*, Molecular fluorescence, phosphorescence, and chemiluminescence spectrometry, *Anal. Chem.* **2008**, *80*, 4551-4574.

[17] H. Wan, A. G. Holmén, Y. Wang*, et al.*, High-throughput screening of pKa values of pharmaceuticals by pressure-assisted capillary electrophoresis and mass spectrometry, *Rapid Commun. Mass Spectrom.* **2003**, *17*, 2639-2648.

[18] E. Fuguet, C. Ràfols, E. Bosch*, et al.*, A fast method for pKa determination by capillary electrophoresis, *Chem. Biodivers.* **2009**, *6*, 1822-1827.

[19] J. Cleveland Jr, M. Benko, S. Gluck*, et al.*, Automated pKa determination at low solute concentrations by capillary electrophoresis, *Journal of Chromatography A* **1993**, *652*, 301-308.

[20] Y. Ishihama, H. Katayama, N. Asakawa*, et al.*, Highly robust stainless steel tips as microelectrospray emitters, *Rapid Commun. Mass Spectrom.* **2002**, *16*, 913-918.

[21] M. Ye, S. Hu, R. M. Schoenherr*, et al.*, On-line protein digestion and peptide mapping by capillary electrophoresis with post-column labeling for laser-induced fluorescence detection, *Electrophoresis* **2004**, *25*, 1319-1326.

[22] R. D. Pensack, R. J. Ashmore, A. L. Paoletta*, et al.*, The Nature of Excimer Formation in Crystalline Pyrene Nanoparticles, *The Journal of Physical Chemistry C* **2018**, *122*, 21004-21017.

[23] J. Aguiar, P. Carpena, J. A. Molina-Bolívar*, et al.*, On the determination of the critical micelle concentration by the pyrene 1:3 ratio method, *Journal of Colloid and Interface Science* **2003**, *258*, 116-122.

[24] M. M. Amiji, Pyrene fluorescence study of chitosan self-association in aqueous solution, *Carbohydr. Polym.* **1995**, *26*, 211-213.

[25] G. Bains, A. B. Patel, V. Narayanaswami, Pyrene: A Probe to Study Protein Conformation and Conformational Changes, *Molecules* **2011**, *16*, 7909.

[26] D. C. Dong, M. A. Winnik, The Py Scale of solvent polarities. Solvent effects on the vibronic fine structure of Pyrene fluorescence and empirical correlations with ET and Y values, *Photochemistry and Photobiology* **1982**, *35*, 17-21.

[27] T. Förster, K. Kasper, Ein Konzentrationsumschlag der Fluoreszenz des Pyrens, *Zeitschrift für Elektrochemie, Berichte der Bunsengesellschaft für physikalische Chemie* **1955**, *59*, 976-980.

[28] Y. Shiraishi, Y. Tokitoh, T. Hirai, pH- and H2O-Driven Triple-Mode Pyrene Fluorescence, *Org. Lett.* **2006**, *8*, 3841-3844.

[29] B. Stevens, E. Hutton, Radiative Life-time of the Pyrene Dimer and the Possible Role of Excited Dimers in Energy Transfer Processes, *Nature* **1960**, *186*, 1045-1046.

[30] P. Geissler, Modelling of lugdunin derivatives, *Unpublished Work*, **2020**.

6.5 Manuscript 5, 2022

D. Ruppelt, T. Dema, S.N. Wirtz, H. Flegel, S. Mönnikes, S. Grond, C. Steinem, unpublished

Paper 5

Towards the mode of action: Fluorescence and IR-spectroscopic analysis of lugdunin in lipid membranes

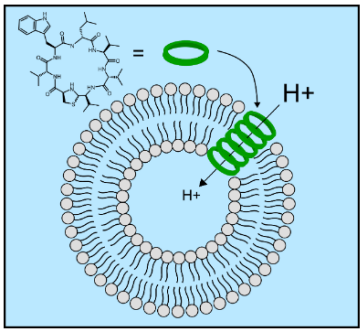

Lord Of The Rings: The mode of action of the first antimicrobial fibupeptide lugdunin depends on the insertion of the peptide into lipid membranes and the accompanying assembly into an antiparallel β-sheet-like nanotube. Due to the characteristic D,L-configuration of lugdunin, these hollow tubes could act as ion channels enabling the efficient transport of protons and presumably other small ions across membranes.

Towards the mode of action: Fluorescence and IR-spectroscopic analysis of lugdunin in lipid membranes

Dominik Ruppelt,[a] Taulant Dema,[b] Sebastian N. Wirtz,[b] Hendrik Flegel,[a] Sophia Mönnikes,[a] Stephanie Grond,[b] Claudia Steinem*[a,c]

The antimicrobial fibupeptide lugdunin is active against methicillin-resistant *Staphylococcus aureus* and vancomycin-resistant enterococci. It is characterized by a seven-membered ring composed of D,L-amino acids and a thiazolidine heterocycle. Recently, we showed that lugdunin is capable of cancelling the membrane potential of bacterial membranes and translocating protons across artificial ones. However, the mode of action is still elusive. Here, we analyzed the insertion propensity of lugdunin into artificial membranes and found that its partitioning is unaffected by the presence of negatively charged lipids but is strongly reduced in bilayers harboring the eukaryotic membrane component cholesterol. ATR-IR spectroscopy revealed that lugdunin adopts a hydrogen-bonded antiparallel β-sheet in lipid bilayers, which can result in tube-like structures. Using bio-inactive methylated lugdunin analogues, which do not assemble into β-sheets and do not transport protons, supports this model.

Introduction

Dissemination of infectious diseases caused by antibiotic-resistant bacterial strains represents a major threat to the global health system.[1] According to recent estimations, multidrug-resistant organism like methicillin-resistant *Staphylococcus aureus* (MRSA) or vancomycin-resistant enterococci (VRE) are expected to cause more deaths than cancer in the near future.[2] Despite the urgency, the development of antibiotics focused primarily on already established structures in the last decades. Only recently, one has started to aim at identifying new antibiotic entities originating from natural products.[3,4] A promising source of novel antibiotic scaffolds is the human microbiota. In particular, bacteria harboured in nutrient-poor environments are believed to, among other mechanisms, secrete antimicrobial peptides (AMPs) killing other bacteria and securing their survival.[5,6] Today, AMPs have emerged to be one of the most promising approaches for the development of potential new antibiotics.[7,8]

In 2016, the novel cyclic AMP lugdunin (**1**, Scheme 1) isolated from a strain of nasal *Staphylococcus lugdunensis* was identified, representing the first member of the class of fibupeptides, which is characterized by a thiazolidine heterocycle in the peptide backbone.[9] *In vivo*, **1** prevents the growth of *S. aureus* in the human nose and has shown promising antimicrobial activity against a plethora of other gram-positive bacteria.[9] In a study with human keratinocytes **1** also displayed synergistic effects with host-derived AMPs and strengthened the immune response.[10] With the development of a synthetic route towards **1**, a variety of structural analogues of **1** became accessible, which allowed us, based on a comprehensive structure–activity relationship study, to identify the essential motifs of **1** for its antimicrobial activity. The results indicate that the thiazolidine ring is pivotal for the activity. Similarly, L-tryptophan, and D-leucine must not be replaced by alanine. Whereas the alternating D,L-configuration is essential for the antimicrobial activity, the enantiomeric compound is as potent as **1** suggesting that for the first attack, a specific AMP-protein interaction is not required. The observation that **1** induces a cancellation of the bacterial membrane potential of *S. aureus* without forming large pores suggested that **1** induces ion transport across the membrane.[11] *In vitro* studies based on simple unilamellar vesicles revealed that **1** is capable of facilitating the transport of protons across membranes, which might be an explanation for the observed cancellation of the membrane potential leading to cell death.[11] Even though these findings points towards a mechanism, in which **1** serves as an ion transporter in the membrane, its partition behavior, and its structure in the membrane remains fully elusive.

To address these questions, we investigated the partitioning of **1** into the membrane of unilamellar vesicles dependent on the lipid composition to unravel whether the specificity of **1** for bacterial membranes and not for human erythrocytes and neutrophils lies in part in the lipid composition. Based on an ATR-FTIR spectroscopic analysis of **1** and methylated derivatives of **1** (Scheme 1) in lipid multi-bilayers, we were able to propose a model of the structure of **1** in lipid membranes that might point towards its mode of action.

[a] D. Ruppelt, H. Flegel, S. Mönnikes, Prof. C. Steinem
Institute of Organic and Biomolecular Chemistry
Georg-August-Universität Göttingen
Tammannstraße 2, 37077 Göttingen (Germany)
E-mail: csteine@gwdg.de

[b] S. N. Wirtz, T. Dema, Prof. S. Grond
Institute of Organic Chemistry
Eberhard Karls Universität Tübingen
Auf der Morgenstelle 18, 72076 Tübingen (Germany)

[c] Prof. C. Steinem
Max Planck Institute for Dynamics and Self-Organization
Am Faßberg 17, 37077 Göttingen (Germany)

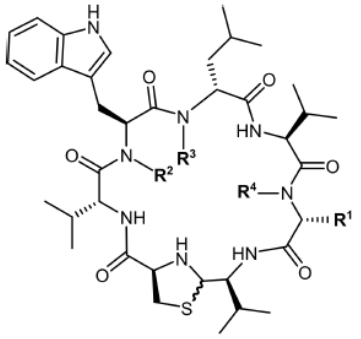

1	Lugdunin	R^1 = D-Val; R^2, R^3, R^4 = H
2	3,6-Ditrp-lugdunin	R^1 = D-Trp; R^2, R^3, R^4 = H
3	3-Methyl-3,6-ditrp-lugdunin	R^1 = D-Trp; R^2 = CH_3; R^3, R^4 = H
4	4-Methyl-3,6-ditrp-lugdunin	R^1 = D-Trp; R^2, R^4 = H; R^3 = CH_3
5	6-Methyl-3,6-ditrp-lugdunin	R^1 = D-Trp; R^2, R^3 = H; R^4 = CH_3

Scheme 1. Chemical structure of lugdunin and lugdunin analogues.

Results and Discussion

Partitioning of lugdunin in POPC membranes

To discern the interaction with and the position of the antimicrobial peptide **1** in lipid bilayers, we exploited the intrinsic fluorescent properties of its tryptophan residue in the absence and presence of POPC vesicles. These simple model membranes enabled us to investigate the partitioning of **1** in a well-defined system without the influence of e.g. bacterial proteins.[12] In aqueous buffer, the fluorescence emission maximum of **1** was at (354 ± 1) nm indicative of a polar environment of the tryptophan residue (Figure 1A, black curve).[13] Upon increasing the POPC concentration, the intensity at the emission maximum increased and the maximum was blue-shifted to lower wavelengths. A maximum blue shift of (18 ± 2) nm in presence of 2000 µM POPC was determined (Figure 1A/B), accompanied by an increase in the maximum fluorescence intensity (Figure 1A/C). The observed blue shift of fluorescence is characteristic for a tryptophan residue that is transferred into a more apolar medium with a lower dielectric constant and is here attributed to a partitioning of the amino acid side chain into the hydrophobic part of a lipid membrane.[14–17] The maximum value of this blue shift depends on the insertion depth of the tryptophan residue into the membrane and can therefore be used to estimate the position of the peptide. For example, the blue shift found for the cationic peptide melittin was around 20 nm indicative of a penetration deep into the hydrophobic membrane core, whereas the antimicrobial peptide cecropin A was located near the lipid head group region with a blue shift of 15 nm.[18,19] With (18 ± 2) nm the tryptophan of peptide **1** appears to be located in between these two areas. To quantify the partition of compound **1** between the aqueous and the membrane phase, its partition coefficient was calculated according to Ladokhin et al.[20] Fitting eq. 3 to the data yielded a partition coefficient of $(9 \pm 2) \times 10^5$ for POPC vesicles, which means that the majority of lugdunin partitions into the membrane phase.

To further corroborate these findings, collisional quenching experiments with water-soluble iodide ions were performed reporting on the accessibility of the tryptophan residue.[21] From the Stern-Volmer plots (Figure 1D), it is evident that quenching is less pronounced in the presence of POPC vesicles, supporting the idea that the tryptophan residue is buried in the lipid bilayer. The corresponding Stern-Volmer constant reads $(7.9 \pm 0.2)\ \mathrm{M}^{-1}$ in buffer solution and was reduced by roughly one half to $(4.5 \pm 0.2)\ \mathrm{M}^{-1}$ in the presence of POPC vesicles.

Lugdunin partitioning is a function of the lipid composition

It has been shown that lugdunin is inactive against human erythrocytes and neutrophils, which raises the question if the lipid composition itself influences the peptide partitioning into a membrane. Thus, we varied the lipid composition and added either POPG to mimic the negative charges of bacterial membranes or cholesterol as an essential component of eukaryotic cell membranes.[22,23] The total blue-shift, the partition coefficients as well as the Stern-Volmer constants for different lipid compositions were determined (Table 1, Fig. S11). Our results clearly show that insertion of **1** into lipid membranes is unaffected by the negative charges introduced by POPG, but hindered in the presence of cholesterol. In case of cholesterol, the observed blue shift ((12 ± 2) nm) and partition coefficient ($(1.0 \pm 0.3) \times 10^5$) were reduced compared to those found for POPC vesicles. Further, the Stern-Volmer constant increased to $(5.8 \pm 0.2)\ \mathrm{M}^{-1}$. An impeding influence of cholesterol on the insertion of antimicrobial peptides has been reported previously.[24] For example, the activity of antimicrobial peptides gramicidin S and S-thanatin was strongly reduced in presence of cholesterol-containing vesicles.[25,26] Cholesterol is known to increase the rigidity of fluid membranes and could thus interfere with the insertion, also affecting the structural assembly of the peptides in the lipid membranes.[27–29]

Table 1. Blue shift $\Delta\lambda_{max}$, partition coefficient K_χ and Stern-Volmer constant K_{SV} for native lugdunin in the absence and presence of lipid vesicles.

Medium	$\Delta\lambda_{max}$ / nm	K_χ / 10^5	K_{SV} / M^{-1}
Buffer	-	-	7.9 ± 0.2
POPC	18 ± 2	9 ± 2	4.5 ± 0.2
25 % POPG	19 ± 3	8 ± 2	-
50 % POPG	17 ± 3	9 ± 2	-
10 % Chol	13 ± 2	1.7 ± 0.2	4.9 ± 0.3
20 % Chol	12 ± 2	1.0 ± 0.3	5.7 ± 0.4

Structural analysis of lugdunin in lipid membranes

The tryptophan fluorescence reports on the insertion of lugdunin into the hydrophobic core of the membrane but does not provide structural information. Thus, we employed IR spectroscopy to gather information about the secondary structure of **1** in lipid membranes. Ordered multi-bilayers composed of DMPC and **1** were analyzed by ATR-FTIR

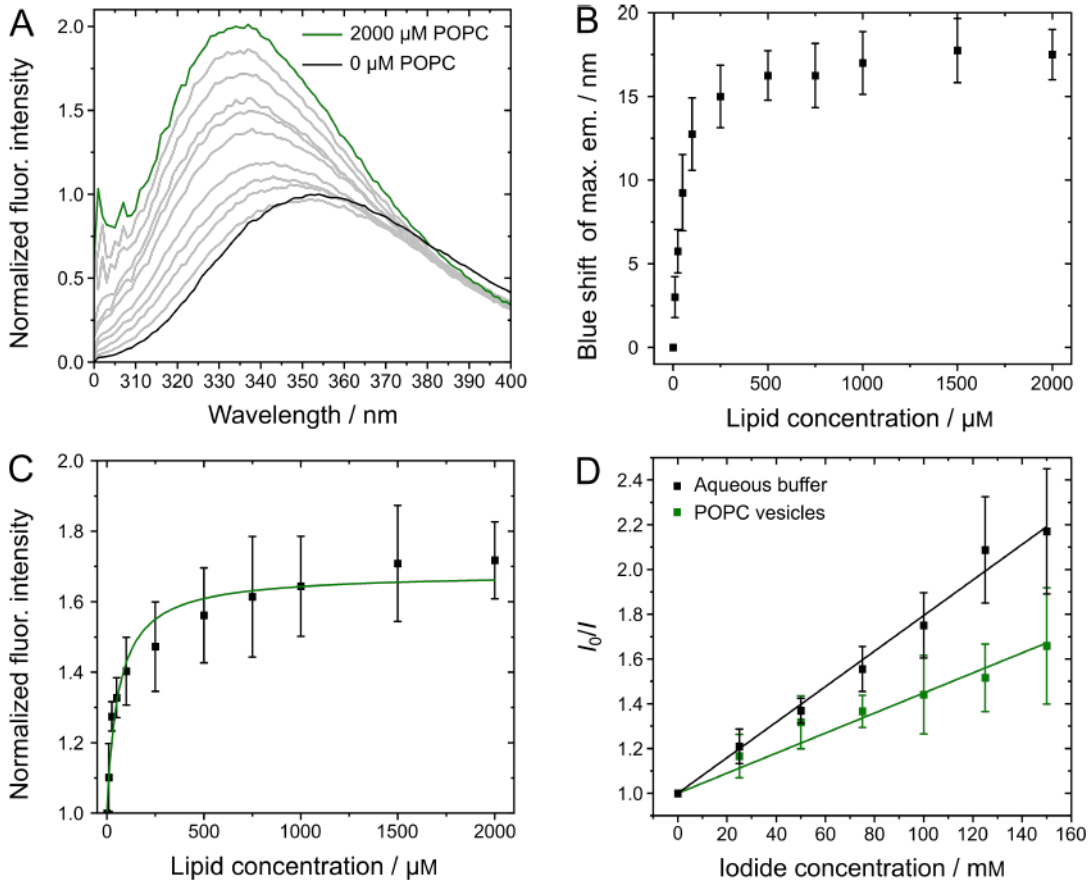

Figure 1. Changes in tryptophan fluorescence properties of lugdunin upon addition of POPC vesicles. A: Fluorescence emission spectra of lugdunin obtained at different lipid concentrations. All measurements were performed with an initial peptide concentration of 10 µM in buffer containing 100 mM KCl, 10 mM HEPES, pH 7.4. The grey curves show measurements at different POPC concentrations between 0-2000 µM. **B:** Blue shift of the maximum emission wavelength of lugdunin dependent on the lipid concentration. **C:** Increase of the fluorescence intensity upon partitioning of the peptide into lipid membranes. ($n \geq 3$ experiments). By fitting equation XX to the data, the partition coefficient of lugdunin in POPC vesicles was obtained. **D:** Stern-Volmer plots of the tryptophan quenching of lugdunin with iodide ions in the absence and presence of POPC vesicles. Measurements were performed with a peptide concentration of 5 µM, a lipid concentration of 500 µM and in buffer containing 100 mM KCl, 10 mM HEPES, pH 7.4 ($n \geq 3$ experiments). All errors are the standard deviation.

spectroscopy (Figure 2A). Next to the absorption bands characteristic for lipids (e.g. $\nu_{as}(N(CH_3)_3^+$ at 3027 cm^{-1}, $\nu_{as}(CH_3)$ at 2957 cm^{-1}, $\nu_{as}(CH_2)$ at 2919 cm^{-1}, $\nu_s(CH_2)$ at 2850 cm^{-1}, ν(C=O) at 1738 cm^{-1}),[30] the IR-spectrum also displays absorption bands representative for the peptide adopting a tightly hydrogen-bonded antiparallel β-sheet structure. Exact peak positions in the amide I region (Figure 2B) were extracted from second derivative spectra revealing peaks at 1641 cm^{-1} (perpendicular component, strong absorption) and 1682 cm^{-1} (parallel component, weak absorption).[31] The amide II region shows a characteristic β-sheet peak at 1543 cm^{-1} (Figure 2A).[32] The amide A peak located at 3282 cm^{-1} supports a tight hydrogen bonding of the N-H groups of the peptide backbone. Assuming intermolecular hydrogen bond interactions between individual peptide molecules, one can estimate the average N–O distance in a hydrogen bond by using Krimm's correlation between the location of the amide A band and the hydrogen bond length.[33] Thus, an amide A peak at 3282 cm^{-1} translates to a N–O distance of around 2.88 Å. To extract the fraction of the secondary structure elements from the amide I band, the peak integrals were taken after deconvoluting the spectra (Table 2). For peptide-to-lipid ratios of 1:40 and 1:30 the deconvolution of the amide I band results in 100 % antiparallel β-sheet structure (Figure 2, Table 2). However, at peptide-to-lipid ratios larger than 1:20 an additional peak in the amide I region prominently emerges at 1624 cm^{-1} (Fig. S12, Table 2). We assume that at this high peptide concentration, peptide aggregates are formed between the multi-bilayer stacks which do not reflect the structure within the lipid bilayers.

The antiparallel β-sheet structure of the cyclic compound **1** with an alternating D,L-configuration might indicate that a tube-like structure is formed in the membrane, similar to synthetic cyclopeptides with D,L-configuration described by Ghadiri and coworkers.[34] These cyclic peptides with an even number of amino acids assemble into tubular β-sheets via hydrogen bonding between the individual molecules under appropriate conditions as shown by electron microscopy

Table 2. Assignment and relative area of peaks attributed to the secondary structure of lugdunin and its derivatives. If not other indicated, data refer to a peptide-to-lipid ratio of 1:10 (n/n).

Peptide	$\tilde{\nu}$ / cm^{-1}	Assignment	Relative area
1[a]	1641, 1683	Antiparallel β-sheet	100 %
1	1624	Aggregation	(50 ± 11) %
	1639, 1682	Antiparallel β-sheet	(49 ± 11) %
2	1626	Aggregation	(9 ± 5) %
	1641, 1683	Antiparallel β-sheet	(73 ± 7) %
	1655	Unordered	(17 ± 12) %
3	1640, 1680	Antiparallel β-sheet	(38 ± 4) %
	1655	Unordered	(62 ± 4) %
4	1636, 1684	Antiparallel β-sheet	(34 ± 2) %
	1654	Unordered	(66 ± 2) %
5	1637, 1684	Antiparallel β-sheet	(36 ± 5) %
	1654	Unordered	(64 ± 5) %

[a] Data refers to a peptide-to-lipid ratio of 1:40 (n/n).

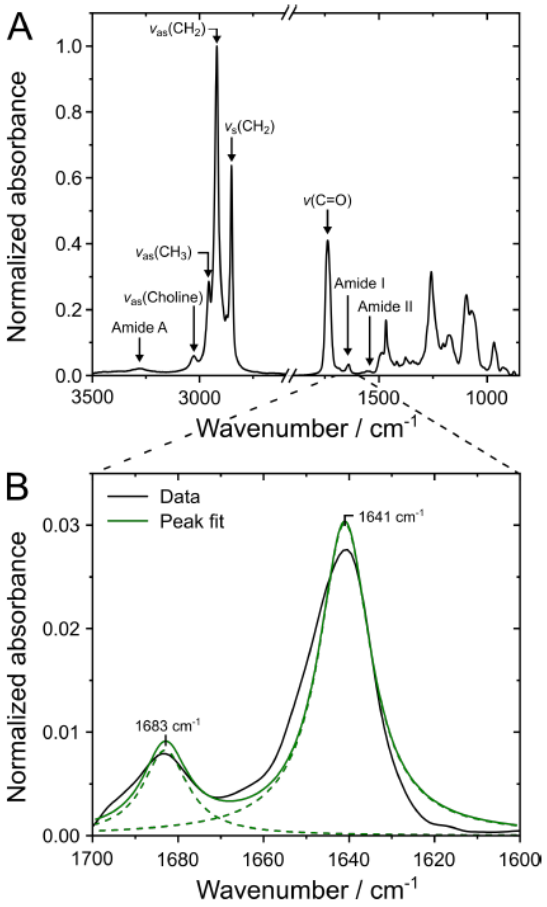

Figure 2. ATR-FTIR spectra of DMPC multi-bilayers with reconstituted lugdunin. A: ATR-FTIR spectrum of DMPC multi-bilayers with peptide **1**. **B:** Amide I region of the spectrum depicted in A. The resulting peak deconvolutions are depicted in green. A nominal peptide-to-lipid ratio of 1:40 (n/n) was used. Spectra are mean values of at least two independent experiments.

and infrared spectroscopy.[35] Furthermore these peptides allowed the passage of small molecules and ions as demonstrated in vesicular transport assays.[36] Owing to the planar ring geometry and the D,L-configuration, a nanotube can be formed with a more polar inner pore and apolar amino acid side chains facing the membrane that can act as a channel with the potential of serving as a new antibiotic.[37] There is one great difference between the synthetic cyclic peptides and **1**, namely **1** is a cyclic peptide composed of an uneven number of amino acids with a thiazolidine heterocycle that might disturb the planarity of the ring. However, despite these differences, the IR spectra of both cyclic peptide species are very similar. For example, the IR spectra of *cyclo*[(L-Trp-D-Leu)$_3$-L-Gln-D-Leu] in DMPC multi-bilayers display amide I peaks located at 1635 cm^{-1} and 1688 cm^{-1}, an amide II peak at 1538 cm^{-1}, and an amide A peak at 3281 cm^{-1}.[38] These results suggest that compound **1** also adopts a quasi-planar ring structure, in which the rings are stacked on each other and are connected via hydrogen bonds. These β-sheet-like 'nanotubes' might act as (ion) channels resulting in the observed antibacterial effect of **1**.

Orientational properties of lugdunin

In addition to the structural information, polarized ATR-FTIR spectroscopy allows to gain insight into the relative orientation of the peptide nanotubes in ordered DMPC multi-bilayers. We determined the orientation of the lipid molecules and peptide **1** in DMPC multi-bilayers by recording polarized ATR-FTIR spectra of the lipid acyl chains (Figure 3A) and the amide I region of the peptide (Figure 3B). The exact experimental approach is described in the supporting information (Fig. S4, Tab. S1). The lipid order was assessed by measuring the dichroic ratio of the antisymmetric and symmetric CH_2-stretch vibrations, whose transition dipole moment is perpendicular to the axis of the all-*trans* hydrocarbon chain. In the absence of peptide **1**, DMPC molecules showed an average tilt angle of (27.5 ± 0.6)°. This value is in good agreement with previously reported values obtained for lipid multi-bilayer systems. Addition of compound **1** alters the tilt angle between 1° and 7° depending on the peptide concentration. For the peptide, we evaluated the dichroic ratio of the amide I peak at ~1640 cm^{-1}. Assuming a nanotube structure, the transition dipole moment of this amide I vibration is oriented rather parallel to the central axis of the nanotube. The intensity of the amide I band shows a substantial change between parallel and perpendicular polarized incident light (Figure 3B). This finding indicates that the hydrogen bonded peptide rings align with the central axis in a parallel orientation to the crystal plate normal. A similar dependency of the intensities was found for the amide A band, which is mainly composed of the N−H-stretch vibration. The tilt angle of the hydrogen bonded peptide rings was determined to (44 ± 2)° relative to the crystal surface, which translates into a tilt angle relative to the membrane of (10 ± 2)° (Table 3). The tilt angle of around 10° is similar to angles of the β-helix formed by gramicidin A in DMPC multi-bilayers determined to 15° and the tilt angle of the synthetic D,L-cyclopeptide *cyclo*[(L-Trp-D-Leu)$_3$-L-Gln-D-Leu] of (7 ± 1)°.[38,39] Note, that even for high peptide-to-lipid ratios in which the additional amide I peak at ~1624 cm^{-1} arises, similar tilt angles for the β-sheet-like nanotube were obtained.

Table 3. Dichroic ratio R^{ATR}, order parameter S Θ) and tilt angle Θ of DMPC multi-bilayers without and with lugdunin (1:40).

	DMPC[a]				DMPC + Lugdunin (P:L 1:40)[a]			
	$\tilde{\nu}$ / cm^{-1}	R^{ATR}	$S(\Theta)$	Θ / °	$\tilde{\nu}$ / cm^{-1}	R^{ATR}	$S(\Theta)$	Θ / °
Stretching	2919, 2851	1.13 ± 0.01	0.68 ± 0.01	27.5 ± 0.6^{b}	2919, 2851	1.28 ± 0.01	0.53 ± 0.02	34.0 ± 0.6^{b}
Amide I	-	-	-	-	1641	3.3 ± 0.2	0.28 ± 0.03	$44 \pm 2^{b,c}$

[a] Data are mean values of 2-3 samples. [b] Tilt angles are relative to the surface of the IRE and were calculated from the transition dipole moment of the respective vibrational mode. [c] The tilt angle relative to the membrane normal was determined to $(10 \pm 2)°$.

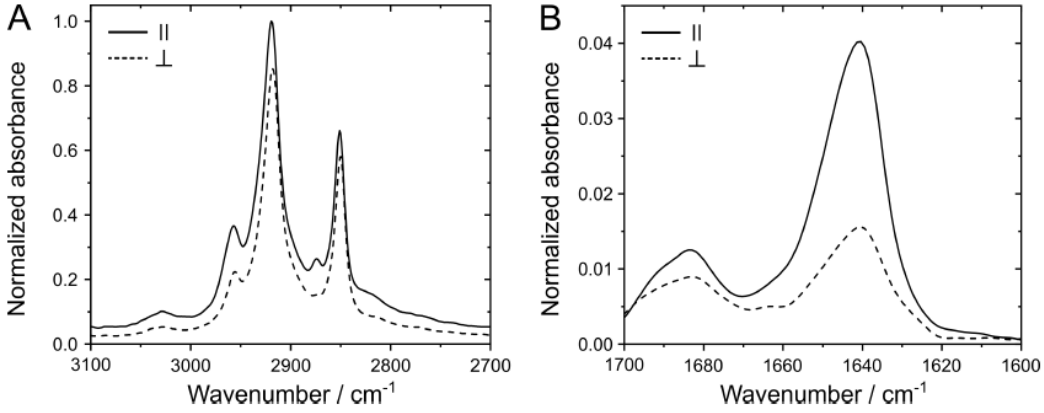

Figure 3. Polarized ATR-FTIR spectra of DMPC multilayer with lugdunin. A: Polarized methylene stretching modes of a pure DMPC multilayer. **B:** Polarized amide I region of peptide **1** in DMPC multi-bilayers. A nominal peptide-to-lipid ratio of 1:40 was used.

Structural and orientational analysis of lugdunin analogues

Our results strongly suggest that nanotubes are the main structure formed by peptide **1** in model membranes and might also be responsible for its *in vivo* activity. To further support this idea, we analyzed the secondary structure of 3,6-ditryptophan-lugdunin (**2**) by IR spectroscopy, as this derivative showed a two-fold increased antimicrobial activity in *in vivo* assays compared to **1**.[11,40] Indeed, compound **2** also adopted an antiparallel β-sheet structure with peaks located at 1641 cm^{-1} and 1680 cm^{-1} (Figure 4A, Table 2). By polarized ATR-IR spectroscopy, the relative tilt angle of the hydrogen bonded peptide rings of **2** was determined, which was $(2 \pm 2)°$ relative to the membrane normal. This finding suggests that the two-fold increased bactericidal activity of peptide **2** is related to a well-aligned nanotube structure. It is known that the planar aromatic structure of the indol ring system of tryptophan favors its position at the lipid-water-interface of membranes in peptides and proteins, thus, stabilizing the interfacial region of the proteins.[41] It is conceivable that the additional tryptophan residue promotes the alignment of β-sheet-like structures, which makes the proton transport more efficient. The IR peak at 1626 cm^{-1} that we found for peptide **1** at peptide-to-lipid ratios larger than 1:20 and which we attributed to aggregated peptides between the multi-bilayer stacks, is for peptide **2** at a peptide-to-lipid ratio of 1:10 much less pronounced. This finding enabled us to use compound **2** and its analogues at a high peptide-to-lipid ratio of 1:10 leading to a high signal-to-noise for further structural studies.

To test our hypothesis of a hydrogen bond-mediated assembly of peptide rings in membranes, we synthesized *N*-methylated derivatives of **2** (Scheme 2). A methylation at the peptide backbone is expected to interfere with the ability of the peptide to form extensive hydrogen-bonded β-sheet structures.[36] Peptide **2** was methylated at position 3, 4 and 6, respectively (Scheme 1, peptides **3**, **4** and **5**), and their IR-spectral properties were investigated. All derivatives showed a secondary structure consisting of 65 % unordered structure (with a peak at around 1655 cm^{-1}) and of 35 % antiparallel β-sheets indicated by peaks at ~1638 cm^{-1} and ~1682 cm^{-1} (Figure 4B). Compared to the non-methylated compound **2**, methylation increased the amount of unordered structural components drastically. With these findings, it is evident that a change in the hydrogen-bonding capability of the peptide results in a fundamental change of the observed structure in lipid membranes further strengthening our idea of a hydrogen-bonded β-sheet.

Proton translocation activity of lugdunin and analogues

To relate our findings of the postulated lugdunin structure in a lipid bilayer to its proton translocation activity, we performed proton translocation assays with the pH-sensitive fluorescent dye pyranine (Figure 5A). Proton translocation across pure POPC bilayers can be unambiguously observed in agreement to our previous findings.[11] Adding negatively charged POPG to the lipid mixture enhanced the proton translocation kinetics of **1** significantly. As the partition coefficients of **1** are the same in POPC and POPC/POPG

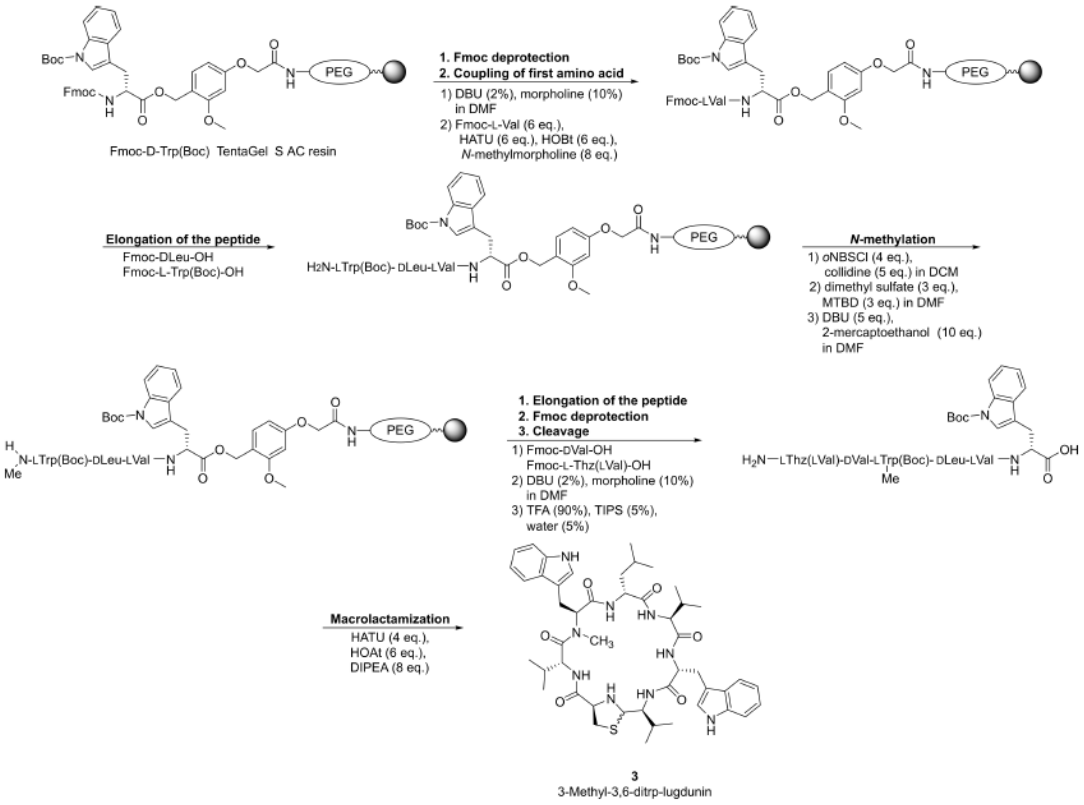

Scheme 2. Solid-phase peptide synthesis of methylated lugdunin analogues 3-5.

bilayers (see Table 1), the faster kinetics can be attributed to the locally increased proton concentration at the negatively charged membrane interface.[42] In case of vesicles composed of POPC and 20 % cholesterol the proton transport activity was significantly reduced. This finding is in agreement with the observed smaller partition coefficients of **1**, which we discuss in terms of membrane rigidification. These results might explain why lugdunin is not active against human erythrocytes and neutrophils.

Furthermore, we probed the proton translocation activity of the methylated peptide analogues **3**, **4** and **5** (Fig. 5B). Even though these peptides exhibit the appropriate hydrophobic surface to partition into bilayers, they only showed a reduced proton transport across lipid membranes and a reduced bioactivity against *S. aureus* compared to **1** (minimal inhibitory concentrations $\geq 100\,\mu g\,mL^{-1}$). This weak proton transport activity suggests that the antiparallel β-sheet structure found for **1** and **2**, but not for **3**, **4** and **5** is pivotal for the activity of the peptide. The reduced ability of the methylated analogues to form ordered intermolecular hydrogen bond-connected ring stacks prevents the formation of functional peptide nanotubes resulting in a reduced proton translocation activity. Like the synthetic D,L-cyclopeptides introduced by Ghadiri and coworkers, the proton transport activity of **1** seems therefore to be tightly associated with the formation of an antiparallel β-sheet structure observed in ATR-FTIR spectra supporting our model of a peptide nanotube inside lipid membranes.

Conclusion

Understanding the mechanism of action of natural occurring antimicrobial peptides, is a prerequisite for the development of novel antimicrobial entities. Here, we used fluorescence and ATR-FTIR spectroscopy to gain insight into the partitioning of the antimicrobial fibupeptide **1** into lipid membranes and its structure. From our results we conclude that **1** strongly partitions into fluid lipid bilayers and forms antiparallel β-sheet structures (Figure 6A). These β-sheets can form nanotubes by the association of individual peptide rings via an extensive hydrogen bonding network (Figure 6B). Such peptide nanotubes can act as ion channels in the lipid bilayer facilitating the transport of ions, such as protons. These results will pave the way for further investigations including molecular dynamics simulations as well as transport kinetics and ion selectivity.

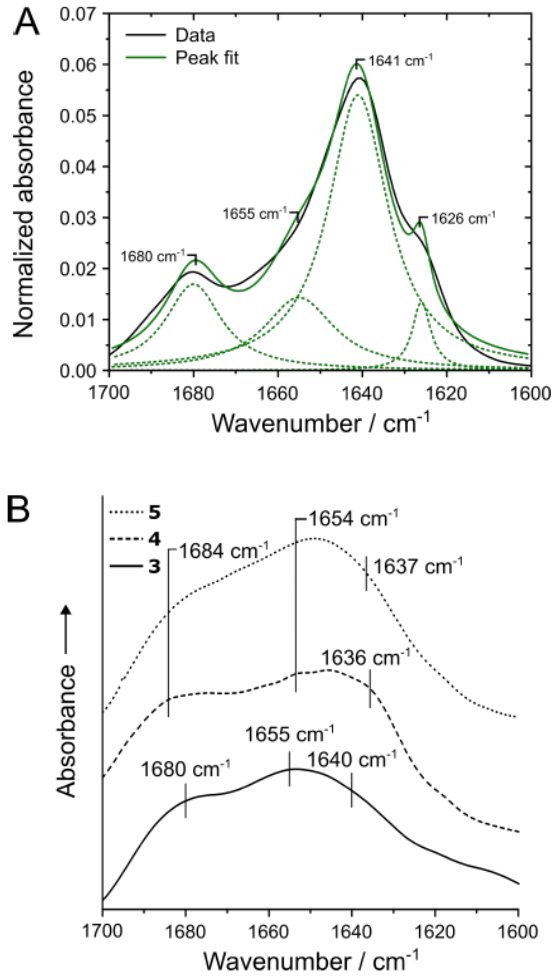

Figure 4. ATR-FTIR spectra of DMPC multi-bilayers with lugdunin analogues. **(A)** ATR-FTIR spectra with peptide **2**. The resulting peak deconvolutions are depicted in green. **(B)** ATR-FTIR spectra with peptides **3**, **4** and **5**. A nominal peptide-to-lipid ratio of 1:10 (n/n) was used. Spectra are mean values of at least three independent experiments.

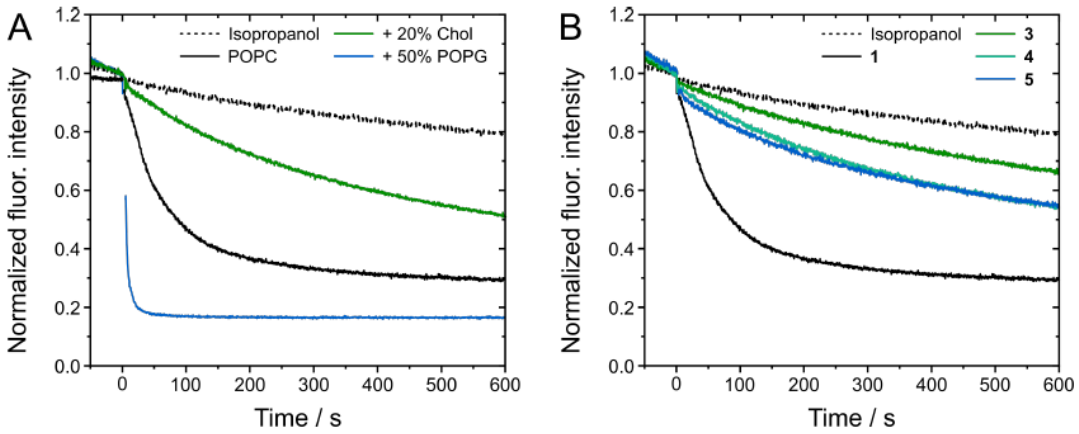

Figure 5. Proton transport activity of lugdunin and its analogues. (A) Proton translocation induced by **1** as a function of the lipid composition. **(B)** Proton translocation induced by peptides **1**, **3**, **4** and **5**. Pure POPC vesicles were used with a peptide to lipid ratio of 1:250 (n/n).

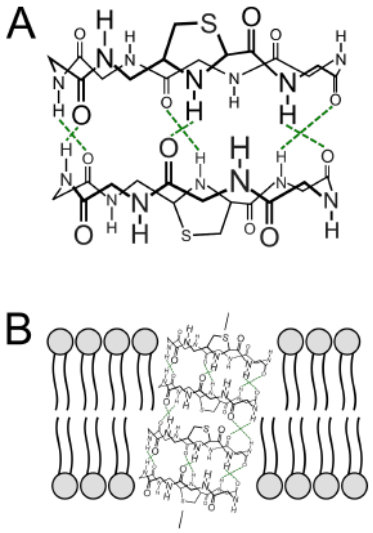

Figure 6. Postulated structural model of lugdunin. (A) Individual lugdunin molecules stack onto each other via hydrogen bonding of the peptide backbone and form an antiparallel β-sheet. **(B)** Dependent on the number of rings, the β-sheet can span lipid membranes and act as an ion channel. Amino acid residues are omitted for clarity, drawing is not to scale.

Acknowledgements

Acknowledgements text.

Conflict of Interest

The authors declare no conflict of interest.

Keywords: Antimicrobial peptides • antiparallel β-sheet • D,L-cyclopeptides • proton translocation • solid-phase peptide synthesis

References

[1] E. Tacconelli, E. Carrara, A. Savoldi, S. Harbarth, M. Mendelson, D. L. Monnet, C. Pulcini, G. Kahlmeter, J. Kluytmans, Y. Carmeli, M. Ouellette, K. Outterson, J. Patel, M. Cavaleri, E. M. Cox, C. R. Houchens, M. L. Grayson, P. Hansen, N. Singh, U. Theuretzbacher, N. Magrini, A. O. Aboderin, S. S. Al-Abri, N. Awang Jalil, N. Benzonana, S. Bhattacharya, A. J. Brink, F. R. Burkert, O. Cars, G. Cornaglia, O. J. Dyar, A. W. Friedrich, A. C. Gales, S. Gandra, C. G. Giske, D. A. Goff, H. Goossens, T. Gottlieb, M. Guzman Blanco, W. Hryniewicz, D. Kattula, T. Jinks, S. S. Kanj, L. Kerr, M.-P. Kieny, Y. S. Kim, R. S. Kozlov, J. Labarca, R. Laxminarayan, K. Leder, L. Leibovici, G. Levy-Hara, J. Littman, S. Malhotra-Kumar, V. Manchanda, L. Moja, B. Ndoye, A. Pan, D. L. Paterson, M. Paul, H. Qiu, P. Ramon-Pardo, J. Rodríguez-Baño, M. Sanguinetti, S. Sengupta, M. Sharland, M. Si-Mehand, L. L. Silver, W. Song, M. Steinbakk, J. Thomsen, G. E. Thwaites, J. W. M. van der Meer, N. van Kinh, S. Vega, M. V. Villegas, A. Wechsler-Fördös, H. F. L. Wertheim, E. Wesangula, N. Woodford, F. O. Yilmaz, A. Zorzet, *Lancet Infect. Dis.* **2018**, *18*, 318.

[2] Jim O'Neill, for The Review on Antimicrobial Resistance, Tackling drug-resistant infections globally: final report and recommendations **2016**.

[3] G. D. Wright, *Can. J. Microbiol.* **2014**, *60*, 147.

[4] a) M. Lakemeyer, W. Zhao, F. A. Mandl, P. Hammann, S. A. Sieber, *Angew. Chem. Int. Ed.* **2018**, *57*, 14440; b) M. Lakemeyer, W. Zhao, F. A. Mandl, P. Hammann, S. A. Sieber, *Angew. Chem.* **2018**, *130*, 14642.

[5] H. Jenssen, P. Hamill, R. E. W. Hancock, *Clin. Microbiol. Rev.* **2006**, *19*, 491.

[6] M. E. Hibbing, C. Fuqua, M. R. Parsek, S. B. Peterson, *Nat. Rev. Microbiol.* **2010**, *8*, 15.

[7] M. Magana, M. Pushpanathan, A. L. Santos, L. Leanse, M. Fernandez, A. Ioannidis, M. A. Giulianotti, Y. Apidianakis, S. Bradfute, A. L. Ferguson, A. Cherkasov, M. N. Seleem, C. Pinilla, C. de La Fuente-Nunez, T. Lazaridis, T. Dai, R. A. Houghten, R. E. W. Hancock, G. P. Tegos, *Lancet Infect. Dis.* **2020**, *20*, e216.

[8] A. Moretta, C. Scieuzo, A. M. Petrone, R. Salvia, M. D. Manniello, A. Franco, D. Lucchetti, A. Vassallo, H. Vogel, A. Sgambato, P. Falabella, *Front. Cell. Infect. Microbiol.* **2021**, *11*, 668632.

[9] A. Zipperer, M. C. Konnerth, C. Laux, A. Berscheid, D. Janek, C. Weidenmaier, M. Burian, N. A. Schilling, C. Slavetinsky, M. Marschal, M. Willmann, H. Kalbacher, B. Schittek, H. Brötz-Oesterhelt, S. Grond, A. Peschel, B. Krismer, *Nature* **2016**, *535*, 511.

[10] K. Bitschar, B. Sauer, J. Focken, H. Dehmer, S. Moos, M. Konnerth, N. A. Schilling, S. Grond, H. Kalbacher, F. C. Kurschus, F. Götz, B. Krismer, A. Peschel, B. Schittek, *Nat. Commun.* **2019**, *10*, 2730.

[11] a) N. A. Schilling, A. Berscheid, J. Schumacher, J. S. Saur, M. C. Konnerth, S. N. Wirtz, J. M. Beltrán-Beleña, A. Zipperer, B. Krismer, A. Peschel, H. Kalbacher, H. Brötz-Oesterhelt, C. Steinem, S. Grond, *Angew. Chem. Int. Ed.* **2019**, *58*, 9234; b) N. A. Schilling, A. Berscheid, J. Schumacher, J. S. Saur, M. C. Konnerth, S. N. Wirtz, J. M. Beltrán-Beleña, A. Zipperer, B. Krismer, A. Peschel, H. Kalbacher, H. Brötz-Oesterhelt, C. Steinem, S. Grond, *Angew. Chem.* **2019**, *131*, 9333.

[12] K. A. Ganzinger, P. Schwille, *J. Cell Sci.* **2019**, *132*.

[13] A. S. Ladokhin, Fluorescence Spectroscopy in Peptide and Protein Analysis, in R. A. Meyers (Editor), *Encyclopedia of Analytical Chemistry*, volume 28, pages 1–18, John Wiley & Sons, Ltd, Chichester, UK **2006**.

[14] G. Beschiaschvili, J. Seelig, *Biochim. Biophys. Acta Biomembr.* **1991**, *1061*, 78.

[15] C. Mollay, G. Krell, *Biochim. Biophys. Acta Lipids Lipid Metab.* **1973**, *316*, 196.

[16] H. Zhao, P. K. J. Kinnunen, *J. Biol. Chem.* **2002**, *277*, 25170.

[17] N. G. Park, U. Silphaduang, H. S. Moon, J.-K. Seo, J. Corrales, E. J. Noga, *Biochemistry* **2011**, *50*, 3288.

[18] D. E. Schlamadinger, J. E. Gable, J. E. Kim, *J. Phys. Chem. B* **2009**, *113*, 14769.

[19] D. E. Schlamadinger, Y. Wang, J. A. McCammon, J. E. Kim, *J. Phys. Chem. B* **2012**, *116*, 10600.

[20] A. S. Ladokhin, S. Jayasinghe, S. H. White, *Anal. Biochem.* **2000**, *285*, 235.

[21] J. R. Lakowicz, *Principles of fluorescence spectroscopy*, Springer, New York, NY, third edition, corrected at 4. printing edition **2010**.

[22] R. F. Epand, P. B. Savage, R. M. Epand, *Biochim. Biophys. Acta Biomembr.* **2007**, *1768*, 2500.

[23] G. van Meer, D. R. Voelker, G. W. Feigenson, *Nat. Rev. Mol. Cell Biol.* **2008**, *9*, 112.

[24] J. R. Brender, A. J. McHenry, A. Ramamoorthy, *Front. Immunol.* **2012**, *3*, 195.

[25] E. J. Prenner, R. N. Lewis, M. Jelokhani-Niaraki, R. S. Hodges, R. N. McElhaney, *Biochim. Biophys. Acta Biomembr.* **2001**, *1510*, 83.

[26] G. Wu, H. Wu, X. Fan, R. Zhao, X. Li, S. Wang, Y. Ma, Z. Shen, T. Xi, *Peptides* **2010**, *31*, 1669.

[27] J. Henriksen, A. C. Rowat, E. Brief, Y. W. Hsueh, J. L. Thewalt, M. J. Zuckermann, J. H. Ipsen, *Biophys. J.* **2006**, *90*, 1639.

[28] S. Chakraborty, M. Doktorova, T. R. Molugu, F. A. Heberle, H. L. Scott, B. Dzikovski, M. Nagao, L.-R. Stingaciu, R. F. Standaert, F. N. Barrera, J. Katsaras, G. Khelashvili, M. F. Brown, R. Ashkar, *Proc. Natl. Acad. Sci. U. S. A.* **2020**, *117*, 21896.

[29] R. Sood, P. K. J. Kinnunen, *Biochim. Biophys. Acta Biomembr.* **2008**, *1778*, 1460.

[30] U. P. Fringeli, H. H. Günthard, *Mol. Biol., Biochem. Biophys.* **1981**, *31*, 270.

[31] A. Barth, C. Zscherp, *Q. Rev. Biophys.* **2002**, *35*, 369.

[32] T. Miyazawa, E. R. Blout, *J. Am. Chem. Soc.* **1961**, *83*, 712.
[33] J. B. Samuel Krimm, Vibrational Spectroscopy and Conformation of Peptides, Polypeptides, and Proteins, in C. B. Anfinsen, J. T. Edsall, F. M. Richards (Editor), *Advances in Protein Chemistry*, volume 38, pages 181–264, Academic Press, New York, NY **1986**.
[34] J. Montenegro, M. R. Ghadiri, J. R. Granja, *Acc. Chem. Res.* **2013**, *46*, 2955.
[35] M. R. Ghadiri, J. R. Granja, R. A. Milligan, D. E. McRee, N. Khazanovich, *Nature* **1993**, *366*, 324.
[36] M. R. Ghadiri, J. R. Granja, L. K. Buehler, *Nature* **1994**, *369*, 301.
[37] S. Fernandez-Lopez, H. S. Kim, E. C. Choi, M. Delgado, J. R. Granja, A. Khasanov, K. Kraehenbuehl, G. Long, D. A. Weinberger, K. M. Wilcoxen, M. R. Ghadiri, *Nature* **2001**, *412*, 452.
[38] H. S. Kim, J. D. Hartgerink, M. R. Ghadiri, *J. Am. Chem. Soc.* **1998**, *120*, 4417.
[39] E. Nabedryk, M. P. Gingold, J. Breton, *Biophys. J.* **1982**, *38*, 243.
[40] J. S. Saur, S. N. Wirtz, N. A. Schilling, B. Krismer, A. Peschel, S. Grond, *J. Med. Chem.* **2021**, *64*, 4034.
[41] K. M. Sanchez, G. Kang, B. Wu, J. E. Kim, *Biophys. J.* **2011**, *100*, 2121.
[42] C. Steinem, A. Janshoff, F. Höhn, M. Sieber, H.-J. Galla, *Chem. Phys. Lipids* **1997**, *89*, 141.

Entry for the Table of Contents

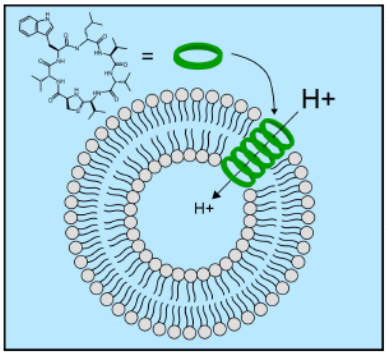

Lord Of The Rings: The mode of action of the first antimicrobial fibupeptide lugdunin depends on the insertion of the peptide into lipid membranes and the accompanying assembly into an antiparallel β-sheet-like nanotube. Due to the characteristic D,L-configuration of lugdunin, these hollow tubes could act as ion channels enabling the efficient transport of protons and presumably other small ions across membranes.